An act of balance: A20/TNFAIP3 in dendritic cells is essential to prevent autoimmunity

Tridib Das

The work described in this thesis was conducted at the Department of Pulmonary Medicine, Erasmus MC, Rotterdam, The Netherlands.

Thesis directors: Prof. dr. R.W.Hendriks
Prof. dr. B.N.M. Lambrecht

Layout and printing: Optima Grafische Communicatie, Rotterdam, The Netherlands.
Cover design: Tridib Das and Olof Borgwit (Optima Grafische Communicatie)

Thesis printing sponsor: Théa Pharma
Department of pulmonary medicine, Erasmus MC

An act of balance: A20/TNFAIP3 in dendritic cells is essential to prevent autoimmunity

Op zoek naar balans: A20/TNFAIP3 in dendritische cellen is essentieel om autoimmuniteit te voorkomen

Thesis

to obtain the degree of Doctor from the
Erasmus University Rotterdam
by command of the
rector magnificus

Prof. dr. F.A. van der Duijn Schouten

and in accordance with the decision of the Doctorate Board.
The public defence shall be held on

Wednesday 24 February 2021 at 13.00hrs
by

Tridib Das
born in New Delhi, India.

Erasmus University Rotterdam

DOCTORAL COMMITTEE

Promotors:	Prof. dr. R.W.Hendriks
	Prof. dr. B.N.M. Lambrecht
Other members:	Prof. dr. F.G.M. Kroese
	Dr. E. Lubberts
	Dr. P.A. Boonstra

In memory of both my grandfathers

Bhagyeswar Das
1926 - 2020

Rabindra Narayan Bhaumik
1927 - 2017

Whom both lived by the principle
to give selflessly

TABLE OF CONTENTS

Chapter 1

General Introduction and Aims

T. Das

GENERAL INTRODUCTION

Dendritic cells: the sentinels of the immune system.

Our immune system consists of cells belonging to the innate immune system and the adaptive immune system. Dendritic cells (DCs) are a family of antigen presenting cells (APCs) that bridge these two systems[1]. They scan the internal milieu for self and foreign antigens and present these to T cells of the adaptive immune system through a process termed 'antigen presentation' (**Figure 1**). T cells express a T cell receptor (TCR) that can specifically recognize a particular antigen in the form of a short peptide bound to major histocompatibility complex (MHC) molecules on APCs. Whereas $CD8^+$ T cells recognize antigens bound to MHC class I molecules, MHC-II is used to present antigens to $CD4^+$ T cells (**Figure 1**). While exogenous antigens, in contrast to intracellular antigens, are normally presented to $CD4^+$ T cells, cross-presentation enables presentation of exogenous antigens onto MHC-I and thereby activation of $CD8^+$ T cells[2] (**Figure 2**).

Ready, set, go: 3 signals necessary for complete T cell activation.

Antigen presentation resulting in TCR stimulation, is a first signal, but it does not automatically result in activation of the receiving T cell. Three signals are necessary in total to achieve full T cell activation[5]. Based on the expressed co-stimulatory molecules or co-inhibitory molecules (**Figure 3**) on the surface of DCs, an activating or inhibiting response is mediated[6, 7], which is known as the second signal. Besides engagement of TCR, the signal via CD28 on T cells which binds CD86 on DCs is crucial for T cells, because without this interaction a T cell will become anergic[8]. Positive stimulation can further be induced by inducible costimulator (ICOS) that binds ICOS-ligand (ICOS-L) (in **Figure 3** as 'B7c')[9]. Inhibitory signals can be mediated via PD-1 and CTLA-4, which can bind PD-L1/PD-L2 or CD80/CD86, respectively. CTLA-4 binds CD80/CD86 with greater affinity and avidity than CD28, thus enabling it to outcompete CD28 for its ligands. Cytokines, either produced by DCs or already available in the milieu, are the third signal, and can further define the T cell response e.g. differentiating them into T helper cell subsets or unlocking their full potential.

DC subsets

Four types of DCs can be distinguished: Conventional type 1 or 2 DCs (cDC1s and cDC2s), plasmacytoid DCs (pDCs)[6] and inflammatory monocyte derived DCs (Mo-DCs)[11]. The functions of DCs are different during steady state or during inflammation. In steady state, cDC1s and cDC2s are primarily involved in peripheral tolerance as they can present tissue-associated self-antigens and effectively induce regulatory T cells (Tregs) and $CD4^+$ and $CD8^+$ T cell tolerance[2, 12-14]. During activation, however, primarily (but not exclusively) $CD8^+$ T cells are activated by cDC1s, and $CD4^+$ T cells by cDC2s[14-16]. pDCs can

also activate both T cell types, but in addition are known for their high type 1 interferon signature[17]. During inflammation, Mo-DCs arise from a monocyte precursor and their functions overlap with dendritic cells[11]. The most used markers to identify DC subsets are listed in **Table 1**.

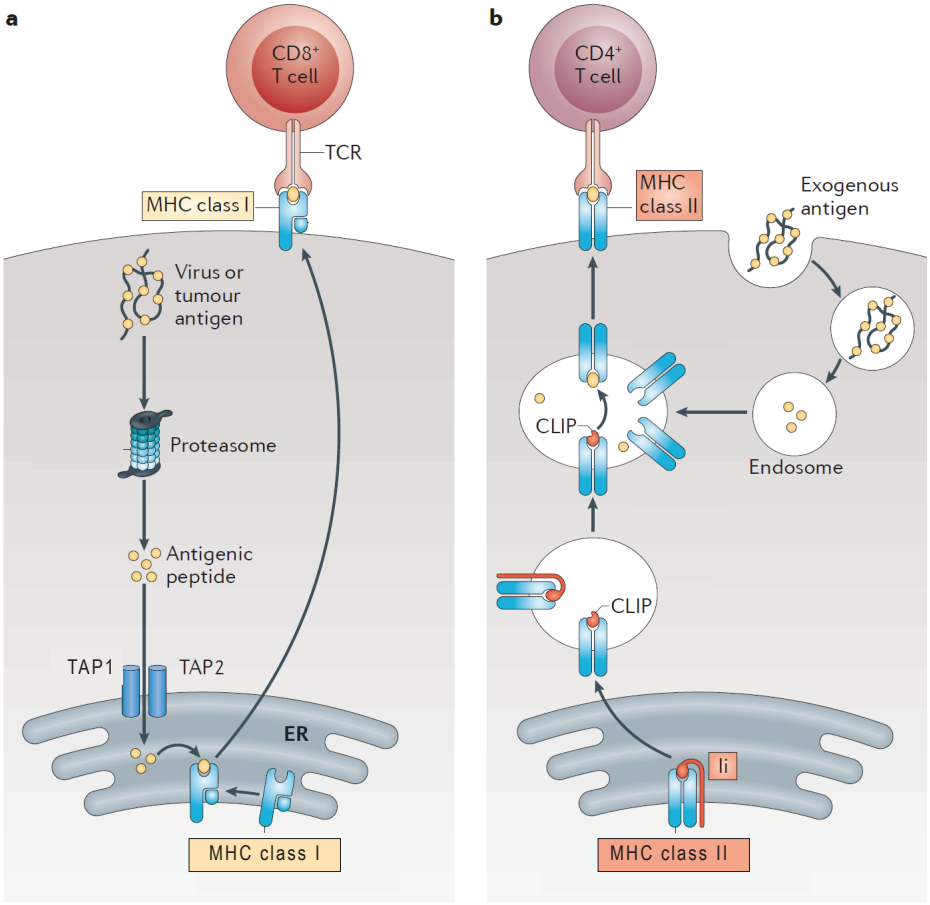

Figure 1: Antigen presentation to CD8$^+$ and CD4$^+$ T cells using MHC-I and MHC-II, respectively (**a**) Virus antigens or tumor antigens are primarily intracellular antigens and are commonly presented on major histocompatibility complex (MHC) class I complex molecules. Proteasomes are large proteins that degrade proteins, such as viral or tumor antigens into smaller peptides. Transporter associated with antigen processing (TAP) 1 and TAP2, carry antigen peptides into the endoplasmic reticulum (ER). Here, antigens are placed onto the presenting groove of MHC-I, which then leave the ER (and are transported via Golgi/secretory vesicles; not shown in figure) to the surface of the cell to present antigen to CD8$^+$ T cells on their T cell receptor (TCR). (**b**) Extracellular antigens, such as bacteria, are commonly presented on MHC-II molecules. The extracellular antigens are processed by endolysosomal enzymes into peptides. The presenting groove of MHC-II first contains Class II-associated invariant chain peptide (CLIP), which is derived from MHC class II-associated invariant chain (Ii). CLIP is displaced by the bacterial peptide and the MHC-II molecule is brought to the surface of the cell in order to present antigens to CD4$^+$ T cells. Adapted from Kobayashi et al[3].

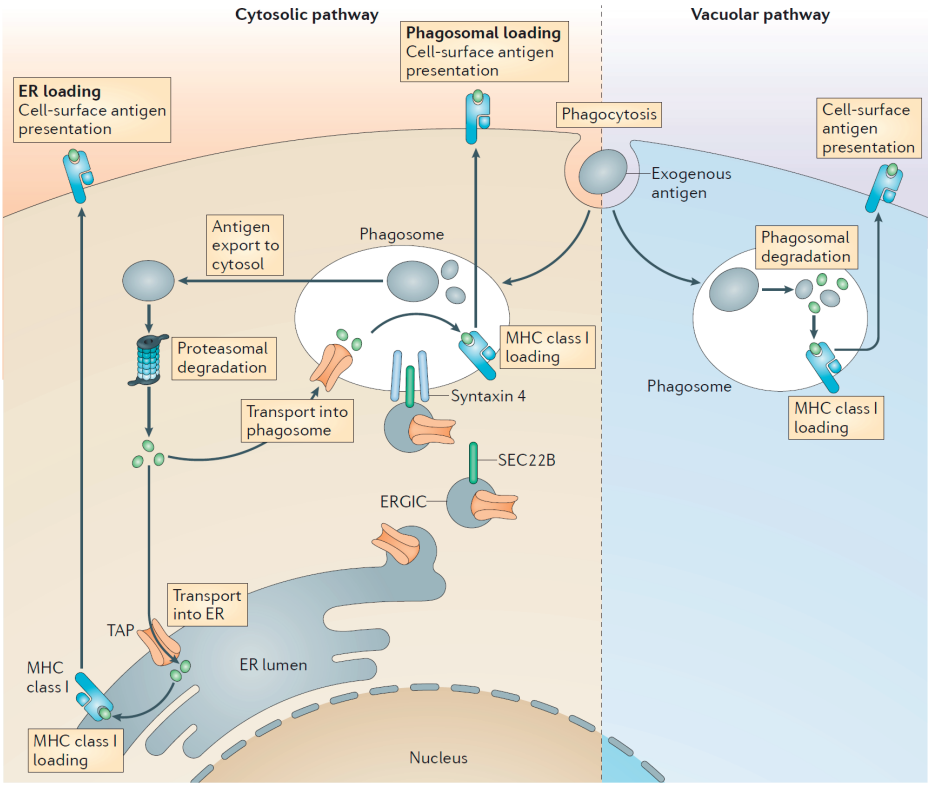

Figure 2: Processing exogenous antigens onto MHC-I molecules within antigen presenting cells in order to cross-present.

Exogenous antigens can be placed onto MHC-I molecules via 2 pathways: the cytosolic pathway or the vacuolar pathway. Within the cytosolic pathway (left), phagocytosed exogenous antigens are processed in an engulfed vesicle called phagosome, then released into cytosol where they can further be degraded by proteasomes. After this, they can be re-transported into the phagosomes, where they can be loaded on available MHC-I molecules and expressed on the cell surface. Alternatively, anitgens can be transported into the ER and loaded on MHC-I molecules there. The ER contains the transporter protein TAP, which is located to phagosomes with the help of other proteins such as the SNARE protein SEC22B and Syntaxin 4. ER-Golgi intermediate compartment (ERGIC) is where SEC22B interacts with Syntaxin 4. The vacuolar pathway (right) allows phagosome-degraded exogenous antigens to be directly loaded on MHC-I molecules and then go to the cell surface for antigen presentation. From Joffre et al[4]

Effector adaptive immune cells in autoimmunity

DCs are central orchestrators of the immune response: they activate T cells and - besides antigen presentation and co-stimulation - produce cytokines to direct naïve T cells into a particular differentiation pathway (**Figure 4**). T helper subsets produce different cytokines (**Figure 4**) and thus have different functions. For a long time, the T helper 1 cell (Th1 cell) and Th2 cell paradigm dominated our understanding of (auto)immune diseases versus allergic diseases, respectively[19, 20]. The Th1 subset is important in host defenses to

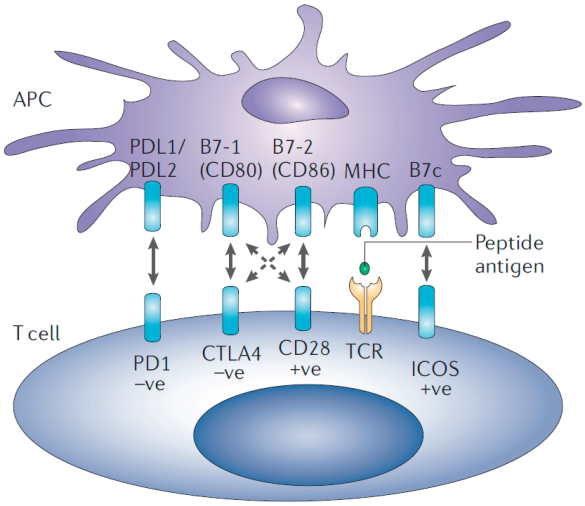

Figure 3: Co-stimulatory and co-inhibitory molecules set thresholds for T cell activation
A selection of common co-stimulatory and co-inhibitory molecules are depicted, that results in positive (+ve) or inhibitory (-ve) effects on T cell activation. The most important co-stimulation for activation is CD28 interaction on T cells with CD80 or CD86 on APCs. Classic interactions are bold arrows, while dashed arrows are weaker affinity connections that are known. From Gregersen et al[10].

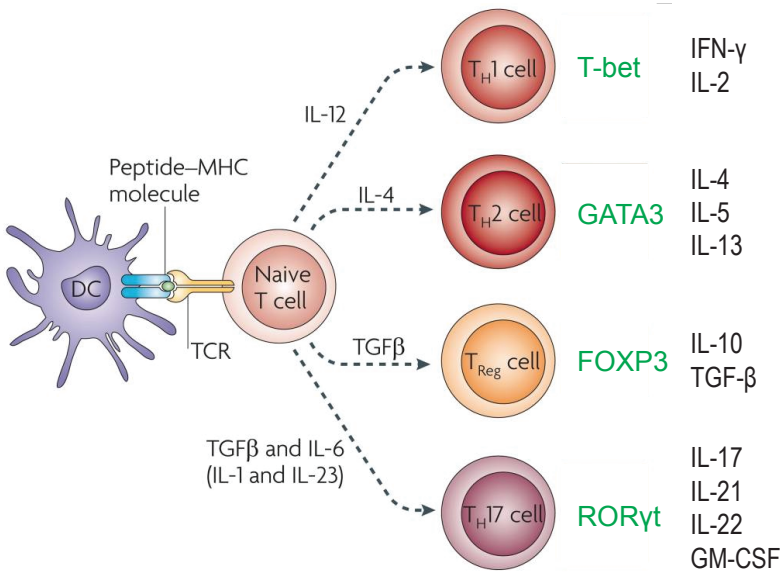

Figure 4: Differentiation of helper T cell (Th) subsets.. Naïve T cells can differentiate into various T helper cell (Th) subsets under influence of differentiating cytokines, that are shown adjacent to the dashed arrows. Responsible key transcription factors (green) and primary cytokines are listed per Th cell subset on the right side. Adapted from Zou et al Nat Rev Immunol 2010[36]

Table 1. Overview of cell surface markers to identify DC subsets in mice.

	Markers *)
cDC1	CD8α / CD103 Clec9a (DNRG1) CD207 (Langerin) XCR1
cDC2	CD4 / CD11b CD172a (SIRPα)
pDCs	B220 Ly6C PDCA.1 Siglec-H
moDCs	FcγRI (CD64) CD14 FcεRI CD11b CD172 (SIRPα) CD206

***) Based on markers listed by Gardner et al[18]**

intracellular bacteria and is involved in autoimmune diseases such as multiple sclerosis and diabetes mellitus. Their development is dependent on transcription factor T-bet, and can be induced by cytokine IL-12[21]. The Th2 subset, developmentally dependent on transcription factor GATA binding protein 3 (GATA3) and induced by cytokine IL-4, mediates protection against helminth infection[21], but also coordinates the characteristic eosinophilic, basophilic and mast cell response in diseases such as allergic asthma[22].

This Th1/Th2 model was challenged when in the early 2000's the Th17 cell was discovered[23]. The Th17 cell is involved in various autoimmune disorders, ranging from psoriasis, inflammatory bowel disease (IBD), rheumatoid arthritis (RA), multiple sclerosis (MS) to systemic lupus erythematosus (SLE)[24, 25]. In order of importance, the cytokines IL-6, IL-1β and TGF-β are relevant for differentiation of naïve T cells into Th17 cells[26], and rely on transcription factor RAR-related orphan receptor gamma (RORγt) for their development[27]. Expansion and survival of Th17 cells are maintained by IL-23[28].

Suppression of excessive immune responses and autoimmune reactions are performed by Tregs, that can be induced from naïve T cells by TGF-β and rely on transcription factor Forkhead box P3 (FoxP3) for their development[29]. Initially, it was thought that only the Th2 subset was important for humoral immunity, until the follicular T helper (Tfh) cell was discovered. It is primarily the Tfh cell that support germinal center B cell responses and plasma cell differentiation[30]. During certain conditions, such as helminth infections, Tfh cells can derive from Th2 cells[31], or the other way around, as has been reported in HDM-driven allergic airway inflammation[32]. This might also be cellular plasticity, which is known to occur for multiple Th-cell subsets[33, 34]. Plasma cells can produce autoreactive antibodies that play a key role in humoral autoimmune diseases such as SLE[35].

Control of the immune system

Homeostasis of the immune system is of crucial importance. During times of foreign pathogens, rapid activation of the immune system is necessary for the extermination of antigens. However, immune cell activation is strictly kept in check, as exaggerated innate and adaptive immune responses can tip the immune system towards autoimmune diseases. The nuclear factor-κB (NF-κB) signaling pathway is a well-studied molecular pathway that promotes cellular activation. The end products of the NF-κB pathway result in a pro-inflammatory milieu, differentiation and cell survival[37]. It also results in transcription of a key regulatory zinc finger (de)ubiquitinating enzyme A20/tumor necrosis factor α-induced protein 3 (TNFAIP3), that is known to contribute largely to the inhibition of NF-κB signaling[38], thereby bringing a balanced halt to inflammation.

A20/TNFAIP3: ubiquitin-modifying enzyme

A20/Tnfaip3 is a ring finger ubiquitin-modifying enzyme, with a dual function being ubiquitination and de-ubiquitination[38]. In the TNFα signaling pathway both functions are utilized to inhibit NF-kB signaling. Briefly, A20/TNFAIP3 removes an activating type of polyubiquitin, (K63–polyubiquitin) from accessory proteins such as RIP1 and NEMO, thereby inhibiting signals to downstream proteins[38]. Furthermore, A20/TNFAIP3 adds an inhibitory type of polyubiquitin (K48-polyubiquitin), to these accessory proteins including RIP1, thereby targeting them for degradation by proteasomes[38].

A20/TNFAIP3 in humans

TNFAIP3 is one of the few genes that has been linked by genome-wide association studies (GWAS) to multiple immune diseases[39, 40]. Single nucleotide polymorphisms (SNPs) in the vicinity of the *TNFAIP3* gene are associated to characteristic autoimmune diseases such as SLE, RA and psoriasis[40]. Over the years, the list of *TNFAIP3* gene SNP-associated clinical diseases keeps expanding, with recent additions of autoimmune hepatitis (AIH), Primary Biliary Cirrhosis (PBC) and colitis ulcerosa (CU)[41-43].

A20/Tnfaip3 in mouse models

The identification of various associations of the *A20/Tnfaip3* gene with diseases has spiked interest of immunologists to study the importance of this gene in cell lines and mouse models. *A20/Tnfaip3* $^{-/-}$ mice develop severe multiorgan inflammation and cachexia, resulting in early death[44]. Cre-LoxP recombination bioengineering made it possible to study cell-specific effects of *A20/Tnfaip3* gene deletion[45]. As an example, *A20/Tnfaip3* deletion in myeloid cells, using LysM-cre, resulted in a spontaneous autoinflammatory disease, characterized by paw inflammation[46]. Furthermore, *A20/Tnfaip3* deletion in B cells using a CD19-cre resulted in a model that resembles SLE[47].

Another key publication in the field was by Kool et al, who utilized a DC-specific cre (CD11c-cre) to ablate *A20/Tnfaip3*[48]. Aged *Tnfaip3*$^{CD11c\text{-}KO}$ mice had activated DCs and developed systemic T and B cell activation. In addition, germinal center B cells, plasma cells and autoantibodies were produced, resulting in an autoimmune phenotype resembling human SLE. Another laboratory used a similar DC-specific *A20/Tnfaip3* deletion strategy, but this resulted in an IBD resembling phenotype[49], indicating that most likely the local microbiome may influence the phenotype.

AIMS AND OUTLINE OF THIS THESIS

The paper by Kool et al.[48] has been the starting point for several chapters in this thesis, which we will touch upon later in our aims. In **chapter 2** we summarize the latest knowledge on A20 as a protein, its molecular function, SNPs associated to human disease, as well as all immune cell-specific conditional deletions of *A20/Tnfaip3* known to date.

Deletion of the *A20/Tnfaip3* gene in all DCs resulted in an SLE[48] or IBD phenotype[49], but it remained unknown which of the DC subsets is mainly responsible for the autoimmune phenotype. To address this issue, we investigated the phenotypic outcome of targeted deletion of A20/*Tnfaip3* in more specific DC subsets. Study of DC ontogeny has revealed several specific markers, such as DNGR1/Clec9a, which are primarily present on cDC1s[50]. In **chapter 3**, we studied the effect of loss of *A20/Tnfaip3* on the activation status of cDCs and moDCs in a *Tnfaip3*$^{DNGR1\text{-}KO}$ mouse model, in which the *Tnfaip3* was mainly deleted in cDC1s. We further analyzed the systemic effects on T cells and B cells that were associated with the activation of these cDCs/moDCs, and explored their immunohistopathology at the age of 31 weeks. Interestingly, while cDC1s were primarily targeted by *A20/Tnfaip3* deletion, cytotoxic $CD8^+$ T cell activation was hardly altered and, unexpectedly, mostly $CD4^+$ T cells and B cells were activated.

The myeloid cell-specific, LysM-cre-driven model of *A20/Tnfaip3* deletion is known to result in an autoinflammatory phenotype with paw inflammation in aged mice[46, 51]. In **chapter 4** we took a step outside of the field of autoimmunity and studied a house-dust mite (HDM)-driven airway inflammation model in *Tnfaip3*$^{LysM\text{-}KO}$ mice. These mice are known to develop a Th17-associated neutrophilic airway inflammation, rather than a Th2-associated eosinophilic airway inflammation[52]. Since neutrophilic recruitment is largely induced by IL-17[53], we wondered whether IL-17RA-signaling was essential for neutrophilic airway inflammation. To determine this, we crossed *Tnfaip3*$^{LysM\text{-}KO}$ mice onto an IL-17RA-signaling knockout background and stimulated the airways with HDM and assessed the responses.

It occurred to us during the study of aged *Tnfaip3*$^{CD11c\text{-}KO}$ mice, that develop an SLE phenotype, that the numbers of B cells were vastly reduced in spleens, pointing to

the possibility that a B cell lineage defect occurred in the bone marrow, resulting in disrupted generation of immature and mature B cell populations. In **chapter 5**, we therefore examined B cell development in the bone marrow of both young 6-week-old mice and 24-week-old *Tnfaip3*$^{CD11c\text{-}KO}$ mice. We further aimed to investigate whether in *Tnfaip3*$^{CD11c\text{-}KO}$ mice mature B cells that were released into the periphery were more responsive and thus more prone to B cell activation or immunoglobulin production than those in wild-type control mice.

B cell activation that is associated with germinal center reactions and plasma cell formation is dependent on help from T cells. In the case of autoimmunity, activated DCs might overly activate T cells, which can positively select autoreactive B cells in pathogenic germinal center reactions[54]. Activated T cells express CD40L which binds CD40 on B cells and thereby provides proliferation and survival signals besides those initiated by B cell receptor (BCR) engagement[55]. Apart from this T cell-dependent response, a T cell-independent activation of B cells by APCs is also known[56, 57]. A20/Tnfaip3-deficient DCs were known to activate B cells independently of T cell help *in vitro*[48]**.** In **chapter 6** we addressed the question whether A20/Tnfaip3-deficient DCs also had the capacity to directly activate B cells *in vivo* and thereby engaged these cells in autoimmune pathology. To this end, we crossed *Tnfaip3*$^{CD11c\text{-}KO}$ mice onto a *CD40lg* deficient background, thereby abrogating T-B cell communication. We also examined whether autoreactive immunoglobulins and kidney remodeling were altered.

It has been demonstrated that stimulated A20/Tnfaip3-deficient DCs *in vitro* have the capacity of highly inducing IL-17 in T cell co-cultures, likely due to elevated production of IL-6 and IL-23[48], both of which are beneficial for their survival. Given the importance of Th17 cells in autoimmune diseases including SLE[58], in **chapter 7** we examined whether IL-23 was dispensable for Th17 homeostasis *in vivo* and cytokine production in the *Tnfaip3*$^{CD11c\text{-}KO}$ SLE mouse model. To achieve this, we crossed *Tnfaip3*$^{CD11c\text{-}KO}$ mice to mice lacking IL-23. Since Th17 cells can stimulate B cells towards class-switched immunoglobulin-producing plasma cells[59], we further examined autoantibody production and kidney remodeling at the age of 24-weeks.

Finally, implications of our work and potential future directions in the field of A20/Tnfaip3 and (auto)immunity are described in **chapter 8.**

REFERENCES

1. Steinman RM. Decisions about dendritic cells: past, present, and future. *Annu Rev Immunol* 2012; 30: 1-22.
2. Bonifaz L, Bonnyay D, Mahnke K, Rivera M, Nussenzweig MC, Steinman RM. Efficient targeting of protein antigen to the dendritic cell receptor DEC-205 in the steady state leads to antigen presentation on major histocompatibility complex class I products and peripheral CD8+ T cell tolerance. *J Exp Med* 2002; 196(12): 1627-1638.
3. Kobayashi KS, van den Elsen PJ. NLRC5: a key regulator of MHC class I-dependent immune responses. *Nat Rev Immunol* 2012; 12(12): 813-820.
4. Joffre OP, Segura E, Savina A, Amigorena S. Cross-presentation by dendritic cells. *Nat Rev Immunol* 2012; 12(8): 557-569.
5. Corthay A. A three-cell model for activation of naive T helper cells. *Scandinavian journal of immunology* 2006; 64(2): 93-96.
6. Steinman RM, Nussenzweig MC. Avoiding horror autotoxicus: the importance of dendritic cells in peripheral T cell tolerance. *Proc Natl Acad Sci U S A* 2002; 99(1): 351-358.
7. Tan JK, O'Neill HC. Maturation requirements for dendritic cells in T cell stimulation leading to tolerance versus immunity. *J Leukoc Biol* 2005; 78(2): 319-324.
8. Lenschow DJ, Walunas TL, Bluestone JA. CD28/B7 system of T cell costimulation. *Annu Rev Immunol* 1996; 14: 233-258.
9. Wikenheiser DJ, Stumhofer JS. ICOS Co-Stimulation: Friend or Foe? *Front Immunol* 2016; 7: 304.
10. Gregersen PK, Behrens TW. Genetics of autoimmune diseases--disorders of immune homeostasis. *Nature reviews Genetics* 2006; 7(12): 917-928.
11. Randolph GJ, Inaba K, Robbiani DF, Steinman RM, Muller WA. Differentiation of phagocytic monocytes into lymph node dendritic cells in vivo. *Immunity* 1999; 11(6): 753-761.
12. Dudziak D, Kamphorst AO, Heidkamp GF, Buchholz VR, Trumpfheller C, Yamazaki S *et al.* Differential antigen processing by dendritic cell subsets in vivo. *Science* 2007; 315(5808): 107-111.
13. Luckashenak N, Schroeder S, Endt K, Schmidt D, Mahnke K, Bachmann MF *et al.* Constitutive crosspresentation of tissue antigens by dendritic cells controls CD8+ T cell tolerance in vivo. *Immunity* 2008; 28(4): 521-532.
14. Schlitzer A, McGovern N, Teo P, Zelante T, Atarashi K, Low D *et al.* IRF4 transcription factor-dependent CD11b+ dendritic cells in human and mouse control mucosal IL-17 cytokine responses. *Immunity* 2013; 38(5): 970-983.
15. Hildner K, Edelson BT, Purtha WE, Diamond M, Matsushita H, Kohyama M *et al.* Batf3 deficiency reveals a critical role for CD8alpha+ dendritic cells in cytotoxic T cell immunity. *Science* 2008; 322(5904): 1097-1100.
16. Plantinga M, Guilliams M, Vanheerswynghels M, Deswarte K, Branco-Madeira F, Toussaint W *et al.* Conventional and monocyte-derived CD11b(+) dendritic cells initiate and maintain T helper 2 cell-mediated immunity to house dust mite allergen. *Immunity* 2013; 38(2): 322-335.
17. Siegal FP, Kadowaki N, Shodell M, Fitzgerald-Bocarsly PA, Shah K, Ho S *et al.* The nature of the principal type 1 interferon-producing cells in human blood. *Science* 1999; 284(5421): 1835-1837.
18. Gardner A, Ruffell B. Dendritic Cells and Cancer Immunity. *Trends Immunol* 2016; 37(12): 855-865.
19. Mosmann TR, Cherwinski H, Bond MW, Giedlin MA, Coffman RL. Two types of murine helper T cell clone. I. Definition according to profiles of lymphokine activities

and secreted proteins. *J Immunol* 1986; 136(7): 2348-2357.
20. Mosmann TR, Coffman RL. TH1 and TH2 cells: different patterns of lymphokine secretion lead to different functional properties. *Annu Rev Immunol* 1989; 7: 145-173.
21. Gagliani N, Huber S. Basic Aspects of T Helper Cell Differentiation. *Methods in molecular biology (Clifton, NJ)* 2017; 1514: 19-30.
22. Robinson DS, Hamid Q, Ying S, Tsicopoulos A, Barkans J, Bentley AM *et al.* Predominant TH2-like bronchoalveolar T-lymphocyte population in atopic asthma. *The New England journal of medicine* 1992; 326(5): 298-304.
23. Park H, Li Z, Yang XO, Chang SH, Nurieva R, Wang YH *et al.* A distinct lineage of CD4 T cells regulates tissue inflammation by producing interleukin 17. *Nat Immunol* 2005; 6(11): 1133-1141.
24. Lubberts E. Th17 cytokines and arthritis. *Seminars in immunopathology* 2010; 32(1): 43-53.
25. Yang J, Sundrud MS, Skepner J, Yamagata T. Targeting Th17 cells in autoimmune diseases. *Trends in pharmacological sciences* 2014; 35(10): 493-500.
26. Ghoreschi K, Laurence A, Yang XP, Tato CM, McGeachy MJ, Konkel JE *et al.* Generation of pathogenic T(H)17 cells in the absence of TGF-beta signalling. *Nature* 2010; 467(7318): 967-971.
27. Ivanov, II, McKenzie BS, Zhou L, Tadokoro CE, Lepelley A, Lafaille JJ *et al.* The orphan nuclear receptor RORgammat directs the differentiation program of proinflammatory IL-17+ T helper cells. *Cell* 2006; 126(6): 1121-1133.
28. Veldhoen M, Hocking RJ, Atkins CJ, Locksley RM, Stockinger B. TGFbeta in the context of an inflammatory cytokine milieu supports de novo differentiation of IL-17-producing T cells. *Immunity* 2006; 24(2): 179-189.
29. Sakaguchi S, Yamaguchi T, Nomura T, Ono M. Regulatory T cells and immune tolerance. *Cell* 2008; 133(5): 775-787.
30. Vinuesa CG, Linterman MA, Yu D, MacLennan IC. Follicular Helper T Cells. *Annu Rev Immunol* 2016; 34: 335-368.
31. Glatman Zaretsky A, Taylor JJ, King IL, Marshall FA, Mohrs M, Pearce EJ. T follicular helper cells differentiate from Th2 cells in response to helminth antigens. *J Exp Med* 2009; 206(5): 991-999.
32. Ballesteros-Tato A, Randall TD, Lund FE, Spolski R, Leonard WJ, León B. T Follicular Helper Cell Plasticity Shapes Pathogenic T Helper 2 Cell-Mediated Immunity to Inhaled House Dust Mite. *Immunity* 2016; 44(2): 259-273.
33. Cannons JL, Lu KT, Schwartzberg PL. T follicular helper cell diversity and plasticity. *Trends Immunol* 2013; 34(5): 200-207.
34. Stadhouders R, Lubberts E, Hendriks RW. A cellular and molecular view of T helper 17 cell plasticity in autoimmunity. *J Autoimmun* 2018; 87: 1-15.
35. Ludwig RJ, Vanhoorelbeke K, Leypoldt F, Kaya Z, Bieber K, McLachlan SM *et al.* Mechanisms of Autoantibody-Induced Pathology. *Front Immunol* 2017; 8: 603.
36. Zou W, Restifo NP. T(H)17 cells in tumour immunity and immunotherapy. *Nat Rev Immunol* 2010; 10(4): 248-256.
37. Liu T, Zhang L, Joo D, Sun SC. NF-kappaB signaling in inflammation. *Signal transduction and targeted therapy* 2017; 2.
38. Wertz IE, O'Rourke KM, Zhou H, Eby M, Aravind L, Seshagiri S *et al.* De-ubiquitination and ubiquitin ligase domains of A20 downregulate NF-kappaB signalling. *Nature* 2004; 430(7000): 694-699.
39. Das T, Chen Z, Hendriks RW, Kool M. A20/Tumor Necrosis Factor alpha-Induced Protein 3 in Immune Cells Controls Development of Autoinflammation and Autoimmunity: Lessons from Mouse Models. *Front Immunol* 2018; 9: 104.

40. Ma A, Malynn BA. A20: linking a complex regulator of ubiquitylation to immunity and human disease. *Nat Rev Immunol* 2012; 12(11): 774-785.
41. Cordell HJ, Han Y, Mells GF, Li Y, Hirschfield GM, Greene CS *et al.* International genome-wide meta-analysis identifies new primary biliary cirrhosis risk loci and targetable pathogenic pathways. *Nat Commun* 2015; 6: 8019.
42. Xu E, Cao H, Lin L, Liu H. rs10499194 polymorphism in the tumor necrosis factor-alpha inducible protein 3 (TNFAIP3) gene is associated with type-1 autoimmune hepatitis risk in Chinese Han population. *PLoS One* 2017; 12(4): e0176471.
43. Jostins L, Ripke S, Weersma RK, Duerr RH, McGovern DP, Hui KY *et al.* Host-microbe interactions have shaped the genetic architecture of inflammatory bowel disease. *Nature* 2012; 491(7422): 119-124.
44. Lee EG, Boone DL, Chai S, Libby SL, Chien M, Lodolce JP *et al.* Failure to regulate TNF-induced NF-kappaB and cell death responses in A20-deficient mice. *Science* 2000; 289(5488): 2350-2354.
45. Maizels N. Genome engineering with Cre-loxP. *J Immunol* 2013; 191(1): 5-6.
46. Matmati M, Jacques P, Maelfait J, Verheugen E, Kool M, Sze M *et al.* A20 (TNFAIP3) deficiency in myeloid cells triggers erosive polyarthritis resembling rheumatoid arthritis. *Nat Genet* 2011; 43(9): 908-912.
47. Tavares RM, Turer EE, Liu CL, Advincula R, Scapini P, Rhee L *et al.* The ubiquitin modifying enzyme A20 restricts B cell survival and prevents autoimmunity. *Immunity* 2010; 33(2): 181-191.
48. Kool M, van Loo G, Waelput W, De Prijck S, Muskens F, Sze M *et al.* The ubiquitin-editing protein A20 prevents dendritic cell activation, recognition of apoptotic cells, and systemic autoimmunity. *Immunity* 2011; 35(1): 82-96.
49. Hammer GE, Turer EE, Taylor KE, Fang CJ, Advincula R, Oshima S *et al.* Expression of A20 by dendritic cells preserves immune homeostasis and prevents colitis and spondyloarthritis. *Nat Immunol* 2011; 12(12): 1184-1193.
50. Schraml BU, van Blijswijk J, Zelenay S, Whitney PG, Filby A, Acton SE *et al.* Genetic tracing via DNGR-1 expression history defines dendritic cells as a hematopoietic lineage. *Cell* 2013; 154(4): 843-858.
51. Vande Walle L, Van Opdenbosch N, Jacques P, Fossoul A, Verheugen E, Vogel P *et al.* Negative regulation of the NLRP3 inflammasome by A20 protects against arthritis. *Nature* 2014; 512(7512): 69-73.
52. Vroman H, Bergen IM, van Hulst JAC, van Nimwegen M, van Uden D, Schuijs MJ *et al.* TNF-alpha-induced protein 3 levels in lung dendritic cells instruct TH2 or TH17 cell differentiation in eosinophilic or neutrophilic asthma. *The Journal of allergy and clinical immunology* 2018; 141(5): 1620-1633. e1612.
53. Jones CE, Chan K. Interleukin-17 stimulates the expression of interleukin-8, growth-related oncogene-alpha, and granulocyte-colony-stimulating factor by human airway epithelial cells. *American journal of respiratory cell and molecular biology* 2002; 26(6): 748-753.
54. Vinuesa CG, Sanz I, Cook MC. Dysregulation of germinal centres in autoimmune disease. *Nat Rev Immunol* 2009; 9(12): 845-857.
55. Casamayor-Palleja M, Feuillard J, Ball J, Drew M, MacLennan IC. Centrocytes rapidly adopt a memory B cell phenotype on co-culture with autologous germinal centre T cell-enriched preparations. *International immunology* 1996; 8(5): 737-744.
56. Xu W, Banchereau J. The antigen presenting cells instruct plasma cell differentiation. *Front Immunol* 2014; 4: 504.
57. Lewis GK, Ranken R, Nitecki DE, Goodman JW. Murine B-cell subpopulations responsive to T-dependent and T-independent antigens. *J Exp Med* 1976; 144(2): 382-397.

58. Furuzawa-Carballeda J, Vargas-Rojas MI, Cabral AR. Autoimmune inflammation from the Th17 perspective. *Autoimmunity reviews* 2007; 6(3): 169-175.
59. Mitsdoerffer M, Lee Y, Jager A, Kim HJ, Korn T, Kolls JK *et al.* Proinflammatory T helper type 17 cells are effective B-cell helpers. *Proceedings of the National Academy of Sciences of the United States of America* 2010; 107(32): 14292-14297.

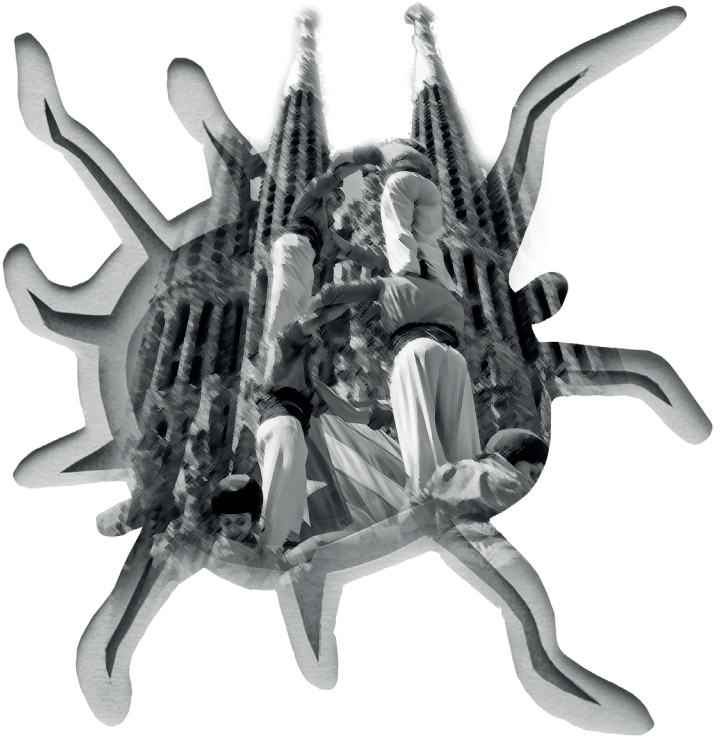

Chapter 2

A20/Tumor Necrosis Factor α-Induced Protein 3 in Immune Cells Controls Development of Autoinflammation and autoimmunity: Lessons from Mouse Models

T. Das, Z. Chen, R.W. Hendriks, M. Kool

Frontiers in Immunology. 2018 Feb 21;9:104

ABSTRACT

Immune cell activation is a stringently regulated process, as exaggerated innate and adaptive immune responses can lead to autoinflammatory and autoimmune diseases. Perhaps the best-characterized molecular pathway promoting cell activation is the nuclear factor-κB (NF-κB) signalling pathway. Stimulation of this pathway leads to transcription of numerous pro-inflammatory and cell-survival genes. Several mechanisms tightly control NF-κB activity, including the key regulatory zinc-finger (de)ubiquitinating enzyme A20/TNFAIP3. Single nucleotide polymorphisms (SNPs) in the vicinity of the *TNFAIP3* gene are associated with a spectrum of chronic systemic inflammatory diseases, indicative of its clinical relevance. Mice harboring targeted cell-specific deletions of the *Tnfaip3* gene in innate immune cells such as macrophages spontaneously develop autoinflammatory disease. When immune cells involved in the adaptive immune response, such as dendritic cells or B-cells, are targeted for A20/TNFAIP3 deletion, mice develop spontaneous inflammation that resembles human autoimmune disease. Therefore, more knowledge on A20/TNFAIP3 function in cells of the immune system is beneficial in our understanding of autoinflammation and autoimmunity. Using the aforementioned mouse models, novel A20/TNFAIP3 functions have recently been described including control of necroptosis and inflammasome activity. In this review, we discuss the function of the A20/TNFAIP3 enzyme, and its critical role in various innate and adaptive immune cells. Lastly, we discuss the latest findings on *TNFAIP3* SNPs in human autoinflammatory and autoimmune diseases and address that genotyping of *TNFAIP3* SNPs may guide treatment decisions.

INTRODUCTION

Autoinflammatory and autoimmune diseases share a spectrum of chronic immune system disorders[1]. Autoinflammatory diseases are rare and occur due to innate immune cell dysfunction with increased cytokines such as IL-1β and TNFα[2,3]. In contrast, autoimmune diseases are caused by adaptive immune system dysfunction and affect millions of people worldwide[4]. Self-reactive T-cells and/or auto-reactive antibodies facilitate responses against harmless tissue[5]. Essential for development of these diseases, is the activation status of immune cells, wherein nuclear factor kappa-light-chain-enhancer of activated B-cells (NF-κB) plays a key role. NF-κB activation is tightly controlled by several mechanisms, including the key regulatory (de)ubiquitinating enzyme A20 or tumor necrosis factor α-induced protein 3 (TNFAIP3)[6]. Genetic studies have demonstrated the association of *TNFAIP3* single nucleotide polymorphisms (SNPs) with multiple human diseases[7], such as systemic lupus erythematosus (SLE)[8-10], rheumatoid arthritis (RA) [9], and Crohn's disease (CD)[11,12]. A20/TNFAIP3 regulates crucial stages in immune cell homeostasis, such as NF-κB activation and apoptosis. Recently new functions have become apparent, including the control of necroptosis and inflammasome activity[13-15]. Here we review the latest understanding of A20/TNFAIP3 as a key regulator of immune signalling and its cell-specific role in the pathogenesis of autoinflammation and autoimmunity as demonstrated in murine models.

1. NF-KB PATHWAY

1.1 NF-κB activation

An important and well-characterized signaling pathway of immune cell activation is the NF-κB pathway[7], which is activated through canonical or non-canonical cascades[16]. The canonical pathway is triggered by several pattern recognition receptors (PRRs), such as Toll-like receptors (TLRs) and nucleotide oligomerization domain (*NOD*)-like *receptors* (NLRs) and cytokine receptors, like tumor necrosis factor receptor (TNFR) and interleukin-1 receptor (IL-1R)[16]. PRRs are essential within the innate immune response in defence against invading pathogens. In addition, T-cell receptor (TCR) or B-cell receptor (BCR) triggering, crucial in the adaptive immune response, also leads to NF-κB activation[17]. In total five NF-κB family members have been identified thusfar, termed p65 (RelA), RelB, c-Rel, NF-κB1, and NF-κB2[18]. These five members can form homo- or heterodimers and distinctive NF-κB dimers bind different DNA-binding sites, resulting in cytokine release, enhanced cell survival, proliferation, differentiation, and changes in metabolism[18,19].

1.2 Regulation of NF-κB activity

Several regulatory mechanisms control NF-κB signaling to maintain tissue homeostasis. One of the proteins that terminate NF-κB signaling is A20/TNFAIP3[6]. A20/TNFAIP3 regulates protein ubiquitination, an important post-translational modification[6]. Ubiquitination is reversible and tightly controlled by opposing actions of ubiquitin ligases and deubiquitinases (DUBs)[20]. Several ubiquitin chains are known, each having specific functions. Lysine (K)48-linked polyubiquitin chains target a protein for proteasomal degradation, whereas K63-linked or linear polyubiquitin chains stabilize protein-protein interactions important for downstream signaling molecules[16]. Interestingly, A20/TNFAIP3 has both DUB and ligase activity to perform both K48-ubiquitination and K63-deubiquitination[6].

2. A20/TNFAIP3

2.1 A20/TNFAIP3 protein structure

In 1990, A20/TNFAIP3 was identified as a primary response gene after TNFα exposure in endothelial cells[21,22]. The structure of A20/TNFAIP3 reveals its dual function (**Figure 1A**). First, the N-terminal OTU domain houses the C103 catalytic cysteine site, responsible for K63-deubiquitination[6,23]. Second, the C-terminal domain ZnF4 domain adds K48-ubiquitin to target proteins for degradation[6]. Both domains cooperate to inhibit NF-κB signaling[24]. Lastly, A20/TNFAIP3 ZnF7 binds linear polyubiquitin, which aids to suppress NF-κB activation[25,26]. To achieve adequate function, A20/TNFAIP3 must bind either target or accessory proteins. The OTU domain binds the target protein TNFR-associated factors (TRAF), while the C-terminus binds accessory molecules like A20-binding protein (ABIN1 and ABIN2), Tax1 Binding Protein 1 (TAX1BP1) and NF-κB essential modulator (NEMO)[27]. These accessory molecules function as adaptor proteins and localize A20/TNFAIP3 near polyubiquitin chains[28-31] (reviewed in [27,32]).

2.2 Function of A20/TNFAIP3 in the TNFR signaling pathway

The multiple functions of A20/TNFAIP3 on NF-κB regulation are most apparent in the TNFR signaling pathway (**Figure 1B**). Briefly, TNFα binding to TNFR recruits receptor-interacting serine/threonine-protein kinase 1 (RIP1) and TRAF2/TRAF5 to shape the TNFR complex[33,34]. RIP1 is K63-polyubiquitinated by ubiquitin-conjugating enzyme (Ubc)13 and cellular inhibitor of apoptosis protein (cIAP)1/2. RIP1-polyubiquitin is a scaffold to recruit NEMO and transforming growth factor beta-activated *kinase* 1 (*TAK1*)-TAB2/3 complex[27]. The linear ubiquitin chain assembly complex (LUBAC) produces linear polyubiquitin on NEMO, recruiting and stabilizing another IKK-NEMO complex[35,36] (**Figure 1B**). TAK1 phosphorylates and activates IκB kinase (IKK), containing IKK2, that

finally phosphorylates IκB[37,38]. Phosphorylated IκB will be K48-polyubiquitined and degradated[19], thereby releasing NF-κB[16] leading to its nuclear translocation.

To terminate NF-κB activation, A20/TNFAIP3 removes K63-polyubiquitin chains from RIP1 and NEMO (**Figure 1B**), thereby disrupting interactions with downstream proteins[6,30]. Furthermore, A20/TNFAIP3 adds K48-polyubiquitin chains to RIP1 and Ubc13, leading to their degradation[6,39]. A20/TNFAIP3 also destabilizes Ubc13 interaction with cIAP1/2 to prevent new K63-ubiquitinating activity[40]. Lastly, the ZnF7 domain of A20/TNFAIP3 binds linear ubiquitin, resulting in dissociation of LUBAC and IKK/NEMO[25,35] and thus inhibits IKK phosphorylation[41].

2.3 Regulation of A20/TNFAIP3 expression and function

A20/TNFAIP3's expression and function is controlled at several levels, e.g. transcriptional, post-transcriptional, and post-translational. During steady state, A20/TNFAIP3 is minimally present in several cell types[27] due to repression by downstream regulatory element antagonist modulator (DREAM)[42]. Transcriptional activation of the *TNFAIP3* gene is facilitated by two NF-κB binding sites in the *TNFAIP3* promoter[43]. *TNFAIP3* promotor activity is also controlled by regulators of cell-instrinsic energy homeostasis such as estrogen-related receptor α (ERRα)[44], linking energy homeostasis to cell activation. The stability of the *TNFAIP3* transcript is regulated by mRNA-binding proteins (e.g. ROQUIN (*Rc3h1*)[45]) and micro-(mi) RNAs, such as miR-125b, miR-19b, miR-29c[46-48]. Interestingly, one of the downstream targets of NF-κB is miR125b, which thereby prolongs NF-κB activity[47]. ROQUIN destabilizes *TNFAIP3* mRNA, leading to lower A20/TNFAIP3 protein expression[45] and mutated ROQUIN is known to induce autoimmunity in mice[49]. Posttranslationally, A20/TNFAIP3 protein function is improved by IKK2-dependent phosphorylation[50] (**Figure 1A**) which enhances K63-deubiquitination and K48-ubiquitination[51]. Also, cell-extrinsic factors control A20/TNFAIP3 protein stability, e.g. high glucose levels target A20/TNFAIP3 for proteasomal degradation and/or reactive oxygen species (ROS) inactivate its deubiquitinating activity[52-54]. Especially the latter is important in RA, in which elevated ROS plays a pathogenic role[55,56], possibly by inhibiting A20/TNFAIP3 function. Lastly, unlike most cell types, resting T-cells constitutively express high levels of A20/TNFAIP3 protein[57], which is degradated after activation by paracaspase MALT1 to facilitate NF-κB translocation[58] (**Figure 1A**).

3. IMMUNE CELL-SPECIFIC DELETION OF A20/*TNFAIP3* IN MICE

A20/TNFAIP3 is critical in inflammation regulation, as mice with germ-line A20/*Tnfaip3*-deletion developed severe multi-organ inflammation and cachexia, resulting in early death[59]. Conditional A20/*Tnfaip3* floxed alleles enabled lineage-specific *Tnfaip3*-deletion and study of cell-specific contributions to autoinflammation and autoimmunity[60].

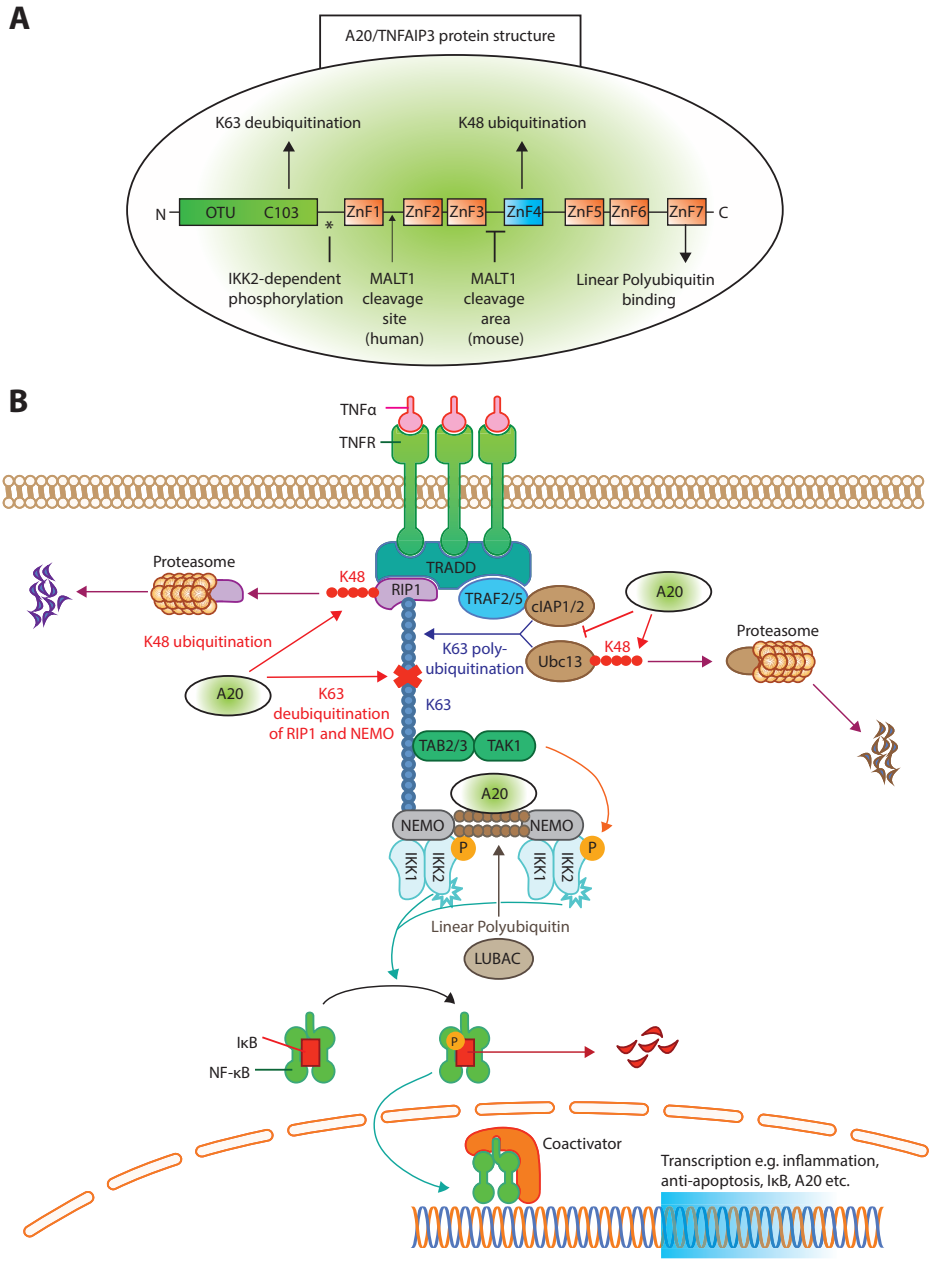

Figure 1: A20/TNFAIP3 protein structure and function in TNFR induced NK-κB inhibition.
(**A**) The protein structure of A20/TNFAIP3. The N-terminus contains the ovarian tumor (OTU) domain, with the C103 cysteine site of K63 deubiquitination. The seven Zinc-Fingers (ZnF) are illustrated, where ZnF4 has K48 ubiquitinating activity and ZnF7 can bind linear polyubiquitin. The asterix (*) indicates the site of IKK2-dependent phosphorylation. An arrow indicates where MALT1 cleaves human A20/TNFAIP3 (after Arginine 439), while for murine A20/TNFAIP3 it is only known that MALT1 cleaves A20/TNFAIP3 between

ZnF3 and ZnF4. (**B**) TNFR activation of the NF-κB pathway. Ligand TNFα binds the TNFR receptor and allows binding of TNFR1-associated death domain protein (TRADD) to the TNFR. This recruits Receptor-interacting serine/threonine-protein kinase 1 (RIP1) and TRAF2 or TRAF5 to form the TNFR complex. RIP1 is K63-polyubiquitinated by E2-E3 ubiquitin-conjugating enzyme (Ubc)13 and cellular inhibitor of apoptosis protein (cIAP)1/2. The polyubiquitin acts as a scaffold for TAB2/TAB3 and *NF-kappa-B essential modulator* (NEMO) to recruit the Transforming growth factor beta-activated *kinase* 1 (*TAK1*)-TAB2/3 complex. TAK1 phosphorylates and activates the IκB Kinase (IKK), composed of IKK1(α), IKK2(β) and NEMO. The linear ubiquitin chain assembly complex (LUBAC), was shown to generate linear polyubiquitin on NEMO (and also RIP1), recruiting and stabilizing another IKK-NEMO complex. IKK2, phosphorylates IκB, allowing IκB K48-polyubiquitination and consequently degrading by proteasomes, thereby releasing NF-κB to translocate to the nucleus. A20/TNFAIP3 acts in different levels of the pathway. A20/TNFAIP3 removes K63-linked polyubiquitin chains from RIP1 and NEMO, thereby disrupting downstream signals. In addition, A20/TNFAIP3 adds K-48-linked polyubiquitin chains to RIP1 and Ubc13, thus targeting them for proteasomal destruction. Beyond (de) ubiquitinating mechanisms, A20/TNFAIP3 also destabilizes Ubc13 interaction with cIAP1/2, thereby preventing new K63-ubiquitinating activity. The ZF7 of A20/TNFAIP3 binds linear ubiquitin, thereby accelerating the dissociation of LUBAC and IKK/NEMO, resulting in NF-κB termination.

3.1 A20/TNFAIP3 function in myeloid cells

To evaluate the role of A20/TNFAIP3 in myeloid cells, *Tnfaip3*$^{fl/fl}$ mice were crossed with lysozyme M (LysM)-cre Tg mice[61], generating *Tnfaip3*^{LysM} mice[13,60,62,63]. The LysM-cre promoter is expressed in ~95-99% of macrophages and neutrophils and ~15% of splenic DCs[61]. *Tnfaip3*$^{LysM\text{-}KO}$ mice developed enthesitis[62] and paw inflammation[63]. While hallmarks of RA comprising increased Th17-cells and serum anti-collagen type II antibodies (anti-CII) were present in *Tnfaip3*$^{LysM\text{-}KO}$ mice, T and B cells were dispensable for paw inflammation[63]. Rather, paw inflammation in *Tnfaip3*$^{LysM\text{-}KO}$ mice depended on IL-1β[13], suggestive of an autoinflammatory disease like Still's disease or juvenile idiopathic arthritis (JIA). *In vitro* cultured *Tnfaip3*-deficient macrophages produced increased amounts of IL-1β, IL-6, IL-18, and TNFα compared to control macrophages[13,63]. IL-1β and IL-18 release is regulated by the NLRP3 inflammasome[64], which is pathogenic in autoinflammatory diseases such as Cryopyrin-associated autoinflammatory syndrome (CAPS)[3,65]. A20/TNFAIP3 directly controls the activity of the NLRP3 inflammasome in macrophages[13,66].

Next, IFNγ or IL-6-induced JAK-STAT signaling is implicated in autoinflammatory diseases[3], which is also regulated by A20/TNFAIP3[62]. *Tnfaip3*-deficient macrophages had elevated STAT1-dependent gene transcription, leading to enhanced chemokine (C-X-C motif) ligand (CXCL)9 and CXCL10 production[62]. Pharmacologic JAK-STAT inhibition by tofacitinib in *Tnfaip3*$^{LysM\text{-}KO}$ mice resulted in reduced enthesitis[62], which is a treatment option for several autoinflammatory diseases[3].

In short, in macrophages A20/TNFAIP3 regulates IL-1β/IL-18 release by controlling NLRP3 inflammasome activity and CXCL9/CXCL10 production through STAT1-signaling. Both pathways are essential in controlling the autoinflammatory arthritis phenotype. However, a role for neutrophils and/or DCs in the pathogenesis of arthritis can not be excluded.

3.2 Function of A20/TNFAIP3 in DCs

DCs play a crucial role in immune homeostasis and arise in two main subsets, comprising conventional DCs type 1 or 2 (cDC1s, cDC2s) and plasmacytoid DCs (pDCs)[67]. When activated, cDCs induce antigen-specific adaptive immune responses and pDCs control anti-viral responses[67]. During inflammation, monocyte-derived DCs (moDCs) are recruited to inflammatory sites[68]. To characterize A20/TNFAIP3 function in DCs *in vivo*, CD11c-cre-mediated[69] targeting was used in mice[70-72]. *Tnfaip3*$^{CD11c\text{-}KO}$ mice had perturbed splenic DC homeostasis as cDC1s, cDC2s, and pDCs were drastically reduced, while moDCs were increased[71]. *In vivo* loss of cDCs and pDCs in *Tnfaip3*$^{CD11c\text{-}KO}$ mice suggested that A20/TNFAIP3 supports their survival. However, *in vitro* generated GM-CSF bone marrow-derived *Tnfaip3*-deficient DCs were more resistant to apoptosis due to upregulated anti-apoptotic molecules[71]. This discrepancy might be caused by contaminating macrophages in GM-CSF-cultures[73]. GM-CSF-cultured DCs from *Tnfaip3*$^{CD11c\text{-}KO}$ mice exhibited an activated phenotype, shown by increased co-stimulatory molecules (e.g. CD80/CD86) and cytokine expression of IL-6, TNFα[70,71], IL-1β and IL-10[71]. In the pathogenesis of SLE, pDCs are pathogenic by secreting type I interferons[74], but increased type I interferon by activated pDCs was observed only *in vitro*[70].

To maintain peripheral tolerance, antigens derived from apoptotic cells are normally not presented in an immunogenic manner to T-cells[75]. Strikingly, *in vitro Tnfaip3*-deficient DCs present these antigens to T-cells and induce T-cell activation[71] leading to a break of tolerance. *In vitro* apoptotic cell-pulsed DCs produce T-cell differentiating cytokines IL-12 and IL-23, leading to increased Th1-cell and Th17-cell differentiation respectively in *Tnfaip3*$^{CD11c\text{-}KO}$ mice[70,71,76]. Surprisingly, three independent studies with *Tnfaip3*$^{CD11c\text{-}KO}$ mice generated different spontaneous phenotypes, i.e. infammatory bowel disease (IBD)[70], systemic autoimmunity resembling SLE[71] and multiorgan inflammation[72]. Serum IL-6 was elevated in mice developing SLE or IBD[70,71], while both TNFα and IFNγ were significantly increased in mice with multiorgan inflammation[72]. As IL-6 depletion ameliorated murine colitis and SLE development[77-80], IL-6 might directly have contributed to IBD and SLE development in *Tnfaip3*$^{CD11c\text{-}KO}$ mice. While CD is recently considered an autoinflammatory disease[81], T-cells were essential for colitis development in *Tnfaip3*$^{CD11c\text{-}KO}$ mice[70]. SLE patients have increased anti-dsDNA autoantibodies[82], which were also observed in *Tnfaip3*$^{CD11c\text{-}KO}$ mice[71]. The diversity of phenotypes observed in *Tnfaip3*$^{CD11c\text{-}KO}$ mice might be due to environmental differences, such as microbiota[70,83], as antibiotics reduced IBD in *Tnfaip3*$^{CD11c\text{-}KO}$ mice[76].

Summarizing, the expression of co-stimulatory molecules, proinflammatory cytokines such as IL-6, and anti-apoptotic proteins in DCs is controlled by A20/TNFAIP3. A20/TNFAIP3 in DCs functions to maintain *in vivo* T-cell and B-cell homeostasis, thereby preventing spontaneous autoinflammation.

3.3 A20/TNFAIP3 functions in T-cells

A20/TNFAIP3 is known to regulate TCR/CD28-mediated NF-κB activation and TCR-mediated survival [84-86], and is highly expressed in naïve T-cells[57]. A20/TNFAIP3's influence on T-cell homeostasis has been examined using maT(mature T cell)-cre and *Cd4*-cre mice, targeting both $CD8^+$ T-cells and $CD4^+$ T-cells[14,15,87]. *Tnfaip3*-deletion efficiency differs between *Tnfaip3*^{maT} and *Tnfaip3*^{CD4} mice. In *Tnfaip3*$^{maT\text{-}KO}$ mice ~80% of $CD8^+$ T-cells and ~30% of $CD4^+$ T-cells are affected[88], whereas in *Tnfaip3*$^{CD4\text{-}KO}$ mice ~100% of both $CD8^+$ and $CD4^+$ T-cells are targeted[89]. Targeted T-cells from both mouse strains showed an activated phenotype[14,87], but only *Tnfaip3*$^{maT\text{-}KO}$ mice developed inflammatory lung and liver infiltrates with increased proportions of $CD8^+$ T-cells[87]. TCR-stimulated $CD8^+$ T-cells from *Tnfaip3*$^{maT\text{-}KO}$ mice had enhanced IL-2 and IFNγ production *in vitro* which correlated with *in vivo* increased serum IFNγ[87]. Serum TNFα and IL-17 were also elevated in *Tnfaip3*$^{maT\text{-}KO}$ mice[87]. Since both IFNγ and TNFα are hepatotoxic factors[90-92], these cytokines likely mediated liver inflammation.

Differences in T-cell specific *Tnfaip3*-deletion between the two mouse strains could indicate that either $CD8^+$ T-cells drive inflammation in *Tnfaip3*$^{maT\text{-}KO}$ mice or $CD4^+$ T-cells have increased regulatory function in *Tnfaip3*$^{CD4\text{-}KO}$ mice. Indeed, regulatory T cell (Treg) proportions were increased in *Tnfaip3*$^{CD4\text{-}KO}$ mice, because of a reduced IL-2 dependence for their development[93]. *In vitro* activated $CD4^+$ T-cells from *Tnfaip3*$^{CD4\text{-}KO}$ mice died quicker than wild-type T-cells[14,15], due to A20/TNFAIP3's control on necroptosis[14] and autophagy[15]. Necroptosis is RIPK3-dependent programmed cell death[94]. Increased necroptosis in A20/*Tnfaip3*-deficient $CD4^+$ T-cells impaired Th1 and Th17-cell differentiation *in vitro*[14]. Interestingly, perinatal death of *Tnfaip3*^{KO} mice was greatly delayed by RIPK3-deficiency, implying that A20/TNFAIP3 may control necroptosis in other cell types[14], such as $CD8^+$ T-cells[95]. Preventing necroptosis did not fully restore survival of A20/*Tnfaip3*-deficient $CD4^+$ T-cells[14], which could be attributed to autophagy, a lysosomal degradation pathway necessary for survival after TCR-stimulation[96]. Autophagy is regulated by mechanistic target of rapamycin (mTOR), which is increased in *Tnfaip3*-deficient $CD4^+$ T-cells after TCR-stimulation[15]. Consequently, treatment with an mTOR inhibitor improves survival by enhancing autophagy[15]. mTOR inhibitors are effective in murine SLE and RA[97], but should not be used in patients with A20/TNFAIP3 alterations, as it may improve pathogenic T-cell survival.

In conclusion, in $CD4^+$ T-cells A20/TNFAIP3 regulates necroptosis and autophagy. In contrast to conventional Th-cells, Treg development is restricted by A20/TNFAIP3. In $CD8^+$ T-cells, A20/TNFAIP3 regulates necroptosis, IL-2 and IFNγ release, of which IFNγ might have contributed to a further undefined lung and liver inflammatory phenotype in *Tnfaip3*$^{maT\text{-}KO}$ mice.

3.4 A20/TNFAIP3 function in B-cells

B-cell homeostasis demands proper integration of TLR, BCR, and CD40-derived signals, all leading to NF-κB activation and controlled by A20/TNFAIP3[98,99]. Using CD19-cre driven *Tnfaip3*-ablation in mice[100-102], B-cell-specific function of A20/TNFAIP3 was examined. *In vitro* activated *Tnfaip3*-deficient B-cells exhibited exaggerated activation as assessed by CD80 and CD95 expression[101,102] and IL-6 production[100,102]. B-cell numbers in *Tnfaip3*$^{CD19\text{-}KO}$ mice are increased in secondary lymphoid organs[100-102], most likely due to increased anti-apoptotic protein B-cell lymphoma-extra large (Bcl-x) expression[102]. Already in 6-week-old *Tnfaip3*$^{CD19\text{-}KO}$ mice, elevated numbers of germinal center B-cells and plasma cells in spleen and peripheral lymph nodes were observed[100-102]. *Tnfaip3*$^{CD19\text{-}KO}$ mice developed autoreactive immunoglobulins, including anti-dsDNA antibodies[100-102] and glomerular immunoglobulin deposits[102], features also observed in SLE patients. Surprisingly, no malignancies developed in *Tnfaip3*$^{CD19\text{-}KO}$ mice[100,102], which might have been expected as A20/TNFAIP3 also functions as a tumor suppressor gene in B-cell lymphomas[103-105].

Summarizing, A20/TNFAIP3 in B-cells controls co-stimulatory molecule expression, IL-6 production, and Bcl-x survival protein expression, thereby preventing autoreactive B-cells formation resulting in an autoimmune SLE phenotype.

4. A20/TNFAIP3 IN AUTOINFLAMMATORY AND AUTOIMMUNE PATIENTS

TNFAIP3 is one of the few genes that has been linked by genome-wide association studies (GWAS) to multiple immune diseases[106,107]. The list of common coding and non-coding variants (SNPs) in the vicinity of the *TNFAIP3* gene region associated with autoimmune conditions keeps expanding, with recently reported associations with autoimmune hepatitis (AIH)[108,109], primary biliary cirrhosis (PBC)[110] and colitis ulcerosa (CU)[111]. Since a comprehensive overview of SNPs within and around the *TNFAIP3* gene has been provided elsewhere[7], we focus on a selection of SNPs with known different functional, clinical, and therapeutical consequences (**Figure 2**). We also discuss a recently described monogenic disease 'Haplo-insufficiency of A20 (HA20)'[112], which clearly illustrates the importance of functional A20/TNFAIP3 protein expression levels (**Figure 2**).

4.1. *TNFAIP3* SNPs and novel mutations affecting A20/TNFAIP3 expression and function

Reduced *TNFAIP3* mRNA expression was observed in peripheral blood mononuclear cells (PBMCs) in SLE and RA patients[113-115] and in disease affected organs, e.g. in colon or skin biopsies from CD and psoriasis patients compared to healthy tissues[116-118].

In RA synovium, reduced A20/TNFAIP3 protein expression was detected compared to non-autoimmune osteoarthritic synovium[119]. SNPs near the *TNFAIP3* gene can result in reduced A20/*TNFAIP3* mRNA expression and consequently protein concentrations. For instance, specific SNPs associated with SLE ("TT>A", **Figure 2H**) are situated in an enhancer region of the *TNFAIP3* gene and hamper DNA-looping, resulting in reduced *TNFAIP3* mRNA expression[120] and reduced A20/TNFAIP3 protein expression in B-cells[8].

Recently, novel rare familial *TNFAIP3* mutations (**Figure 2B,G**) causing HA20 have been described[112]. These mutations lead to severely reduced functional A20/TNFAIP3 protein expression[112,121]. HA20 is a dominantly inherited disease caused by high-penetrance heterozygous germline (mostly nonsense or frameshift) mutations in *TNFAIP3*[112]. Previously, A20/TNFAIP3 loss-of-function mutations were only identified as somatic variants in lymphomas[105] (reviewed in [122]). HA20-associated mutations were first reported in 7 unrelated families with an early-onset inflammatory disease resembling the common polygenic Behçet disease[112]. Some patients diagnosed with Behçet-like disease were found to have similar HA20 mutations[123,124]. Recently, in a Japanese cohort the majority (59%) of HA20 patients did not fulfill criteria of Behçet disease[125], thus carefull evaluation of clinical characteristics of HA20 and Behçet disease will aid disease diagnosis[126]. Also HA20 patients with autoimmune disease were recognized[121] with excess Th17-cell differentiation[126], including autoimmune lymphoproliferative syndrome (ALPS)[127]. All HA20 patients identified thusfar have a strong inflammatory signature as demonstrated by elevated levels of many pro-inflammatory cytokines (e.g. IL-1β, IL-6, TNFα, IL-17, IFNγ) and most patients respond to treatment with cytokine inhibitors (anti-TNF, anti-IL-1)[112,125,126]. Interestingly, *Tnfaip3*$^{+/-}$ mice do not have an overt inflammatory phenotype despite elevated inflammatory cytokines (e.g. IL-1β and IL-6) in serum[128] and brain[129]. Nevertheless, *Tnfaip3*$^{+/-}$ mice are more susceptible to experimental psoriasis[118] and atherosclerosis[128], but these specific symptoms are not commonly reported for HA20. Increased NLRP3 activity was detected in PBMCs of HA20 patients after LPS stimulation, leading to elevated IL-1β[112]. Transfection of mutant truncated A20/TNFAIP3 prolonged NF-κB activation due to reduced deubituinating function[112] (**Figure 2B**). PBMCs of a patient with HA20 also demonstrated prolonged NF-κB activation[112,121]. Mutant truncated A20/TNFAIP3 proteins do not exert a dominant-negative effect on protein function and this indicates that sustained NF-κB activation in HA20 is due to haploinsufficiency rather than an aberrant protein function[112]. It remains unclear whether missense high penetrance mutations may have a different impact on A20/TNFAIP3 function.

Two SNPs, rs5029941 (A125V) and rs2230926 (F127C), are located in close proximity of each other near the C103 catalytic site in the OTU domain and result in nonsynonymous coding changes in the A20/TNFAIP3 protein (**Figure 2D,E**). The rs2230926 (F127C) SNP, associated with multiple autoimmune diseases (**Figure 2E**) hampers A20/TNFAIP3

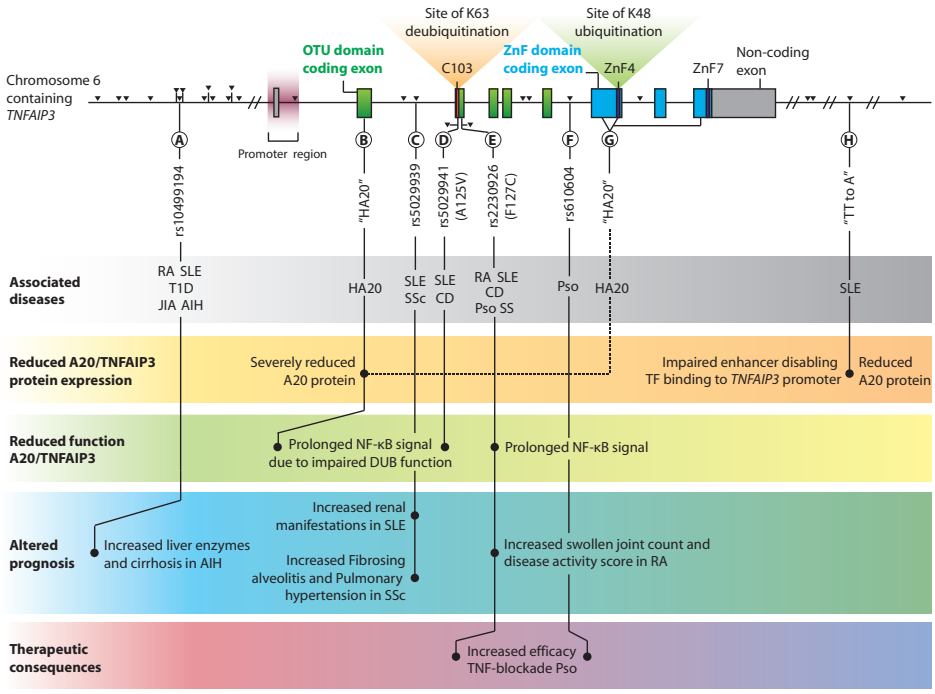

Novel mutations causing HA20				"TT to A"
Mutation	**Location**	**Mutation**	**Location**	
p.Arg45*	OTU	p.Gln415fs	ZnF1	rs148314165
p.Trp85Glyfs*11	OTU	p.Lys417Serfs*4	Between ZnF1-ZnF2	rs200820567
p.Leu227*	OTU	p.Asn449Thrfs*28	Between ZnF1-ZnF2	
p. Phe224Serfs*4	OTU	p.V489Afs*7	ZnF2	
p.Cys243Tyr	OTU	p.Ala588Valfs*80	Between ZnF3-ZnF4	
p.Arg271*	OTU	p.Thr604Argfs*93	ZnF4	
p.Tyr306*	OTU	p.His636Glufs*55	ZnF4	
p.Pro268Leufs*19	OTU	p.Phe637Glu*2	Between ZnF4-ZnF5	
		p.Gln737Serfs*79	ZnF6	

Figure 2: Overview of Single Nucleotide Polymorphisms (SNPs) and novel HA20 mutations in the proximity of *TNFAIP3* which are highlighted in this review

TNFAIP3 gene SNPs, adapted from Ma et al. Nat Rev Immunol; 2012. Exons contributing to the OTU domain are depicted green and exons forming the zinc-finger (ZnF) domains are blue. Non-coding exons are grey. The catalytic C103 site, ZnF4 and ZnF7 are highlighted. Black triangles indicate all known SNPs in the *TNFAIP3*-gene with associations to autoimmune diseases. Among the various documented SNPs/novel mutations, several lead to (1) reduced A20/TNFAIP3 protein level, (2) reduced A20/TNFAIP3 efficiency, (3) altered disease prognosis or (4) therapeutic implications and are thus highlighted in this figure (**A-G**). Known associations to (autoimmune) diseases for SNPs are indicated in the top grey bar. Multiple novel mutations causing "HA20" and two SNPs termed "TT>A" (associated to SLE) are listed in the box in the lower left corner. The reported p.Gln415fs mutation[127], should be reported as p.Lys417Serfs*4 to stay consistent with Human Genome Variation Society nomenclature[142]. Abbreviations: OTU; Ovarian Tumor, ZnF; Zinc Finger, TF; transcription factors, TNFAIP3; HA20; Haploinsufficiency of A20, AIH; autoimmune hepatitis, SLE; systemic lupus erythematosus, SSc; Systemic Sclerosis, RA; Rheumatoid arthritis, T1D; Type 1 Diabetes, JIA; Juvenile Idiopathic Arthritis, CD; Crohn's disease, Pso; Psoriasis, SS; Sjögren syndrome.

function after TNFα-stimulation[10]. The SNP location within the OTU domain (**Figure 2E**) suggests that the K63-deubiquitinating efficacy is decreased, although this was not evaluated. The A125V mutation (**Figure 2D**) results in reduced DUB activity and was shown to impair A20-mediated degradation and deubiquitination of TRAF2[130]. Although the A125V mutation was associated with protection from SLE, surprisingly the same allele was associated with increased risk of IBD[130].

In conclusion, specific SNPs functionally alter A20/TNFAIP3 expression or function and HA20 is a disease with generalized inflammation due to severely reduced functional A20/TNFAIP3 protein expression.

4.2 *TNFAIP3* SNPs affecting disease progression and treatment in patients

Common, presumably hypomorphic, variants in *TNFAIP3* can have clinical consequences. For instance, lower *TNFAIP3* mRNA expression in PBMCs correlates with SLE disease activity as susceptibility to lupus nephritis is increased[113]. SLE or SSc patients with an intron SNP (**Figure 2C**) predisposes for increased risk for either renal involvement[131] or aggravated disease with fibrosing alveolitis and pulmonary hypertension[132]. Similarly, RA patients with a previously described functional SNP (**Figure 2E**) had more swollen joints and increased disease activity scores (DAS28) compared to RA patients without this SNP, indicating worse clinical prognosis[9,115]. Lastly, AIH patients with an upstream SNP (**Figure 2A**) harboured increased liver enzymes and more cirrhosis at disease presentation compared to patients without this SNP[109]. These findings illustrate that within autoimmune patients certain SNPs around the *TNFAIP3* gene predispose a worse clinical prognosis.

Analysis of *TNFAIP3* SNPs might guide treatment choices, e.g. with TNF-blocking therapy. For RA and CD patients, reduced *TNFAIP3* mRNA in PBMCs or colonic biopsies respectively is correlated with effective TNF-blocking therapy[116,133]. Psoriasis patients harbouring specific *TNFAIP3* SNPs (**Figure 2E,F**) respond more effectively to TNF-blockade[134]. This indicates that *TNFAIP3* SNP analysis before TNF-blocking therapy initiation is worthwhile to perform in several autoimmune diseases and may be more practical than evaluating *TNFAIP3* mRNA expression.

4.3 Treatment of autoinflammation and autoimmunity.

Knowledge from cell-specific targeting studies in mice illustrate that loss of A20/TNFAIP3 results in either autoinflammation or autoimmunity. The pathophysiologic distinction between these conditions has therapeutic implications. Autoinflammatory diseases such as Still's disease, Behçet's disease, and most cases of HA20 are well treated with IL-1 blockade, which has only marginal effect in autoimmune diseases including RA[135]. Autoinflammation may also underlie other chronic disorders such as atherosclerosis, as these patients benefit from anti-IL-1 therapy[136,137]. In contrast, autoimmune

disorders (e.g. SLE) have a strong contribution of IL-6 highlighted by successful anti-IL-6 treatment[138]. This is in line with mouse studies in which innate cell activation (e.g. *Tnfaip3*$^{LysM\text{-}KO}$ mice) leads to increased IL-1β[13] and adaptive immune cell activation (e.g. *Tnfaip3*$^{CD19\text{-}KO}$ mice) lead to enhanced IL-6[70,71,100,102]. In line with the adaptive nature of the disease, several autoimmune diseases also improve after treatments targeting adaptive immune cells (e.g. T-cell suppression using cyclosporine[139,140] or B-cell depletion using Rituximab)[141].

CONCLUSION

Control of immune system activation is crucial to prevent both autoinflammation and autoimmunity. A20/TNFAIP3 hereby plays an important role in several innate and adaptive immune cells. Through analysis of cell-specific deletion of A20/*Tnfaip3* in mice, it became apparent that innate myeloid cells require A20/TNFAIP3 to suppress autoinflammation, while the development of autoimmunity is primarily controlled by A20/TNFAIP3 in DCs and B-cells. In addition, novel functions of A20/TNFAIP3 on inflammasome activity and necroptosis are uncovered. It would be of great value to examine in patient material cell-specific profiles of A20/TNFAIP3 and its effector function. The direct consequence of many SNPs on A20/TNFAIP3 is yet unknown. However, it is becoming increasingly clear that specific *TNFAIP3* SNPs can alter A20/TNFAIP3 function, can affect its expression level, or are associated to poor clinical outcomes. Lastly, future studies on *TNFAIP3* SNPs to predict therapeutic effectivity would greatly benefit patient healthcare to obtain personalized therapy.

Acknowledgements

This project was supported by grants from the Dutch Arthritis Association (12-2-410) and European Framework program 7 (FP7-MC-CIG grant 304221).

Conflict of interest

The authors declare no conflict of interest.

REFERENCES

1. McGonagle D, McDermott MF. A proposed classification of the immunological diseases. PLoS medicine 2006;3(8):e297.
2. McDermott MF, Aksentijevich I. The autoinflammatory syndromes. Current opinion in allergy and clinical immunology 2002;2(6):511-6.
3. Peckham D, Scambler T, Savic S, McDermott MF. The burgeoning field of innate immune-mediated disease and autoinflammation. The Journal of pathology 2017;241(2):123-39.
4. Ngo ST, Steyn FJ, McCombe PA. Gender differences in autoimmune disease. Front Neuroendocrinol 2014;35(3):347-69.
5. Ma WT, Chang C, Gershwin ME, Lian ZX. Development of autoantibodies precedes clinical manifestations of autoimmune diseases: A comprehensive review. J Autoimmun 2017.
6. Wertz IE, O'Rourke KM, Zhou H, Eby M, Aravind L, Seshagiri S, et al. De-ubiquitination and ubiquitin ligase domains of A20 downregulate NF-kappaB signalling. Nature 2004;430(7000):694-9.
7. Ma A, Malynn BA. A20: linking a complex regulator of ubiquitylation to immunity and human disease. Nat Rev Immunol 2012;12(11):774-85.
8. Adrianto I, Wen F, Templeton A, Wiley G, King JB, Lessard CJ, et al. Association of a functional variant downstream of TNFAIP3 with systemic lupus erythematosus. Nat Genet 2011;43(3):253-8.
9. Moaaz M, Mohannad N. Association of the polymorphisms of TRAF1 (rs10818488) and TNFAIP3 (rs2230926) with rheumatoid arthritis and systemic lupus erythematosus and their relationship to disease activity among Egyptian patients. Cent Eur J Immunol 2016;41(2):165-75.
10. Musone SL, Taylor KE, Lu TT, Nititham J, Ferreira RC, Ortmann W, et al. Multiple polymorphisms in the TNFAIP3 region are independently associated with systemic lupus erythematosus. Nat Genet 2008;40(9):1062-4.
11. Nair RP, Duffin KC, Helms C, Ding J, Stuart PE, Goldgar D, et al. Genome-wide scan reveals association of psoriasis with IL-23 and NF-kappaB pathways. Nat Genet 2009;41(2):199-204.
12. Indhumathi S, Rajappa M, Chandrashekar L, Ananthanarayanan PH, Thappa DM, Negi VS. TNFAIP3 and TNIP1 polymorphisms confer psoriasis risk in South Indian Tamils. Br J Biomed Sci 2015;72(4):168-73.
13. Vande Walle L, Van Opdenbosch N, Jacques P, Fossoul A, Verheugen E, Vogel P, et al. Negative regulation of the NLRP3 inflammasome by A20 protects against arthritis. Nature 2014;512(7512):69-73.
14. Onizawa M, Oshima S, Schulze-Topphoff U, Oses-Prieto JA, Lu T, Tavares R, et al. The ubiquitin-modifying enzyme A20 restricts ubiquitination of the kinase RIPK3 and protects cells from necroptosis. Nat Immunol 2015;16(6):618-27.
15. Matsuzawa Y, Oshima S, Takahara M, Maeyashiki C, Nemoto Y, Kobayashi M, et al. TNFAIP3 promotes survival of CD4 T cells by restricting MTOR and promoting autophagy. Autophagy 2015;11(7):1052-62.
16. Catrysse L, Vereecke L, Beyaert R, van Loo G. A20 in inflammation and autoimmunity. Trends Immunol 2014;35(1):22-31.
17. Siebenlist U, Brown K, Claudio E. Control of lymphocyte development by nuclear factor-kappaB. Nat Rev Immunol 2005;5(6):435-45.
18. Hoesel B, Schmid JA. The complexity of NF-kappaB signaling in inflammation and cancer. Molecular cancer 2013;12:86.
19. Hayden MS, Ghosh S. NF-kappaB, the first quarter-century: remarkable progress and outstanding questions. Genes Dev 2012;26(3):203-34.

20. Hershko A, Ciechanover A. The ubiquitin system. Annu Rev Biochem 1998;67:425-79.
21. Opipari AW, Jr., Boguski MS, Dixit VM. The A20 cDNA induced by tumor necrosis factor alpha encodes a novel type of zinc finger protein. J Biol Chem 1990;265(25):14705-8.
22. Dixit VM, Green S, Sarma V, Holzman LB, Wolf FW, O'Rourke K, et al. Tumor necrosis factor-alpha induction of novel gene products in human endothelial cells including a macrophage-specific chemotaxin. J Biol Chem 1990;265(5):2973-8.
23. Makarova KS, Aravind L, Koonin EV. A novel superfamily of predicted cysteine proteases from eukaryotes, viruses and Chlamydia pneumoniae. Trends Biochem Sci 2000;25(2):50-2.
24. Lu TT, Onizawa M, Hammer GE, Turer EE, Yin Q, Damko E, et al. Dimerization and ubiquitin mediated recruitment of A20, a complex deubiquitinating enzyme. Immunity 2013;38(5):896-905.
25. Verhelst K, Carpentier I, Kreike M, Meloni L, Verstrepen L, Kensche T, et al. A20 inhibits LUBAC-mediated NF-kappaB activation by binding linear polyubiquitin chains via its zinc finger 7. Embo J 2012;31(19):3845-55.
26. Tokunaga F, Nishimasu H, Ishitani R, Goto E, Noguchi T, Mio K, et al. Specific recognition of linear polyubiquitin by A20 zinc finger 7 is involved in NF-kappaB regulation. Embo j 2012;31(19):3856-70.
27. Shembade N, Harhaj EW. Regulation of NF-kappaB signaling by the A20 deubiquitinase. Cell Mol Immunol 2012;9(2):123-30.
28. Shembade N, Harhaj NS, Liebl DJ, Harhaj EW. Essential role for TAX1BP1 in the termination of TNF-alpha-, IL-1- and LPS-mediated NF-kappaB and JNK signaling. Embo J 2007;26(17):3910-22.
29. Oshima S, Turer EE, Callahan JA, Chai S, Advincula R, Barrera J, et al. ABIN-1 is a ubiquitin sensor that restricts cell death and sustains embryonic development. Nature 2009;457(7231):906-9.
30. Mauro C, Pacifico F, Lavorgna A, Mellone S, Iannetti A, Acquaviva R, et al. ABIN-1 binds to NEMO/IKKgamma and co-operates with A20 in inhibiting NF-kappaB. J Biol Chem 2006;281(27):18482-8.
31. Iha H, Peloponese JM, Verstrepen L, Zapart G, Ikeda F, Smith CD, et al. Inflammatory cardiac valvulitis in TAX1BP1-deficient mice through selective NF-kappaB activation. Embo J 2008;27(4):629-41.
32. Verstrepen L, Verhelst K, van Loo G, Carpentier I, Ley SC, Beyaert R. Expression, biological activities and mechanisms of action of A20 (TNFAIP3). Biochem Pharmacol 2010;80(12):2009-20.
33. Micheau O, Tschopp J. Induction of TNF receptor I-mediated apoptosis via two sequential signaling complexes. Cell 2003;114(2):181-90.
34. Brenner D, Blaser H, Mak TW. Regulation of tumour necrosis factor signalling: live or let die. Nat Rev Immunol 2015;15(6):362-74.
35. Tokunaga F. Linear ubiquitination-mediated NF-kappaB regulation and its related disorders. J Biochem 2013;154(4):313-23.
36. Tokunaga F, Sakata S, Saeki Y, Satomi Y, Kirisako T, Kamei K, et al. Involvement of linear polyubiquitylation of NEMO in NF-kappaB activation. Nat Cell Biol 2009;11(2):123-32.
37. Chen ZJ, Parent L, Maniatis T. Site-specific phosphorylation of IkappaBalpha by a novel ubiquitination-dependent protein kinase activity. Cell 1996;84(6):853-62.
38. Alkalay I, Yaron A, Hatzubai A, Orian A, Ciechanover A, Ben-Neriah Y. Stimulation-dependent I kappa B alpha phosphorylation marks the NF-kappa B inhibitor for degradation via the ubiquitin-proteasome pathway. Proc Natl Acad Sci U S A 1995;92(23):10599-603.
39. Bosanac I, Wertz IE, Pan B, Yu C, Kusam S, Lam C, et al. Ubiquitin binding to A20 ZnF4 is required for modulation of NF-kappaB signaling. Mol Cell 2010;40(4):548-57.

40. Shembade N, Ma A, Harhaj EW. Inhibition of NF-kappaB signaling by A20 through disruption of ubiquitin enzyme complexes. Science 2010;327(5969):1135-9.
41. Skaug B, Chen J, Du F, He J, Ma A, Chen ZJ. Direct, noncatalytic mechanism of IKK inhibition by A20. Mol Cell 2011;44(4):559-71.
42. Tiruppathi C, Soni D, Wang DM, Xue J, Singh V, Thippegowda PB, et al. The transcription factor DREAM represses the deubiquitinase A20 and mediates inflammation. Nat Immunol 2014;15(3):239-47.
43. Krikos A, Laherty CD, Dixit VM. Transcriptional activation of the tumor necrosis factor alpha-inducible zinc finger protein, A20, is mediated by kappa B elements. J Biol Chem 1992;267(25):17971-6.
44. Yuk JM, Kim TS, Kim SY, Lee HM, Han J, Dufour CR, et al. Orphan Nuclear Receptor ERRalpha Controls Macrophage Metabolic Signaling and A20 Expression to Negatively Regulate TLR-Induced Inflammation. Immunity 2015;43(1):80-91.
45. Murakawa Y, Hinz M, Mothes J, Schuetz A, Uhl M, Wyler E, et al. RC3H1 post-transcriptionally regulates A20 mRNA and modulates the activity of the IKK/NF-kappaB pathway. Nat Commun 2015;6:7367.
46. Gantier MP, Stunden HJ, McCoy CE, Behlke MA, Wang D, Kaparakis-Liaskos M, et al. A miR-19 regulon that controls NF-kappaB signaling. Nucleic Acids Res 2012;40(16):8048-58.
47. Kim SW, Ramasamy K, Bouamar H, Lin AP, Jiang D, Aguiar RC. MicroRNAs miR-125a and miR-125b constitutively activate the NF-kappaB pathway by targeting the tumor necrosis factor alpha-induced protein 3 (TNFAIP3, A20). Proc Natl Acad Sci U S A 2012;109(20):7865-70.
48. Wang CM, Wang Y, Fan CG, Xu FF, Sun WS, Liu YG, et al. miR-29c targets TNFAIP3, inhibits cell proliferation and induces apoptosis in hepatitis B virus-related hepatocellular carcinoma. Biochem Biophys Res Commun 2011;411(3):586-92.
49. Vinuesa CG, Cook MC, Angelucci C, Athanasopoulos V, Rui L, Hill KM, et al. A RING-type ubiquitin ligase family member required to repress follicular helper T cells and autoimmunity. Nature 2005;435(7041):452-8.
50. Hutti JE, Turk BE, Asara JM, Ma A, Cantley LC, Abbott DW. IkappaB kinase beta phosphorylates the K63 deubiquitinase A20 to cause feedback inhibition of the NF-kappaB pathway. Mol Cell Biol 2007;27(21):7451-61.
51. Wertz IE, Newton K, Seshasayee D, Kusam S, Lam C, Zhang J, et al. Phosphorylation and linear ubiquitin direct A20 inhibition of inflammation. Nature 2015;528(7582):370-5.
52. Kulathu Y, Garcia FJ, Mevissen TE, Busch M, Arnaudo N, Carroll KS, et al. Regulation of A20 and other OTU deubiquitinases by reversible oxidation. Nat Commun 2013;4:1569.
53. Lee JG, Baek K, Soetandyo N, Ye Y. Reversible inactivation of deubiquitinases by reactive oxygen species in vitro and in cells. Nat Commun 2013;4:1568.
54. Shrikhande GV, Scali ST, da Silva CG, Damrauer SM, Csizmadia E, Putheti P, et al. O-glycosylation regulates ubiquitination and degradation of the anti-inflammatory protein A20 to accelerate atherosclerosis in diabetic ApoE-null mice. PLoS One 2010;5(12):e14240.
55. Di Dalmazi G, Hirshberg J, Lyle D, Freij JB, Caturegli P. Reactive oxygen species in organ-specific autoimmunity. Auto Immun Highlights 2016;7(1):11.
56. Kienhofer D, Boeltz S, Hoffmann MH. Reactive oxygen homeostasis - the balance for preventing autoimmunity. Lupus 2016;25(8):943-54.
57. Tewari M, Wolf FW, Seldin MF, O'Shea KS, Dixit VM, Turka LA. Lymphoid expression and regulation of A20, an inhibitor

of programmed cell death. J Immunol 1995;154(4):1699-706.
58. Coornaert B, Baens M, Heyninck K, Bekaert T, Haegman M, Staal J, et al. T cell antigen receptor stimulation induces MALT1 paracaspase-mediated cleavage of the NF-kappaB inhibitor A20. Nat Immunol 2008;9(3):263-71.
59. Lee EG, Boone DL, Chai S, Libby SL, Chien M, Lodolce JP, et al. Failure to regulate TNF-induced NF-kappaB and cell death responses in A20-deficient mice. Science 2000;289(5488):2350-4.
60. Maizels N. Genome engineering with Cre-loxP. J Immunol 2013;191(1):5-6.
61. Clausen BE, Burkhardt C, Reith W, Renkawitz R, Forster I. Conditional gene targeting in macrophages and granulocytes using LysMcre mice. Transgenic Res 1999;8(4):265-77.
62. De Wilde K, Martens A, Lambrecht S, Jacques P, Drennan MB, Debusschere K, et al. A20 inhibition of STAT1 expression in myeloid cells: a novel endogenous regulatory mechanism preventing development of enthesitis. Ann Rheum Dis 2016.
63. Matmati M, Jacques P, Maelfait J, Verheugen E, Kool M, Sze M, et al. A20 (TNFAIP3) deficiency in myeloid cells triggers erosive polyarthritis resembling rheumatoid arthritis. Nat Genet 2011;43(9):908-12.
64. Agostini L, Martinon F, Burns K, McDermott MF, Hawkins PN, Tschopp J. NALP3 forms an IL-1beta-processing inflammasome with increased activity in Muckle-Wells autoinflammatory disorder. Immunity 2004;20(3):319-25.
65. de Torre-Minguela C, Mesa Del Castillo P, Pelegrin P. The NLRP3 and Pyrin Inflammasomes: Implications in the Pathophysiology of Autoinflammatory Diseases. Front Immunol 2017;8:43.
66. Duong BH, Onizawa M, Oses-Prieto JA, Advincula R, Burlingame A, Malynn BA, et al. A20 restricts ubiquitination of pro-interleukin-1beta protein complexes and suppresses NLRP3 inflammasome activity. Immunity 2015;42(1):55-67.
67. Steinman RM, Hemmi H. Dendritic cells: translating innate to adaptive immunity. Curr Top Microbiol Immunol 2006;311:17-58.
68. Naik SH, Metcalf D, van Nieuwenhuijze A, Wicks I, Wu L, O'Keeffe M, et al. Intrasplenic steady-state dendritic cell precursors that are distinct from monocytes. Nat Immunol 2006;7(6):663-71.
69. Caton ML, Smith-Raska MR, Reizis B. Notch-RBP-J signaling controls the homeostasis of CD8- dendritic cells in the spleen. J Exp Med 2007;204(7):1653-64.
70. Hammer GE, Turer EE, Taylor KE, Fang CJ, Advincula R, Oshima S, et al. Expression of A20 by dendritic cells preserves immune homeostasis and prevents colitis and spondyloarthritis. Nat Immunol 2011;12(12):1184-93.
71. Kool M, van Loo G, Waelput W, De Prijck S, Muskens F, Sze M, et al. The ubiquitin-editing protein A20 prevents dendritic cell activation, recognition of apoptotic cells, and systemic autoimmunity. Immunity 2011;35(1):82-96.
72. Xuan NT, Wang X, Nishanth G, Waisman A, Borucki K, Isermann B, et al. A20 expression in dendritic cells protects mice from LPS-induced mortality. Eur J Immunol 2015;45(3):818-28.
73. Helft J, Bottcher J, Chakravarty P, Zelenay S, Huotari J, Schraml BU, et al. GM-CSF Mouse Bone Marrow Cultures Comprise a Heterogeneous Population of CD11c(+) MHCII(+) Macrophages and Dendritic Cells. Immunity 2015;42(6):1197-211.
74. Crow MK. Advances in understanding the role of type I interferons in systemic lupus erythematosus. Current opinion in rheumatology 2014;26(5):467-74.
75. Cummings RJ, Barbet G, Bongers G, Hartmann BM, Gettler K, Muniz L, et al. Different tissue phagocytes sample apoptotic cells

to direct distinct homeostasis programs. Nature 2016;539(7630):565-69.
76. Liang J, Huang HI, Benzatti FP, Karlsson AB, Zhang JJ, Youssef N, et al. Inflammatory Th1 and Th17 in the Intestine Are Each Driven by Functionally Specialized Dendritic Cells with Distinct Requirements for MyD88. Cell Rep 2016;17(5):1330-43.
77. Cash H, Relle M, Menke J, Brochhausen C, Jones SA, Topley N, et al. Interleukin 6 (IL-6) deficiency delays lupus nephritis in MRL-Faslpr mice: the IL-6 pathway as a new therapeutic target in treatment of autoimmune kidney disease in systemic lupus erythematosus. J Rheumatol 2010;37(1):60-70.
78. Atreya R, Mudter J, Finotto S, Mullberg J, Jostock T, Wirtz S, et al. Blockade of interleukin 6 trans signaling suppresses T-cell resistance against apoptosis in chronic intestinal inflammation: evidence in crohn disease and experimental colitis in vivo. Nat Med 2000;6(5):583-8.
79. Jacob N, Stohl W. Cytokine disturbances in systemic lupus erythematosus. Arthritis Res Ther 2011;13(4):228.
80. Neurath MF. Current and emerging therapeutic targets for IBD. Nat Rev Gastroenterol Hepatol 2017;14(5):269-78.
81. Ciccarelli F, De Martinis M, Ginaldi L. An update on autoinflammatory diseases. Current medicinal chemistry 2014;21(3):261-9.
82. Holman HR, Kunkel HG. Affinity between the lupus erythematosus serum factor and cell nuclei and nucleoprotein. Science 1957;126(3265):162-3.
83. Hammer GE, Ma A. Molecular control of steady-state dendritic cell maturation and immune homeostasis. Annu Rev Immunol 2013;31:743-91.
84. Duwel M, Welteke V, Oeckinghaus A, Baens M, Kloo B, Ferch U, et al. A20 negatively regulates T cell receptor signaling to NF-kappaB by cleaving Malt1 ubiquitin chains. J Immunol 2009;182(12):7718-28.
85. Malewicz M, Zeller N, Yilmaz ZB, Weih F. NF kappa B controls the balance between Fas and tumor necrosis factor cell death pathways during T cell receptor-induced apoptosis via the expression of its target gene A20. J Biol Chem 2003;278(35):32825-33.
86. Shi L, Chen S, Lu Y, Wang X, Xu L, Zhang F, et al. Changes in the MALT1-A20-NF-kappaB expression pattern may be related to T cell dysfunction in AML. Cancer Cell Int 2013;13(1):37.
87. Giordano M, Roncagalli R, Bourdely P, Chasson L, Buferne M, Yamasaki S, et al. The tumor necrosis factor alpha-induced protein 3 (TNFAIP3, A20) imposes a brake on antitumor activity of CD8 T cells. Proc Natl Acad Sci U S A 2014;111(30):11115-20.
88. Roncagalli R, Hauri S, Fiore F, Liang Y, Chen Z, Sansoni A, et al. Quantitative proteomics analysis of signalosome dynamics in primary T cells identifies the surface receptor CD6 as a Lat adaptor-independent TCR signaling hub. Nat Immunol 2014;15(4):384-92.
89. Lee PP, Fitzpatrick DR, Beard C, Jessup HK, Lehar S, Makar KW, et al. A critical role for Dnmt1 and DNA methylation in T cell development, function, and survival. Immunity 2001;15(5):763-74.
90. Bae HR, Leung PS, Tsuneyama K, Valencia JC, Hodge DL, Kim S, et al. Chronic expression of interferon-gamma leads to murine autoimmune cholangitis with a female predominance. Hepatology (Baltimore, Md) 2016;64(4):1189-201.
91. Morita M, Watanabe Y, Akaike T. Protective effect of hepatocyte growth factor on interferon-gamma-induced cytotoxicity in mouse hepatocytes. Hepatology (Baltimore, Md) 1995;21(6):1585-93.
92. Toyonaga T, Hino O, Sugai S, Wakasugi S, Abe K, Shichiri M, et al. Chronic active hepatitis in transgenic mice expressing interferon-gamma in the liver. Proc Natl Acad Sci U S A 1994;91(2):614-8.

93. Fischer JC, Otten V, Kober M, Drees C, Rosenbaum M, Schmickl M, et al. A20 Restrains Thymic Regulatory T Cell Development. J Immunol 2017.
94. He S, Wang L, Miao L, Wang T, Du F, Zhao L, et al. Receptor interacting protein kinase-3 determines cellular necrotic response to TNF-alpha. Cell 2009;137(6):1100-11.
95. Just S, Nishanth G, Buchbinder JH, Wang X, Naumann M, Lavrik I, et al. A20 Curtails Primary but Augments Secondary CD8+ T Cell Responses in Intracellular Bacterial Infection. Sci Rep 2016;6:39796.
96. McLeod IX, Jia W, He YW. The contribution of autophagy to lymphocyte survival and homeostasis. Immunol Rev 2012;249(1):195-204.
97. Thomson AW, Turnquist HR, Raimondi G. Immunoregulatory functions of mTOR inhibition. Nat Rev Immunol 2009;9(5):324-37.
98. Bekeredjian-Ding I, Jego G. Toll-like receptors--sentries in the B-cell response. Immunology 2009;128(3):311-23.
99. Ferch U, zum Buschenfelde CM, Gewies A, Wegener E, Rauser S, Peschel C, et al. MALT1 directs B cell receptor-induced canonical nuclear factor-kappaB signaling selectively to the c-Rel subunit. Nat Immunol 2007;8(9):984-91.
100. Chu Y, Vahl JC, Kumar D, Heger K, Bertossi A, Wojtowicz E, et al. B cells lacking the tumor suppressor TNFAIP3/A20 display impaired differentiation and hyperactivation and cause inflammation and autoimmunity in aged mice. Blood 2011;117(7):2227-36.
101. Hovelmeyer N, Reissig S, Xuan NT, Adams-Quack P, Lukas D, Nikolaev A, et al. A20 deficiency in B cells enhances B-cell proliferation and results in the development of autoantibodies. Eur J Immunol 2011;41(3):595-601.
102. Tavares RM, Turer EE, Liu CL, Advincula R, Scapini P, Rhee L, et al. The ubiquitin modifying enzyme A20 restricts B cell survival and prevents autoimmunity. Immunity 2010;33(2):181-91.
103. Honma K, Tsuzuki S, Nakagawa M, Tagawa H, Nakamura S, Morishima Y, et al. TNFAIP3/A20 functions as a novel tumor suppressor gene in several subtypes of non-Hodgkin lymphomas. Blood 2009;114(12):2467-75.
104. Novak U, Rinaldi A, Kwee I, Nandula SV, Rancoita PM, Compagno M, et al. The NF-{kappa}B negative regulator TNFAIP3 (A20) is inactivated by somatic mutations and genomic deletions in marginal zone lymphomas. Blood 2009;113(20):4918-21.
105. Schmitz R, Hansmann ML, Bohle V, Martin-Subero JI, Hartmann S, Mechtersheimer G, et al. TNFAIP3 (A20) is a tumor suppressor gene in Hodgkin lymphoma and primary mediastinal B cell lymphoma. J Exp Med 2009;206(5):981-9.
106. Dieguez-Gonzalez R, Calaza M, Perez-Pampin E, Balsa A, Blanco FJ, Canete JD, et al. Analysis of TNFAIP3, a feedback inhibitor of nuclear factor-kappaB and the neighbor intergenic 6q23 region in rheumatoid arthritis susceptibility. Arthritis Res Ther 2009;11(2):R42.
107. Vereecke L, Beyaert R, van Loo G. Genetic relationships between A20/TNFAIP3, chronic inflammation and autoimmune disease. Biochemical Society transactions 2011;39(4):1086-91.
108. de Boer YS, van Gerven NM, Zwiers A, Verwer BJ, van Hoek B, van Erpecum KJ, et al. Genome-wide association study identifies variants associated with autoimmune hepatitis type 1. Gastroenterology 2014;147(2):443-52 e5.
109. Xu E, Cao H, Lin L, Liu H. rs10499194 polymorphism in the tumor necrosis factor-alpha inducible protein 3 (TNFAIP3) gene is associated with type-1 autoimmune hepatitis risk in Chinese Han population. PLoS One 2017;12(4):e0176471.
110. Cordell HJ, Han Y, Mells GF, Li Y, Hirschfield GM, Greene CS, et al. International genome-wide meta-analysis identifies

new primary biliary cirrhosis risk loci and targetable pathogenic pathways. Nat Commun 2015;6:8019.
111. Jostins L, Ripke S, Weersma RK, Duerr RH, McGovern DP, Hui KY, et al. Host-microbe interactions have shaped the genetic architecture of inflammatory bowel disease. Nature 2012;491(7422):119-24.
112. Zhou Q, Wang H, Schwartz DM, Stoffels M, Park YH, Zhang Y, et al. Loss-of-function mutations in TNFAIP3 leading to A20 haploinsufficiency cause an early-onset autoinflammatory disease. Nat Genet 2016;48(1):67-73.
113. Li D, Wang L, Fan Y, Song L, Guo C, Zhu F, et al. Down-regulation of A20 mRNA expression in peripheral blood mononuclear cells from patients with systemic lupus erythematosus. J Clin Immunol 2012;32(6):1287-91.
114. Wang Z, Zhang Z, Yuan J, Li LI. Altered TNFAIP3 mRNA expression in peripheral blood mononuclear cells from patients with rheumatoid arthritis. Biomed Rep 2015;3(5):675-80.
115. Zhu L, Wang L, Wang X, Zhou L, Liao Z, Xu L, et al. Characteristics of A20 gene polymorphisms and clinical significance in patients with rheumatoid arthritis. J Transl Med 2015;13:215.
116. Arsenescu R, Bruno ME, Rogier EW, Stefka AT, McMahan AE, Wright TB, et al. Signature biomarkers in Crohn's disease: toward a molecular classification. Mucosal Immunol 2008;1(5):399-411.
117. Bruno ME, Rogier EW, Arsenescu RI, Flomenhoft DR, Kurkjian CJ, Ellis GI, et al. Correlation of Biomarker Expression in Colonic Mucosa with Disease Phenotype in Crohn's Disease and Ulcerative Colitis. Dig Dis Sci 2015;60(10):2976-84.
118. Aki A, Nagasaki M, Malynn BA, Ma A, Kagari T. Hypomorphic A20 expression confers susceptibility to psoriasis. PLoS One 2017;12(6):e0180481.
119. Elsby LM, Orozco G, Denton J, Worthington J, Ray DW, Donn RP. Functional evaluation of TNFAIP3 (A20) in rheumatoid arthritis. Clin Exp Rheumatol 2010;28(5):708-14.
120. Wang S, Wen F, Tessneer KL, Gaffney PM. TALEN-mediated enhancer knockout influences TNFAIP3 gene expression and mimics a molecular phenotype associated with systemic lupus erythematosus. Genes Immun 2016;17(3):165-70.
121. Duncan CJA, Dinnigan E, Theobald R, Grainger A, Skelton AJ, Hussain R, et al. Early-onset autoimmune disease due to a heterozygous loss-of-function mutation in TNFAIP3 (A20). Ann Rheum Dis 2017.
122. Malynn BA, Ma A. A20 takes on tumors: tumor suppression by an ubiquitin-editing enzyme. J Exp Med 2009;206(5):977-80.
123. Ohnishi H, Kawamoto N, Seishima M, Ohara O, Fukao T. A Japanese family case with juvenile onset Behcet's disease caused by TNFAIP3 mutation. Allergology international : official journal of the Japanese Society of Allergology 2017;66(1):146-48.
124. Shigemura T, Kaneko N, Kobayashi N, Kobayashi K, Takeuchi Y, Nakano N, et al. Novel heterozygous C243Y A20/TNFAIP3 gene mutation is responsible for chronic inflammation in autosomal-dominant Behcet's disease. RMD Open 2016;2(1):e000223.
125. Kadowaki T, Ohnishi H, Kawamoto N, Hori T, Nishimura K, Kobayashi C, et al. Haploinsufficiency of A20 causes autoinflammatory and autoimmune disorders. J Allergy Clin Immunol 2017.
126. Aeschlimann FA, Batu ED, Canna SW, Go E, Gul A, Hoffmann P, et al. A20 haploinsufficiency (HA20): clinical phenotypes and disease course of patients with a newly recognised NF-kB-mediated autoinflammatory disease. Ann Rheum Dis 2018.
127. Takagi M, Ogata S, Ueno H, Yoshida K, Yeh T, Hoshino A, et al. Haploinsufficiency of TNFAIP3 (A20) by germline mutation is involved in autoimmune lymphoprolif-

erative syndrome. J Allergy Clin Immunol 2017;139(6):1914-22.

128. Wolfrum S, Teupser D, Tan M, Chen KY, Breslow JL. The protective effect of A20 on atherosclerosis in apolipoprotein E-deficient mice is associated with reduced expression of NF-kappaB target genes. Proc Natl Acad Sci U S A 2007;104(47):18601-6.
129. Guedes RP, Csizmadia E, Moll HP, Ma A, Ferran C, da Silva CG. A20 deficiency causes spontaneous neuroinflammation in mice. Journal of neuroinflammation 2014;11:122.
130. Lodolce JP, Kolodziej LE, Rhee L, Kariuki SN, Franek BS, McGreal NM, et al. African-derived genetic polymorphisms in TNFAIP3 mediate risk for autoimmunity. J Immunol 2010;184(12):7001-9.
131. Bates JS, Lessard CJ, Leon JM, Nguyen T, Battiest LJ, Rodgers J, et al. Meta-analysis and imputation identifies a 109 kb risk haplotype spanning TNFAIP3 associated with lupus nephritis and hematologic manifestations. Genes Immun 2009;10(5):470-7.
132. Dieude P, Guedj M, Wipff J, Ruiz B, Riemekasten G, Matucci-Cerinic M, et al. Association of the TNFAIP3 rs5029939 variant with systemic sclerosis in the European Caucasian population. Ann Rheum Dis 2010;69(11):1958-64.
133. Koczan D, Drynda S, Hecker M, Drynda A, Guthke R, Kekow J, et al. Molecular discrimination of responders and nonresponders to anti-TNF alpha therapy in rheumatoid arthritis by etanercept. Arthritis Res Ther 2008;10(3):R50.
134. Tejasvi T, Stuart PE, Chandran V, Voorhees JJ, Gladman DD, Rahman P, et al. TNFAIP3 gene polymorphisms are associated with response to TNF blockade in psoriasis. J Invest Dermatol 2012;132(3 Pt 1):593-600.
135. Dayer JM, Oliviero F, Punzi L. A Brief History of IL-1 and IL-1 Ra in Rheumatology. Frontiers in pharmacology 2017;8:293.
136. Ridker PM, Everett BM, Thuren T, MacFadyen JG, Chang WH, Ballantyne C, et al. Antiinflammatory Therapy with Canakinumab for Atherosclerotic Disease. The New England journal of medicine 2017;377(12):1119-31.
137. Ridker PM, MacFadyen JG, Thuren T, Everett BM, Libby P, Glynn RJ. Effect of interleukin-1beta inhibition with canakinumab on incident lung cancer in patients with atherosclerosis: exploratory results from a randomised, double-blind, placebo-controlled trial. Lancet (London, England) 2017;390(10105):1833-42.
138. Illei GG, Shirota Y, Yarboro CH, Daruwalla J, Tackey E, Takada K, et al. Tocilizumab in systemic lupus erythematosus: data on safety, preliminary efficacy, and impact on circulating plasma cells from an open-label phase I dosage-escalation study. Arthritis and rheumatism 2010;62(2):542-52.
139. Kronke M, Leonard WJ, Depper JM, Arya SK, Wong-Staal F, Gallo RC, et al. Cyclosporin A inhibits T-cell growth factor gene expression at the level of mRNA transcription. Proc Natl Acad Sci U S A 1984;81(16):5214-8.
140. Szamel M, Bartels F, Resch K. Cyclosporin A inhibits T cell receptor-induced interleukin-2 synthesis of human T lymphocytes by selectively preventing a transmembrane signal transduction pathway leading to sustained activation of a protein kinase C isoenzyme, protein kinase C-beta. Eur J Immunol 1993;23(12):3072-81.
141. Dorner T, Isenberg D, Jayne D, Wiendl H, Zillikens D, Burmester G. Current status on B-cell depletion therapy in autoimmune diseases other than rheumatoid arthritis. Autoimmunity reviews 2009;9(2):82-9.
142. Aksentijevich I, Zhou Q. NF-kappaB Pathway in Autoinflammatory Diseases: Dysregulation of Protein Modifications by Ubiquitin Defines a New Category of Autoinflammatory Diseases. Front Immunol 2017;8:399.

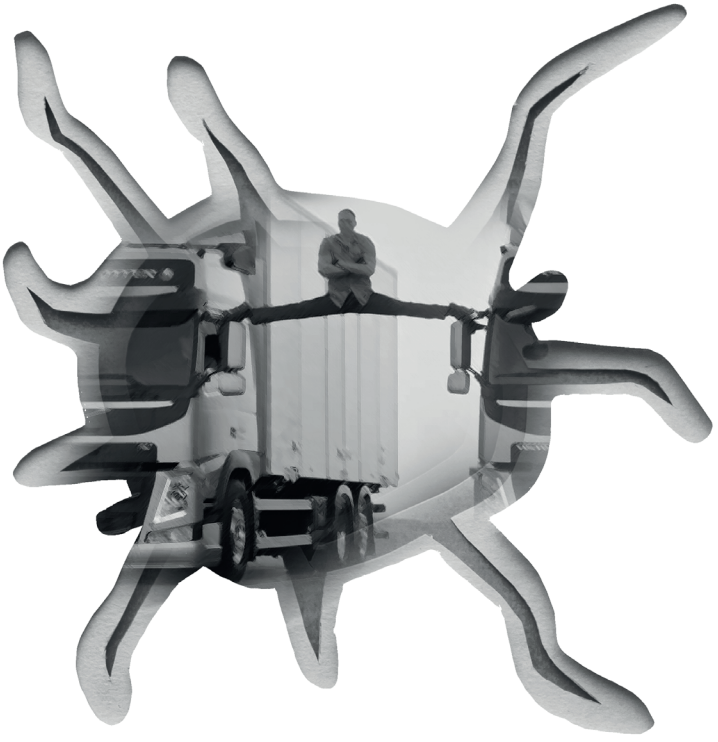

Chapter 3

DNGR1-mediated Deletion of A20/Tnfaip3 in Dendritic Cells Alters T and B-cell Homeostasis and Promotes Autoimmune Liver Pathology

T. Das, I.M. Bergen, T. Koudstaal, J.A.C. van Hulst, G. van Loo, A. Boonstra, T. Vanwolleghem, P.S.C. Leung, M.E. Gershwin, R.W. Hendriks, M. Kool

Journal of Autoimmunity. 2019 Aug;102:167-178.

ABSTRACT

Dendritic cells (DCs) are central regulators of tolerance versus immunity. The outcome depends amongst others on DC subset and activation status. Whereas $CD11b^+$ type 2 conventional DCs (cDC2s) initiate proinflammatory helper T (Th)-cell responses, $CD103^+$ cDC1s are crucial for regulatory T-cell (Treg) induction and $CD8^+$ T-cell activation. DC activation is controlled by the transcription factor NF-κB. Ablation of A20/Tnfaip3, a critical regulator of NF-κB activation, in DCs leads to constitutive DC activation and development of systemic autoimmunity. We hypothesized that the activation status of cDCs controls the development of autoimmunity.

To target cDCs, DNGR1(*Clec9a)*-mediated excision of A20/Tnfaip3 was used through generation of *Tnfaip3*$^{fl/fl}$x*Clec9a*$^{+/cre}$ (*Tnfaip3*$^{DNGR1\text{-}KO}$) mice. Immune cell activation was evaluated at 31-weeks of age.

We found that DNGR1-mediated deletion of A20/Tnfaip3 resulted in liver pathology characterized by inflammatory infiltrates adjacent to the portal triads. Both cDC subsets as well as monocyte-derived DCs (moDCs) in *Tnfaip3*$^{DNGR1\text{-}KO}$ livers harbored an activated phenotype. Specifically, the costimulatory molecule CD40 in liver cDCs and moDCs was regulated by A20/Tnfaip3 expression. Livers from *Tnfaip3*$^{DNGR1\text{-}KO}$ mice had augmented proportions of Th1, Th17, Treg, and follicular Th (Tfh)-cells compared to control mice, accompanied by an increase in IgA-producing plasma cells. Serum IgA from *Tnfaip3*$^{DNGR1\text{-}KO}$ mice recognized self-proteins, specifically cytoplasmic proteins in liver periportal regions.

These data show that enhanced activation of cDCs and moDCs, due to A20/Tnfaip3 ablation, promotes the development of organ-specific autoimmunity but not systemic autoimmunity. This model could be useful to examine the pathobiological processes contributing to autoimmune liver diseases.

1. INTRODUCTION

The adaptive immune response is critically altered in autoimmune diseases, where activation of T-cells is induced by dendritic cells (DCs). DCs are also known as central regulators in the delicate balance between tolerance and immunity[1]. During steady state, immature DCs present self-antigens to T-cells, thereby inducing regulatory $CD4^+$ T-cell (Tregs), T-cell anergy or autoreactive T-cell deletion[2-4]. These mechanisms prevent T-cell mediated autoimmunity[5]. The balance between tolerance and immunity depends on the maturation status of DCs, a process that is strictly regulated[6, 7]. During infections and inflammation, DCs are activated through ligand-receptor interaction on DCs, which initiates the NF-κB pathway is initiated and provokes proinflammatory cytokine production[8]. NF-κB activation is tightly controlled by several mechanisms. One major inhibitor of NF-κB signalling is the ubiquitin-editing enzyme TNFα-induced protein 3 (TNFAIP3) or A20[9]. DC-specific deletion of *Tnfaip3*/A20 using the *Cd11c* promotor in mice (*Tnfaip3*$^{CD11c\text{-}KO}$ mice) resulted in spontaneous activation of DCs and induction of autoreactive $CD4^+$ T helper (Th)1-cells and Th17-cells differentiation, causing a severe and complex autoimmune inflammatory phenotype[10, 11]. *Tnfaip3*$^{CD11c\text{-}KO}$ mice developed features of inflammatory bowel disease[10] (IBD) and systemic lupus erythematosus (SLE)[11]. Importantly, genetic polymorphisms in the *TNFAIP3* gene are associated with several human autoimmune disorders[12, 13].

DCs comprise different subsets with specialized functions[5]. Both conventional DCs (cDCs) and plasmacytoid DCs (pDCs) are present during steady state. $CD103^+$/$CD8^+$ type 1 cDCs (cDC1s) are important for peripheral tolerance as they can present tissue-associated self-antigens[5]. During steady state, cDC1s can induce Tregs[14-16], Th-cell deletion[17], $CD8^+$ T-cell tolerance[17, 18], and once activated, cDC1s also provoke cytotoxic T-cell responses[19]. Strikingly, ablation of cDC1s does not cause spontaneous autoimmunity[19, 20], it only alters intestinal T-cell homeostasis[21]. Under steady state, $CD11b^+$/$CD4^+$ type 2 cDCs (cDC2s) also induce T-cell tolerance[22], and provoke Treg proliferation and differentiation[16, 23]. Activated cDC2s strongly promote Th-cell activation and induce Th-cell differentiation into Th2[24] or Th17-cells[25]. During inflammation, monocyte-derived DCs (moDCs) arise and produce chemokines to attract immune cells to the inflammatory lesion[26].

It is unclear what the contribution of different DC subsets is to the autoimmune phenotype in *Tnfaip3*$^{CD11c\text{-}KO}$ mice. As cDCs are important instructors of T-cell tolerance, we hypothesized that cDCs crucially contribute to the autoimmune phenotype. To determine cDC function, we used DNGR1-driven[27] deletion of *Tnfaip3*/A20 (*Tnfaip3*$^{DNGR1\text{-}KO}$ mice) as DNGR1-driven cre-expression can induce efficient deletion of target genes in ~95% of organ cDC1s, 25-40% of cDC2s, and ~5-25% of moDCs in wildtype mice [27].

2. MATERIAL & METHODS

2.1. Mice

Male and female mice harbouring a conditional *Tnfaip3* allele flanked by LoxP sites[28] were crossed to mice expressing the Cre recombinase under the *Clec9a* promotor (DNGR1)[27], generating *Tnfaip3*$^{fl/fl}$x*Clec9a*$^{+/cre}$ mice (*Tnfaip3*$^{DNGR1\text{-}KO}$ mice). Mice were >10 times back-crossed to obtain a C57Bl/6 background. *Tnfaip3*$^{fl/fl}$x*Clec9a*$^{+/+}$ littermates (*Tnfaip3*$^{DNGR1\text{-}WT}$ mice) served as controls. All mice were sacrificed between 11-31 weeks of age.

To trace Tnfaip3-deletion and function in cDCs, we crossed *Tnfaip3*$^{+/+}$x*Clec9a*$^{+/cre}$ mice to Rosa26-Stop$^{fl/fl}$-YFP mice[29] (*Tnfaip3*$^{DNGR1\text{-}ROSA\text{-}WT}$ mice) and *Tnfaip3*$^{fl/fl}$x*Clec9a*$^{+/cre}$ mice to Rosa26-Stop$^{fl/fl}$-YFP mice (*Tnfaip3*$^{DNGR1\text{-}ROSA\text{-}KO}$ mice). Mice were housed under specific pathogen-free conditions and had ad libitum access to food and water. All experiments were approved by the animal ethical committee of the Erasmus MC, Rotterdam, The Netherlands and comply to the EU Directive 2010/63/EU for animal experiments.

2.2. Cell suspension preparation

Spleen and liver were isolated and used for flow cytometry. Spleens were homogenized through a 100-µm cell strainer. Erythroid cells present in the spleen cell suspensions were lysed using osmotic lysis buffer (8.3% NH_4CL, 1% $KHCO_3$, and 0.04% NA_2EDTA in Milli-Q). Liver single-cell suspensions were obtained, as previously described[30], by digesting with Liberase TM (Roche, Basel, Switzerland) for 30 minutes at 37°C. After digestion, the livers were homogenized using a 100-µm cell strainer (Fischer Scientific). Hepatocytes were discarded using two low speed centrifuge steps. Lastly, erythroid cells were lysed using osmotic lysis buffer.

2.3. Flow cytometry procedures

Flow cytometry surface and intracellular staining procedures have been described previously[31]. Monoclonal antibodies used for flow cytometric analyses are listed in **Supplementary table 1**. For all experiments, dead cells were excluded using fixable Amcyan viability dye (eBioscience, San Diego, CA, USA). To measure cytokine production, cells were stimulated with 10 ng/mL PMA (Sigma-Aldrich, St. Louis, MI, USA) and 250 ng/mL ionomycin (Sigma-Aldrich) in the presence of GolgiStop (BD Biosciences, San Jose, CA, USA) for 4 h at 37°C. Flow cytometry absolute counting beads (Polysciences, Warrington, PA, USA) were added to liver flow cytometry samples. Data were acquired using an LSR II flow cytometer (BD Biosciences) with FACS Diva™ software and analyzed by FlowJo version 9 (Tree Star Inc software, Ashland, OR, USA).

2.4. Liver histology

The right lobe of the liver was fixated with 4% PFA (Carl Roth, Karlsruhe, Germany) for 24 hr before paraffin embedding. Six-µm-thick paraffin embedded liver sections were stained with hematoxylin and eosin, and using Sirius Red (Sigma-Aldrich) and Fast Green (Sigma-Aldrich) to stain for collagen fibers, as previously described[32]. Liver pathology was scored using the histopathologic scoring system according to Ishak et al.[33] For immunohistochemical stainings, antigen retrieval on paraffin-sections was established using citrate buffer (Sigma-Aldrich).

Paraffin sections were stained for Cytokeratin 7, CD3 and B220. The primary antibodies used for immunohistochemistry are listed in **Supplementary table 2**. Sections were incubated for 1 hr with the primary antibodies. After washing, slides were incubated for 30 minutes with secondary antibodies (**Supplementary table 2**). On paraffin sections which were stained for Cytokeratin 7 and CD3, the anti-Rabbit ABC Peroxidase Kit was utilized (Vector Labs, Burlingame, CA, USA). Diaminobenzene (DAB) and Fast Blue Alkaline phosphatase substrates were used to retrieve specific staining.

2.5. Serum measurements

To determine liver function, aspartate aminotransferase (AST) and alanine aminotransferase (ALT) enzymes were measured in serum.

For total immunoglobulin concentrations, Nunc Microwell plates (Life technologies, Carlsbad, CA, USA) were coated with 1 µg/ml goat-anti-mouse IgM, IgA, IgG1, IgG2a, IgG2b, or IgG3 (Southern Biotech, Birmingham, AL, USA) overnight at 4C°. Wells were blocked with 10% FCS (Capricorn Scientific, Ebsdorfergrund, Germany) in PBS (Thermo Scientific, Waltham, MA, USA) for 1 hr. Standards and serum were diluted in PBS and incubated for 3 hrs at room temperature. Depending on the isotype of interest, anti-mouse biotin-labeled IgM, IgA, IgG1, IgG2a, IgG2b, or IgG3 (Southern Biotech) was incubated for 1 hr. Streptavidin-HRP (eBioscience) and TMB substrate (eBioscience) was used to develop the ELISA and then optical density (OD) was measured at 450 nm on a Microplate Reader (Bio-Rad, Hercules, CA, USA).

For detection of anti-cardiolipin antibodies, Nunc Microwell plates were coated with 10 µg/ml cardiolipin from bovine heart (Sigma) in ethanol and left to dry overnight. For detection of dsDNA, 20µg/ml dsDNA from calf thymus (Sigma) was coated overnight on pre-coated poly-l-lysine microwells. Wells were blocked with 2% BSA/PBS for 2 hrs, after which serum was incubated for 2 hrs. Anti-mouse IgG1 biotin/streptavidin-HRP (eBioscience) was used to develop the ELISA with TMB substrate (eBioscience). Detection of immunoglobulin IgG/IgA versus PDC-E2, sp100 and gp210 was performed as previously described[34].

For detection of autoreactive IgA binding to tissues, we used 5µm cryo-sectioned liver and pancreas from $Rag1^{KO}$ mouse[35], as these mice lack mature B-cells and conse-

quently endogenous immunoglobulins are absent. After 10 minutes acetone fixation (Sigma) and 10 minutes block with 10% normal goat serum (NGS), sera from *Tnfaip3*$^{DNGR1\text{-}WT}$ mice (dilution 1/33) and *Tnfaip3*$^{DNGR1\text{-}KO}$ mice (dilution 1/100) were incubated for 1 hr. Different dilutions were used to correct for total IgA concentrations in serum from *Tnfaip3*$^{DNGR1\text{-}WT}$ and *Tnfaip3*$^{DNGR1\text{-}KO}$ mice. Incubation with anti-mouse IgA biotin/streptavidin (BD) and subsequently goat anti-Rat-AP (Sigma), followed by New Fuchsine (Sigma) staining were used to visualize liver-specific IgA. Slides were counterstained with Gills hematoxylin (Sigma).

2.6. Statistics

Statistical significance of data was calculated using the non-parametric Mann Whitney U test. P-values <0.05 were considered significant. All analyses were performed using Prism (GraphPad Software version 9, La Jolla, CA, USA). All data are presented as the mean with the standard error of the mean (SEM).

3. RESULTS

3.1. *Tnfaip3*$^{DNGR1\text{-}KO}$ mice have spontaneous periportal liver infiltrates and signs of chronic inflammation.

To investigate whether immune homeostasis is altered when cDCs harbor a DNGR1-mediated deletion of the A20/*Tnfaip3* gene, we evaluated 31-week-old *Tnfaip3*^{DNGR1} mice. *Tnfaip3*$^{DNGR1\text{-}KO}$ mice had splenomegaly and hyper cellularity in contrast to *Tnfaip3*$^{DNGR1\text{-}WT}$ littermate controls (**Supplementary Figure 1A**). Splenic DC and T-cell numbers did not differ between *Tnfaip3*$^{DNGR1\text{-}KO}$ mice and *Tnfaip3*$^{DNGR1\text{-}WT}$ mice (**Supplementary Figure 1B-C**). Mainly marginal zone B-cells contributed to the increase of total splenic B-cells numbers in *Tnfaip3*$^{DNGR1\text{-}KO}$ mice compared to *Tnfaip3*$^{DNGR1\text{-}WT}$ mice (**Supplementary Figure 1D**).

We next evaluated kidneys, pancreas, intestines, and livers in 31-week-old *Tnfaip3*$^{DNGR1\text{-}KO}$ mice for signs of inflammation. Spleens of *Tnfaip3*$^{DNGR1\text{-}KO}$ mice showed mild architectural changes of the white pulp lymphoid follicles in comparison to WT mice (**Supplementary Figure 2A**). Pancreas, terminal ileum, colon, and kidneys of *Tnfaip3*$^{DNGR1\text{-}KO}$ mice did not show any sign of inflammation or remodelling (**Supplementary Figure 2B-E**). In contrast, livers of all *Tnfaip3*$^{DNGR1\text{-}KO}$ mice showed periportal inflammatory infiltrates at 31-weeks of age compared to WT mice (**Figure 1A/B**). Mild interface hepatitis (also known as piecemeal necrosis) and focal necrosis with inflammation, that are often seen in autoimmune hepatitis (AIH)[36], could also be observed *Tnfaip3*$^{DNGR1\text{-}KO}$ mice, but not in WT mice (**Figure 1C/D**). Mild liver fibrosis also occurred around portal triads of *Tnfaip3*$^{DNGR1\text{-}KO}$ mice compared to controls (**Figure 1E/F**). These features resulted in

a significantly higher liver histopathologic score for *Tnfaip3*$^{DNGR1\text{-}KO}$ mice compared to WT mice (**Figure 1G**). Also increased cytokeratin 7 expression, a protein expressed in bile ducts and indicative for ductular reaction, could be observed in *Tnfaip3*$^{DNGR1\text{-}KO}$ mice compared to littermate controls (**Figure 1H**). Furthermore, a mild, but significant, in-

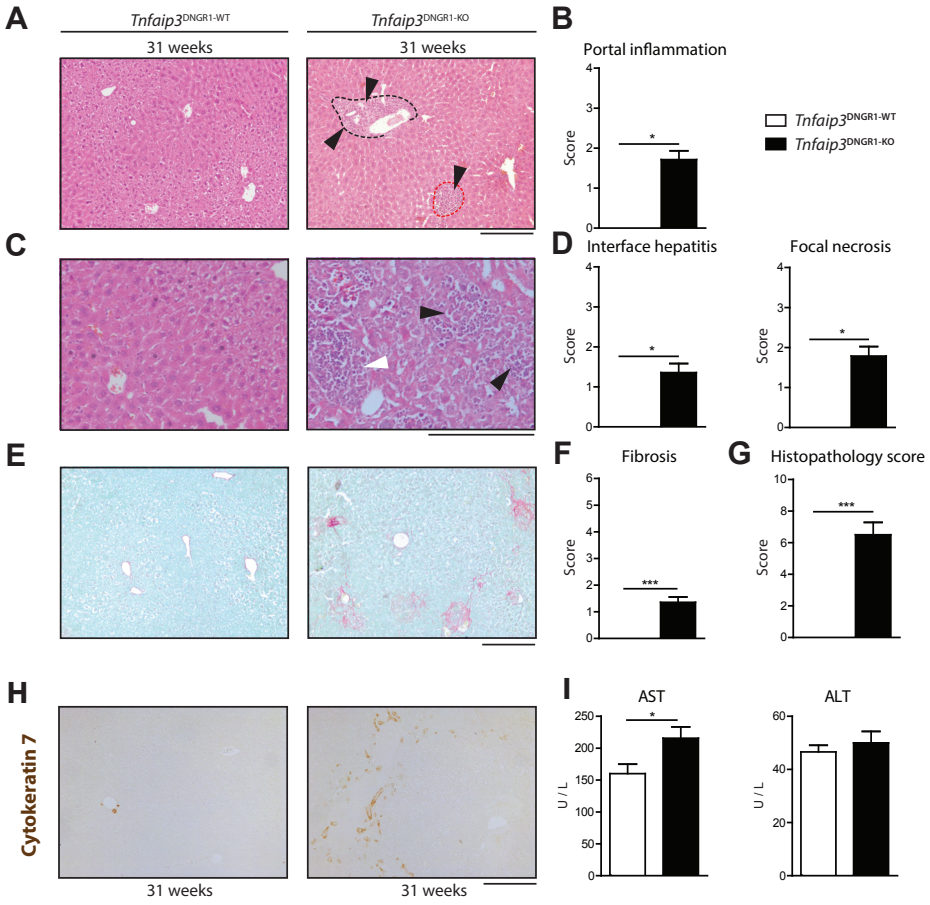

Figure 1: *Tnfaip3*$^{DNGR1\text{-}KO}$ mice have spontaneous periportal liver infiltrates and signs of chronic inflammation.

Tnfaip3$^{DNGR1\text{-}WT}$ mice and *Tnfaip3*$^{DNGR1\text{-}KO}$ mice were analyzed at 31-weeks of age. (A) Hematoxylin and eosin (H&E) stained liver histology with periportal infiltrates (black dashed line) and lobular infiltrates (red dashed line). (B) Quantification of the portal inflammation score (max. 4). (C) Larger magnification H&E stained liver histology indicating areas of interface hepatitis (white arrow) and focal necrosis with inflammation (black arrows). (D) Quantified interface hepatitis and focal necrosis with inflammation score (max. 4). (E-F) Sirius Red staining to stain collagen fibers (E) and enumeration of the resulting fibrosis score (max. 6) (F). (G) Quantification of the total histopathology score (max. 18). (H) Immunohistochemistry of livers for Cytokeratin 7 (brown). (I) Quantification of serum liver enzymes AST and ALT in 31-week-old *Tnfaip3*$^{DNGR1\text{-}WT}$ mice and *Tnfaip3*$^{DNGR1\text{-}KO}$ mice. Scale bars represent 200 µm. Results of pooled data from 3 experiments and are presented as mean ± SEM of $n = 15$ mice per group. $^{*}P < 0.05$, $^{***}P < 0.001$.

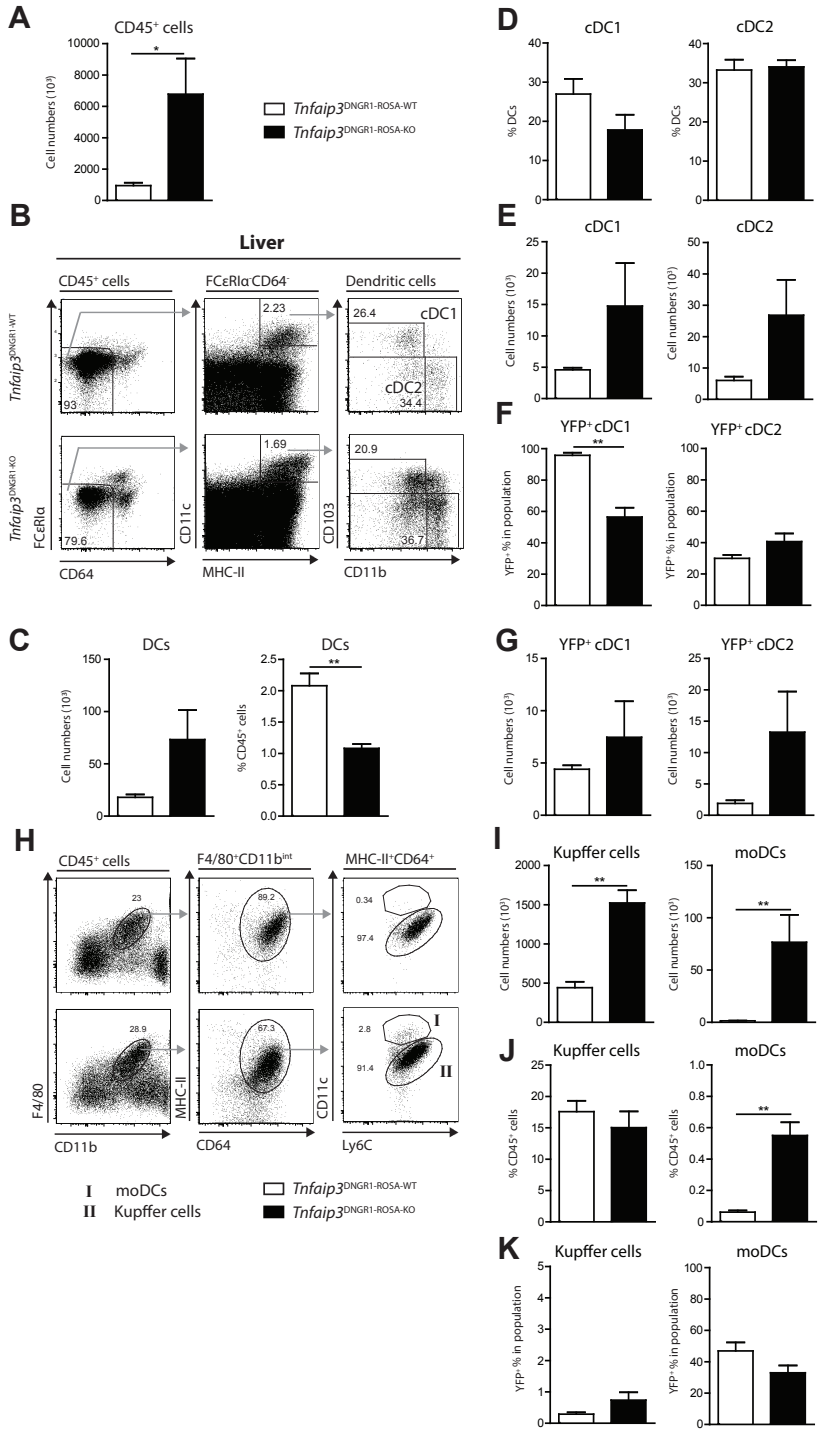

Figure 2: DNGR1-mediated deletion of A20/*Tnfaip3* targets both cDCs and mo-DCs

Tnfaip3$^{DNGR1\text{-}ROSA\text{-}WT}$ mice and *Tnfaip3*$^{DNGR1\text{-}ROSA\text{-}KO}$ mice were analyzed at 31-weeks of age. (A) Enumeration of liver CD45$^+$ cells. (B) Flow cytometric gating strategy of liver cDC1s (CD103$^+$ CD11b$^-$CD11c^{hi}MHC-II^{hi}FcεRIα$^-$CD64$^-$) and cDC2s (CD11b$^+$CD103$^-$CD11c^{hi}MHC-II^{hi}FcεRIα$^-$CD64$^-$). Representative flow cytometry examples are shown from *Tnfaip3*$^{DNGR1\text{-}ROSA\text{-}WT}$ mice and *Tnfaip3*$^{DNGR1\text{-}ROSA\text{-}KO}$ mice. (C) Total DC number and proportion of CD45$^+$ cells. (D-G) Quantification of cDC1s and cDC2s as a proportion of liver DCs (D), cell numbers (E), proportion of YFP$^+$ expressing cells (F) and the YFP$^+$ cell numbers (G). (H) Flow cytometric gating strategy of liver Kupffer cells (F4/80$^+$CD11b^{int}MHC-II^{hi}CD64$^+$CD11c$^{lo/int}$) and moDCs (F4/80$^+$CD11b^{int}MHC-II^{hi}CD64$^+$CD11c^{hi}) in *Tnfaip3*$^{DNGR1\text{-}WT}$ mice and *Tnfaip3*$^{DNGR1\text{-}KO}$ mice. (I-K) Quantification of Kupffer cell and moDC numbers (I), proportion of CD45$^+$ hematopoietic cells (J), and proportion of YFP$^+$ expressing cells (K) using flow cytometry. Representative data is shown from one experiment of 2 independent experiments. Results are presented as mean ± SEM of n = 4-7 mice per group. *P<0.05, **P<0.01.

crease in serum aspartate aminotransferase (AST) was observed in *Tnfaip3*$^{DNGR1\text{-}KO}$ mice compared to WT controls (**Figure 1I**). No differences were observed between male or female *Tnfaip3*$^{DNGR1\text{-}KO}$ mice (data not shown).

Summarizing, these data illustrate that aged *Tnfaip3*$^{DNGR1\text{-}KO}$ mice develop a spontaneous liver pathology characterized by the presence of periportal inflammatory infiltrates and signs of chronic inflammation.

3.2. DNGR1-mediated deletion of A20/*Tnfaip3* targets both cDCs and mo-DCs.

In line with histological findings, the total number of liver CD45$^+$ hematopoietic cells was increased in *Tnfaip3*$^{DNGR1\text{-}ROSA\text{-}KO}$ mice compared to *Tnfaip3*$^{DNGR1\text{-}ROSA\text{-}WT}$ mice (**Figure 2A**). Within liver CD45$^+$ cells, we determined the different DC subsets (**Figure 2B**). The proportion of DCs from total CD45$^+$ cells was lower in *Tnfaip3*$^{DNGR1\text{-}ROSA\text{-}KO}$ mice compared to *Tnfaip3*$^{DNGR1\text{-}ROSA\text{-}WT}$ mice, but total liver DC numbers were not significantly different (**Figure 2C**). Conventional DC1s and cDC2s were neither significantly altered as proportions of DCs nor in cell numbers between the two genotypes (**Figure 2D/E**). To investigate DNGR1-cre mediated deletion efficiency and the effect of A20/Tnfaip3 ablation on liver cDC homeostasis, we examined *Tnfaip3*$^{DNGR1\text{-}ROSA\text{-}WT}$ mice and *Tnfaip3*$^{DNGR1\text{-}ROSA\text{-}KO}$ mice, in which YFP expression can be used as a lineage tracer of DNGR1 expression. DNGR1-lineage tracing studies revealed that DNGR1-mediated cre-recombinase activity targeted almost all mature cDC1s and ~30% of cDC2s. As mature cDC2s do not express DNGR1[27], this ~30% deletion is caused by DNGR1-cre efficacy in cDC progenitors, which do express DNGR1 although to a lower extent[27]. Similar to other organs[27], in livers of *Tnfaip3*$^{DNGR1\text{-}ROSA\text{-}WT}$ mice ~95% of cDC1s showed YFP expression, which was reduced to ~55% in *Tnfaip3*$^{DNGR1\text{-}ROSA\text{-}KO}$ mice (**Figure 2F**). YFP expression in liver cDC2s did not differ between *Tnfaip3*$^{DNGR1\text{-}ROSA\text{-}WT}$ mice and *Tnfaip3*$^{DNGR1\text{-}ROSA\text{-}KO}$ mice and remained ~35% (**Figure 2F**). The absolute number of YFP$^+$ cDC1s was similar between *Tnfaip3*$^{DNGR1\text{-}ROSA\text{-}WT}$ mice and *Tnfaip3*$^{DNGR1\text{-}ROSA\text{-}KO}$ mice (**Figure 2G**). Plasmacytoid DCs in liver were unaffected by DNGR1-mediated deletion (~2% YFP$^+$; data not shown). We next determined Kupffer cells and monocyte-derived DCs (moDCs) (**Figure 2H**). The total number of both Kupffer

cells and moDCs was increased in *Tnfaip3*$^{DNGR1\text{-}KO}$ mice compared to *Tnfaip3*$^{DNGR1\text{-}WT}$ mice (**Figure 2I**). While Kupffer cell proportions of CD45^{+} cells were similar, moDCs significantly expanded as a proportion of CD45^{+} cells in *Tnfaip3*$^{DNGR1\text{-}KO}$ mice compared to littermate controls (**Figure 2J**). YFP expression was almost absent in Kupffer cells (<1%) in both genotypes (**Figure 2K**). Liver moDCs, albeit present in low numbers in *Tnfaip3*$^{DNGR1\text{-}ROSA\text{-}WT}$ mice, harbored a slightly higher YFP expression WT mice (~45%) compared to and in *Tnfaip3*$^{DNGR1\text{-}ROSA\text{-}WT}$ and *Tnfaip3*$^{DNGR1\text{-}ROSA\text{-}KO}$ mice (~30%) (**Figure 2K**).

Concluding, DNGR1-lineage tracing indicated that in livers of control mice respectively 95% and 35% of cDC1s and cDC2s, as well as 45% of moDCs express or once expressed DNGR1. Furthermore, due to deletion of A20/Tnfaip3 55% and 35% of liver cDC1s and cDC2s, along with 30% of liver moDCs were affected by DNGR1-targeting.

3.3. Surface CD40 expression is increased through both cell-intrinsic and cell-extrinsic effects of Tnfaip3-deficiency in cDC1s, cDC2s, and moDCs.

In livers of *Tnfaip3*$^{DNGR1\text{-}KO}$ mice, both cDC1s and cDC2s showed significantly enhanced surface expression of the costimulatory molecule CD40 compared to *Tnfaip3*$^{DNGR1\text{-}WT}$ mice (**Figure 3A/B**). In *Tnfaip3*$^{DNGR1\text{-}WT}$ mice, expression of the co-inhibitory molecule PD-L1 was higher in cDC2s than in cDC1s (**Figure 3B**). Both cDC1s and cDC2s in *Tnfaip3*$^{DNGR1\text{-}KO}$ mice significantly increased PD-L1 expression in comparison to *Tnfaip3*$^{DNGR1\text{-}WT}$ mice (**Figure 3A/B**). No differences were observed for MHC-I or MHC-II expression in cDCs (data not shown).

We next analyzed whether the altered co-stimulatory molecule expression was a direct consequence of A20/Tnfaip3-deletion, and compared YFP^{+} and YFP^{-} cDCs, indicative of A20/Tnfaip3-deficient or A20/Tnfaip3-sufficient cDCs respectively in Tnfaip3$^{DNGR1\text{-}ROSA\text{-}KO}$ mice. YFP^{+} cDC1s and YFP^{+} cDC2s from *Tnfaip3*$^{DNGR1\text{-}ROSA\text{-}KO}$ mice harboured significantly higher CD40 expression in comparison to YFP^{-} cDCs within the same livers (**Figure 3C**), whereas PD-L1 expression was similar in YFP^{+} and YFP^{-} cDC1s/cDC2s from *Tnfaip3*$^{DNGR1\text{-}ROSA\text{-}KO}$ mice (**Figure 3D**). CD40 and PD-L1 expression was already enhanced on YFP-negative Tnfaip3-sufficient cDC1s/cDC2s from *Tnfaip3*$^{DNGR1\text{-}ROSA\text{-}KO}$ mice compared to Tnfaip3-sufficient cDC1s/cDC2s in *Tnfaip3*$^{DNGR1\text{-}ROSA\text{-}WT}$ mice (**Figure 3C/D**). CD40 expression on liver moDCs did not differ between *Tnfaip3*$^{DNGR1\text{-}KO}$ mice and WT controls (**Figure 3E/F**). In contrast, YFP^{+} moDCs of *Tnfaip3*$^{DNGR1\text{-}ROSA\text{-}KO}$ mice showed a higher CD40 expression than YFP^{-} moDCs (**Figure 3G/H**). Liver moDCs also harboured higher PD-L1 expression in *Tnfaip3*$^{DNGR1\text{-}KO}$ mice compared to *Tnfaip3*$^{DNGR1\text{-}WT}$ controls (**Figure 3E/F**), but this did not differ between YFP^{+} or YFP^{-} moDCs in *Tnfaip3*$^{DNGR1\text{-}ROSA\text{-}KO}$ mice (**Figure 3G/H**).

In summary, both liver cDC1s and cDC2s of *Tnfaip3*$^{DNGR1\text{-}KO}$ mice show an activated phenotype, e.g. increased CD40 and PD-L1 expression, irrespective of Tnfaip3 deletion. Only CD40 expression is specifically enhanced due to cell-intrinsic loss of Tnfaip3. Liver moDCs of *Tnfaip3*$^{DNGR1\text{-}KO}$ mice show elevated PD-L1 expression compared to

Tnfaip3$^{DNGR1\text{-}WT}$ mice. Strikingly, enhanced CD40 expression is specifically observed in *Tnfaip3*-deficient moDCs.

3.4. Livers of *Tnfaip3*$^{DNGR1\text{-}KO}$ mice have increased proportions of Th1-cells, Th17-cells and Tregs.

The proportion of CD8$^+$ T-cells and natural killer (NK)-cells within CD45$^+$ cells were elevated in the livers of *Tnfaip3*$^{DNGR1\text{-}KO}$ mice compared to control mice (**Figure 4A**). The percentage of CD4$^+$ Th-cells and neutrophils were reduced in *Tnfaip3*$^{DNGR1\text{-}KO}$ mice compared to *Tnfaip3*$^{DNGR1\text{-}WT}$ controls (**Figure 4A**). Liver F4/80$^+$ macrophages and Kupffer cells, monocytes, and B-cell percentages were not significantly different (**Figure 4A**). Due to an increase in absolute numbers of CD45$^+$ hematopoietic cells (**Figure 2A**), the total number of CD8$^+$ T-cells, CD4$^+$ Th-cells, and B-cells were significantly increased in *Tnfaip3*$^{DNGR1\text{-}KO}$ mice compared to controls (**Figure 4B**). Clusters of T-cells and B-cells were observed in the periportal infiltrates of *Tnfaip3*$^{DNGR1\text{-}KO}$ mice, while only occasionally among hepatocytes in *Tnfaip3*$^{DNGR1\text{-}WT}$ mice (**Figure 4C**). In *Tnfaip3*$^{DNGR1\text{-}KO}$ mice, the majority of inflammatory lesions in the portal triads consisted of T-cells only (**Figure 4C**). In addition, clusters of DCs and CD8$^+$ T-cells were localised in periportal infiltrates in *Tnfaip3*$^{DNGR1\text{-}KO}$ mice, compared to sparsely located DCs and CD8$^+$ T-cells in control mice (**Supplementary Figure 3A**). DNGR1$^+$ cells, most likely cDC1s, were also localised within these periportal infiltrates of *Tnfaip3*$^{DNGR1\text{-}KO}$ mice (**Supplementary Figure 3B**).

The percentage of effector CD44$^+$ CD8$^+$ T-cells was increased in *Tnfaip3*$^{DNGR1\text{-}KO}$ mice compared to WT controls, however the percentage of granzyme B or interferon gamma (IFNγ)-positive CD8$^+$ T-cells was unaltered (**Supplementary Figure 4**). No differences were observed in the proportions of CD44$^+$ effector liver Th-cells (**Figure 4D**), but the proportions of liver Foxp3$^+$CD25$^+$ Tregs were augmented in *Tnfaip3*$^{DNGR1\text{-}KO}$ mice in comparison to WT mice (**Figure 4E**). Increased percentages of IFNγ single-positive, IFNγ/IL-10 double-producing, and IL-17A single-positive Th-cells were found in livers of *Tnfaip3*$^{DNGR1\text{-}KO}$ mice compared to WT mice (**Figure 4F/G/H**). No differences were observed in IL-10 single-positive Th-cells (**Figure 4G**). Interleukin-12-positive cells could also be observed within the periportal infiltrates in *Tnfaip3*$^{DNGR1\text{-}KO}$ mice (**Supplementary Figure 3C**).

In summary, liver CD8$^+$ T-cells, Th-cells, and B-cells in *Tnfaip3*$^{DNGR1\text{-}KO}$ mice increase in number due to a total increase in hematopoietic cells and they accumulate in the periportal regions. Th-cells within livers from *Tnfaip3*$^{DNGR1\text{-}KO}$ mice showed augmented proportions of IFNγ and IL-17A single-producing Th-cells and IFNγ/IL-10 double-producing Th-cells.

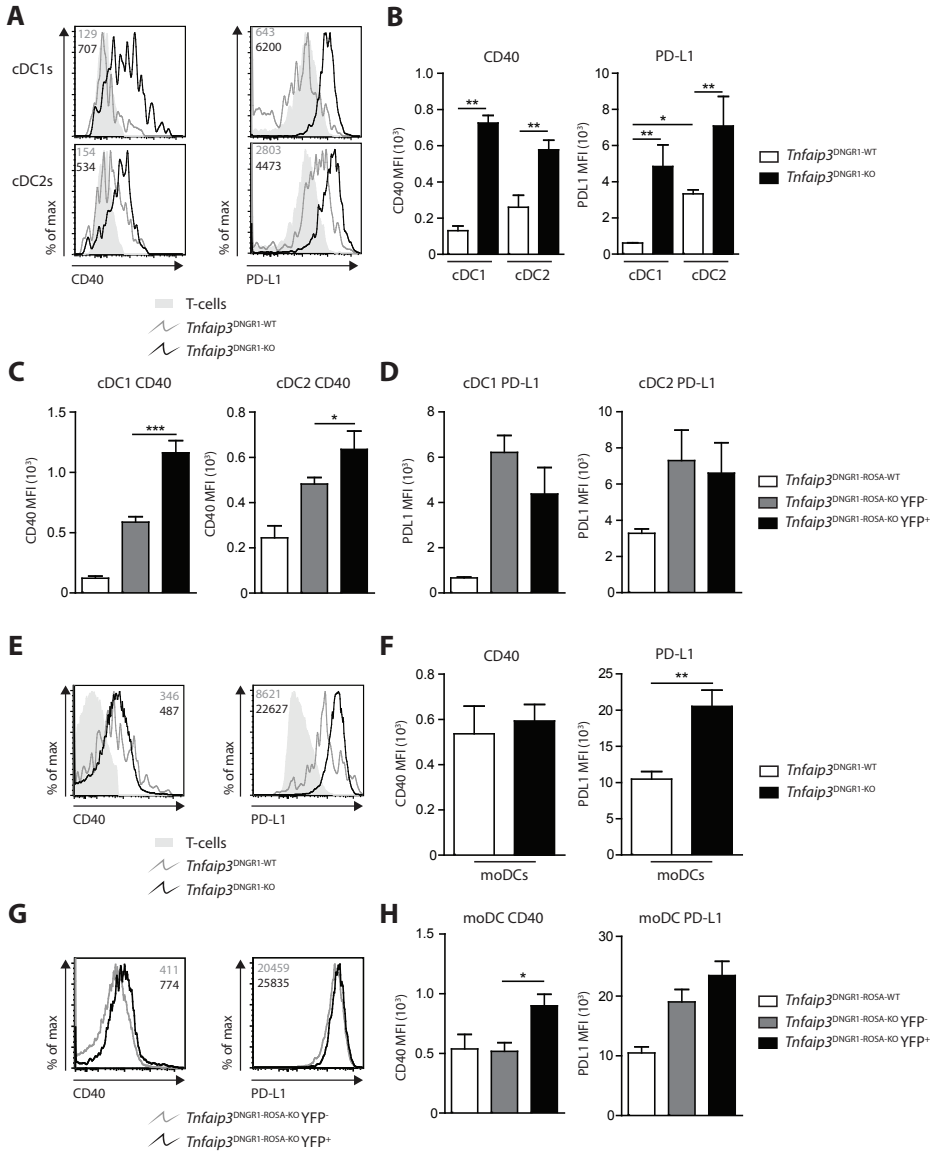

Figure 3: CD40 expression is increased through both cell-intrinsic and cell-extrinsic effects of Tnfaip3-deficiency in cDC1s, cDC2s, and moDCs.

Tnfaip3$^{DNGR1\text{-}ROSA\text{-}WT}$ mice and *Tnfaip3*$^{DNGR1\text{-}ROSA\text{-}KO}$ mice were sacrificed at 31-weeks of age. (A) Histograms showing expression of CD40 and PD-L1 on liver cDC1s and cDC2s. (B) Quantification of CD40 and PD-L1 by median fluorescence intensity (MFI) on liver cDC1s and cDC2s. (C-D) Quantification of CD40 MFI (C) and PD-L1 MFI (D) in YFP-positive and YFP-negative liver cDC1s and cDC2s. (E) Histograms showing expression of CD40 and PD-L1 on liver moDCs. (F) Quantification of CD40 and PD-L1 by MFI on liver moDCs. (G) Histograms illustrating expression of CD40 and PD-L1 on liver YFP$^+$ and YFP$^-$ moDCs in *Tnfaip3*$^{DNGR1\text{-}ROSA\text{-}KO}$ mice. (H) Quantification of CD40 and PD-L1 by MFI in YFP-positive and YFP-negative liver moDCs in *Tnfaip3*$^{DNGR1\text{-}ROSA\text{-}KO}$ mice. Representative data is shown from one experiment of 2 independent experiments.

Results are presented as mean ± SEM of n = 4-7 mice per group. Significance in (C,H) is only shown for YFP$^+$ and YFP$^-$ cells in *Tnfaip3*$^{DNGR1\text{-}ROSA\text{-}KO}$ mice. *P < 0.05, **P<0.01.

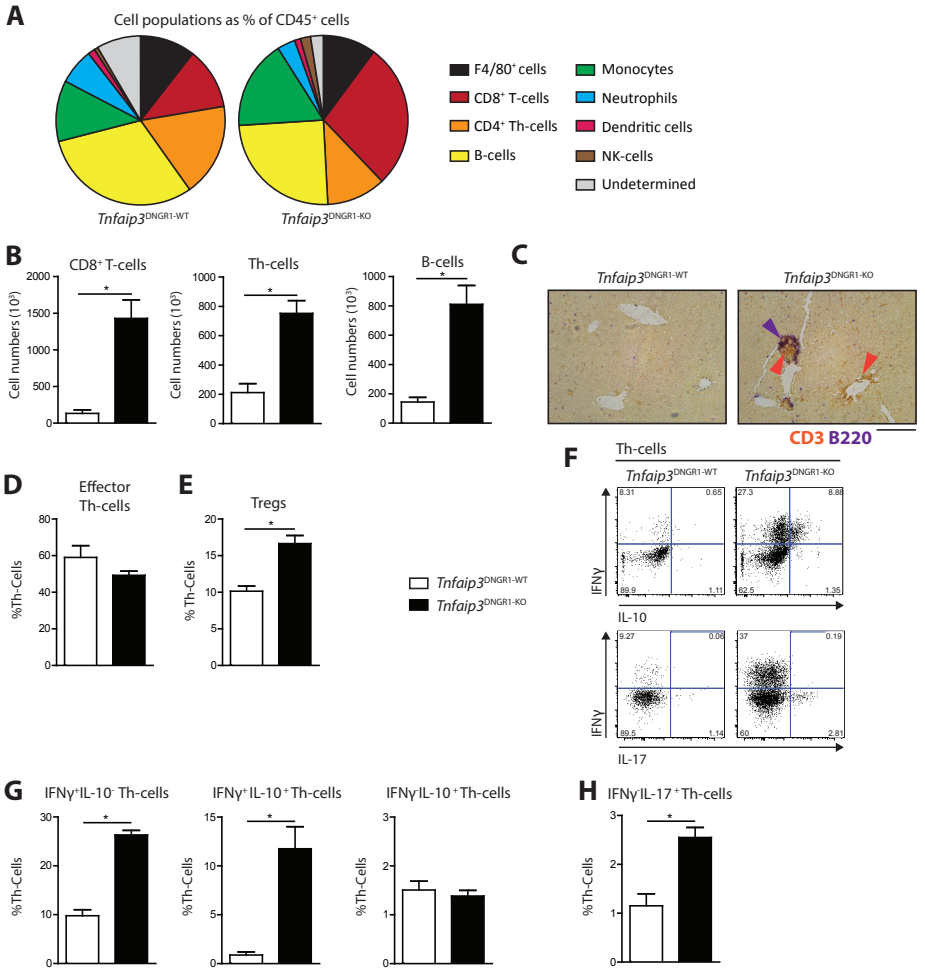

Figure 4: Livers of *Tnfaip3*$^{DNGR1\text{-}KO}$ mice have increased proportions of Th1-cells, Th17-cells and Tregs. *Tnfaip3*$^{DNGR1\text{-}WT}$ mice and *Tnfaip3*$^{DNGR1\text{-}KO}$ mice were sacrificed at 31-weeks of age. (A) Representation of liver immune cell proportions, being F4/80$^+$ cells (CD45$^+$F4/80$^+$CD11b^{int}), CD8$^+$ T-cells (CD3$^+$CD8$^+$), Th-cells (CD3$^+$CD4$^+$), B-cells (CD19$^+$), monocytes (CD11b$^+$CD11c$^-$GR1$^-$NK1.1$^-$), neutrophils (CD11b$^+$GR1$^+$NK1.1$^-$), total DCs, and NK-cells (NK1.1$^+$, GR1$^-$). (B) Quantification of CD8$^+$ T-cells, Th-cells and B-cells (CD19$^+$B220$^+$) in liver. (C) Immunohistochemistry of livers for CD3$^+$ (brown, T-cells) and B220$^+$ (purple, B-cells) cells in 31-week-old *Tnfaip3*$^{DNGR1\text{-}KO}$ mice and *Tnfaip3*$^{DNGR1\text{-}WT}$ mice also indicated by arrowheads. (D-E) Quantification of the proportion activated (CD44$^+$) Th-cells (D) and Tregs (E) using flow cytometry. (F) A representative example of flow cytometry data of liver CD4$^+$ Th-cells with IFNγ, IL-10 and IL-17A production is shown for *Tnfaip3*$^{DNGR1\text{-}WT}$ mice and *Tnfaip3*$^{DNGR1\text{-}KO}$ mice. (G-H) Percentages of cytokine-producing Th-cells is shown, being IFNγ single-positive, IFNγ/IL-10 double-positive, IL-10 single-positive (G) and IL-17A single-positive (H) using flow cytometry. Representative data from one experiment is shown out of 4 experiments for (B, D), 2 experiments (G-H) or 1 experiment (A,C). Results are presented as mean ± SEM of n =4 mice per group. *P < 0.05.

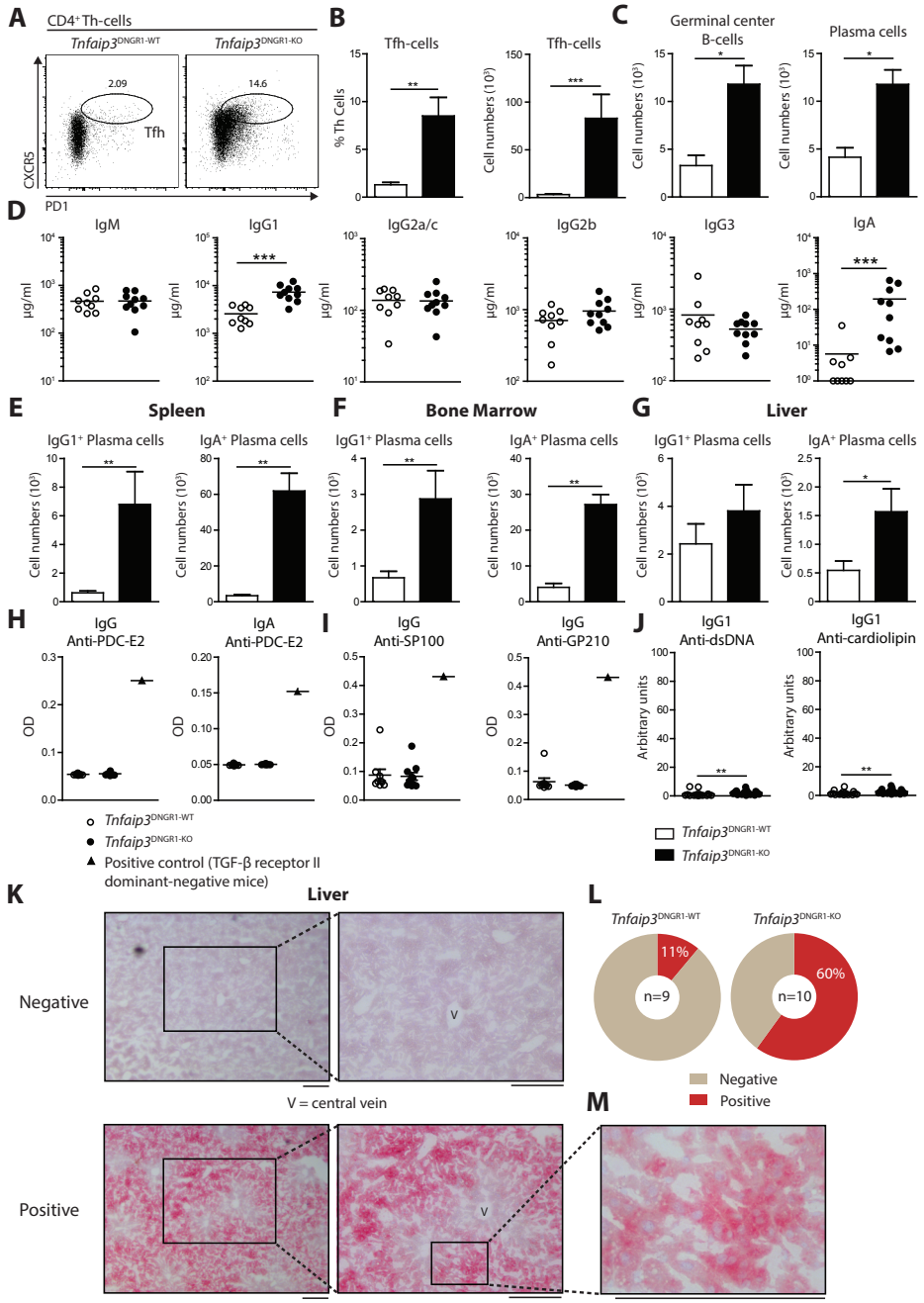

Figure 5: Livers of *Tnfaip3*$^{DNGR1-KO}$ mice contain increased Tfh-cells and plasma cells, likely producing liver-specific IgA antibodies.

Tnfaip3$^{DNGR1-WT}$ mice and *Tnfaip3*$^{DNGR1-KO}$ mice were sacrificed at 31-weeks of age. (A) Flow cytometry data of liver Tfh-cells ($CD3^+CD4^+CXCR5^+PD1^+$) from *Tnfaip3*$^{DNGR1-KO}$ mice and control mice. (B) Quantification of

the proportion Tfh-cells and cell numbers. (C) Enumeration of liver GC B-cells ($CD19^+B220^+CD95^+IgD^-$) and plasma cells ($B220^-CD138^+$). (D) Quantification of all serum immunoglobulin isotypes in 31-week-old mice. (E-G) Enumeration of $IgG1^+$ plasma cells ($B220^-CD138^+IgG1^+$) and IgA^+ plasma cells ($B220^-CD138^+IgGA^+$) in spleen (E), bone marrow (F), and liver (G). (H-J) Assessment of autoreactive IgG and IgA immunoglobulins towards PDC-E2 (H), IgG towards sp100 and gp210 (I) and IgG1 towards dsDNA and cardiolipin (J) in serum from 31-week-old mice using ELISA. 100 arbitrary units represent the average level of lupus-prone *lpr* mice in (J). (K) Livers from *Rag1*^{KO} mice were incubated with serum from 31-week-old *Tnfaip3*$^{DNGR1\text{-}WT}$ and *Tnfaip-3*$^{DNGR1\text{-}KO}$ mice and assessed for IgA binding. (L) Negative and positive autoreactive IgA staining numbers on *Rag1*^{KO} livers using serum from *Tnfaip3*$^{DNGR1\text{-}KO}$ mice or *Tnfaip3*$^{DNGR1\text{-}KO}$ mice, depicted in pie-chart format, and in (M) higher magnification of bound IgA on *Rag1*^{KO} livers. Results are presented as mean ± SEM of $n = 4$-19 mice per group. *$P < 0.05$, **$P < 0.01$, ****$P < 0.0001$. Scale bars represent 200µm.

3.5. Livers of *Tnfaip3*$^{DNGR1\text{-}KO}$ mice contain increased Tfh-cells and plasma cells, likely producing liver-specific IgA antibodies.

The presence of liver inflammatory lesion with both T-cells and B-cells could indicate direct communication of follicular T-helper (Tfh)-cells with germinal center (GC) B-cells. In *Tnfaip3*$^{DNGR1\text{-}KO}$ mice, the proportions and absolute numbers of Tfh-cells (**Figure 5A/B**) as well as the number GC B-cells and plasma cells (**Figure 5C**) were significantly increased in the livers compared to littermate controls. Moreover, total IgG1 and IgA concentrations were significantly elevated in the serum of 31-week-old *Tnfaip3*$^{DNGR1\text{-}KO}$ mice compared to WT controls (**Figure 5D**). This increase coincided with significantly increased numbers of $IgG1^+$ and IgA^+ plasma cells in spleens and bone marrow (BM) (**Figure 5E/F**). In liver, only IgA^+ plasma cells were significantly increased in *Tnfaip3*$^{DNGR1\text{-}KO}$ mice compared to control mice (**Figure 5G**). Remarkably, we detected increased serum IgG1 and IgA already in 11-week-old mice (**Supplementary Figure 5A**).

We next investigated whether IgG1 and IgA from *Tnfaip3*$^{DNGR1\text{-}KO}$ mice recognised self-antigens, but could not detect significant differences for antibodies against pyruvate dehydrogenase complex subunit E2 (PDC-E2), sp100, glycoprotein 210 (gp210), dsDNA or cardiolipin (**Figure 5H/I/J**). While IgG1 anti-dsDNA and anti-cardiolipin was enhanced in *Tnfaip3*$^{DNGR1\text{-}KO}$ mice compared to WT mice, these concentrations were very low in comparison to the reference serum of lupus-prone *lpr* mice (**Figure 5J**) and most likely not physiological relevant as no IgG deposition nor pathology was observed in the kidneys of *Tnfaip3*$^{DNGR1\text{-}KO}$ mice (**Supplementary Figure 2D/E**).

We next examined whether serum IgG1 or IgA of *Tnfaip3*$^{DNGR1\text{-}KO}$ mice recognized liver-specific proteins. Serum IgG1 from *Tnfaip3*$^{DNGR1\text{-}KO}$ mice did not bind proteins present in liver or pancreas (data not shown). In contrast, serum IgA from 6 out of 10 mice from a panel of 31-week-old *Tnfaip3*$^{DNGR1\text{-}KO}$ mice recognized antigens in the liver periportal regions, while this was only detected by serum IgA from 1 out of 9 WT mice (**Figure 5K/L**). Primarily liver cytoplasmic proteins were recognized by serum IgA from *Tnfaip-3*$^{DNGR1\text{-}KO}$ mice (**Figure 5M**). Importantly, serum IgA from 11-week-old *Tnfaip3*$^{DNGR1\text{-}KO}$ mice did not recognize liver-specific proteins, whereas total IgA was elevated at that age

(**Supplementary Figure 5A/B**), indicating that the auto-reactivity of IgA developed after the age of 11 weeks. Serum IgA from ~30% of *Tnfaip3*$^{DNGR1\text{-}KO}$ mice recognized pancreas-specific proteins, albeit with reduced staining intensity compared to liver tissue (**Supplementary figure 5C/D**).

In summary, livers of *Tnfaip3*$^{DNGR1\text{-}KO}$ mice contain increased number of Tfh-cells, GC B-cells, and IgA^{+} plasma cells, accompanied by elevated serum IgG1 and IgA concentrations. Importantly, IgA from *Tnfaip3*$^{DNGR1\text{-}KO}$ mice recognized self-proteins, specifically cytoplasmic proteins of cells within the hepatic periportal regions, which could be involved in the pathogenesis of liver inflammation.

4. DISCUSSION

DCs play a crucial role in the maintenance of tolerance during steady state. The activation status of DCs can act like a switch in the development of tolerance or immunity[6]. Previously we and others have shown that DC-specific ablation of A20/Tnfaip3 led to spontaneous DC activation and subsequently T and B-cell activation, resulting in an inflammatory phenotype resembling SLE[11] or IBD[10]. DCs comprise different subsets and cDCs are primarily known to maintain tolerance[17, 22]. To investigate whether A20/Tnfaip3 deletion in cDCs induces autoimmunity, we crossed *Tnfaip3*-floxed mice to *Clec9a*/DNGR1-cre recombinase mice, as previously this promotor was shown to mainly target cDCs in wild-type mice[27].

In contrast to A20/Tnfaip3 ablation in all DC subsets, which induced systemic autoimmune disease resembling SLE[11] or IBD[10] in mice, *Tnfaip3*$^{DNGR1\text{-}KO}$ mice develop organ-specific autoimmune disease. Aged *Tnfaip3*$^{DNGR1\text{-}KO}$ mice acquired aggravated liver inflammatory infiltrates, consisting mainly of T-cells and some B-cells, adjacent to the portal triads and in lobules. This was accompanied by increased autoreactive IgA in serum, recognizing liver cytoplasmic proteins. DNGR1-driven targeting of DCs in the liver of control mice was similar to other organs[27], being ~95% in cDC1s, ~35% in cDC2s and ~45% in moDCs. However, in *Tnfaip3*$^{DNGR1\text{-}KO}$ mice we found a striking decrease in the proportions of targeted cDC1s (~55%). It is not very likely that the DNGR1-driven excision in cDC1s was reduced in *Tnfaip3*$^{DNGR1\text{-}KO}$ mice. Rather, this finding indicates that due to A20/Tnfaip3-ablation, DC homeostasis was disturbed. Furthermore, liver cDC1s, cDC2s and moDCs show an enhanced activation status (e.g., increased CD40 expression) upon A20/Tnfaip3-ablation.

First signs of chronic liver inflammation, shown by increased cytokeratin 7 expression[37] and liver fibrosis, were found in 24-week-old *Tnfaip3*$^{DNGR1\text{-}KO}$ mice (data not shown) and further increased at 31-weeks of age. Kidneys and intestines, did not show inflammatory lesions, and only very mild inflammation was observed in pancreas. Inflammation plays

an important role in several liver pathologies, and genome-wide association studies (GWAS) have revealed *TNFAIP3* single nucleotide polymorphisms (SNPs) associated to primary biliary cirrhosis (PBC)[38, 39] and autoimmune hepatitis (AIH)[40, 41]. Our data show that A20/Tnfaip3-deletion in cDCs and moDCs leads to spontaneous (auto) immune responses in the liver.

Strikingly, DNGR1-cre mediated deletion of A20/Tnfaip3 in cDC1s reduces the proportion of cells targeted by DNGR1 from ~95% in *Tnfaip3*$^{DNGR1\text{-}WT}$ mice to ~55% in *Tnfaip3*$^{DNGR1\text{-}KO}$ mice. This could be induced by an enhanced sensitivity of cDC1s to undergo apoptosis, which is also regulated by A20/Tnfaip3[42]. As the total number of DNGR1-targeted cDC1s was similar between *Tnfaip3*$^{DNGR1\text{-}WT}$ mice and *Tnfaip3*$^{DNGR1\text{-}KO}$ mice, this suggests that *Tnfaip3*-deficient cDC1s do not undergo apoptosis. The reduced proportion of *Tnfaip3*-deleted cDC1s in *Tnfaip3*$^{DNGR1\text{-}KO}$ mice could be a consequence of a robust selective advantage for the residual *Tnfaip3*-sufficient cDC1s in the *Tnfaip3*$^{DNGR1\text{-}KO}$ mice, as total CD45^{+} hematopoietic cells and thus total DCs increase in the liver. Alternatively, monocytes can adopt to a cDC1-phenotype in the presence of inflammatory signals[43] and start expressing cDC1-typical molecules, like CD103, XCR1, and IRF8. Additional studies are needed to identify the cause for the increase in Tnfaip3-sufficient cDC1s in *Tnfaip3*$^{DNGR1\text{-}KO}$ mice.

Next to DCs, the liver contains other myeloid antigen presenting cells (APCs) such as Kupffer cells and moDCs. Kupffer cell proportions in *Tnfaip3*$^{DNGR1\text{-}KO}$ mice remained constant, while moDCs slightly increased in *Tnfaip3*$^{DNGR1\text{-}KO}$ mice livers, most likely recruited due to liver inflammation[44, 45]. Approximately 30% of moDCs in *Tnfaip3*$^{DNGR1\text{-}KO}$ mice were targeted by DNGR1-driven Cre expression and consequently deleted Tnfaip3. While kidneys are also known to have a similar proportion of DNGR1-Cre-mediated deletion[27], we saw no inflammation in kidneys in *Tnfaip3*$^{DNGR1\text{-}KO}$ mice. Nevertheless, the liver phenotype observed in *Tnfaip3*$^{DNGR1\text{-}KO}$ mice will most likely not be solely induced by Tnfaip3 ablation in cDCs, because affected moDCs may also contribute. Liver cDC1s, cDC2s, and moDCs are activated upon A20/Tnfaip3-ablation, indicated by enhanced co-stimulatory CD40 expression. Subtle differences in CD40 expression on cDCs can lead to substantial differences in T-cell activation, possibly due to a threshold effect. For instance, a 2-fold higher CD40 increase on cDC1s in non-obese diabetic (NOD) mice turns the balance from tolerant Tregs to effector Th1-cell responses[46]. In contrast, absence of CD40 on APCs/DCs during inflammatory conditions expands the number of Tregs[47, 48]. Thus, enhanced CD40 expression on cDCs and a proportion of moDCs in *Tnfaip3*$^{DNGR1\text{-}KO}$ could well explain the increased induction of Th1-cells in the liver. Remarkably, transgenic mice with constitutive CD11c-specific CD40-signalling have a break in tolerance, which coincided with increased Th1 and Th17-cell responses and strikingly also elevated serum IgA[49]. These features are also observed in *Tnfaip3*$^{DNGR1\text{-}KO}$ mice. Evaluating CD40 expression on A20/Tnfaip3-deficient and A20/Tnfaip3-sufficient cDCs within the same *Tnfaip3*$^{DNGR1\text{-}KO}$ mouse

demonstrated that CD40 expression is largely, but not completely regulated by A20/Tnfaip3 in a cell-autonomous way. Suppression of CD40 expression by A20/Tnfaip3 has also been demonstrated in *in vitro* mesothelial cells[50]. However, elevated CD40 expression was also observed on A20/Tnfaip3-sufficient cDCs from *Tnfaip3*$^{DNGR1\text{-}KO}$ mice compared to control mice, suggesting CD40 expression is additionally influenced by cell-extrinsic factors. In *Tnfaip3*$^{DNGR1\text{-}KO}$ mice both cDCs and moDCs expressed higher surface levels of the co-inhibitory molecule PD-L1 which was most likely regulated cell-extrinsically as both A20/Tnfaip3-deficient and A20/Tnfaip3-sufficient cDCs within the same Tnfaip3$^{DNGR1\text{-}KO}$ mouse harbored similar elevated expression compared to control mice. Increased PD-L1 expression is probably driven by enhanced IFNγ[51], produced by liver Th1-cells and CD8$^+$ T-cells (data not shown) in *Tnfaip3*$^{DNGR1\text{-}KO}$ mice.

The inflammatory infiltrates in *Tnfaip3*$^{DNGR1\text{-}KO}$ mouse livers contained CD8$^+$ T-cells, Th-cells, and B-cells. These lymphocytes were detected next to DCs in the periportal inflammatory infiltrates, which could imply local T- and B-cell activation. A number of genes involved in T-cell activation, such as *IL12A*, *IL12RB2* and *STAT4*, all involved in IL-12R signaling, are strongly associated to liver autoimmune biliary diseases[52], and involved in Th1 and Th17-cell polarization. *Tnfaip3*$^{DNGR1\text{-}KO}$ mice showed increased liver Th1-cells and Th17-cells, together with augmented IL-12$^+$ cells, which are present around periportal infiltrates.

Although the percentage of IFNγ-producing CD8$^+$ T-cells did not increase in livers of *Tnfaip3*$^{DNGR1\text{-}KO}$ mice, their total cell number did (data not shown). While the Th1 cytokine IFNγ is hepatotoxic[53] and plays pathological roles in mouse models of autoimmune liver disease[54, 55], controversy exists regarding the function of the Th17 cytokine IL-17A, being either protective[56] or pathogenic[54, 57]. In our study, Th17-cells appeared dispensable for liver inflammation in *Tnfaip3*$^{DNGR1\text{-}KO}$ mice, as the liver pathology was unaltered in the absence of liver IL-17A$^+$ Th-cells (data not shown). Since Th-cell transfer from IFNγ-overexpressing mice induced similar liver pathology[58] as observed in *Tnfaip3*$^{DNGR1\text{-}KO}$ mice, this could be indicative that Th1-cells are pathogenic in *Tnfaip3*$^{DNGR1\text{-}KO}$ mice. Strikingly, the majority of IFNγ-producing Th-cells co-expressed IL-10 in livers from *Tnfaip3*$^{DNGR1\text{-}KO}$ mice, which has broad anti-inflammatory properties. Expression of IL-10 by Th1-cells could be a self-regulatory mechanism to prevent excessive local inflammation[59], as IL-10 can reduce IL-12 secretion from DCs[60].

Aggregation of DCs, T-cells, and B-cells in the livers of *Tnfaip3*$^{DNGR1\text{-}KO}$ mice could promote active TLO formation, in which a GC reaction with help of Tfh-cells would support B-cell activation, class switching, and antibody production. Indeed, liver Tfh-cells, GC B-cells, and plasma cells are increased in *Tnfaip3*$^{DNGR1\text{-}KO}$ mice. In autoimmune liver disease patients, liver Tfh-cells are expanded compared to healthy controls[61] and Tfh-cells even correlate with serum anti-nuclear antibody (ANA) titers[62]. Elevated IgG[63] or IgM[64] are

often seen in autoimmune liver diseases, which are known to correlate with circulating Tfh-cells[65]. The increased liver Tfh-cells in *Tnfaip3*$^{DNGR1\text{-}KO}$ mice may have contributed to establishing elevated serum total IgG and IgA from a young age. In autoimmune liver disease, increased autoreactive IgA is observed[66], which we also find in *Tnfaip3*$^{DNGR1\text{-}KO}$ mice. Serum of *Tnfaip3*$^{DNGR1\text{-}KO}$ mice contained autoreactive IgA specifically recognizing cytoplasmic proteins within the periportal regions. The explicit increase in liver IgA^{+} plasma cells, and not liver IgG1^{+} plasma cells, might explain why only liver-specific autoreactive IgA is observed. As liver periportal inflammation was already present on 11-weeks of age, but autoreactive IgA was not yet detected in *Tnfaip3*$^{DNGR1\text{-}KO}$ mice at that time, this could indicate that auto-antibodies do not initiate liver pathology but rather exacerbate the phenotype.

In summary, DNGR1-cre-mediated deletion of A20/Tnfaip3 in cDCs and moDCs provokes chronic liver inflammatory infiltrates surrounding the portal triads. A20/Tnfaip3 directly controls CD40 expression in liver cDC1s, cDC2s and moDCs *in vivo*, with increased proportions of Th1-cells, Th17-cells, and Tfh-cells and autoreactive B-cell activation. Our data illustrate that activation of conventional DCs and moDCs is sufficient to shift the balance between tolerance and immunity and induces organ-specific autoimmunity, especially in the liver.

Acknowledgements

This project was supported by The Dutch Arthritis Association (12-2-410) and the European Framework program 7 (FP7-MC-CIG grant 304221). We would like to thank Prof. Caetano Reis e Sousa for providing critical mouse strains, Jacobus Hagoort for reviewing the manuscript and Fatemeh Ahmedi and the Erasmus MC Animal Facility (EDC) staff for their assistance during the project.

Conflict of interest

The authors declare no conflict of interest.

REFERENCES

1. Steinman RM. Decisions about dendritic cells: past, present, and future. *Annu Rev Immunol* 2012; 30: 1-22.
2. Hawiger D, Inaba K, Dorsett Y, Guo M, Mahnke K, Rivera M *et al.* Dendritic cells induce peripheral T cell unresponsiveness under steady state conditions in vivo. *J Exp Med* 2001; 194(6): 769-779.
3. Mahnke K, Qian Y, Knop J, Enk AH. Induction of CD4+/CD25+ regulatory T cells by targeting of antigens to immature dendritic cells. *Blood* 2003; 101(12): 4862-4869.
4. Hernandez J, Aung S, Redmond WL, Sherman LA. Phenotypic and functional analysis of CD8(+) T cells undergoing peripheral deletion in response to cross-presentation of self-antigen. *J Exp Med* 2001; 194(6): 707-717.
5. Steinman RM, Hawiger D, Nussenzweig MC. Tolerogenic dendritic cells. *Annu Rev Immunol* 2003; 21: 685-711.
6. Steinman RM, Nussenzweig MC. Avoiding horror autotoxicus: the importance of dendritic cells in peripheral T cell tolerance. *Proc Natl Acad Sci U S A* 2002; 99(1): 351-358.
7. Tan JK, O'Neill HC. Maturation requirements for dendritic cells in T cell stimulation leading to tolerance versus immunity. *J Leukoc Biol* 2005; 78(2): 319-324.
8. Yoshimura S, Bondeson J, Foxwell BM, Brennan FM, Feldmann M. Effective antigen presentation by dendritic cells is NF-kappaB dependent: coordinate regulation of MHC, co-stimulatory molecules and cytokines. *International immunology* 2001; 13(5): 675-683.
9. Wertz IE, O'Rourke KM, Zhou H, Eby M, Aravind L, Seshagiri S *et al.* De-ubiquitination and ubiquitin ligase domains of A20 downregulate NF-kappaB signalling. *Nature* 2004; 430(7000): 694-699.
10. Hammer GE, Turer EE, Taylor KE, Fang CJ, Advincula R, Oshima S *et al.* Expression of A20 by dendritic cells preserves immune homeostasis and prevents colitis and spondyloarthritis. *Nat Immunol* 2011; 12(12): 1184-1193.
11. Kool M, van Loo G, Waelput W, De Prijck S, Muskens F, Sze M *et al.* The ubiquitin-editing protein A20 prevents dendritic cell activation, recognition of apoptotic cells, and systemic autoimmunity. *Immunity* 2011; 35(1): 82-96.
12. Ma A, Malynn BA. A20: linking a complex regulator of ubiquitylation to immunity and human disease. *Nat Rev Immunol* 2012; 12(11): 774-785.
13. Das T, Chen Z, Hendriks RW, Kool M. A20/Tumor Necrosis Factor alpha-Induced Protein 3 in Immune Cells Controls Development of Autoinflammation and Autoimmunity: Lessons from Mouse Models. *Front Immunol* 2018; 9: 104.
14. Coombes JL, Siddiqui KR, Arancibia-Carcamo CV, Hall J, Sun CM, Belkaid Y *et al.* A functionally specialized population of mucosal CD103+ DCs induces Foxp3+ regulatory T cells via a TGF-beta and retinoic acid-dependent mechanism. *J Exp Med* 2007; 204(8): 1757-1764.
15. Khare A, Krishnamoorthy N, Oriss TB, Fei M, Ray P, Ray A. Cutting edge: inhaled antigen upregulates retinaldehyde dehydrogenase in lung CD103+ but not plasmacytoid dendritic cells to induce Foxp3 de novo in CD4+ T cells and promote airway tolerance. *J Immunol* 2013; 191(1): 25-29.
16. Yamazaki S, Dudziak D, Heidkamp GF, Fiorese C, Bonito AJ, Inaba K *et al.* CD8+ CD205+ splenic dendritic cells are specialized to induce Foxp3+ regulatory T cells. *J Immunol* 2008; 181(10): 6923-6933.
17. Bonifaz L, Bonnyay D, Mahnke K, Rivera M, Nussenzweig MC, Steinman RM. Efficient targeting of protein antigen to the dendritic cell receptor DEC-205 in the steady state leads to antigen presentation on

major histocompatibility complex class I products and peripheral CD8+ T cell tolerance. *J Exp Med* 2002; 196(12): 1627-1638.

18. Luckashenak N, Schroeder S, Endt K, Schmidt D, Mahnke K, Bachmann MF *et al.* Constitutive crosspresentation of tissue antigens by dendritic cells controls CD8+ T cell tolerance in vivo. *Immunity* 2008; 28(4): 521-532.
19. Hildner K, Edelson BT, Purtha WE, Diamond M, Matsushita H, Kohyama M *et al.* Batf3 deficiency reveals a critical role for CD8alpha+ dendritic cells in cytotoxic T cell immunity. *Science* 2008; 322(5904): 1097-1100.
20. Edelson BT, Kc W, Juang R, Kohyama M, Benoit LA, Klekotka PA *et al.* Peripheral CD103+ dendritic cells form a unified subset developmentally related to CD8alpha+ conventional dendritic cells. *J Exp Med* 2010; 207(4): 823-836.
21. Luda KM, Joeris T, Persson EK, Rivollier A, Demiri M, Sitnik KM *et al.* IRF8 Transcription-Factor-Dependent Classical Dendritic Cells Are Essential for Intestinal T Cell Homeostasis. *Immunity* 2016; 44(4): 860-874.
22. Dudziak D, Kamphorst AO, Heidkamp GF, Buchholz VR, Trumpfheller C, Yamazaki S *et al.* Differential antigen processing by dendritic cell subsets in vivo. *Science* 2007; 315(5808): 107-111.
23. Guilliams M, Crozat K, Henri S, Tamoutounour S, Grenot P, Devilard E *et al.* Skin-draining lymph nodes contain dermis-derived CD103(-) dendritic cells that constitutively produce retinoic acid and induce Foxp3(+) regulatory T cells. *Blood* 2010; 115(10): 1958-1968.
24. Plantinga M, Guilliams M, Vanheerswynghels M, Deswarte K, Branco-Madeira F, Toussaint W *et al.* Conventional and monocyte-derived CD11b(+) dendritic cells initiate and maintain T helper 2 cell-mediated immunity to house dust mite allergen. *Immunity* 2013; 38(2): 322-335.
25. Schlitzer A, McGovern N, Teo P, Zelante T, Atarashi K, Low D *et al.* IRF4 transcription factor-dependent CD11b+ dendritic cells in human and mouse control mucosal IL-17 cytokine responses. *Immunity* 2013; 38(5): 970-983.
26. Randolph GJ, Inaba K, Robbiani DF, Steinman RM, Muller WA. Differentiation of phagocytic monocytes into lymph node dendritic cells in vivo. *Immunity* 1999; 11(6): 753-761.
27. Schraml BU, van Blijswijk J, Zelenay S, Whitney PG, Filby A, Acton SE *et al.* Genetic tracing via DNGR-1 expression history defines dendritic cells as a hematopoietic lineage. *Cell* 2013; 154(4): 843-858.
28. Vereecke L, Sze M, Mc Guire C, Rogiers B, Chu Y, Schmidt-Supprian M *et al.* Enterocyte-specific A20 deficiency sensitizes to tumor necrosis factor-induced toxicity and experimental colitis. *J Exp Med* 2010; 207(7): 1513-1523.
29. Srinivas S, Watanabe T, Lin CS, William CM, Tanabe Y, Jessell TM *et al.* Cre reporter strains produced by targeted insertion of EYFP and ECFP into the ROSA26 locus. *BMC Dev Biol* 2001; 1: 4.
30. van de Garde MD, Movita D, van der Heide M, Herschke F, De Jonghe S, Gama L *et al.* Liver Monocytes and Kupffer Cells Remain Transcriptionally Distinct during Chronic Viral Infection. *PLoS One* 2016; 11(11): e0166094.
31. Vroman H, Bergen IM, Li BW, van Hulst JA, Lukkes M, van Uden D *et al.* Development of eosinophilic inflammation is independent of B-T cell interaction in a chronic house dust mite-driven asthma model. *Clin Exp Allergy* 2017; 47(4): 551-564.
32. Marlow SL, Blennerhassett MG. Deficient innervation characterizes intestinal strictures in a rat model of colitis. *Exp Mol Pathol* 2006; 80(1): 54-66.
33. Ishak K, Baptista A, Bianchi L, Callea F, De Groote J, Gudat F *et al.* Histological grading

and staging of chronic hepatitis. *Journal of hepatology* 1995; 22(6): 696-699.

34. Yang CY, Leung PS, Yang GX, Kenny TP, Zhang W, Coppel R *et al.* Epitope-specific anti-nuclear antibodies are expressed in a mouse model of primary biliary cirrhosis and are cytokine-dependent. *Clin Exp Immunol* 2012; 168(3): 261-267.
35. Mombaerts P, Iacomini J, Johnson RS, Herrup K, Tonegawa S, Papaioannou VE. RAG-1-deficient mice have no mature B and T lymphocytes. *Cell* 1992; 68(5): 869-877.
36. Washington MK. Autoimmune liver disease: overlap and outliers. *Mod Pathol* 2007; 20 Suppl 1: S15-30.
37. Bateman AC, Hubscher SG. Cytokeratin expression as an aid to diagnosis in medical liver biopsies. *Histopathology* 2010; 56(4): 415-425.
38. Cordell HJ, Han Y, Mells GF, Li Y, Hirschfield GM, Greene CS *et al.* International genome-wide meta-analysis identifies new primary biliary cirrhosis risk loci and targetable pathogenic pathways. *Nat Commun* 2015; 6: 8019.
39. Juran BD, Hirschfield GM, Invernizzi P, Atkinson EJ, Li Y, Xie G *et al.* Immunochip analyses identify a novel risk locus for primary biliary cirrhosis at 13q14, multiple independent associations at four established risk loci and epistasis between 1p31 and 7q32 risk variants. *Human molecular genetics* 2012; 21(23): 5209-5221.
40. de Boer YS, van Gerven NM, Zwiers A, Verwer BJ, van Hoek B, van Erpecum KJ *et al.* Genome-wide association study identifies variants associated with autoimmune hepatitis type 1. *Gastroenterology* 2014; 147(2): 443-452 e445.
41. Xu E, Cao H, Lin L, Liu H. rs10499194 polymorphism in the tumor necrosis factor-alpha inducible protein 3 (TNFAIP3) gene is associated with type-1 autoimmune hepatitis risk in Chinese Han population. *PLoS One* 2017; 12(4): e0176471.
42. Onizawa M, Oshima S, Schulze-Topphoff U, Oses-Prieto JA, Lu T, Tavares R *et al.* The ubiquitin-modifying enzyme A20 restricts ubiquitination of the kinase RIPK3 and protects cells from necroptosis. *Nat Immunol* 2015; 16(6): 618-627.
43. Sharma MD, Rodriguez PC, Koehn BH, Baban B, Cui Y, Guo G *et al.* Activation of p53 in Immature Myeloid Precursor Cells Controls Differentiation into Ly6c(+)CD103(+) Monocytic Antigen-Presenting Cells in Tumors. *Immunity* 2018; 48(1): 91-106.
44. Dominguez PM, Ardavin C. Differentiation and function of mouse monocyte-derived dendritic cells in steady state and inflammation. *Immunol Rev* 2010; 234(1): 90-104.
45. Sutti S, Locatelli I, Bruzzi S, Jindal A, Vacchiano M, Bozzola C *et al.* CX3CR1-expressing inflammatory dendritic cells contribute to the progression of steatohepatitis. *Clinical science (London, England : 1979)* 2015; 129(9): 797-808.
46. Price JD, Beauchamp NM, Rahir G, Zhao Y, Rieger CC, Lau-Kilby AW *et al.* CD8+ dendritic cell-mediated tolerance of autoreactive CD4+ T cells is deficient in NOD mice and can be corrected by blocking CD40L. *J Leukoc Biol* 2014; 95(2): 325-336.
47. Richer MJ, Lavallee DJ, Shanina I, Horwitz MS. Immunomodulation of antigen presenting cells promotes natural regulatory T cells that prevent autoimmune diabetes in NOD mice. *PLoS One* 2012; 7(2): 15.
48. Zheng X, Suzuki M, Ichim TE, Zhang X, Sun H, Zhu F *et al.* Treatment of autoimmune arthritis using RNA interference-modulated dendritic cells. *J Immunol* 2010; 184(11): 6457-6464.
49. Barthels C, Ogrinc A, Steyer V, Meier S, Simon F, Wimmer M *et al.* CD40-signalling abrogates induction of RORgammat(+) Treg cells by intestinal CD103(+) DCs and causes fatal colitis. *Nat Commun* 2017; 8: 14715.
50. Zou XL, Pei DA, Yan JZ, Xu G, Wu P. A20 overexpression inhibits lipopolysaccha-

ride-induced NF-kappaB activation, TRAF6 and CD40 expression in rat peritoneal mesothelial cells. *Int J Mol Sci* 2014; 15(4): 6592-6608.

51. Freeman GJ, Long AJ, Iwai Y, Bourque K, Chernova T, Nishimura H *et al.* Engagement of the PD-1 immunoinhibitory receptor by a novel B7 family member leads to negative regulation of lymphocyte activation. *J Exp Med* 2000; 192(7): 1027-1034.
52. Webb GJ, Siminovitch KA, Hirschfield GM. The immunogenetics of primary biliary cirrhosis: A comprehensive review. *J Autoimmun* 2015; 64: 42-52.
53. Kano A, Watanabe Y, Takeda N, Aizawa S, Akaike T. Analysis of IFN-gamma-induced cell cycle arrest and cell death in hepatocytes. *J Biochem* 1997; 121(4): 677-683.
54. Kawata K, Tsuda M, Yang GX, Zhang W, Tanaka H, Tsuneyama K *et al.* Identification of potential cytokine pathways for therapeutic intervention in murine primary biliary cirrhosis. *PLoS One* 2013; 8(9): e74225.
55. Toyonaga T, Hino O, Sugai S, Wakasugi S, Abe K, Shichiri M *et al.* Chronic active hepatitis in transgenic mice expressing interferon-gamma in the liver. *Proc Natl Acad Sci U S A* 1994; 91(2): 614-618.
56. Yang W, Yao Y, Yang YQ, Lu FT, Li L, Wang YH *et al.* Differential modulation by IL-17A of Cholangitis versus Colitis in IL-2Ralpha deleted mice. *PLoS One* 2014; 9(8): e105351.
57. Yu H, Huang J, Liu Y, Ai G, Yan W, Wang X *et al.* IL-17 contributes to autoimmune hepatitis. *J Huazhong Univ Sci Technolog Med Sci* 2010; 30(4): 443-446.
58. Bae HR, Leung PS, Tsuneyama K, Valencia JC, Hodge DL, Kim S *et al.* Chronic expression of interferon-gamma leads to murine autoimmune cholangitis with a female predominance. *Hepatology* 2016; 64(4): 1189-1201.
59. Jankovic D, Kullberg MC, Feng CG, Goldszmid RS, Collazo CM, Wilson M *et al.* Conventional T-bet(+)Foxp3(-) Th1 cells are the major source of host-protective regulatory IL-10 during intracellular protozoan infection. *J Exp Med* 2007; 204(2): 273-283.
60. De Smedt T, Van Mechelen M, De Becker G, Urbain J, Leo O, Moser M. Effect of interleukin-10 on dendritic cell maturation and function. *European journal of immunology* 1997; 27(5): 1229-1235.
61. Wang L, Sun Y, Zhang Z, Jia Y, Zou Z, Ding J *et al.* CXCR5+ CD4+ T follicular helper cells participate in the pathogenesis of primary biliary cirrhosis. *Hepatology* 2015; 61(2): 627-638.
62. Kimura N, Yamagiwa S, Sugano T, Setsu T, Tominaga K, Kamimura H *et al.* Possible involvement of chemokine C-C receptor 7(-) programmed cell death-1(+) follicular helper T-cell subset in the pathogenesis of autoimmune hepatitis. *Journal of gastroenterology and hepatology* 2018; 33(1): 298-306.
63. Hennes EM, Zeniya M, Czaja AJ, Pares A, Dalekos GN, Krawitt EL *et al.* Simplified criteria for the diagnosis of autoimmune hepatitis. *Hepatology* 2008; 48(1): 169-176.
64. Taal BG, Schalm SW, de Bruyn AM, de Rooy FW, Klein F. Serum IgM in primary biliary cirrhosis. *Clinica chimica acta; international journal of clinical chemistry* 1980; 108(3): 457-463.
65. Ma L, Qin J, Ji H, Zhao P, Jiang Y. Tfh and plasma cells are correlated with hypergammaglobulinaemia in patients with autoimmune hepatitis. *Liver Int* 2014; 34(3): 405-415.
66. Nishio A, Van de Water J, Leung PS, Joplin R, Neuberger JM, Lake J *et al.* Comparative studies of antimitochondrial autoantibodies in sera and bile in primary biliary cirrhosis. *Hepatology* 1997; 25(5): 1085-1089.

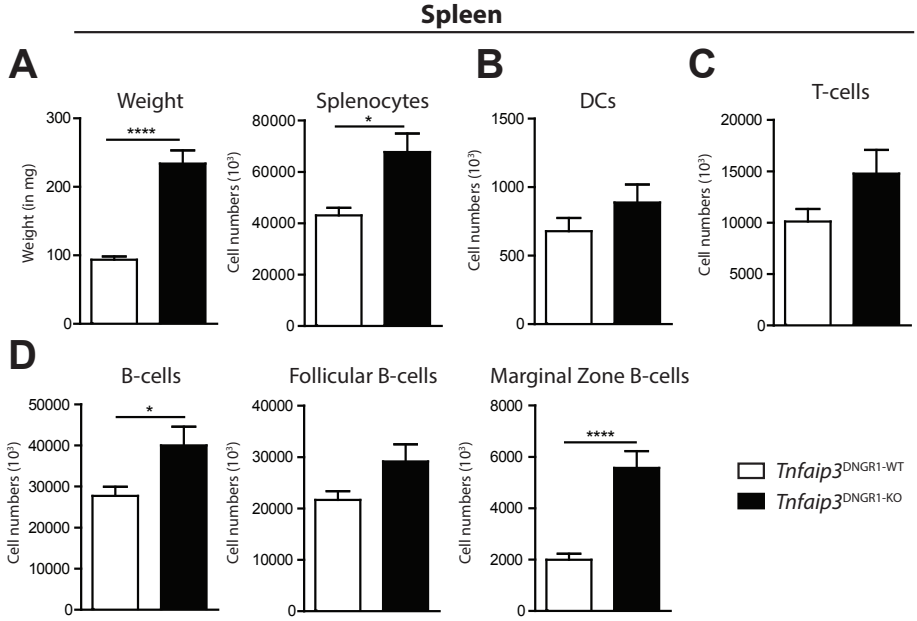

Supplementary Figure 1: *Tnfaip3*$^{DNGR1\text{-}KO}$ mice have splenomegaly with increased marginal zone B-cells.

Tnfaip3$^{DNGR1\text{-}WT}$ mice and *Tnfaip3*$^{DNGR1\text{-}KO}$ mice were analyzed at 31-weeks of age. (**A**) Quantification of both spleen weight and total cell count. (**B-C**) Enumeration of dendritic cells (CD11c^{hi}MHC-II^{hi}) (**B**) T-cells (CD3^{+}) (**C**), B-cells (CD19^{+}B220^{+}), Follicular B-cells (CD19^{+}B220^{+}CD23^{+}) and marginal zone B-cells (CD19^{+}B220^{+}CD21/35^{+}) (**D**) in spleen cell suspensions by flow cytometry. Results are presented as mean ± SEM and is pooled data from 3 independent experiments, n = 9-15 per group. *$P < 0.05$, ****$P < 0.0001$.

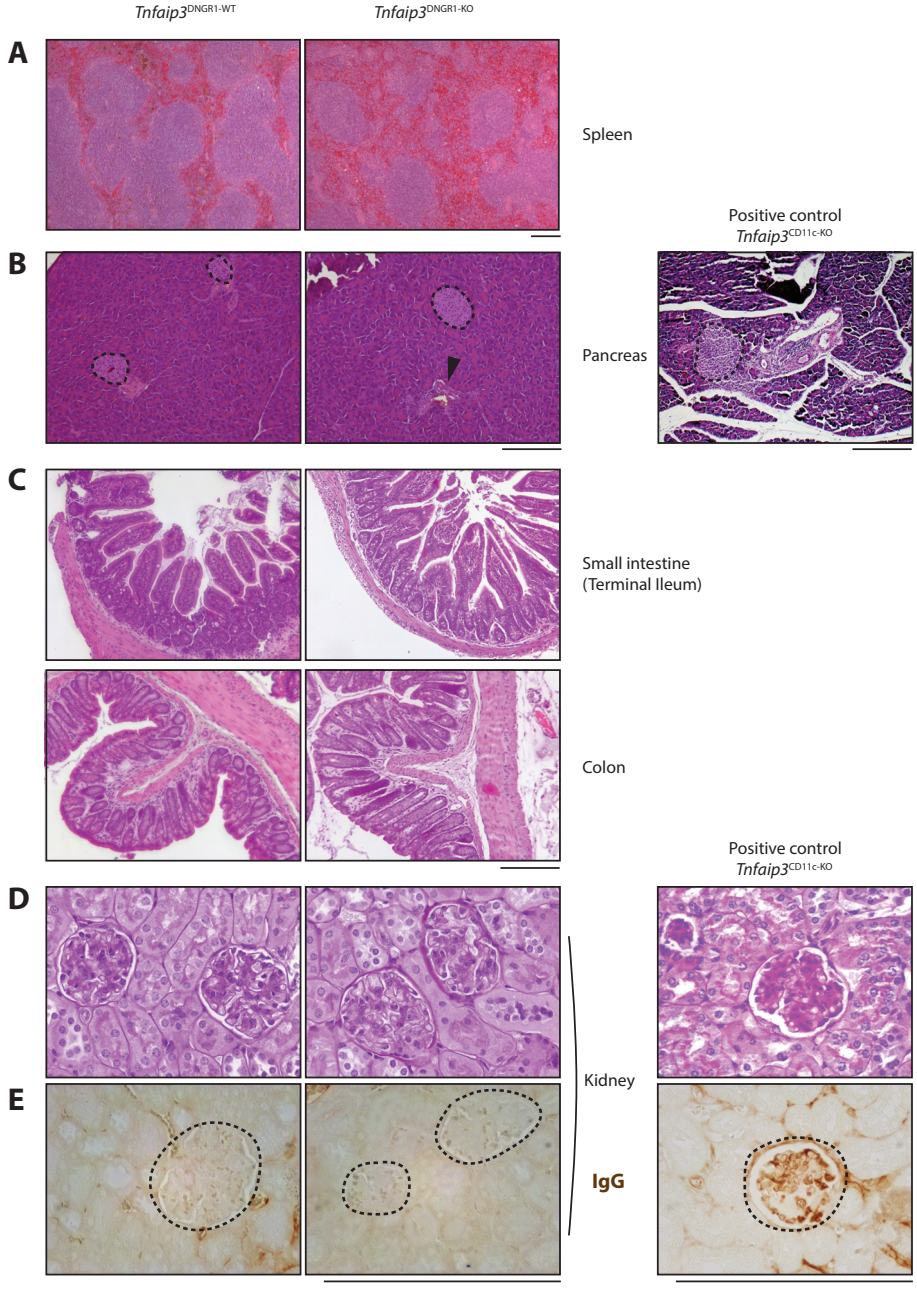

Supplementary Figure 2: Most tissues have absence of inflammation in *Tnfaip3*$^{DNGR1\text{-}KO}$ mice.
(**A-C**) H&E staining of spleens (**A**), pancreas (**B**) and terminal ileum and colon (**C**) from 31-week-old *Tnfaip3*$^{DNGR1\text{-}KO}$ mice. Arrowheads indicate mild inflammatory infiltrate. (**D**) Periodic acid-Schiff (PAS)$^{+}$ staining of kidneys from 31-week-old *Tnfaip3*$^{DNGR1\text{-}WT}$ mice and *Tnfaip3*$^{DNGR1\text{-}KO}$ mice. (**E**) Immunohistochemistry for glomerular IgG^{+} (brown) depositions in kidneys of 31-week-old mice. Dashed line highlights glomeruli. A lupus mouse positive control (*Cd11c*-cre mediated *Tnfaip3*-deleted mice) is also illustrated for comparison. Scale bars represent 200μm.

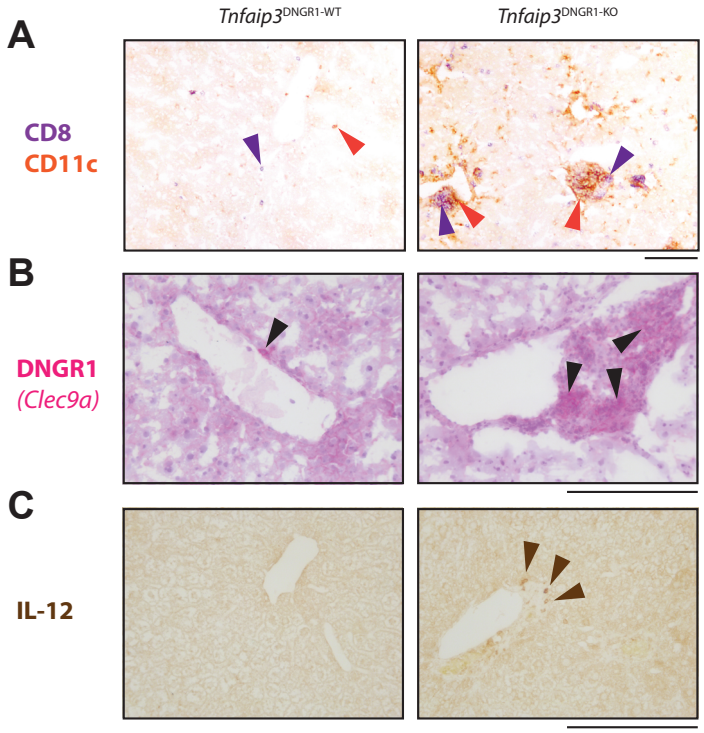

Supplementary Figure 3: Inflammatory infiltrates in *Tnfaip3*$^{DNGR1-KO}$ mice contain DCs, CD8$^+$ T-cells and DNGR1$^+$ cells.
(**A-C**) Immunohistochemistry for CD8$^+$ (purple, arrowhead) and CD11c$^+$ cells (orange, arrowhead) (**A**) DNGR1$^+$ cells (pink, arrowhead, positive in n=5/5 mice) (**B**) and IL-12 (brown, arrowhead, positive in n=4/6 mice) (**C**) in livers of 31-week-old *Tnfaip3*$^{DNGR1-WT}$ mice and *Tnfaip3*$^{DNGR1-KO}$ mice. Scale bars represent 200µm.

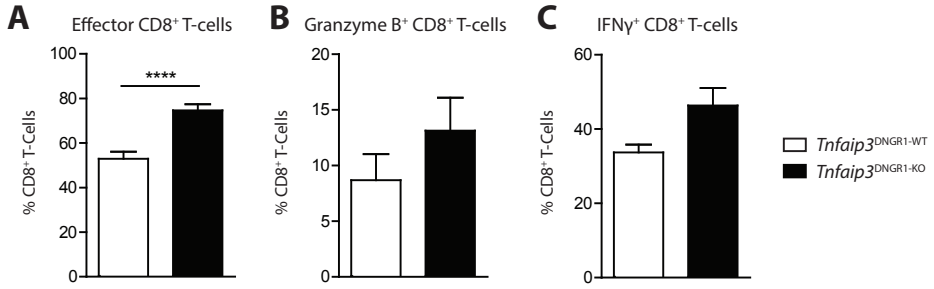

Supplementary Figure 4: *Tnfaip3*$^{DNGR1-KO}$ mice have increased liver CD8$^+$ T-cell activation.
Tnfaip3$^{DNGR1-WT}$ mice and *Tnfaip3*$^{DNGR1-KO}$ mice were sacrificed at 31-weeks of age under naïve conditions and the livers were examined. (**A-C**) Quantification of the proportion activated (CD44$^+$) (**A**), Granzyme B$^+$ (**B**) and IFNγ$^+$ (**C**) CD8$^+$ T-cells using flow cytometry. Pooled data from 4 experiments is shown for (**A**), 3 experiments for (**B**) and representative data from one out of 2 experiment is shown for (**C**). Results are presented as mean ± SEM of n = 4-19 per group. ****P < 0.0001.

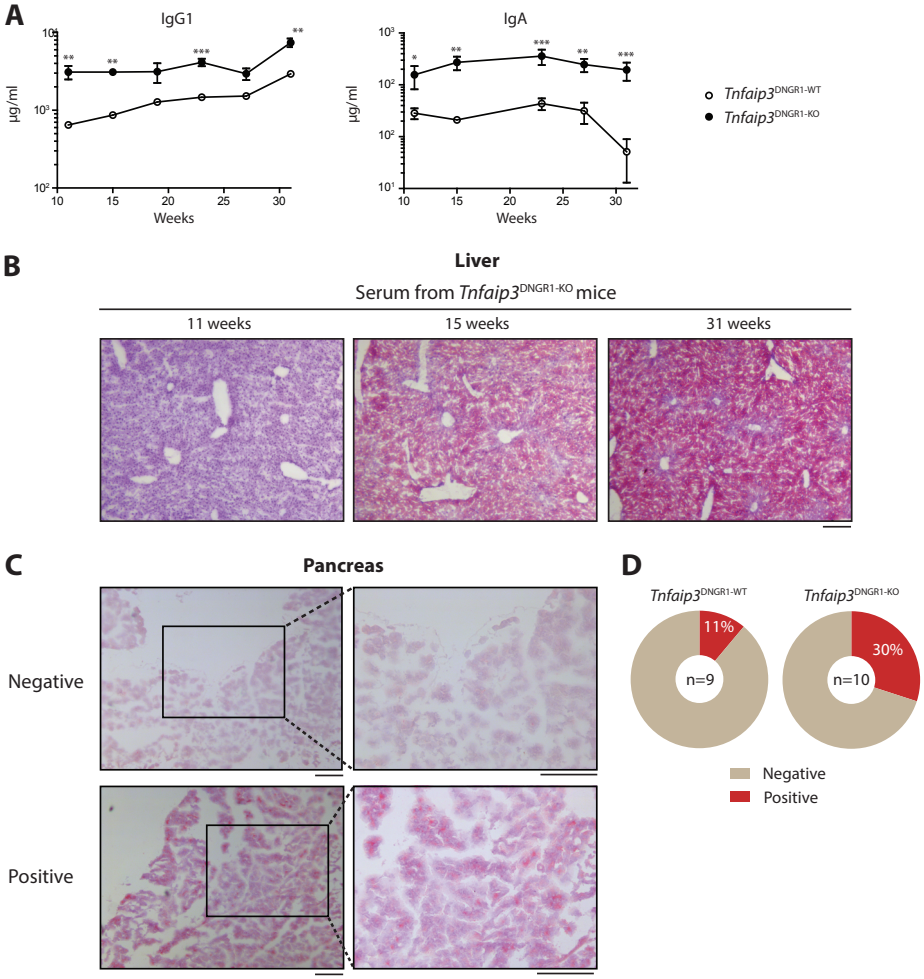

Supplementary Figure 5: IgA from *Tnfaip3*$^{DNGR1-KO}$ mice are primarily directed to liver antigens.
Serum of *Tnfaip3*$^{DNGR1-WT}$ mice and *Tnfaip3*$^{DNGR1-KO}$ mice was obtained. (**A**) Quantification of IgG1 and IgA immunoglobulin levels over time between 11 and 31-week-old mice. (**B**) Representative illustration of IgA autoreactivity towards liver proteins on liver of *Rag1*^{KO} mice in serum of 11, 15 and 31-week-old *Tnfaip-3*$^{DNGR1-KO}$ mice. (**C-D**) Representative negative and positive IgA staining on pancreas of *Rag1*^{KO} mice (**C**) and illustrated in pie chart format from both *Tnfaip3*$^{DNGR1-WT}$ mice and *Tnfaip3*$^{DNGR1-KO}$ mice (**D**). Results are from 2 experiments presented as mean ± SEM of *n* = 6-10 per group. *P<0.05, **$P < 0.01$, ***$P < 0.001$. Scale bars represent 200µm.

SUPPLEMENTARY MATERIAL METHODS:

Liver and Kidney (immuno)histochemistry

Liver cryosections were stained for DNGR1 (*Clec9a*, included in **Supplementary table 2**) and CD11c with CD8 (also included in **Supplementary table 2**). Cryo-sections were initially fixed in acetone. Sections were then incubated for 1hr with the primary antibodies. After washing, slides were incubated for 30 min with secondary antibodies (**Supplementary table 2**). Diaminobenzene (DAB) (for CD11c), Fast blue alkaline phosphatase (for CD8) and new fuchsin alkaline phosphatase (for DNGR1) substrates were used to retrieve specific staining. Counterstaining was performed with Gills hematoxylin (Sigma) (only for DNGR1-staining).

Six-µm-thick paraffin embedded kidney sections were stained with Periodic Acid Schiff (PAS; Sigma). For immunohistochemical stainings, antigen retrieval on paraffin-sections were established using citrate buffer (Sigma Aldrich). Paraffin kidney sections were stained for IgG with the primary antibody (**Supplementary table 2**) and paraffin liver sections were stained for IL-12 (**Supplementary table 2**). After washing, slides were incubated for 30 min with secondary antibodies (**Supplementary table 2**). The anti-Rabbit ABC Peroxidase Kit was utilized (Vector Labs, Burlingame, CA, USA). Diaminobenzene (DAB) was used to retrieve specific staining.

Supplementary Table 1: Antibodies used for flow cytometry.

Antibody	Conjugate	Clone	Company
B220	Alexa Fluor 700	RA3-6B2	eBioscience
B220	Pe-Cy7	RA3-6B2	eBioscience
CD103	ef450	2E7	eBioscience
CD11b	Biotin	M1/70	BD
CD11c	PE-Texas Red	N418	Invitrogen
CD138	Brilliant Violet 605	281-2	BD
CD19	APC-Cy7	1D3	BD
CD25	Biotin	PC61.5	eBioscience
CD3	PE-CF594	145-2C11	BD
CD4	Brilliant Violet 605	RM4-5	BD
CD4	Brilliant Violet 711	RM4-5	BD
CD44	FITC	IM7	eBioscience
CD44	APC-Cy7	IM7	BD
CD45	Brilliant Violet 711	30-F11	BD
CD45	PerCP-ef710	30-F11	eBioscience
CD62L	APC-ef780	MEL-14	eBioscience
CD64	Alexa Fluor 647	X54-5/7.1	BD
CD8	PE-Cy7	53-6.7	eBioscience
CD95	PE-Texas Red	Jo2	BD
CXCR5	Biotin	J43	eBioscience
F4/80	APC-ef780	BM8	eBioscience
FCƐRIα	Biotin	MAR-1	eBioscience
Foxp3	Alexa Fluor 700	FJK-16s	eBioscience
Granzyme B	PE	MHGB04	Caltag
IFN-γ	ef450	XMG1.2	eBioscience
IgA	FITC	C10-3	BD
IgD	APC	11-26c	eBiosicence
IgG1	PE	A85-1	BD
IgM	PE-Cy7	II/41	eBioscience
IL-10	Alexa Fluor 488	JES5-16E3	eBioscience
IL-17A	Alexa Fluor 700	TC11-18H10.1	BD
Ly6G/GR1	FITC	RB6.8C5	eBioscience
MHC-II	Alexa Fluor 700	M5/114.15.3	eBioscience
NK1.1	PE	PK136	eBioscience
PD1	Brilliant Violet 421	J43	BD
RORγt	PerCP-Cy5.5	Q31-378	BD
Streptavidin	Brilliant Violet 786		BD
Streptavidin	Brilliant Violet 711		BD

Supplementary Table 2: Primary and secondary antibodies for Immunohistochemistry

Primary Antibody	Clone	Company	Secondary Antibody	Product code	Company
Rat anti-CD8-PE	53-6.7	eBioscience, San Diego, CA, USA	**Goat anti-R-phycoerythrin AP**	600-105-387	Rockland, Limerick, PA, USA
Hamster anti-CD11c	N418	eBioscience, San Diego, CA, USA	**Goat anti-Hamster PO**	127-035-099	Jackson Immunoresearch, West Grove, PA, USA
Rabbit anti-Cytokeratin 7	EPR17078	Abcam, Cambridge,UK	**Goat anti-Rabbit PO**	PK-4001	Vector Laboratories, Burlingame, CA, USA
Rat anti-CLEC9a	MAB67761	R&D, Minneapolis, MN, USA	**Goat anti-RAT AP**	112-055-167	Jackson Immunoresearch
Rabbit anti-CD3	Polyclonal	DAKO, Glostrup, Denmark	**Goat anti-Rabbit PO**	PK-4001	Vector Laboratories
Rat anti-B220	RA3-6B2	Bioceros, Utrecht, The Netherlands	**Goat anti-RAT AP**	112-055-167	Jackson Immunoresearch
Goat anti-IgG-Biotin		Southern Biotech, Birmingham, AL, USA	**VECTASTAIN® ABC-HRP Kit**	PK-6100	Vector Laboratories, Burlingame, CA, USA
Rabbit anti-IL-12	EP5737	Abcam, Cambridge,UK	**Goat anti-Rabbit PO**	PK-4001	Vector Laboratories, Burlingame, CA, USA

Chapter 4

House dust mite-driven neutrophilic airway inflammation in mice with TNFAIP3-deficient myeloid cells is IL-17-independent

H. Vroman, T. Das, I.M. Bergen, J.A.C. van Hulst, F. Ahmadi, G. van Loo, E. Lubberts, R.W. Hendriks, M. Kool

Clinical Experimental Allergy. 2018;48:1705–171

ABSTRACT

Background: Asthma is a heterogeneous disease of the airways that involves several types of granulocytic inflammation. Recently, we have shown that the activation status of myeloid cells regulated by TNFAIP3/A20 is a crucial determinant of eosinophilic or neutrophilic airway inflammation. However, whether neutrophilic inflammation observed in this model is dependent on IL-17 remains unknown.

Objective: In this study, we investigated whether IL-17RA-signalling is essential for eosinophilic or neutrophilic inflammation in house dust mite (HDM)-driven airway inflammation.

Methods: *Tnfaip3*$^{fl/fl}$x*Lyz2*$^{+/cre}$ (*Tnfaip3*$^{LysM\text{-}KO}$) mice were crossed to *Il17ra*^{KO} mice, generating *Tnfaip3*^{LysM}*Il17ra*^{KO} mice and subjected to an HDM-driven airway inflammation model.

Results: Both eosinophilic and neutrophilic inflammation observed in HDM-exposed WT and *Tnfaip3*$^{LysM\text{-}KO}$ mice respectively, was unaltered in the absence of IL-17RA. Production of IL-5, IL-13 and IFNγ by CD4^{+} T cells was similar between WT, *Tnfaip3*$^{LysM\text{-}KO}$, and *Il17ra*^{KO} mice, whereas mucus-producing cells in *Tnfaip3*$^{LysM\text{-}KO}$*Il17ra*^{KO} mice were reduced compared to controls. Strikingly, spontaneous accumulation of pulmonary Th1, Th17 and $\gamma\delta$-17 T-cells was observed in *Tnfaip3*$^{LysM\text{-}KO}$*Il17ra*^{KO} mice, but not in the other genotypes. Th17 cell-associated cytokines such as GM-CSF and IL-22 were increased in the lungs of HDM-exposed *Tnfaip3*$^{LysM\text{-}KO}$*Il17ra*^{KO} mice, compared to IL-17RA-sufficient controls. Moreover, neutrophilic chemo-attractants CXCL1, CXCL2, CXCL12, and Th17-promoting cytokines IL-1β and IL-6 were unaltered between *Tnfaip3*$^{LysM\text{-}KO}$ and *Tnfaip3*$^{LysM\text{-}KO}$*Il17ra*^{KO} mice.

Conclusion and Clinical Relevance: These findings show that neutrophilic airway inflammation induced by activated TNFAIP3/A20-deficient myeloid cells can develop in the absence of IL-17RA-signalling. Neutrophilic inflammation is likely maintained by similar quantities of pro-inflammatory cytokines IL-1β and IL-6, that can independently of IL-17 signalling, induce the expression of neutrophil chemo-attractants.

INTRODUCTION

Asthma is characterized by reversible airway obstruction, airway remodelling and mucus production, together with increased pulmonary inflammation[1]. Granulocytic cells observed in pulmonary inflammation of asthmatic patients can comprise eosinophils, neutrophils, or a mixture of both cell types[2]. Eosinophilic inflammation is induced by interleukin (IL)-5, a type 2 cytokine produced by both Th2 cells and innate lymphoid cells type 2 (ILC2s)[3]. Neutrophilic inflammation is triggered by IL-8 produced by airway epithelial cells after activation by IL-17[4]. IL-17 furthermore contributes to asthma symptoms, because (1) it induces airway remodelling by promoting fibroblast proliferation, (2) reduces apoptosis of smooth muscle cells, and (3) increases the expression of mucin genes in airway epithelial cells[5-7]. Th17 cells primarily produce IL-17 and Th17-associated neutrophilic inflammation is particularly found in late-onset asthma patients with a severe phenotype[8, 9]. Unfortunately, severe asthma patients are often unresponsive to corticosteroid treatment, leading to frequent asthma exacerbations and higher morbidity[10]. Neutrophils and Th17 cells are likely contributing to this phenotype, as both cell types are corticosteroid insensitive[11-13]. Therefore, it is imperative to investigate the contribution of IL-17-signalling to the development of neutrophilic asthma.

Dendritic cell (DC) activation is essential for Th cell differentiation as antigen load, expression of costimulatory molecules, and DC-derived cytokines determine whether Th2 or Th17 cell differentiation is induced[14]. DC activation is controlled by TNFAIP3 (TNFα-induced protein 3, also known as A20), an ubiquitin modifying enzyme that deubiquitinates several key intermediate NF-κB signalling molecules, and thereby controls NF-κB-mediated cell activation[15]. TNFAIP3 is also implicated in Th2-associated disorders, as genetic polymorphisms in *TNFAIP3* and TNFAIP3 interacting protein (*TNIP*) have been associated with risk of developing allergies and asthma[16, 17]**.** Recently, we found that increasing the activation status of DCs by ablation of the *Tnfaip3* gene in myeloid cells induced a neutrophilic inflammation in house dust mite (HDM)-mediated asthma protocols, which was accompanied with enhanced number of IL-17-producing $CD4^+$ T cells[18].

To investigate whether the HDM-driven neutrophilic airway inflammation is dependent on IL-17, we crossed myeloid-specific *Tnfaip3* knockout mice (*Tnfaip3*$^{LysM\text{-}KO}$ mice)[19] to *Il17ra*^{KO} mice, generating *Tnfaip3*^{LysM}*Il17ra*^{KO} mice, in which IL-17A, IL-17E and IL-17F-signalling is disabled[20]. Absence of IL-17RA-signalling in *Tnfaip3*$^{LysM\text{-}KO}$ mice does not significantly affect neutrophilic inflammation, most likely due to enhanced amounts of IL-1β and IL-6 that can also promote the production of several neutrophil chemoattractants.

MATERIALS AND METHODS

Mice

Male and female C57BL/6 mice harbouring a conditional *Tnfaip3* allele between LoxP-flanked sites[21] were crossed to transgenic mice expressing the Cre recombinase under the LysM promotor[22], generating *Tnfaip3*$^{fl/fl}$x*Lyz2*$^{+/cre}$ mice, in which *Tnfaip3* will be deleted in cells that express or have expressed LysM[19] (*Tnfaip3*$^{LysM\text{-}KO}$ mice). *Tnfaip3*$^{fl/fl}$*Lyz2*$^{+/+}$ littermates (wild type (WT) mice) were used as controls. *Tnfaip3*^{LysM} mice were crossed with conventional *Il17ra*^{KO} mice[23], creating *Tnfaip3*$^{fl/fl}$x*Lyz2*$^{+/cre}$x*Il17ra*$^{-/-}$ mice (*Tnfaip3*$^{LysM\text{-}KO}$*Il17ra*^{KO} mice) and *Tnfaip3*$^{fl/fl}$x*Lyz2*$^{+/+}$x*Il17ra*$^{-/-}$ mice (*Il17ra*^{KO} mice). Mice were housed under specific pathogen-free conditions and were analysed at ~8 weeks (naïve and House Dust Mite (HDM) experiments) or at ~18 weeks (arthritis experiments). All experiments were approved by the animal ethical committee of the Erasmus MC, Rotterdam, The Netherlands (EMC3328 and EMC3333).

HDM-induced allergic airway inflammation

During intranasal (i.n.) exposures, mice were anesthetized using isofluorane. On day 0, mice were sensitized with 1 µg/40 µL HDM (Greer Laboratories Inc, Lenoir, NC, USA) i.n. or with 40 µL PBS (GIBCO Life Technologies, Carlsbad, CA, USA) as a control and challenged with 10 µg/40 µl HDM on days 7-11. Four days after the last challenge, bronchoalveolar lavage (BAL), lung, and mediastinal lymph node (MLN) were collected.

Cell suspension preparation

BAL was obtained by flushing the lungs three times with 1 mL PBS containing 0.5 mM EDTA (Sigma-Aldrich, St. Louis, MO, USA). The right lung was inflated with either 1:1 PBS/Tissue-TEK O.C.T. (VWR International, Darmstadt, Germany) solution, or snap-frozen in liquid nitrogen, and kept at −80°C until further processing for histology. The left lung was used for flow cytometry. Single-cell suspensions of the left lung were obtained by digesting using DNase (Sigma-Aldrich) and Liberase (Roche, Basel, Switzerland) for 30 min at 37°C. After digestion, the lungs were homogenized using a 100-µm cell strainer (Fischer Scientific, Waltham, MA, USA) and red blood cells were lysed using osmotic lysis buffer (8.3% NH_4CL, 1% $KHCO_3$, and 0.04% NA_2EDTA in Milli-Q). MLN and spleen were isolated for flow cytometry, for which they were homogenized through a 100-µm cell strainer.

Flow cytometry procedures

Flow cytometry surface and intracellular staining procedures have been described previously[24]. Monoclonal antibodies used for flow cytometric analyses are listed in **Supplementary table 1**. For all experiments, dead cells were excluded using fixable viability

dye (eBioscience, San diego, CA, USA). For measuring cytokine production, cells were stimulated with 10 ng/mL PMA (Sigma-Aldrich), 250 ng/mL ionomycin (Sigma-Aldrich), and GolgiStop (BD Biosciences, San Jose, CA, USA) for 4 h at 37°C. Data were acquired using a LSR II flow cytometer (BD Biosciences) with FACS DivaTM software and analysed with FlowJo version 9 (Tree Star Inc software, Ashland, OR, USA).

Lung histology

Six-µm-thick paraffin embedded lung sections were stained with periodic acid-Schiff (PAS) to visualize goblet cell hyperplasia.

Cytokine mRNA assessment by Quantitative Real-Time PCR

Homogenized left lower lung lobe was used to isolate and purify total RNA using the GeneElute mammalian total RNA miniprep system (Sigma-Aldrich) and RNA quantity was determined using a NanoDrop 1000 (VWR International). Up to 0.5 µg of total RNA was reverse-transcribed with SuperScript II reverse transcriptase (Invitrogen). Gene expression was analysed for *Gapdh, Cxcl1, Cxcl2, Cxcl12, Il1b, Il6, Il22, Il23*, *Csf2,* and *Muc5a* in SYBR Green Master Mixes (Qiagen, Hilden, Germany) using an ABI Prism 7300 Sequence Detector and ABI Prism Sequence Detection Software version 1.4 (Applied Biosystems, Foster City, CA, USA). Forward and reverse primers for each gene are listed in **Supplementary table 2**. Samples were analysed simultaneously for *Gapdh* mRNA as internal control. Each sample was assayed in duplicate and relative expression was calculated as 2^(-ΔCt), where ΔCt is the difference between Ct of the gene of interest and GAPDH.

Statistical analysis

All data was presented as means ± SEM. Mann–Whitney *U*-tests were used for comparison between two groups, and a *P*-value of <0.05 was considered statistically significant. All analyses were performed using Prism (Version 5, GraphPad Software, La Jolla, CA, USA).

RESULTS

Loss of IL-17RA-signalling combined with myeloid TNFAIP3 deficiency increases splenic monocytes, neutrophils and γδ T cells with progressing age.

To investigate the role of IL-17RA-signalling in HDM-driven neutrophilic airway inflammation responses, we crossed *Tnfaip3*^{LysM} mice[18, 19] with conventional *Il17ra*^{KO} mice[23]. It has been demonstrated that aged *Tnfaip3*$^{LysM\text{-}KO}$ mice develop arthritis[19] and that *Il17ra*^{KO} mice have altered monocyte[25] and neutrophil[26, 27] homeostasis. We therefore first examined whether abrogation of IL-17RA-signalling in *Tnfaip3*$^{LysM\text{-}KO}$ mice induces additional

alterations in the immune system. We assessed spleens of 8 and 18-week-old mice, as a representation of the systemic immune state. Both 8 and 18-week-old *Tnfaip3*$^{LysM\text{-}KO}$ and *Tnfaip3*$^{LysM\text{-}KO}$*Il17ra*^{KO} mice showed splenomegaly in comparison to WT and *Il17ra*^{KO} control mice (**Figure 1A**), whereas total splenic cell counts were only increased in 8 and 18-week old *Tnfaip3*$^{LysM\text{-}KO}$*Il17ra*^{KO} mice (**Figure 1B**). Monocytes and neutrophils (gated as shown in **Supplementary Figure 1**) were significantly increased in 8-week-old *Tnfaip3*$^{LysM\text{-}KO}$ mice in comparison to WT mice (**Figure 1C-D**), however only neutrophils were significantly increased in 18-week-old *Tnfaip3*$^{LysM\text{-}KO}$ mice compared to WT mice (**Figure 1D**), confirming previous findings[19]. Interestingly, both neutrophils and monocytes were significantly increased in 18-week-old *Tnfaip3*$^{LysM\text{-}KO}$*Il17ra*^{KO} mice compared to *Tnfaip3*$^{LysM\text{-}KO}$ mice (**Figure 1C-D**). Despite elevated monocyte and neutrophil numbers in *Tnfaip3*$^{LysM\text{-}KO}$*Il17ra*^{KO} mice, the macroscopic and microscopic arthritis phenotype was similar between *Tnfaip3*$^{LysM\text{-}KO}$ mice and *Tnfaip3*$^{LysM\text{-}KO}$*Il17ra*^{KO} mice (**Supplementary Figure 2**).

As IL-17 controls its own expression in CD4$^+$ T cells[26], we assessed conventional TCRαβ T cells and γδ T cells in the spleen (gating shown in **Figure 1E**). Total CD4$^+$ T helper (Th) cell numbers were not different between the genotypes in 8-week old mice, but were significantly increased in 18-week-old *Il17ra*^{KO} mice compared to WT mice (**Figure 1F**). Splenic RORγt$^+$ Th17 cells were elevated in 8-week-old *Tnfaip3*$^{LysM\text{-}KO}$*Il17ra*^{KO} mice compared to *Tnfaip3*$^{LysM\text{-}KO}$ mice, but this was no longer seen in 18-week-old mice (**Figure 1G**). Only 18-week-old *Il17ra*^{KO} mice and *Tnfaip3*$^{LysM\text{-}KO}$*Il17ra*^{KO} mice had increased splenic γδ T cell numbers compared to respective *Il17ra*^{WT} controls (**Figure 1H**). Splenic CD8$^+$ T cells were reduced in *Tnfaip3*$^{LysM\text{-}KO}$ mice and *Tnfaip3*$^{LysM\text{-}KO}$*Il17ra*^{KO} mice compared to respective *Tnfaip3*$^{LysM\text{-}WT}$ littermate controls at both ages (**Figure 1I**). Splenic B cell numbers did not differ between genotypes in both 8-week-old and 18-week-old mice (**Figure 1J**).

Taken together, these data show that myeloid TNFAIP3 deficiency with additional loss of IL-17RA-signalling induces minimal systemic immune changes at a young age, as only splenic Th17 cells are increased and CD8$^+$ T cells are decreased. In contrast, with progressing age myeloid TNFAIP3 deficient mice with abrogated IL-17RA-signalling accumulate splenic monocytes, neutrophils and γδ T cells.

House dust mite-induced eosinophilic and neutrophilic airway inflammation is unaltered in the absence of IL-17RA-signalling.

To investigate the requirement of IL-17RA-signalling on neutrophilic airway inflammation, we exposed young *Tnfaip3*^{LysM}*Il17ra* mice to an HDM-driven airway inflammation model (**Figure 2A**). As previously shown[18], HDM-sensitization and challenge induced a predominant eosinophilic inflammation in WT mice compared to PBS-sensitization, whereas *Tnfaip3*$^{LysM\text{-}KO}$ mice developed a primarily neutrophilic inflammation in the bronchoalveolar lavage (BAL) (**Figure 2B**). Absence of IL-17RA-signalling did not significantly

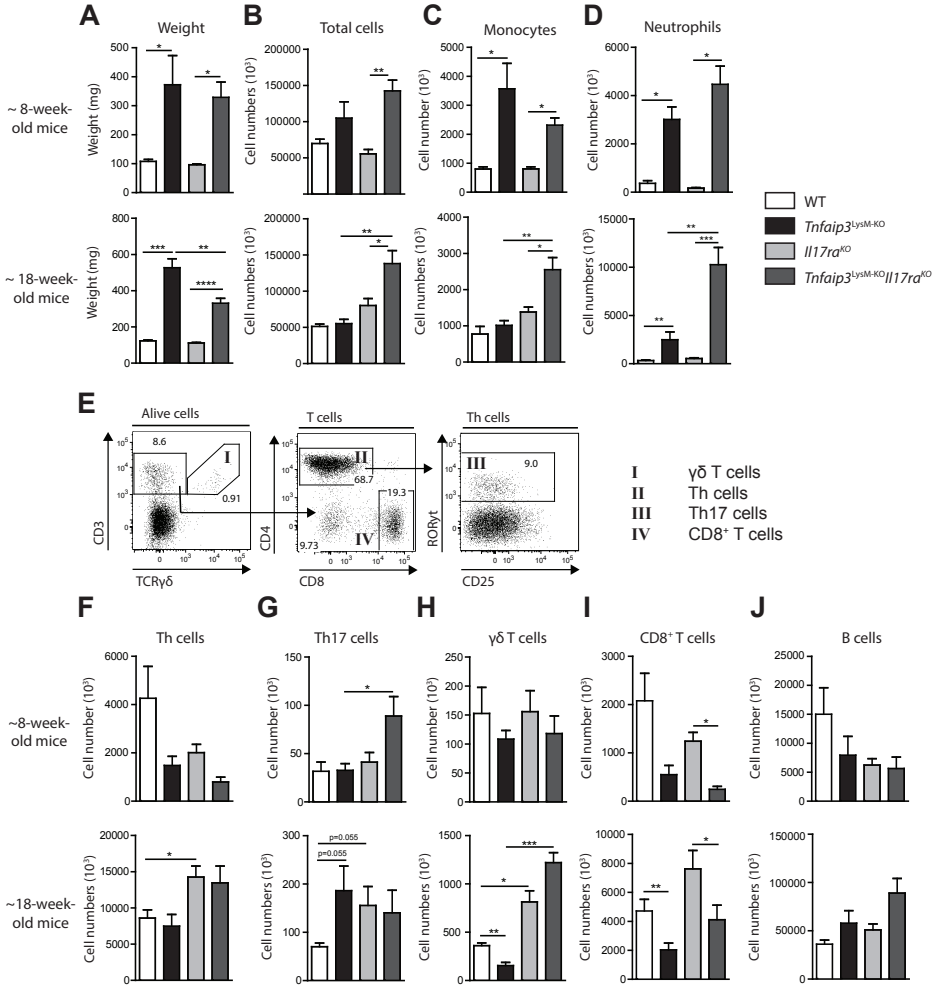

Figure 1: Loss of IL-17RA-signalling combined with myeloid TNFAIP3 deficiency increases splenic monocytes, neutrophils and γδ T cells with progressing age.

Tnfaip3^{LysM}*Il17ra* mice were analysed at 8 weeks and 18 weeks of age. (**A-B**) Quantification of spleen weight (**A**) and total cell numbers (**B**). (**C-D**) Enumeration of monocytes (**C**) and neutrophils (**C**) analysed in spleen cell suspensions by flow cytometry. (**E**) Flow cytometric gating strategy of T cells and γδ T cells. Example is shown from a spleen obtained from a WT mouse. (**F-H**) Cell numbers are depicted of Th cells (**F**), Th17 cells (**G**), γδ T cells (**H**), CD8$^+$ T cells (**I**) and B cells (**J**) in spleen cell suspensions by flow cytometry. Results are presented as mean ± SEM of n = 4-10 per group and are pooled from several experiments. *$P < 0.05$, **$P <$ 0.01, ***$P < 0.001$.

alter eosinophilic or neutrophilic inflammation in HDM-sensitized *Tnfaip3*$^{LysM\text{-}KO}$*Il17ra*^{KO} mice compared to HDM-sensitized *Tnfaip3*$^{LysM\text{-}KO}$ mice (**Figure 2B**). BAL DCs were increased in both HDM-sensitized WT mice and *Il17ra*^{KO} mice compared to their respective PBS-sensitized littermates (**Figure 2B**). However, in HDM-sensitized *Tnfaip3*$^{LysM\text{-}KO}$ mice,

DC numbers were reduced compared to HDM-sensitized WT mice and were increased in HDM-sensitized *Tnfaip3*$^{LysM\text{-}KO}$*Il17ra*^{KO} mice compared to HDM-sensitized *Tnfaip3*$^{LysM\text{-}KO}$ mice (**Figure 2B**). The absence of IL-17RA did not significantly alter the number of BAL macrophages in comparison to IL-17RA sufficient controls (**Figure 2B**).

HDM-sensitized WT and *Il17ra*^{KO} mice exhibited enhanced small airway mucus-producing goblet cells and inflammatory cells compared to their PBS-sensitized controls (**Figure 2C**). HDM-sensitized *Tnfaip3*$^{LysM\text{-}KO}$ mice had similar numbers of mucus-positive cells in both small and large airways compared to HDM-sensitized WT mice (**Figure 2C**). Remarkably, with additional loss of IL-17RA-signalling, the amount of goblet cells in small and large airways and lung *Muc5a* mRNA levels were severely reduced in HDM-sensitized *Tnfaip3*$^{LysM\text{-}KO}$*Il17ra*^{KO} mice compared to HDM-sensitized *Il17ra*^{KO} mice (**Figure 2C-D**).

In HDM-sensitized WT mice, the numbers of total T cells and CD4^{+} T cells in BAL fluid increased compared to PBS-sensitized WT mice (**Figure 2E**). Total BAL T cells, Th cells and γδ T cells were prominently elevated in HDM-sensitized *Tnfaip3*$^{LysM\text{-}KO}$*Il17ra*^{KO} mice compared to HDM-sensitized *Tnfaip3*$^{LysM\text{-}KO}$ mice (**Figure 2E**). HDM-sensitized *Il17ra*^{KO} mice had a slight increase in γδ T cells compared to HDM-sensitized WT mice (**Figure 2E**). Differences in total T cells and γδ T cells were not observed in the MLN (**Supplementary Figure 3**).

In conclusion, absence of IL-17RA-signalling did not significantly alter eosinophilic or neutrophilic airway inflammation in respectively HDM-treated *Il17ra*^{KO} and *Tnfaip3*$^{LysM\text{-}KO}$*Il17ra*^{KO} mice. In contrast, abrogated IL-17RA-signalling in combination with *Tnfaip3*-deficient myeloid cells hampered goblet cell hyperplasia. While Th cells and γδ T cells increase equally in *Tnfaip3*$^{LysM\text{-}KO}$ and WT mice upon HDM sensitisation, these populations remarkably increase with loss of IL-17RA-signalling.

Loss of IL-17RA-signalling does not reduce lung Th2 cytokines in an HDM-sensitized model, but increases IL-17 production.

The effects of IL-17 on Th2 differentiation in allergic asthma models depend on the allergen used and the timing of IL-17 exposure[28-30]. As eosinophilia and neutrophilia were only moderately affected by the loss of IL-17RA in HDM-sensitized *Tnfaip3*$^{LysM\text{-}WT}$ and *Tnfaip3*$^{LysM\text{-}KO}$ mice, we determined the effects of IL-17RA-signalling on cytokine secretion by T cells upon HDM-provoked airway inflammation. As expected, IL-13 and IL-5-expressing Th cells were increased within the BAL of HDM-sensitized WT mice compared to PBS-sensitized WT mice (**Figure 3A-B**). IL-13^{+} and IL-5^{+} Th cells were unaltered in HDM-sensitized *Il17ra*^{KO} and *Tnfaip3*$^{LysM\text{-}KO}$*Il17ra*^{KO} mice compared to their respective controls with functional IL-17RA-signalling (**Figure 3B**). HDM-sensitized *Tnfaip3*$^{LysM\text{-}KO}$*Il-17ra*^{KO} mice had reduced IL-13^{+} and IL-5^{+} Th cells compared to HDM-sensitized *Il17ra*^{KO} mice (**Figure 3B**). As previously shown[18], BAL IL-17^{+} Th cells increased in HDM-sensitized

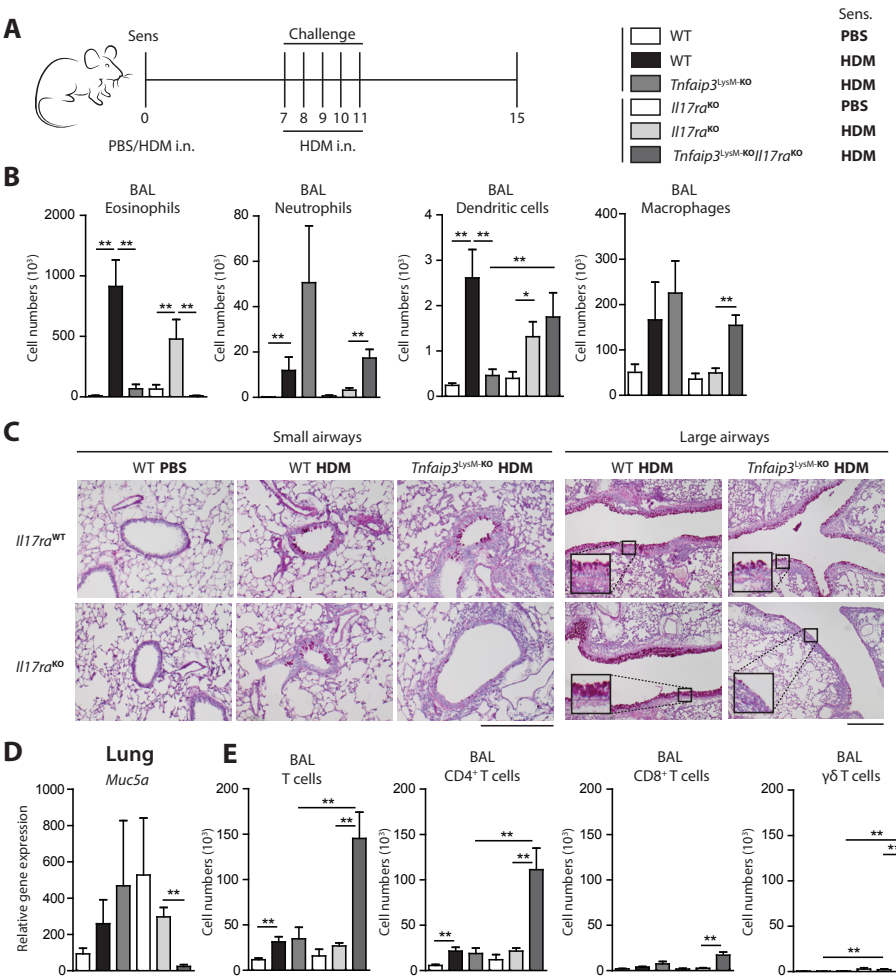

Figure 2: House dust mite induced eosinophilic and neutrophilic airway inflammation is unaltered in the absence of IL-17RA-signalling.

(**A**) Mice were sensitized with PBS or HDM (1 µg) on day 0 and challenged with 10 µg HDM from day 7-11. Analysis was performed at day 15. (**B**) Quantification of bronchoalveolar lavage (BAL) fluid eosinophils, neutrophils, dendritic cells and macrophages by flow cytometry. (**C**) Periodic Acid Schiff (PAS) stained lung small airway and large airway histology of *Tnfaip3*^{LysM}*Il17ra* mice after HDM exposure. Scale bar indicates 200µM. (**D**) *Muc5a* mRNA levels within lung homogenates of PBS and HDM challenged *Tnfaip3*^{LysM}*Il17ra* mice. (**E**) Enumeration of total CD3$^+$ T cells, CD4$^+$ Th cells, CD8$^+$ T cells and γδ T cells in BAL by flow cytometry. Results are presented as mean ± SEM of $n = 6$ per group and are representative of two independent experiments. *$P < 0.05$, **$P < 0.01$.

Tnfaip3$^{LysM\text{-}KO}$ mice compared to HDM-sensitized WT controls. Already in PBS-sensitized *Il17ra*^{KO} mice, an increase of BAL IL-17$^+$ Th cells was observed compared to PBS-sensitized WT mice, which was even more enhanced in HDM-sensitized *Tnfaip3*$^{LysM\text{-}KO}$*Il17ra*^{KO} mice (**Figure 3B**). BAL IFNγ-producing Th cells were only increased in HDM-sensitized

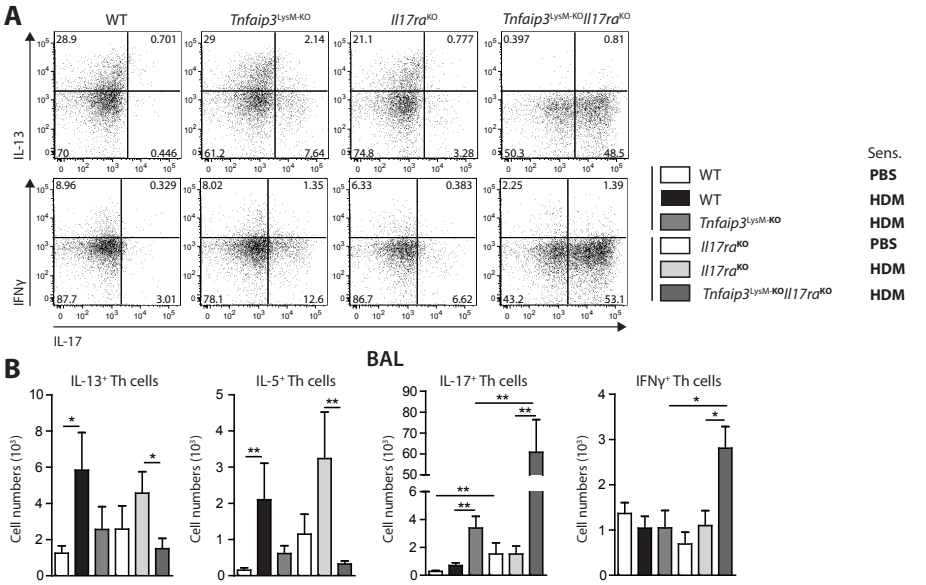

Figure 3: Loss of IL-17RA-signalling does not affect lung Th2 cytokines in a HDM-sensitized model, but increase IL-17 production.

Tnfaip3^{LysM}*Il17ra* mice were analysed after completion of the HDM exposure protocol. (**A**) Flow cytometry data is shown of intracellular cytokine expression within Th cells of broncho-alveolar lavage (BAL) of representative HDM exposed mice. (**B**) Quantification of BAL Th cell cytokines IL-13, IL-5, IL-17 and IFNγ as determined by flow cytometry. Results are presented as mean ± SEM of $n = 6$ per group and are representative of two independent experiments. *$P < 0.05$, **$P < 0.01$.

Tnfaip3$^{LysM\text{-}KO}$*Il17ra*^{KO} mice compared to either HDM-sensitized *Il17ra*^{KO} or *Tnfaip3*$^{LysM\text{-}KO}$ mice (**Figure 3B**).

In conclusion, lack of IL-17RA-signalling did not alter Th2 cytokines in HDM-sensitized mice, which correlated with the previously seen eosinophilic infiltrate. In contrast, IL-17-production and IFNγ-production by Th cells significantly increased in HDM-sensitized mice lacking myeloid TNFAIP3 with absent IL-17RA-signalling.

Myeloid TNFAIP3-deficient mice have IL-17RA-independent increases of neutrophil chemokines upon HDM-sensitization.

IL-17 may contribute to neutrophil chemokine (C-X-C motif) ligand (CXCL)1[31, 32], CXCL2[23, 33], and CXCL12 release[34]. Since neutrophilic inflammation persisted in lungs of HDM-sensitized *Tnfaip3*$^{LysM\text{-}KO}$*Il17ra*^{KO} mice, we assessed mRNA expression levels of these chemokines. HDM-sensitized lungs of *Tnfaip3*$^{LysM\text{-}KO}$ mice expressed increased amounts of *Cxcl1, Cxcl2* and *Cxcl12 mRNA* compared to HDM-sensitized WT mice (**Figure 4A**). Surprisingly, *Cxcl1* and *Cxcl12* mRNA expression did not differ between HDM-sensitized lungs of *Tnfaip3*$^{LysM\text{-}KO}$*Il17ra*^{KO} mice and *Tnfaip3*$^{LysM\text{-}KO}$ mice (**Figure 4A**). In contrast, lung

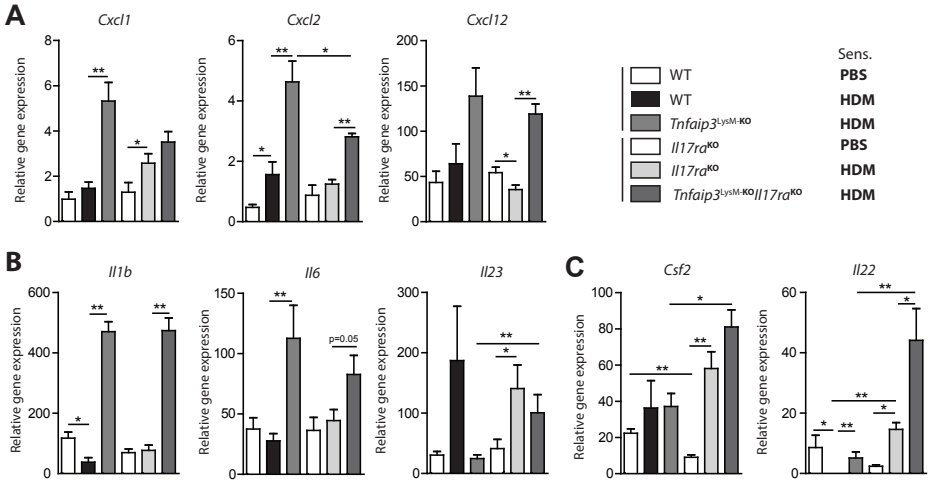

Figure 4: Myeloid TNFAIP3-deficient mice have IL-17RA-independent increases of neutrophil chemokines upon HDM-sensitization.

Total lung homogenates of HDM-challenged *Tnfaip3*^{LysM}*Il17ra* were analysed by RT-PCR. (**A-C)** Quantification of neutrophil chemokines *Cxcl1, Cxcl2, Cxcl12* gene expression (A), pro-inflammatory cytokines *Il1b, Il6* and *Il23* gene expression **(B)** and Th17-associated cytokines *Csf2* and *Il22* gene expression **(C)** in lung homogenates of PBS and HDM challenged *Tnfaip3*^{LysM}*Il17ra* mice. Results are presented as mean ± SEM of $n = 6$ per group. *$P < 0.05$, **$P < 0.01$.

Cxcl2 mRNA expression was partially reduced in HDM-sensitized *Tnfaip3*$^{LysM\text{-}KO}$*Il17ra*^{KO} mice as compared to HDM-sensitized *Tnfaip3*$^{LysM\text{-}KO}$ mice (**Figure 4A**). As absence of IL-17RA-signalling only moderately influenced chemokine expression, we evaluated other pro-inflammatory cytokines that can promote their expression, such as IL-1β[31, 35], IL-6[36] and IL-23[37]. HDM-treated *Tnfaip3*$^{LysM\text{-}KO}$ mice demonstrated elevated *Il1b* and *Il6* expression as compared to HDM-treated WT controls (**Figure 4B**). Abrogated IL-17RA-signalling in HDM-exposed *Tnfaip3*$^{LysM\text{-}KO}$*Il17ra*^{KO} mice resulted in similar *Il1b* and *Il6* cytokine expression as *Tnfaip3*$^{LysM\text{-}KO}$ mice (**Figure 4B**). In contrast, *Il23* expression was markedly increased in HDM-exposed *Tnfaip3*$^{LysM\text{-}KO}$*Il17ra*^{KO} mice compared to *Tnfaip3*$^{LysM\text{-}KO}$ controls (**Figure 4B**).

Next to IL-17A, Th17 cells can produce other cytokines, such as granulocyte-macrophage colony-stimulating factor (GM-CSF)[38] and IL-22[39, 40], which are known to regulate neutrophil chemokines CXCL1/CXCL2 and directly attract neutrophils respectively. mRNA expression of *Csf2* and *Il22* were augmented in HDM-sensitized *Il17ra*^{KO} mice compared to PBS-sensitized *Il17ra*^{KO} mice (**Figure 4C**). Only *Il22* gene expression was further increased in HDM-sensitized *Tnfaip3*$^{LysM\text{-}KO}$*Il17ra*^{KO} mice lungs compared to HDM-sensitized *Il17ra*^{KO} mice (**Figure 4C**). Both lung *Csf2* and *Il22* mRNA expression was enhanced in HDM-sensitized *Tnfaip3*$^{LysM\text{-}KO}$*Il17ra*^{KO} mice compared to HDM-exposed

Tnfaip3$^{LysM\text{-}KO}$ mice (**Figure 4C**), which corresponded to the number of Th17 cells (**Figure 3B**).

In summary, myeloid TNFAIP3-deficient HDM-sensitized mice had elevated lung mRNA expression of the neutrophil chemokines *Cxcl1, Cxcl2* and *Cxcl12,* despite abrogated IL-17RA-signalling. IL-17RA-signalling partially contributes to *Cxcl2* expression in response to HDM-sensitization in myeloid TNFAIP3-deficient mice. Neutrophil chemo-attractants are probably maintained in the absence of IL-17RA-signalling by equal quantities of IL-1β and IL-6, that are most likely derived from activated myeloid cells.

DISCUSSION

IL-17 is implicated in severe and uncontrolled asthma, as patients who suffer from severe asthma display increased levels of IL-17 in lung tissue[41]. Recently we have shown that the presence of intrinsically activated myeloid cells, obtained through TNFAIP3/A20 ablation, induces development of neutrophilic inflammation accompanied by increased Th17 cells in contrast to Th2 cell-driven eosinophilic inflammation induced in control mice[18]. To investigate whether neutrophilic inflammation development as observed in HDM-treated *Tnfaip3*^{LysM} mice is dependent on IL-17-signalling, *Tnfaip3*^{LysM} mice were crossed to IL-17RA-deficient mice.

Surprisingly, absence of IL-17RA-signalling had only limited effects on neutrophilic inflammation, and neutrophil chemo-attractants in our HDM-driven airway inflammation mouse model. Ablation of IL-17RA-signalling increased the number of Th1 and Th17 cells, whereas Th2 cell differentiation and eosinophilic inflammation was not hampered. Strikingly, the presence of mucus-producing cells was severely reduced in mice with deficient IL-17RA-signalling and TNFAIP3-deficient myeloid cells.

The IL-17RA subunit forms a heterodimer with either the IL-17RC or IL-17RB subunit. IL-17RA/C heterodimer is used by IL-17A, IL-17F, and IL-17A/F and the IL-17RA/B heterodimer is activated by IL-17E (also known as IL-25)[20]. Ablation of the IL-17RA subunit will therefore affect the signalling of IL-17A, IL-17F, IL-17A/F, and IL-25. We observed that neutrophilic inflammation and neutrophil chemo-attractants persisted in the absence of IL-17RA-signalling, indicating that neutrophilia can develop without the presence of the described IL-17R family members IL-17A, IL-17F, and IL-25. This is in contrast to other reports that showed dependency of neutrophil influx on IL-17RA-signalling not only in asthma and COPD, but also in pulmonary bacterial and viral infections[9, 11, 23, 42-44]. Neutrophil chemo-attractants CXCL1, CXCL2 and CXCL12 were not altered upon ablation of IL-17RA-signalling indicating that these chemo-attractants can be induced by factors independent of IL-17RA-signalling. Similar quantities of Th17-promoting cytokines IL-1β and IL-6 were found in the lungs of HDM-exposed *Tnfaip3*$^{LysM\text{-}KO}$ and *Tnfaip3*$^{LysM\text{-}KO}$*Il17ra*^{KO}

mice, whereas IL-23 expression was increased in HDM-exposed *Tnfaip3*$^{LysM\text{-}KO}$*Il17ra*^{KO} as compared to *Tnfaip3*$^{LysM\text{-}KO}$ mice. IL-1β has been shown to induce CXCL1 as efficiently as IL-17 by mouse embryonic fibroblasts[31]. Furthermore, IL-1β-deficient mice have defective neutrophil mobilization upon group B streptococcus infection, most likely caused by strongly reduced CXCL1 and CXCL2 production[35]. Likewise, IL-6 can induce CXCL1 transcription in endothelial cells[36]. This could indicate that pulmonary IL-1β and IL-6 expression in *Tnfaip3*$^{LysM\text{-}KO}$*Il17ra*^{KO} mice can induce CXCL1 expression by lung epithelial cells, independent of IL-17RA-signalling.

Ablation of IL-17RA-signalling alone only slightly increases the presence of IL-17-expressing T cells, however combined with *Tnfaip3*-deficient myeloid cells, pulmonary Th17 cells were massively enhanced in allergen-exposed *Tnfaip3*$^{LysM\text{-}KO}$*Il17ra*^{KO} mice. Increased pulmonary IL-23-expression, high levels of IL-1β and IL-6, and defective negative feedback normally provided by IL-17 in *Tnfaip3*$^{LysM\text{-}KO}$*Il17ra*^{KO} mice, could be responsible for this massive increase. It is known that IL-23 expression by myeloid cells, such as DCs and macrophages drives clonal expansion of Th17 cells[45], whereas IL-17 acts as a negative feedback to control its own expression[26]. Strikingly, only IL-23, and not IL-1β and IL-6, was specifically increased in *Tnfaip3*$^{LysM\text{-}KO}$*Il17ra*^{KO} mice when compared to *Tnfaip3*$^{LysM\text{-}KO}$ mice, suggesting that IL-17RA-signalling also controls IL-23 production.

We found limited effects of defective IL-17RA-signalling on all features observed in HDM-mediated allergic airway inflammation including Th2 differentiation and eosinophilic inflammation. This implicates that IL-17A, IL-17A/F, IL-17F and IL-25 are dispensable for Th2-mediated eosinophilic inflammation upon HDM treatment. Blockade of IL-17A also did not influence eosinophilic inflammation and Th2 cytokine secretion upon exposure to the HDM Der f allergen[42]. This is in contrast to ovalbumin (OVA)-mediated allergic airway models, where reduced eosinophilic inflammation, Th2 cytokines, and airway hyper responsiveness (AHR) were observed in either IL-17RA-deficient or IL-17-deficient mice[28, 29]. This suggests that the importance of IL-17 depends on the allergen/model used. While IL-17-depletion during HDM challenges has no effect on eosinophilia and Th2 cytokines[42], blockade of IL-17 during challenge in OVA-mediated models promotes Th2-mediated eosinophilic inflammation[28]. Treatment with recombinant IL-17 promotes inflammatory resolution upon OVA-mediated airway inflammation[30], indicating that IL-17 during the resolution phase can be beneficial.

Next to airway type-2 inflammation, goblet cell hyperplasia was also almost completely absent in *Tnfaip3*$^{LysM\text{-}KO}$*Il17ra*^{KO} mice. This suggests that the presence of Th2 cytokines in WT mice, or Th17 cytokines in *Tnfaip3*$^{LysM\text{-}KO}$ are essential for goblet cell hyperplasia. Indeed, mucus production by goblet cells is induced by Th2 cytokines IL-4, IL-13[46-49], and Th17 cytokines IL-17A[7] and IL-17F[50]. Furthermore, IL-25 (e.g. IL-17E) is also implicated in goblet cell hyperplasia[51, 52]. The combination of OVA-specific Th2 and Th17 cells was shown to induce more mucus-producing goblet cells than OVA-specific Th2

cells alone[53]. This indicates that both Th2 and Th17 cytokines can induce hyperplasia of mucus-producing cells separately and can even take over each other function, as combined absence of Th2 cytokines and abrogated IL-17RA-signalling in *Tnfaip3*$^{LysM\text{-}KO}$*Il17ra*^{KO} mice completely hampers the induction of goblet cell hyperplasia. Furthermore, mucus production by goblet cells in *Il17ra*^{KO} mice develops independent of IL-25.

In conclusion, our results show that neutrophilic airway inflammation induced by activated TNFAIP3/A20-deficient myeloid cells can develop in the absence of IL-17RA-signalling. Increased pulmonary pro-inflammatory cytokines IL-1β and IL-6 quantities are not influenced by IL-17RA-deficiency in mice with activated myeloid cells after HDM exposure. Both IL-1b and IL-6 can induce the expression of neutrophil chemo-attractants, contributing to neutrophilic airway inflammation independently of IL-17 signalling.

Acknowledgements

These studies were partly supported by NWO-VENI (916.11.067), European Framework program 7 (FP7-MC-CIG grant 304221), Dutch Arthritis Foundation (12-2-410) and the Netherlands Lung Foundation (3.2.12.087, 4.2.13.054JO). We would like to thank Dr. Louis Boon (Bioceros), Anne Huber and the Erasmus MC Animal Facility (EDC) staff for their assistance during the project.

Conflict of interest

The authors declare no conflict of interest.

REFERENCES

1. Holgate ST. Innate and adaptive immune responses in asthma. *Nature medicine* 2012; 18(5): 673-683.
2. Wenzel SE. Asthma phenotypes: the evolution from clinical to molecular approaches. *Nat Med* 2012; 18(5): 716-725.
3. Li BWS, Hendriks RW. Group 2 innate lymphoid cells in lung inflammation. *Immunology* 2013; 140(3): 281-287.
4. Wonnenberg B, Jungnickel C, Honecker A, Wolf L, Voss M, Bischoff M *et al.* IL-17A attracts inflammatory cells in murine lung infection with P. aeruginosa. *Innate immunity* 2016; 22(8): 620-625.
5. Chang Y, Al-Alwan L, Risse PA, Roussel L, Rousseau S, Halayko AJ *et al.* TH17 cytokines induce human airway smooth muscle cell migration. *J Allergy Clin Immunol* 2011; 127(4): 1046-1053 e1041-1042.
6. Chang Y, Al-Alwan L, Risse PA, Halayko AJ, Martin JG, Baglole CJ *et al.* Th17-associated cytokines promote human airway smooth muscle cell proliferation. *Faseb J* 2012; 26(12): 5152-5160.
7. Chen Y, Thai P, Zhao YH, Ho YS, DeSouza MM, Wu R. Stimulation of airway mucin gene expression by interleukin (IL)-17 through IL-6 paracrine/autocrine loop. *J Biol Chem* 2003; 278(19): 17036-17043.
8. Shaw DE, Berry MA, Hargadon B, McKenna S, Shelley MJ, Green RH *et al.* Association between neutrophilic airway inflammation and airflow limitation in adults with asthma. *Chest* 2007; 132(6): 1871-1875.
9. Manni ML, Trudeau JB, Scheller EV, Mandalapu S, Elloso MM, Kolls JK *et al.* The complex relationship between inflammation and lung function in severe asthma. *Mucosal Immunol* 2014; 7(5): 1186-1198.
10. Wenzel SE. Asthma phenotypes: the evolution from clinical to molecular approaches. *Nature medicine* 2012; 18(5): 716-725.
11. McKinley L, Alcorn JF, Peterson A, Dupont RB, Kapadia S, Logar A *et al.* TH17 cells mediate steroid-resistant airway inflammation and airway hyperresponsiveness in mice. *J Immunol* 2008; 181(6): 4089-4097.
12. Green RH, Brightling CE, Woltmann G, Parker D, Wardlaw AJ, Pavord ID. Analysis of induced sputum in adults with asthma: identification of subgroup with isolated sputum neutrophilia and poor response to inhaled corticosteroids. *Thorax* 2002; 57(10): 875-879.
13. Zhang Z, Biagini Myers JM, Brandt EB, Ryan PH, Lindsey M, Mintz-Cole RA *et al.* beta-Glucan exacerbates allergic asthma independent of fungal sensitization and promotes steroid-resistant TH2/TH17 responses. *J Allergy Clin Immunol* 2017; 139(1): 54-65 e58.
14. Vroman H, van den Blink B, Kool M. Mode of dendritic cell activation: the decisive hand in Th2/Th17 cell differentiation. Implications in asthma severity? *Immunobiology* 2015; 220(2): 254-261.
15. Wertz IE, O'Rourke KM, Zhou H, Eby M, Aravind L, Seshagiri S *et al.* De-ubiquitination and ubiquitin ligase domains of A20 downregulate NF-kappaB signalling. *Nature* 2004; 430(7000): 694-699.
16. Li X, Ampleford EJ, Howard TD, Moore WC, Torgerson DG, Li H *et al.* Genome-wide association studies of asthma indicate opposite immunopathogenesis direction from autoimmune diseases. *J Allergy Clin Immunol* 2012; 130(4): 861-868.e867.
17. Schuijs MJ, Willart MA, Vergote K, Gras D, Deswarte K, Ege MJ *et al.* Farm dust and endotoxin protect against allergy through A20 induction in lung epithelial cells. *Science (New York, NY)* 2015; 349(6252): 1106-1110.
18. Vroman H, Bergen IM, van Hulst JAC, van Nimwegen M, van Uden D, Schuijs MJ *et al.* TNF-alpha-induced protein 3 levels in lung dendritic cells instruct TH2 or TH17 cell differentiation in eosinophilic or neutrophilic

asthma. *J Allergy Clin Immunol* 2017; 6(17): 31422-31427.

19. Matmati M, Jacques P, Maelfait J, Verheugen E, Kool M, Sze M *et al.* A20 (TNFAIP3) deficiency in myeloid cells triggers erosive polyarthritis resembling rheumatoid arthritis. *Nat Genet* 2011; 43(9): 908-912.
20. Gaffen SL. Structure and signalling in the IL-17 receptor family. *Nat Rev Immunol* 2009; 9(8): 556-567.
21. Vereecke L, Sze M, Mc Guire C, Rogiers B, Chu Y, Schmidt-Supprian M *et al.* Enterocyte-specific A20 deficiency sensitizes to tumor necrosis factor-induced toxicity and experimental colitis. *J Exp Med* 2010; 207(7): 1513-1523.
22. Clausen BE, Burkhardt C, Reith W, Renkawitz R, Forster I. Conditional gene targeting in macrophages and granulocytes using LysMcre mice. *Transgenic Res* 1999; 8(4): 265-277.
23. Ye P, Rodriguez FH, Kanaly S, Stocking KL, Schurr J, Schwarzenberger P *et al.* Requirement of interleukin 17 receptor signaling for lung CXC chemokine and granulocyte colony-stimulating factor expression, neutrophil recruitment, and host defense. *J Exp Med* 2001; 194(4): 519-527.
24. Vroman H, Bergen IM, Li BW, van Hulst JA, Lukkes M, van Uden D *et al.* Development of eosinophilic inflammation is independent of B-T cell interaction in a chronic house dust mite-driven asthma model. *Clin Exp Allergy* 2016.
25. Ge S, Hertel B, Susnik N, Rong S, Dittrich AM, Schmitt R *et al.* Interleukin 17 receptor A modulates monocyte subsets and macrophage generation in vivo. *PLoS One* 2014; 9(1): e85461.
26. Smith E, Stark MA, Zarbock A, Burcin TL, Bruce AC, Vaswani D *et al.* IL-17A inhibits the expansion of IL-17A-producing T cells in mice through "short-loop" inhibition via IL-17 receptor. *J Immunol* 2008; 181(2): 1357-1364.
27. Stark MA, Huo Y, Burcin TL, Morris MA, Olson TS, Ley K. Phagocytosis of apoptotic neutrophils regulates granulopoiesis via IL-23 and IL-17. *Immunity* 2005; 22(3): 285-294.
28. Schnyder-Candrian S, Togbe D, Couillin I, Mercier I, Brombacher F, Quesniaux V *et al.* Interleukin-17 is a negative regulator of established allergic asthma. *J Exp Med* 2006; 203(12): 2715-2725.
29. Nakae S, Komiyama Y, Nambu A, Sudo K, Iwase M, Homma I *et al.* Antigen-specific T cell sensitization is impaired in IL-17-deficient mice, causing suppression of allergic cellular and humoral responses. *Immunity* 2002; 17(3): 375-387.
30. Murdoch JR, Lloyd CM. Resolution of allergic airway inflammation and airway hyperreactivity is mediated by IL-17-producing gamma delta T cells. *Am J Respir Crit Care Med* 2010; 182(4): 464-476.
31. Park H, Li Z, Yang XO, Chang SH, Nurieva R, Wang YH *et al.* A distinct lineage of CD4 T cells regulates tissue inflammation by producing interleukin 17. *Nat Immunol* 2005; 6(11): 1133-1141.
32. Witowski J, Pawlaczyk K, Breborowicz A, Scheuren A, Kuzlan-Pawlaczyk M, Wisniewska J *et al.* IL-17 stimulates intraperitoneal neutrophil infiltration through the release of GRO alpha chemokine from mesothelial cells. *J Immunol* 2000; 165(10): 5814-5821.
33. Zhang Y, Chen L, Gao W, Hou X, Gu Y, Gui L *et al.* IL-17 neutralization significantly ameliorates hepatic granulomatous inflammation and liver damage in Schistosoma japonicum infected mice. *Eur J Immunol* 2012; 42(6): 1523-1535.
34. Fleige H, Ravens S, Moschovakis GL, Bolter J, Willenzon S, Sutter G *et al.* IL-17-induced CXCL12 recruits B cells and induces follicle formation in BALT in the absence of differentiated FDCs. *J Exp Med* 2014; 211(4): 643-651.

35. Biondo C, Mancuso G, Midiri A, Signorino G, Domina M, Lanza Cariccio V *et al.* The interleukin-1beta/CXCL1/2/neutrophil axis mediates host protection against group B streptococcal infection. *Infection and immunity* 2014; 82(11): 4508-4517.
36. Roy M, Richard JF, Dumas A, Vallieres L. CXCL1 can be regulated by IL-6 and promotes granulocyte adhesion to brain capillaries during bacterial toxin exposure and encephalomyelitis. *Journal of neuroinflammation* 2012; 9: 18.
37. McDermott AJ, Falkowski NR, McDonald RA, Pandit CR, Young VB, Huffnagle GB. Interleukin-23 (IL-23), independent of IL-17 and IL-22, drives neutrophil recruitment and innate inflammation during Clostridium difficile colitis in mice. *Immunology* 2016; 147(1): 114-124.
38. Khajah M, Millen B, Cara DC, Waterhouse C, McCafferty DM. Granulocyte-macrophage colony-stimulating factor (GM-CSF): a chemoattractive agent for murine leukocytes in vivo. *Journal of leukocyte biology* 2011; 89(6): 945-953.
39. Aujla SJ, Chan YR, Zheng M, Fei M, Askew DJ, Pociask DA *et al.* IL-22 mediates mucosal host defense against Gram-negative bacterial pneumonia. *Nat Med* 2008; 14(3): 275-281.
40. Liang SC, Nickerson-Nutter C, Pittman DD, Carrier Y, Goodwin DG, Shields KM *et al.* IL-22 induces an acute-phase response. *J Immunol* 2010; 185(9): 5531-5538.
41. Al-Ramli W, Prefontaine D, Chouiali F, Martin JG, Olivenstein R, Lemiere C *et al.* T(H)17-associated cytokines (IL-17A and IL-17F) in severe asthma. *J Allergy Clin Immunol* 2009; 123(5): 1185-1187.
42. Chesne J, Braza F, Chadeuf G, Mahay G, Cheminant MA, Loy J *et al.* Prime role of IL-17A in neutrophilia and airway smooth muscle contraction in a house dust mite-induced allergic asthma model. *J Allergy Clin Immunol* 2015; 135(6): 1643-1643 e1643.
43. Crowe CR, Chen K, Pociask DA, Alcorn JF, Krivich C, Enelow RI *et al.* Critical role of IL-17RA in immunopathology of influenza infection. *J Immunol* 2009; 183(8): 5301-5310.
44. Yanagisawa H, Hashimoto M, Minagawa S, Takasaka N, Ma R, Moermans C *et al.* Role of IL-17A in murine models of COPD airway disease. *American journal of physiology Lung cellular and molecular physiology* 2017; 312(1): L122-l130.
45. McGeachy MJ, Chen Y, Tato CM, Laurence A, Joyce-Shaikh B, Blumenschein WM *et al.* The interleukin 23 receptor is essential for the terminal differentiation of interleukin 17-producing effector T helper cells in vivo. *Nat Immunol* 2009; 10(3): 314-324.
46. Webb DC, McKenzie AN, Koskinen AM, Yang M, Mattes J, Foster PS. Integrated signals between IL-13, IL-4, and IL-5 regulate airways hyperreactivity. *J Immunol* 2000; 165(1): 108-113.
47. Temann UA, Prasad B, Gallup MW, Basbaum C, Ho SB, Flavell RA *et al.* A novel role for murine IL-4 in vivo: induction of MUC5AC gene expression and mucin hypersecretion. *Am J Respir Cell Mol Biol* 1997; 16(4): 471-478.
48. Dabbagh K, Takeyama K, Lee HM, Ueki IF, Lausier JA, Nadel JA. IL-4 induces mucin gene expression and goblet cell metaplasia in vitro and in vivo. *J Immunol* 1999; 162(10): 6233-6237.
49. Cohn L, Homer RJ, MacLeod H, Mohrs M, Brombacher F, Bottomly K. Th2-induced airway mucus production is dependent on IL-4Ralpha, but not on eosinophils. *J Immunol* 1999; 162(10): 6178-6183.
50. Oda N, Canelos PB, Essayan DM, Plunkett BA, Myers AC, Huang SK. Interleukin-17F induces pulmonary neutrophilia and amplifies antigen-induced allergic response. *Am J Respir Crit Care Med* 2005; 171(1): 12-18.
51. Angkasekwinai P, Park H, Wang YH, Wang YH, Chang SH, Corry DB *et al.* Interleukin

25 promotes the initiation of proallergic type 2 responses. *J Exp Med* 2007; 204(7): 1509-1517.

52. Ballantyne SJ, Barlow JL, Jolin HE, Nath P, Williams AS, Chung KF *et al.* Blocking IL-25 prevents airway hyperresponsiveness in allergic asthma. *J Allergy Clin Immunol* 2007; 120(6): 1324-1331.

53. Wang YH, Voo KS, Liu B, Chen CY, Uygungil B, Spoede W *et al.* A novel subset of CD4(+) T(H)2 memory/effector cells that produce inflammatory IL-17 cytokine and promote the exacerbation of chronic allergic asthma. *J Exp Med* 2010; 207(11): 2479-2491.

Supplementary Table 1: Antibodies used for flow cytometry.

Antibody	Conjugate	Clone	Company
CD3	APC-eF780	17A2	ebioscience
CD4	PE-CF594	RM4-5	BD
CD4	BV711	RM4-5	BD
CD8	PE-Cy7	53-6.7	ebioscience
CD11b	PerCP-cy5.5	M1/70	BD Bioscience
CD11c	PE Texas Red	N418	ebioscience
CD25	Pe-Cy7	PC61.5	ebioscience
CD27	Biotin	LG.7F9	ebioscience
CD44	FITC	IM7	ebioscience
CD44	APC-cy7	IM7	BD
CD45	PE Texas Red	I3/2.3	Abcam
CD64	APC	X54-5/7.1	BD
CD64	PE	X54-5/7.1	BD
CD86	PE Cy7	GL1	BD
CD103	APC	2E7	ebioscience
FcƐRI	Biotin	MAR-1	ebioscience
GR1	Pe-cy7	1A8	BD
IFNγ	eF450	XMG1.2	ebioscience
IL-5	PE	TRFK-5	BD
IL-5	APC	TRFK-5	BD
IL-13	AF647	eBio13A	ebioscience
IL-17A	AF700	TC11-18H10.1	BD
MHC-II	Alexa Fluor 700	M5/114.15.3	ebioscience
RORγt	PE	Q31-378	BD
Streptavidin	PerCP-Cy5.5		BD
Streptavidin	APC-eF 780		ebioscience
Streptavidin	Brilliant Violet 786		BD
TCRγδ	Biotin	UC7-13D5	ebioscience
Ter119	APC	TER-119	ebioscience

Supplementary Table 2: The RT-PCR primers have been listed with the gene name, corresponding encoded protein and forward/reverse sequence.

Gene name	Encoded Protein	Forward sequence	Reverse sequence
Csf2	GM-CSF	AAAGGGACCAAGAGATGTGGC	GTTTGTCTTCCGCTGTCCAAG
Cxcl1	CXCL1	CTGGGATTCACCTCAAGAACATC	CAGGGTCAAGGCAAGCCTC
Cxcl12	CXCL12	GTCAGCCTGAGCTACCGATG	TTCTTCAGCCGTGCAACAATC
Cxcl2	CXCL2	CGCTGTCAATGCCTGAAG	GGCGTCACACTCAAGCTCT
Gapdh	GAPDH	TTCACCACCATGGAGAAGGC	GGCATGGACTGTGGTCATGA
Il1b	IL-1β	AGTTGACGGACCCCAAAAG	TTTGAAGCTGGATGCTCTCAT
Il22	IL-22	GTGACGACCAGAACATCCAG	TCCACTCTCTCCAAGCTTTTTC
Il23	IL-23	CCAGCGGGACATATGAATCT	TGGATACGGGGCACATTATT
Il6	IL-6	ACACATGTTCTCTGGGAAATCGT	AAGTGCATCATCGTTGTTCATACA
Muc5a	Mucin 5AC	ACCACTTTCTCCTTCTCCACAC	CCCCTGAGGACCCTACACTC

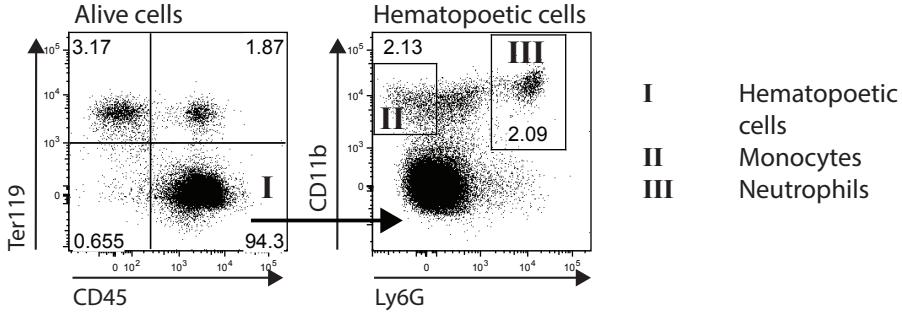

Supplementary Figure 1: Flow cytometric gating strategy of myeloid cells. An example is shown of a spleen derived from a WT mouse.

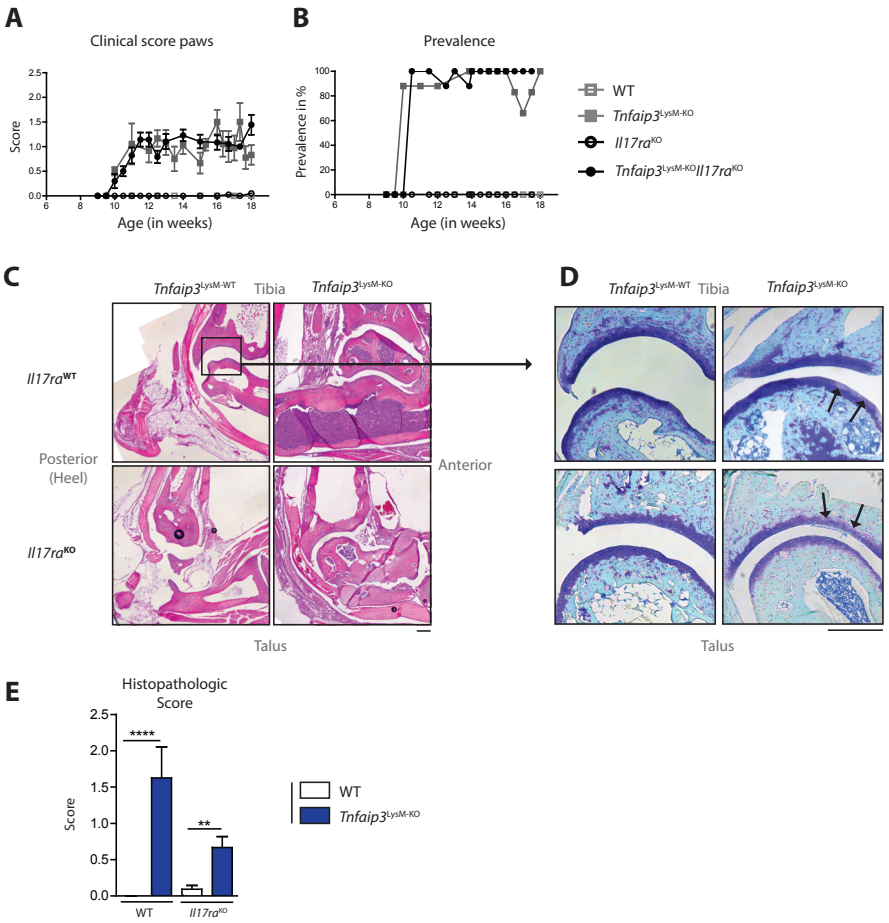

Supplementary Figure 2: Aged myeloid *Tnfaip3*-deficient mice develop arthritis, regardless of IL-17RA-signalling.

Mice were analysed at 18 weeks of age when arthritis had spontaneously developed. (**A-B**) Paws were scored biweekly for severity (**A**) and the derived prevalence graph (**B**) of spontaneous arthritis is shown. (**C**) Hematoxylin and eosin (H&E) stained paraffin embedded, EDTA decalcified, talo-tibial joints at a magnification of 50x is shown. (**D**) Tolluidine blue stain of the talo-tibial cartilage region is depicted at a magnification of 200x. Arrows represent areas of cartilage loss. Scale bars (200µm) are at the lower right corner of the microscopic images. (**E**) Histopathologic score of talo-tibial joints as assessed by combining H&E and toluidine blue stain scores. Results are presented as mean ± SEM of n = 4-10 per group and are pooled from several experiments. $^{**}P < 0.01$, $^{**}P < 0.001$, $^{****}P < 0.0001$.

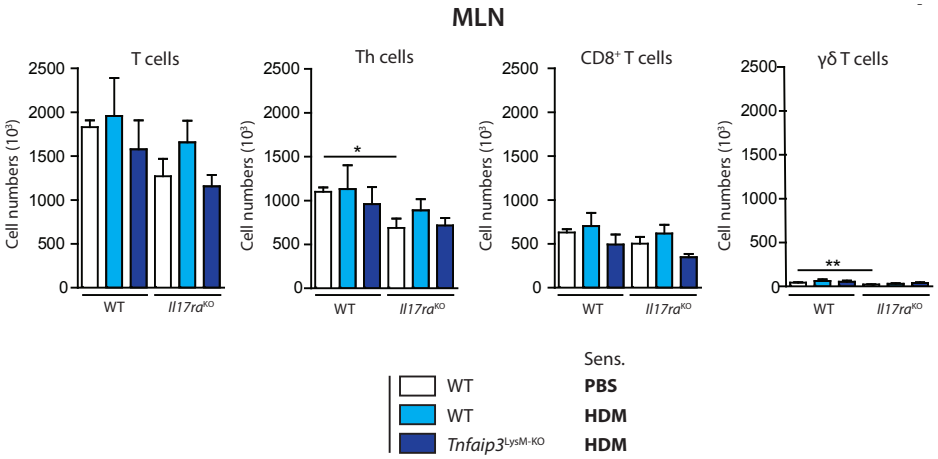

Supplementary Figure 3: HDM exposure does not lead to increased T cells or γδ T cells in the MLN of myeloid *Tnfaip3*-deficient and IL-17RA-signalling deficient mice.
Quantification of total CD3+ T cells, Th cells, CD8+ T cells and γδ T cells in cell suspensions of the mediastinal lymph node (MLN) using flow cytometry. Results are presented as mean ± SEM of $n = 6$ per group. *$P < 0.05$, **$P < 0.01$.

SUPPLEMENTARY MATERIAL METHODS:

Assessment of joint swelling

To assess the degree of joint swelling, we evaluated hind and front paws swelling of mice from 6 weeks of age giving a maximum score of 2 per paw (Corneth et al, Arthritis Rheum, 2014), rising to a theoretical total of 8 per mouse. Mice were removed from the experiment with scores of 6 to alleviate suffering. Disease severity and incidence were monitored.

Histology

Ankle joints were fixed in formalin, decalcified in EDTA and embedded in paraffin. The tissues were stained with Hematoxylin and Eosin (H&E) to visualize the structure of bone. Toluidine blue staining was done to assess the cartilage integrity (Schmitz et al, Osteoarthritis Cartilage, 2010). Each histology slide was arbitrarily scored for tissue inflammation and cartilage integrity by two independent blinded researchers.

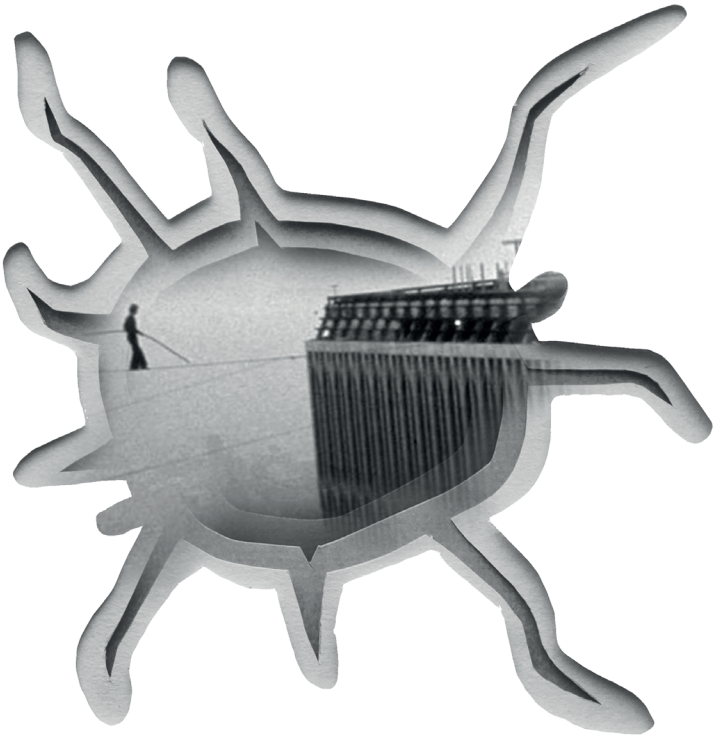

Chapter 5

Developmental B-cell defects within a model of A20/Tnfaip3-deficient dendritic cells.

Tridib Das, Ingrid Bergen, Menno van Nimwegen, Jennifer van Hulst, Marjolein de Bruijn, Geert van Loo, Bart N. Lambrecht, Rudi W. Hendriks

Manuscript in preparation

ABSTRACT

Background: Dendritic cells (DCs) are central regulators of tolerance versus immunity. Mice with a DC-specific deficiency of deubiquitinating enzyme A20/*Tnfaip3* (*Tnfaip3*$^{CD11c\text{-}cre}$), a major negative regulator of NF-κB signaling, exhibit increased DC activation. Aged *Tnfaip3*$^{CD11c\text{-}cre}$ mice show activation of mature B cells and develop humoral autoimmunity resembling systemic lupus erythematosus (SLE). In addition, mature B cells are severely decreased in numbers.

Objective: To identify the arrest in B cell development in *Tnfaip3*$^{CD11c\text{-}cre}$ mice and to investigate whether mature peripheral B cells have functional defects.

Methods: B cell development was studied in bone marrow and spleen of 6-week-old and 24-week-old *Tnfaip3*$^{CD11c\text{-}cre}$ mice. Splenic naïve B cells were stimulated *in vitro* to measure cellular activation and immunoglobulin production capacity. *In vivo* B cell responses were determined.

Results: B cell development in the bone marrow was hampered at the immature B cell stage in 6-week-old *Tnfaip3*$^{CD11c\text{-}KO}$ mice and at the pre-B cell stage in 24-week-old *Tnfaip3*$^{CD11c\text{-}KO}$ mice. The observed age-dependent developmental arrest of B-lineage cells most likely reflected changes in the bone marrow micro-environment. Although development of B-1 cells in *Tnfaip3*$^{CD11c\text{-}KO}$ appeared impaired, the IgM and IgG3 B cell responses to T cell independent antigen DNP-Ficoll were unaffected. While serum immunoglobulin levels were increased, *Tnfaip3*$^{CD11c\text{-}KO}$ mice displayed a defective T cell-dependent B cell response *in vivo*. In addition, mature naïve peripheral B cells from *Tnfaip3*$^{CD11c\text{-}KO}$ mice showed increased activation upon *in vitro* stimulation compared with control mice.

Conclusion: DC-specific deficiency of A20/*Tnfaip3* is associated with defective B cell development, reflecting a dysfunctional bone marrow micro-environment. The observed defects may contribute to defective immune homeostasis and autoimmunity in *Tnfaip3*$^{CD11c\text{-}KO}$ mice.

INTRODUCTION

Systemic lupus erythematosus (SLE) is a multifactorial disease[1]. Often malfunction of multiple innate and adaptive immune cell types, such as dendritic cells (DCs), T cells and B cells lies at the base of the autoimmune phenotype[1]. B cells can contribute to pathology by autoantigen presentation, secretion of pro-inflammatory cytokines, ectopic germinal center generation and autoantibody secretion[2]. DCs have a crucial role in the maintenance of tolerance[3]. Control of immune cell activation is essential to prevent autoimmunity. For example, transgenic removal of regulatory proteins such as the tyrosine kinase Lyn or Src homology region 2 domain–containing phosphatase-1 (SHP1) in B cells[4, 5] or DCs[6, 7] in mice results in the spontaneous development of SLE symptoms.

Proper signals within the NF-κB pathway are also essential to maintain tolerance[8]. Tumor necrosis factor alpha-induced protein 3 (TNFAIP3), also known as A20, is one of the major negative regulators of the NF-κB pathway[9]. Targeted deletion of the *Tnfaip3* gene in B cells or DCs in mice resulted in spontaneous autoimmunity resembling SLE and was characterized by increased germinal center (GC) responses, autoantibody production and glomerulonephritis[10, 11]. Interestingly, in mature 24-week-old mice in which the *Tnfaip3* gene was conditionally deleted in DCs, the numbers of B cells in the periphery were reduced, indicating that B cell development may be disturbed.

Development of autoreactive B cells in the bone marrow is prevented by various central tolerance mechanisms, including receptor editing[12, 13] and clonal deletion[14]. Tolerance mechanisms that function at later stages, such as B cell anergy[15], are referred to as peripheral tolerance. Because defects due to central tolerance can be observed in autoimmune patients with rheumatoid arthritis (RA)[16, 17], type 1 diabetes (T1D)[16] and SLE[18-20], as well as in corresponding mouse models[21, 22], we investigated B cell development in the bone marrow and peripheral B cell function in A20/*Tnfaip3*$^{CD11c\text{-}KO}$ mice.

In this study, we demonstrate that B cell development is hampered in the bone marrow of *Tnfaip3*$^{CD11c\text{-}KO}$ mice in an age-dependent fashion. Mature B cells that reach the periphery exhibit various abnormalities. They display a more activated phenotype upon activation *in vitro*, but fail to efficiently respond to a T cell-dependent antigen *in vivo*. Thus, hyperactivation of DCs, due to loss of A20/*Tnfaip3*, did not only deregulate mature T and B cells, but also disturbed B cell development in the bone marrow.

MATERIAL & METHODS

Mice

Male and female C57BL/6 mice harbouring a conditional *Tnfaip3* allele flanked by LoxP sites[23], were crossed onto a transgenic line expressing the Cre recombinase under the

control of the *CD11c* promotor[24], generating CD11c-Cre transgenic *Tnfaip3*$^{fl/fl}$ mice (*Tnfaip3*$^{CD11c\text{-}KO}$ mice). CD11c-Cre non-transgenic *Tnfaip3*$^{fl/fl}$ littermates (*Tnfaip3*$^{CD11c\text{-}WT}$ mice) served as controls and heterozygous CD11c-Cre transgenic *Tnfaip3*$^{fl/+}$ mice (*Tnfaip3*$^{CD11c\text{-}HZ}$) mice were also analyzed. Mice were sacrificed at ~6-8 weeks or ~24-26 weeks of age. Mice were housed under specific pathogen-free conditions and attained food and water ad libitum. All experiments were approved by the animal ethical committee of the Erasmus MC, Rotterdam, The Netherlands.

Cell suspension preparation

Spleen, bone marrow (BM) and mesenteric lymph node (MesLN) were obtained using standard procedures. The hind legs were crushed initially, and spleen and MesLN were homogenized through a 100-µm cell strainer to obtain single-cell suspensions. To remove erythrocytes, spleens and BM were lysed using an osmotic lysis buffer (8.3% NH_4CL, 1% $KHCO_3$, and 0.04% NA_2EDTA in Milli-Q).

Flow cytometry procedures

Flow cytometry surface and intracellular staining procedures have been described previously[25]. Monoclonal antibodies used for flow cytometric analyses are listed in **Supplementary Table 1**. For all experiments, dead cells were excluded using fixable AmCyan viability dye (eBioscience, San diego, CA, USA). To measure cytokine production (in the case of B cells), cells were stimulated with 10 ng/mL Phorbol 12-myristate 13-acetate PMA (Sigma-Aldrich, St. Louis, MI, USA) and 250 ng/mL ionomycin (Sigma-Aldrich) in the presence of GolgiStop (BD Biosciences, San Jose, CA, USA) for 4 hrs at 37°C. To measure cytokine production in DCs, cells were kept in the presence of GolgiPlug (BD Biosciences) for 4 hrs at 37 °C. Data were acquired using an LSR II flow cytometer (BD Biosciences) with FACS Diva™ software and analysed by FlowJo version 9 (Tree Star Inc software, Ashland, OR, USA).

In vitro B cell stimulation

Via MACS separation (Miltenyi Biotec, Bergisch Gladbach, Germany) naïve B cells were isolated from spleen single-cell suspensions via negative selection. Cells were labeled with the biotin-conjugated markers NK1.1, CD4, CD8, Ter119, CD11c, GR-1, FcRI, CD5, CD43, CD138, CD11b, CD95 and Streptavidin Microbreads (Miltenyi Biotec).

For investigating B cell activation markers, naïve B cells were stimulated with 10 µg/ml anti-IgM F'ab fragments (Jackson Immunoresearch, West Grove, PA, USA), 5 ng/ml LPS (Enzo Life Sciences, Farmingdale, NY, USA), 1 µM CpG (Invitrogen, Carlsbad, CA, USA) or 20 µg/ml anti-CD40 (BD Biosciences, San Jose, CA, USA) overnight in RPMI medium (Thermo Fisher, Waltham, Massachusetts) supplemented with gentamycin (Thermo Fisher), β-mercapto-ethanol (Sigma) and 5% Fetal Bovine Serum (Capricorn Scientific,

Ebsdorfergrund, Germany). To investigate immunoglobulin production, naïve B cell fractions were stimulated for 4 days in context of LPS (Enzo Life Sciences) with/without IL-4 (Peprotech, Rocky Hill, NJ, USA).

IL-7 culture of small pre-B cells and immature B cells

Hind legs of *Tnfaip3*$^{CD11c\text{-}KO}$ and *Tnfaip3*$^{CD11c\text{-}WT}$ mice were crushed and erythrocytes were lysed. After labeling with anti-CD19 beads, B cells were positively separated from the CD19^{neg} fraction that also contains stromal cells, using a MACS column. In a 24-wells plate, 2 x 10^6 stroma cells and 300.000 B cells, from either *Tnfaip3*$^{CD11c\text{-}KO}$ or *Tnfaip3*$^{CD11c\text{-}WT}$ mice, were cultured in 1 ml IMDM medium supplemented with gentamycin (Thermo Fisher), β-mercaptoethanol (Sigma), 5% Fetal Bovine Serum (Capricorn Scientific, Ebsdorfergrund, Germany), Glutamine (Gibco) and 100U/ml recombinant IL-7 (Peprotech) per well. B cell and stromal cell suspensions were sex-matched. On day 4, cells were harvested, washed and cultured with or without the presence of IL-7 for 2 days. At day 7, cells were prepared for FACS analysis.

DNP-Ficoll and OVA-Alum immunization

For T cell–independent immunization, 50 μg of DNP(49)-Ficoll (Biosearch Technologies, Petaluma, CA, USA) in PBS was injected i.p. Serum was collected at baseline and 7 days after immunization.

For T cell-dependent immunization, mice received 10 μg OVA (Worthington Biochemical Corp, Lakewood, NJ, USA) i.p. in a saline solution containing 1:20 Imject-alum adjuvant (Thermo Scientific). The mixture was left stirring for 1hr, and then 500μl of OVA-Alum solution was injected per mouse. A booster was given after 1 week. Serum was collected at a pre-immune timepoint, at 8 days and 15 days after booster immunization.

Immunoglobulin levels

For quantification of total immunoglobulin (Ig) levels, Nunc Microwell plates (Life technologies, Carlsbad, CA, USA) were coated overnight at 4C^{o} with 1 μg/ml goat-anti-mouse Ig$_x$ (being the immunoglobulin isotype, Southern Biotech, Birmingham, AL, USA). Wells were blocked with 10% FCS/PBS for 1 hr. Subsequently, standards and serum (diluted in multiple series) were incubated for 3 hrs. Depending on the isotype, anti-mouse Ig$_x$ biotin/streptavidin-HRP were used to develop the ELISA.

For DNP-specific sandwich ELISA assays, Nunc Microwell plates were coated with DNP-Ficoll in 0.1M carbonate buffer (pH 9.5); the standard curve wells were plated with purified unlabeled goat anti-IgM or IgG3 (Southern Biotech) in PBS overnight at 4C^{o}. Wells were blocked with 1% BSA for 1 hr, followed by 3 hrs of incubation with serum samples (diluted in multiple series) and standard IgM or IgG3. Anti-mouse Ig$_x$ biotin/streptavidin-HRP was used to develop the ELISA.

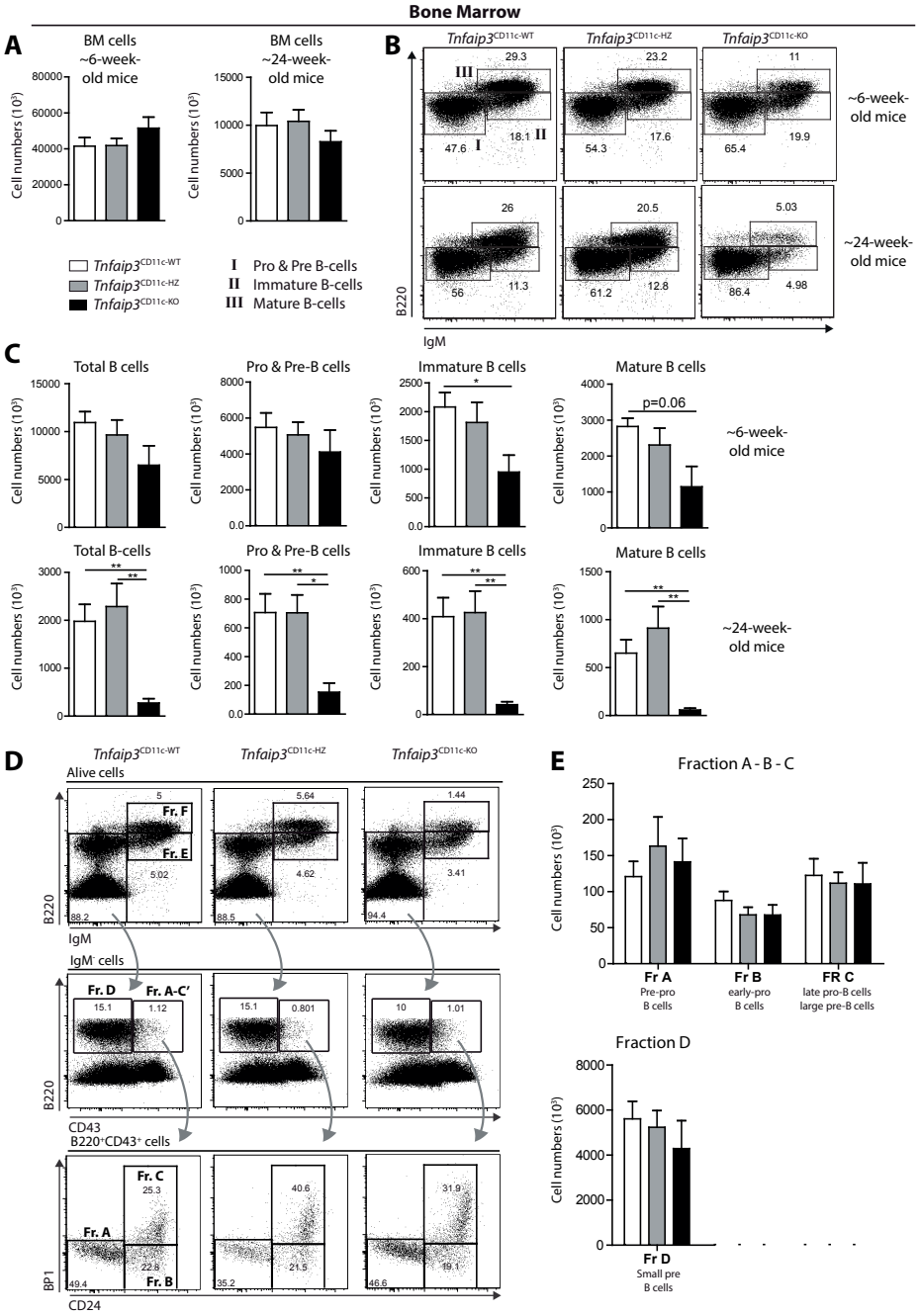

Figure 1: Age-dependent arrest in B cell development in the bone marrows of *Tnfaip3*$^{CD11c\text{-}KO}$ mice.
(**A**) Enumeration of total bone marrow cells in *Tnfaip3*$^{CD11c\text{-}WT}$, *Tnfaip3*$^{CD11c\text{-}HZ}$ and *Tnfaip3*$^{CD11c\text{-}KO}$ mice at the indicated age, using flow cytometry. (**B**) Flow cytometric analysis of bone marrow Pro-/Pre-B cells ($CD19^+B220^{lo}IgM^-$), immature B cells ($CD19^+B220^{lo}IgM^+$) and mature B cells ($CD19^+B220^{hi}IgM^+$). Representa-

tive examples of gated CD19$^+$ lymphoid cells fractions are shown from *Tnfaip3*$^{CD11c\text{-}WT}$, *Tnfaip3*$^{CD11c\text{-}HZ}$ and *Tnfaip3*$^{CD11c\text{-}KO}$ mice. (**C**) Quantification of total B cells, Pro-/Pre-B cells, immature B cells and mature B cells in bone marrow of mice (legend shown in panel A) at the indicated age. (**D**) Flow cytometric analysis of bone marrow total lymphoid cells, showing B cell stages according to Hardy et al.[26] in representative examples from three genotypes in 6-week-old mice. (**E**) Quantification of Hardy fraction A (B220^{lo}IgM$^-$CD43$^+$BP1$^-$CD24$^-$), Hardy fraction B (B220^{lo}IgM$^-$CD43$^+$BP1$^-$CD24$^+$), Hardy fraction C (B220^{lo}IgM$^-$CD43$^+$BP1$^+$CD24$^+$), Hardy fraction D (B220^{lo}IgM$^-$CD43$^-$), Hardy fraction E (B220^{lo}IgM$^+$) and Hardy fraction F (B220^{hi}IgM$^+$), using flow cytometry in 6-week-old mice. Results are representative of 3 independent experiments and are presented as mean values ± SEM of n = 4-6 per group. *P<0.05, **P < 0.01 using the Mann-whitney U statistical test.

Statistics

Statistical significance of data was calculated using the non-parametric Mann Whitney U test. P-values <0.05 were considered significant. All data were plotted as mean values with the standard error of the mean (SEM).

RESULTS

Age-dependent arrest in B cell development in the bone marrows of *Tnfaip3*$^{CD11c\text{-}KO}$ mice.

To investigate how DC-specific A20/*Tnfaip3* deficiency affects B cell development, we analyzed bone marrows of ~6-week-old and ~24-week-old *Tnfaip3*$^{CD11c\text{-}KO}$ mice, as well as *Tnfaip3*$^{CD11c\text{-}HZ}$ and *Tnfaip3*$^{CD11c\text{-}WT}$ controls. Bone marrow total cell counts did not differ between the three genotypes at either age (**Figure 1A**). We used flow cytometry to quantify the populations of developing B cells in the bone marrow and found that at the age of ~6 weeks the *Tnfaip3*$^{CD11c\text{-}KO}$ mice had significantly lower numbers of immature B cells compared to *Tnfaip3*$^{CD11c\text{-}WT}$ controls (**Figure 1B,1C**). These young mice showed a near-significant reduction of mature B cells. However, at the age of 24 weeks, the total numbers of bone marrow B cells, pro/pre B cells, immature B cells and mature B cells were significantly reduced in *Tnfaip3*$^{CD11c\text{-}KO}$ mice compared to WT and *Tnfaip3*$^{CD11c\text{-}HZ}$ mice (**Figure 1C**), indicating a progressive loss of mature B cell development over time.

Because we found evidence for a B cell development disorder already at ~6 weeks of age, we investigated mice at this age for the remaining experiments. To identify the individual stages of early B cell development, we used the classification according to Hardy et al[26]. The total numbers of pre/pro-B cells within Hardy fractions A, B or C were not different between the three genotypes (**Figure 1D,1E**). Accordingly, as proportions of these fractions from live cells, all these fractions showed no differences across the genotypes (**Supplementary Figure 1**). Although a significant decrease of the proportions of small pre-B cells (Hardy fraction D) was noticed in *Tnfaip3*$^{CD11c\text{-}KO}$ mice compared to *Tnfaip3*$^{CD11c\text{-}WT}$ mice (**Supplementary Figure 1**), there was no significant reduction of the absolute cell numbers of fraction D small pre-B cells (**Figure 1E**). As a proportion

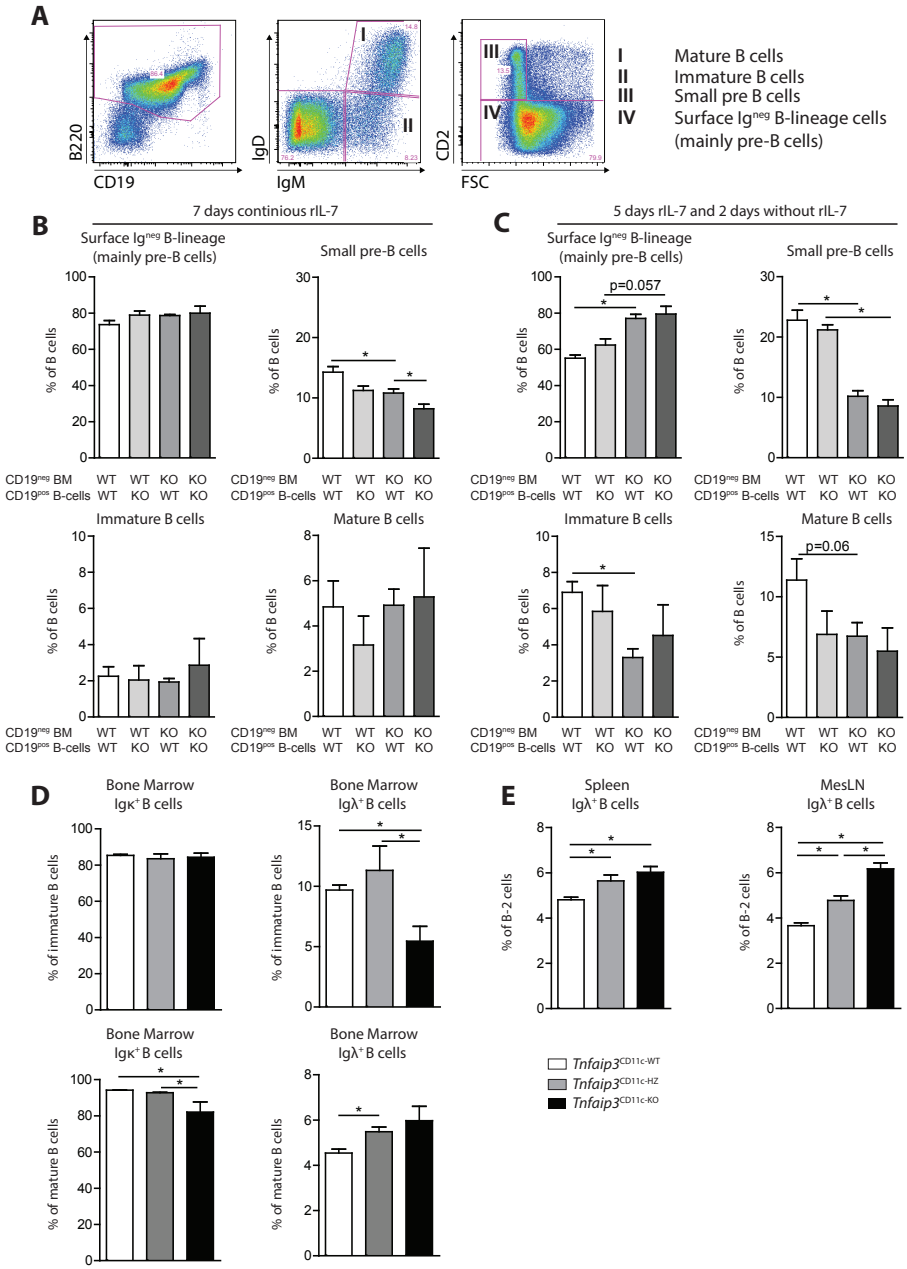

Figure 2: Cell non-intrinsic defect in B lineage cells and evidence for aberrant BCR repertoire selection of Igλ B cells in *Tnfaip3*$^{CD11c\text{-}KO}$ mice.

Combinations of CD19^{pos} and CD19^{neg} fractions from bone marrows of *Tnfaip3*$^{CD11c\text{-}WT}$ mice (termed 'WT') and *Tnfaip3*$^{CD11c\text{-}KO}$ mice (termed 'KO') were cultured in vitro. (A) Flow cytometric analysis of *in vitro* Mature B cells (B220^{+}CD19^{+}IgD^{hi}IgM^{hi}), immature B cells (B220^{+}CD19^{+}IgD^{lo}IgM^{hi}), small pre-B cells (B220^{+}CD19^{+}IgD^{lo}IgM^{lo}CD2^{+}FSC^{lo}) and remaining surface Ig^{neg} B-lineage cells containing mainly large cy-

cling pre-B cells ($B220^+CD19^+IgD^{neg}IgM^{lo/neg}CD2^-$). (**B-C**) Quantification of previously described (in **A**) B cell proportions in continuous presence of IL-7 (**B**) and in absence of IL-7 during the last 2 days of culture (**C**) using flow cytometry. (**D**) Quantification of the proportion of $Ig\kappa^+$ and $Ig\lambda^+$ light chain of immature B cells and mature B cells in the bone marrow using flow cytometry. (**E**) The percentage $Ig\lambda^+$ B cells in spleen and Mesenteric Lymph node (MesLN) quantified using flow cytometry. Results are presented as mean values ± SEM of $n = 4$-6 per group. *$P<0.05$ using the Mann-whitney U statistical test.

of live cells, immature B cells and mature B cells (Fractions E and F, respectively), were decreased in *Tnfaip3*$^{CD11c\text{-}KO}$ mice compared to *Tnfaip3*$^{CD11c\text{-}WT}$ mice (**Supplementary Figure 1**).

In conclusion, ~6-week-old *Tnfaip3*$^{CD11c\text{-}KO}$ mice have a B cell development disorder at the transition of small pre-B cells to immature B cells. This progresses over time, resulting in a reduction of all B cell stages at 24 weeks of age.

Cell non-intrinsic defect in B lineage cells in *Tnfaip3*$^{CD11c\text{-}KO}$ mice.

Since the *Tnfaip3* gene was specifically deleted in DCs, it was highly unlikely that the observed B cell arrest in *Tnfaip3*$^{CD11c\text{-}KO}$ mice was due to an intrinsic B cell defect. Rather, the defective B cell development in these mice might be explained by changes in the cytokine milieu or cell-cell interactions in the bone marrow micro-environment. For example, it has been reported that cytokines such as IL-1α[27] or IL-1β[28], interferon **(**IFN) α or β [29, 30], IFNγ[31] or TNFα[32] can hamper B cell development in the bone marrow. It is therefore conceivable that high systemic levels of pro-inflammatory cytokines – associated with the autoimmune phenotype – affect B lymphopoiesis.

We utilized an *in vitro* co-culture system to distinguish whether the small pre-B cell to immature B cell transition was hampered due to local cytokines signals or due to anomalous cell-cell interactions between developing B cells and stromal components or myeloid cells, including DCs, present in the bone marrow. We assumed that in such an *in vitro* co-culture all inhibitory cytokines present that would have been present in the bone marrow *in vivo* were removed by the extensive washing procedures. As IL-7 is crucial for B cell development, we performed *in vitro* IL-7-driven bone marrow co-cultures of magnetically sorted $CD19^{pos}$ B-lineage cell fractions in combination with $CD19^{neg}$ fractions containing bone marrow stromal cells as well as myeloid cells. In these experiments, we used various combinations of $CD19^{pos}$ and $CD19^{neg}$ fractions of *Tnfaip3*$^{CD11c\text{-}KO}$ or *Tnfaip3*$^{CD11c\text{-}WT}$ bone marrows. Continuous IL-7 supplementation is known to support pre-B cell survival and proliferation and to limit the developmental progression of pre-B cells into IgM^+ immature B cells[33]. This condition resulted in a major population (~80%) of surface Ig^{neg} B cells that precede small pre-B cells, such as large pre-B cells (**Figure 2B**; for gating strategy see **Figure 2A**). This condition also results in a low percentage of small pre-B cells, immature B cells and mature B cells of about ~10%, ~2% and ~4%, respectively, irrespective of the genotypes of the $CD19^{pos}$ and $CD19^{neg}$ cell fractions (**Fig-**

ure 2B). A moderate, yet significant, reduction of the proportions of small pre-B cells was observed in the co-cultures of *Tnfaip3*$^{CD11c\text{-}WT}$ CD19^{pos} B cell fractions and *Tnfaip3*$^{CD11c\text{-}KO}$ CD19^{neg} supporting cells, in comparison to WT cultures of CD19^{pos} and CD19^{neg} fractions, and also in comparison to the condition with both CD19^{pos} and CD19^{neg} fractions from *Tnfaip3*$^{CD11c\text{-}KO}$ mice (**Figure 2B**).

Upon removal of IL-7 after 5 days of culture, pre-B cells stop cycling and a proportion of the pre-B cells generally proceeds to the IgM^{+} immature B cell stage[33]. Thus, the proportions of small pre-B cells were expected to rise, which however only occurred in conditions whereby B-lineage cells were cultured with *Tnfaip3*$^{CD11c\text{-}WT}$ CD19^{neg} supporting cells, irrespective of the *Tnfaip3*$^{CD11c\text{-}WT}$ or *Tnfaip3*$^{CD11c\text{-}KO}$ genotype of the B-lineage cell fractions (**Figure 2C**). In contrast, the CD19^{neg} fraction from *Tnfaip3*$^{CD11c\text{-}KO}$ bone marrow hampered the efficient generation of small pre-B cells, both from *Tnfaip3*$^{CD11c\text{-}KO}$ and *Tnfaip3*$^{CD11c\text{-}WT}$ CD19^{pos} B-lineage cells (**Figure 2C**). Consistently, the largest population cells that contained the pre-B cells, were reduced in the conditions that gave rise to high small pre-B cells (**Figure 2C**). After withdrawal of IL-7, the proportions of immature B cells were also higher in the presence of *Tnfaip3*$^{CD11c\text{-}WT}$ than *Tnfaip3*$^{CD11c\text{-}KO}$ CD19^{neg} supporting cells, which reached significance for B-lineage cells from *Tnfaip3*$^{CD11c\text{-}WT}$ bone marrow (**Figure 2C**).

Taken together, these *in vitro* experiments support a cell non-intrinsic defect in B lineage cells in *Tnfaip3*$^{CD11c\text{-}KO}$ mice. Our finding that the function of *Tnfaip3*$^{CD11c\text{-}KO}$ CD19^{neg} supporting cells *in vitro* was impaired, suggest that inhibitory signals from cytokines are not directly responsible for the defective B cell development in *Tnfaip3*$^{CD11c\text{-}KO}$ mice.

Evidence for aberrant BCR repertoire selection of Igλ B cells in *Tnfaip3*$^{CD11c\text{-}KO}$ mice.

After successful rearrangement of the Ig heavy chain, immunoglobulin light (IgL) chain rearrangement is initiated at the transition from large to small pre-B cells[33]. The light chain can be either Igκ or Igλ[34], whereby Igλ^{+} B cells often contain non-productive Igκ rearrangements or productive Igκ rearrangements that are associated with autoreactivity[35]. We thus investigated Igκ and Igλ light chain usage in immature B cells and mature B cells within the bone marrow samples (For gating strategy according to Dingjan et al[36], see **Supplementary Figure 2A**). As expected, the majority of immature B cells was Igκ^{+}, irrespective of the genotype (**Figure 2D**). Importantly, we found that the proportions of Igλ^{+} immature B cells was significantly reduced in *Tnfaip3*$^{CD11c\text{-}KO}$ mice compared to WT controls (**Figure 2D**). In contrast, mature B cells had significantly reduced Igκ^{+} proportions in *Tnfaip3*$^{CD11c\text{-}KO}$ compared to WT mice, while a non-significant rise of the proportions of Igλ^{+} cells in the population of recirculating mature B cells was observed (**Figure 2D**).

Mature B cell populations in peripheral organs such as spleen (For gating strategy according to Dingjan et al[36], see **Supplementary Figure 2B**) and mesenteric lymph node (MesLN) from *Tnfaip3*$^{CD11c\text{-}KO}$ mice and *Tnfaip3*$^{CD11c\text{-}HZ}$ mice displayed significantly increased usage of Ig λ chain, compared to B cells from WT littermates (**Figure 2E**), in line with the observed (non-significant) rise of the proportions of Igλ^{+} recirculating mature B cells. Subpopulation analysis or the splenic B cell population indicated that IgD^{hi}IgM^{hi} and IgD^{hi}IgM^{lo} B cell splenic fractions were responsible for the elevated Igλ proportions (**Supplementary Figure 2B**). Likewise, we found elevated proportions of Igλ^{+} B cells in the IgD^{hi} B cell fraction in the MesLN of *Tnfaip3*$^{CD11c\text{-}KO}$ mice (data not shown).

Taken together, these data show that immature B cells in *Tnfaip3*$^{CD11c\text{-}KO}$ mice had significantly decreased proportions of Igλ^{+} cells, compared to *Tnfaip3*$^{CD11c\text{-}HZ}$ or *Tnfaip3*$^{CD11c\text{-}KO}$ control mice. Remarkably, during B cell maturation in the spleen these Igλ^{+} B cell proportions increased in *Tnfaip3*$^{CD11c\text{-}KO}$ mice, resulting in elevated Igλ usage in IgD^{hi}IgM^{lo} B cells in spleen, MesLN and bone marrow. Although we cannot exclude that *Tnfaip3*$^{CD11c\text{-}KO}$ mice have a reduced Igλ locus accessibility affecting Igλ recombination, it is more likely that in these mice BCR repertoire selection is abnormal. This would then explain reduced receptor editing in the bone marrow and decreased selection against Igλ^{+} B cells in the periphery[37].

Defects in the B-1 cell compartment in *Tnfaip3*$^{CD11c\text{-}KO}$ mice.

Since in contrast to B-2 cell development, B-1 cell precursors do not abide in the bone marrow[38] and develop independently of IL-7[39], we studied B-1 cells in *Tnfaip3*$^{CD11c\text{-}KO}$ mice.

We investigated B-1 and B-2 cells in the peritoneal (**Figure 3A**) and pleural cavities. While total B cell numbers were unchanged, the proportions of B-1 cells (from total B cells) were reduced in *Tnfaip3*$^{CD11c\text{-}HZ}$ and *Tnfaip3*$^{CD11c\text{-}KO}$ mice compared with WT controls, both in the peritoneal cavity (**Figure 3B**) and in the pleural cavity (**Figure 3C**). B-1 cells have a restricted B cell receptor (BCR) repertoire and a considerable fraction of these cells recognize neutral phospholipids such as phosphatidylcholine PtC[40, 41]. When we stained peritoneal B cells for PtC-specificity, we observed reduced PtC binding in *Tnfaip3*$^{CD11c\text{-}HZ}$ mice and *Tnfaip3*$^{CD11c\text{-}KO}$ mice compared with *Tnfaip3*$^{CD11c\text{-}WT}$ controls (**Figure 3D,3E**). The frequency of intracellular IL-10^{+} B-1 and B-2 cells in the peritoneum of *Tnfaip3*$^{CD11c\text{-}KO}$ mice was decreased compared to *Tnfaip3*$^{CD11c\text{-}WT}$ mice and *Tnfaip3*$^{CD11c\text{-}HZ}$ mice (**Figure 3F**).

Potential mechanisms for the observed abnormalities in peritoneal B-1-cells may involve changes in DC activity. We did not detect differences in surface expression of co-stimulatory molecules on DCs or in the capacity of T-cells to produce cytokines across the three genotypes (data not shown). However, we did find increased proportions of IL-6^{+} and IL-10^{+} DCs in the peritoneum of *Tnfaip3*$^{CD11c\text{-}HZ}$ mice and *Tnfaip3*$^{CD11c\text{-}KO}$ mice compared to controls (**Supplementary Figure 3**). Conversely, the frequencies of IFNγ^{+} DCs were decreased in the peritoneum of *Tnfaip3*$^{CD11c\text{-}KO}$ mice compared to WT controls (**Supplementary Figure 3**).

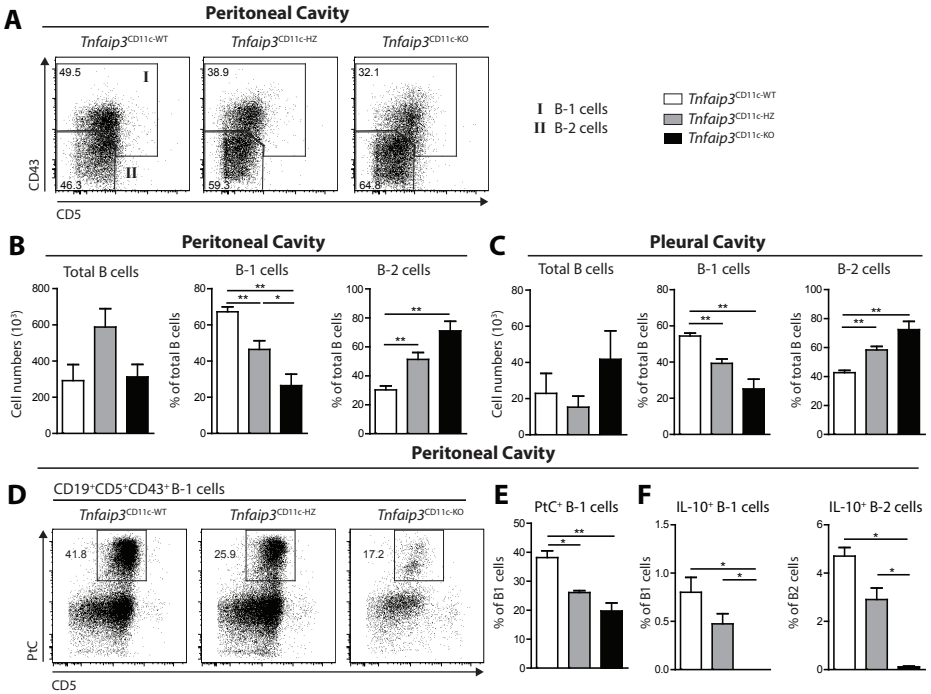

Figure 3: Defects in the B-1 cell compartment in *Tnfaip3*$^{CD11c\text{-}KO}$ mice.
(**A**) Flow cytometric analysis of peritoneal cavity B-1 cells ($CD19^+B220^+CD43^+CD5^{int}$) and B-2 cells ($CD19^+B220^+CD43^-CD5^-$). FACS profiles of gated $CD19^+$ lymphoid cells fractions are shown for the indicated mice. (**B-C**) Enumeration of total B cells, B-1 cells and B-2 cells in peritoneal (**B**) and pleural (**C**) cavity, using flow cytometry. (**D**) Flow cytometry plots of peritoneal PtC^+ B-1 cells, identified by CD5/PtC profiles of $CD19^+CD43^+$ B cells. Representative examples are shown from *Tnfaip3*$^{CD11c\text{-}WT}$, *Tnfaip3*$^{CD11c\text{-}HZ}$ and *Tnfaip3*$^{CD11c\text{-}KO}$ mice. (**E**) Quantification of PtC^+ B-1 cells as a proportion of B-1 cells in the peritoneal cavity, using flow cytometry. (**F**) Quantification intracellular IL-10^+ cells in the B-1 and B-2 cell population in peritoneal cavity from the three mouse groups, using flow cytometry. Legend for the individual mouse groups is shown in panel A. Results of (A-C) are representative of 3 independent experiments, and (D-F) are from 2 independent experiment and are presented as me an values ± SEM of $n = 4$-7 per group. *$P<0.05$, **$P < 0.01$ using the Mann-whitney U statistical test.

Summarizing, these data show that the absence of *Tnfaip3* in the DC-lineage affected the numbers of peritoneal B cells. The reduction in PtC-binding and the changes in cytokine profile furthermore suggest altered B-1 cell function.

Reduction of B cell numbers in the spleen of *Tnfaip3*$^{CD11c\text{-}KO}$ mice.

Given that B cell development was disturbed in *Tnfaip3*$^{CD11c\text{-}KO}$ mice, we next characterized the B cell populations in peripheral lymphoid organs. Total splenic B-2 cell numbers were reduced in *Tnfaip3*$^{CD11c\text{-}KO}$ mice compared to WT controls (**Figure 4A**). Splenic transitional B cells did not differ between the three genotypes (**Figure 4B**). Marginal zone (MZ) B cells were decreased in *Tnfaip3*$^{CD11c\text{-}KO}$ mice compared to *Tnfaip3*$^{CD11c\text{-}HZ}$ and

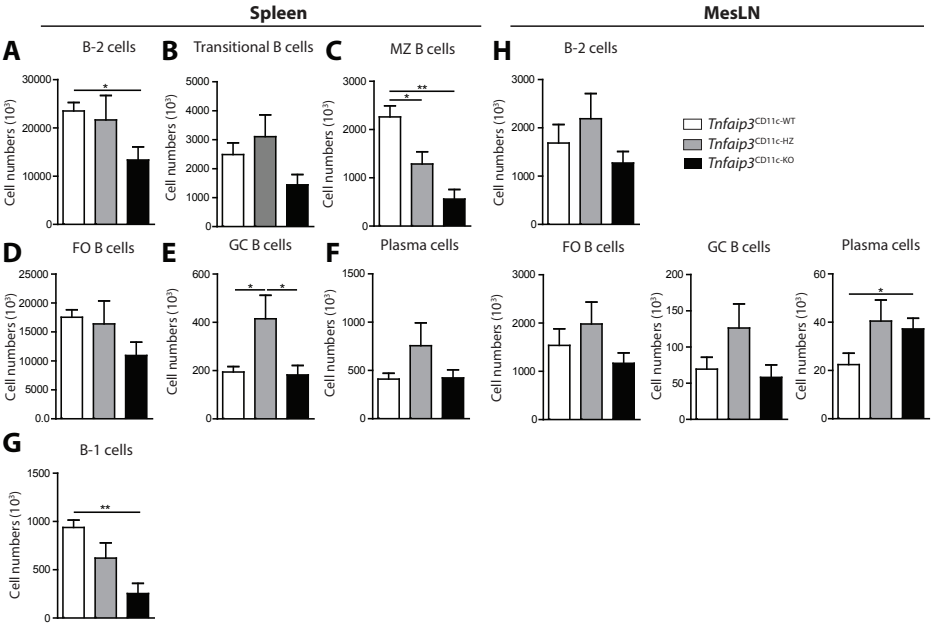

Figure 4: Reduction of B cell numbers in the spleen of *Tnfaip3*$^{CD11c\text{-}KO}$ mice.
(**A-G**) Enumeration of splenic B-2 cells ($CD19^+B220^+CD43^-CD5^-$) (**A**), Transitional B cells ($CD19^+B220^+CD21/35^-CD23^-$) (**B**), marginal zone B cells ($CD19^+B220^+CD21/35^+CD23^-$) (**C**), follicular B cells ($CD19^+B220^+CD21/35^-CD23^+$) (**D**), Germinal center B cells ($CD19^+B220^+CD95^+IgD^-$) (**E**), plasma cells ($B220^-CD138^+$) (**F**) and B-1 cells ($CD19^+B220^+CD43^+CD5^{int}$) (**G**) using flow cytometry. (**H**) Quantification of all B cell subsets from (**A-G**) except transitional B-cells, MZ and B-1 B cells within the MesLN, using flow cytometry. Mice were 6 weeks of age. Results are from representative of 2 independent experiments and are presented as mean values ± SEM of $n = 6$ per group. *P<0.05, **P < 0.01 using the Mann-whitney U statistical test.

Tnfaip3$^{CD11c\text{-}WT}$ mice (**Figure 4C**), but the numbers of total follicular (FO) B cells did not differ significantly between the three genotypes (**Figure 4D**). While the numbers of splenic germinal center (GC) B cells were highest in *Tnfaip3*$^{CD11c\text{-}HZ}$ mice, GC B cells and plasma cells were not different between *Tnfaip3*$^{CD11c\text{-}WT}$ and *Tnfaip3*$^{CD11c\text{-}KO}$ mice (**Figure 4E, 4F**). Parallel to our findings in the peritoneal cavity, also the number of splenic B-1 cells were reduced in *Tnfaip3*$^{CD11c\text{-}KO}$ mice compared to WT littermate controls (**Figure 4G**). The numbers of B cell subpopulations in MesLN were similar between *Tnfaip3*$^{CD11c\text{-}WT}$ and *Tnfaip3*$^{CD11c\text{-}KO}$ mice, except for a small but significant increase in the total numbers of plasma cells in *Tnfaip3*$^{CD11c\text{-}KO}$ mice (**Figure 4H**).

Taken together, at ~6 weeks of age defective B cell development in the bone marrow of *Tnfaip3*$^{CD11c\text{-}KO}$ mice was associated with a reduction of the numbers of splenic B cells, in particular of the mature B-2 cell and MZ B cell fractions.

B cells from *Tnfaip3*$^{CD11c\text{-}KO}$ mice show normal T-cell independent and defective T-cell dependent antibody responses.

Since supernatants of WT B cells that were co-cultured with *Tnfaip3*$^{CD11c\text{-}KO}$ DCs contained increased amounts of IgA and IgG1, when compared to co-cultures with *Tnfaip3*$^{CD11c\text{-}WT}$ DCs[10], we determined total Ig levels in serum of ~6-week-old mice. Total IgM was highest in *Tnfaip3*$^{CD11c\text{-}HZ}$ mice, compared to *Tnfaip3*$^{CD11c\text{-}WT}$ and *Tnfaip3*$^{CD11c\text{-}KO}$ mice (**Figure 5A**). Total IgA and IgG was increased in the serum of *Tnfaip3*$^{CD11c\text{-}HZ}$ and *Tnfaip3*$^{CD11c\text{-}KO}$ mice, compared with *Tnfaip3*$^{CD11c\text{-}WT}$ controls (**Figure 5A**). Specifically, the IgG1, IgG2b and IgG2c isotypes were increased in these two genotypes (**Figure 5B**). In contrast, IgG3 serum levels were specifically elevated in *Tnfaip3*$^{CD11c\text{-}HZ}$ mice, paralleling our findings for serum IgM levels (**Figure 5B**).

We next examined the specific Ig response against the T-cell dependent antigen ovalbumin (OVA). While *Tnfaip3*$^{CD11c\text{-}WT}$ and *Tnfaip3*$^{CD11c\text{-}HZ}$ mice elicited an anti-OVA IgG1 response at day 8 and day 15 after booster immunization, this response was severely reduced in *Tnfaip3*$^{CD11c\text{-}KO}$ mice (**Figure 5C**). On the other hand, a T-cell independent antigen such as DNP-Ficoll, elicited anti-DNP-Ficoll IgM and IgG3 responses in *Tnfaip3*$^{CD11c\text{-}KO}$ mice that were in the normal range (**Figure 5D**).

In summary, *Tnfaip3*$^{CD11c\text{-}KO}$ mice had increased serum levels of several Ig subclasses including IgG1, but showed a severely reduced T-cell dependent IgG1 response. In these mice IgM and IgG3 levels, as well as type II T cell-independent IgM and IgG3 responses, were not affected.

Splenic naïve mature B cells in *Tnfaip3*$^{CD11c\text{-}KO}$ mice show enhanced responsiveness to activating stimuli.

Because spontaneous Ig production by B cells from aging *Tnfaip3*$^{CD11c\text{-}KO}$ mice was increased[10], we wondered whether mature naïve splenic B cells from 6-week-old *Tnfaip3*$^{CD11c\text{-}KO}$ mice displayed an increased capacity to produce pro-inflammatory cytokines. Indeed, splenic B cells in *Tnfaip3*$^{CD11c\text{-}HZ}$ and *Tnfaip3*$^{CD11c\text{-}KO}$ mice showed an increased capacity to produce IFNγ, compared with *Tnfaip3*$^{CD11c\text{-}WT}$ mice, as measured by intracellular cytokine staining upon short *in vitro* activation with PMA and ionomycin (**Figure 6A**).

This prompted us to investigate whether naïve mature B cells in the periphery from *Tnfaip3*$^{CD11c\text{-}KO}$ mice showed evidence for enhanced activation by stimuli such as lipopolysaccharide (LPS) in comparison to B cells from control mice. Indeed, stimulating naïve B cells *in vitro* with LPS or the TLR9 ligand CpG, resulted in higher surface expression levels of CD86 and CD80 on B cells from *Tnfaip3*$^{CD11c\text{-}KO}$ mice, compared to *Tnfaip3*$^{CD11c\text{-}WT}$ controls (**Figure 6B-6D**). The GC marker Fas Ligand or CD95 was more readily induced upon anti-IgM, LPS, CpG or anti-CD40 stimulation of naïve splenic B cells from *Tnfaip3*$^{CD11c\text{-}KO}$ mice, compared with B cells from WT control mice (**Figure 6E**). The stimulation-induced expression of CD69 did not differ across the genotypes (**Figure 6F**).

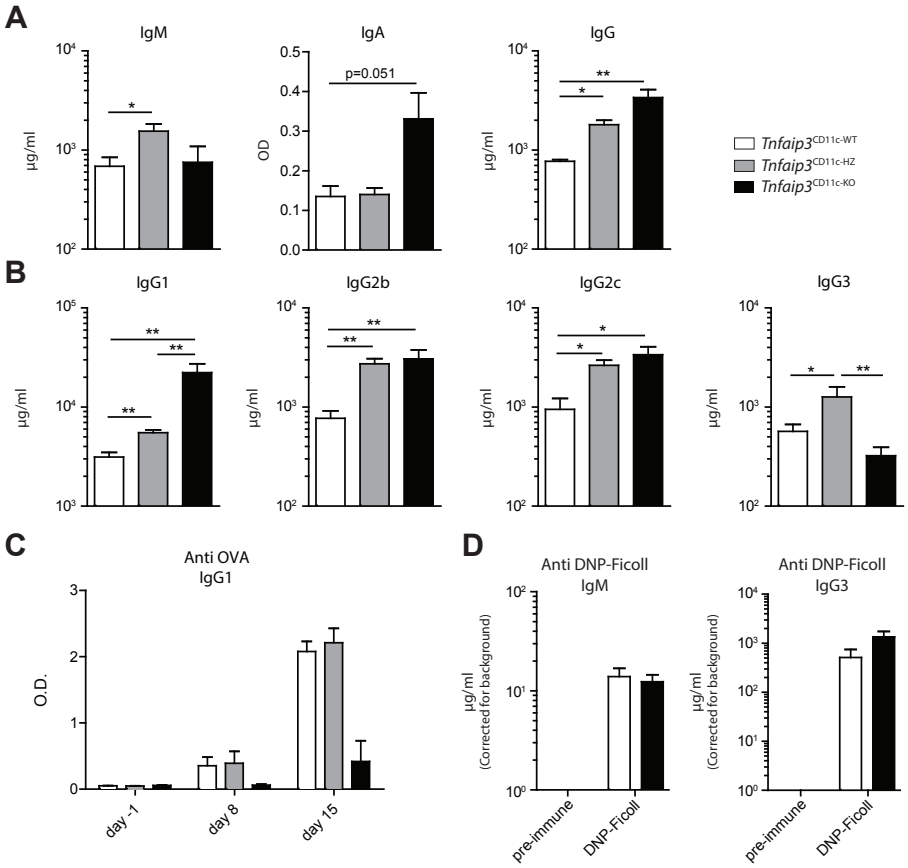

Figure 5: B cells from *Tnfaip3*$^{CD11c\text{-}KO}$ mice show normal T-cell independent and defective T-cell dependent antibody responses.

(**A-B**) Measurement of total serum levels of IgM, IgA and IgG (**A**) and subclasses IgG1, IgG2b, IgG2c and IgG3 (**B**) using ELISA. (**C**) T-cell dependent B cell response: pre-immune and post-OVA immunisation assessment of OVA-specific IgG1 serum levels using ELISA. (**D**) T-cell independent type II B cell response: pre-immune and post-immunisation assessment of DNP-specific IgM and IgG3 serum levels, using ELISA. Results are presented as mean values ± SEM of n = 3-10 per group. *P<0.05, **P < 0.01 using the Mann-whitney U statistical test.

We next evaluated *in vitro* plasma cell differentiation upon LPS stimulation in the presence or absence of IL-4. Increased proportions of IgG1^{+}CD138^{+} plasmablasts were found upon LPS/IL-4 stimulation of purified B cell fractions from *Tnfaip3*$^{CD11c\text{-}KO}$ mice, compared with WT mice (**Figure 6G**). After LPS stimulation alone, the proportions of IgG3^{+} B cells or plasmablasts were not different between cultures from *Tnfaip3*$^{CD11c\text{-}KO}$ or *Tnfaip3*$^{CD11c\text{-}WT}$ mice (**Figure 5H**).

In conclusion, these data illustrate that following *in vitro* activation naïve splenic B cells from *Tnfaip3*$^{CD11c\text{-}KO}$ mice display a more activated phenotype and an increased differentiation capacity towards IgG1^{+} plasmablasts, compared to B cells from *Tnfaip3*$^{CD11c\text{-}WT}$ mice.

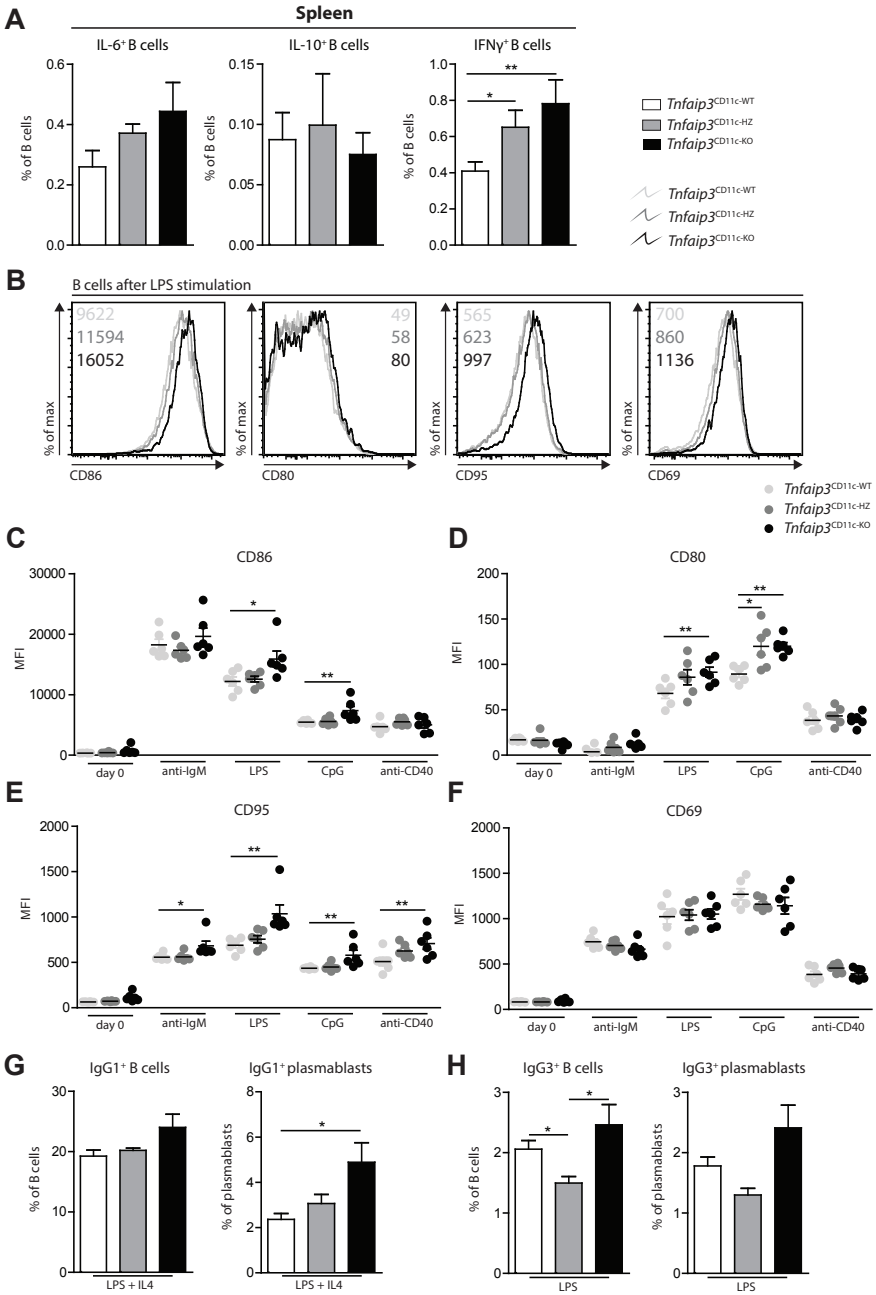

Figure 6: Splenic naïve mature B cells in *Tnfaip3*$^{CD11c\text{-}KO}$ mice show enhanced responsiveness to activating stimuli.

(**A**) Quantification of the proportions of IL-6$^+$, IL-10$^+$ and IFNγ$^+$ splenic B cells in the indicated mice. (**B-F**) Purified naïve B cells (CD19$^+$B220$^+$NK1.1$^-$CD4$^-$CD8$^-$Ter119$^-$CD11c$^-$GR1$^-$FCRla$^-$CD5$^-$CD43$^-$CD138$^-$CD11b$^-$CD95$^-$) were *in vitro* stimulated using LPS (**B**) and assessed for the indicated activation markers. Data are shown as

histogram overlays (**B**) or quantifications of expression of the activation markers CD86 (**C**), CD80 (**D**), CD95 (**E**) and CD69 (**F**), as determined by flow cytometry, on B cells that were cultured in the presence of the indicated activating stimuli. (**G-H**) Naïve B cells were cultured *in vitro* with LPS in the presence or absence of IL-4, as indicated, and assessed for $IgG1^+$ (**G**) and $IgG3^+$ (**H**) B cells or plasmablasts ($CD19^+B220^+CD138^+$), using flow cytometry. Results are representative of 2 independent experiments and are presented as mean values ± SEM of $n = 6$ per group. $^*P<0.05$, $^{**}P < 0.01$ using the Mann-whitney U statistical test.

DISCUSSION

B cells are crucial in autoimmune diseases[2, 42] and therefore the immune system has several checkpoints to remove autoreactive B cells from the repertoire. In a lupus mouse model of DC-specific deletion of A20/*Tnfaip3* (*Tnfaip3*$^{CD11c\text{-}cre}$), we previously demonstrated that B cells are more activated and engaged in autoreactive Ig production associated with glomerulo-nephritis[10]. Because aged *Tnfaip3*$^{CD11c\text{-}cre}$ mice displayed severely reduced numbers of peripheral B cells and B cell tolerance is initiated in the bone marrow[12-15], we studied bone marrow B cell development in *Tnfaip3*$^{CD11c\text{-}cre}$ mice.

We observed an age-dependent developmental arrest of B-lineage cells: B cell development was hampered at the immature B cell stage in 6-week-old *Tnfaip3*$^{CD11c\text{-}KO}$ mice and at the pre-B cell stage in 24-week-old *Tnfaip3*$^{CD11c\text{-}KO}$ mice. Various molecular mechanisms may explain these findings. An intrinsic defect in B cell differentiation affecting the pre-B cell stage is not very likely, since deletion of the *Tnfaip3* gene was specifically targeted to the DC-lineage. Secondly, B cell development might be hampered as a result of the circulating pro-inflammatory cytokines arising during autoimmune pathology. For example, IFN α/β[30] and IFNγ[31] can directly induce apoptosis of IL-7 dependent B cell precursors. In addition, cytokines such as IL-4[43], IL-1(α/β)[27, 28] and transforming growth factor (TGF)-β[44, 45] can exert inhibitory effects on B cell development. Thirdly, B cells in *Tnfaip3*$^{CD11c\text{-}KO}$ mice might be subjected to improper cell-cell interaction signals, because of an altered activation status of DCs or because activated DCs affected stromal cells or other supportive cells in the bone marrow environment. Finally, a possible scenario could be that B-lineage cells have a reduced migration capacity into $IL\text{-}7R^{lo}$ niches in the bone marrow, e.g. due to reduced expression of CXCL12[32].

To address this issue, we performed IL-7-driven bone marrow cultures *in vitro* using combinations of *Tnfaip3*$^{CD11c\text{-}KO}$ and *Tnfaip3*$^{CD11c\text{-}WT}$ B cells and supporting stromal/myeloid cells. We found that *Tnfaip3*$^{CD11c\text{-}KO}$ stromal/myeloid cells were less beneficial for developmental progression of pre-B cells, indicating that cell-cell contact rather than external cytokines or chemokine gradients hampered B cell development in *Tnfaip3*$^{CD11c\text{-}KO}$ mice. With this *in vitro* experiment, however, we cannot formally exclude the possibility that *Tnfaip3*$^{CD11c\text{-}KO}$ stromal/myeloid cells in our culture system produced soluble factors that hamper B cell development.

Small pre-B cells rearrange their Ig κ or λ light chains, with a 95:5 ratio respectively in the peripheral B cell population in mice[46]. We found that immature B cells in the bone marrow of *Tnfaip3*$^{CD11c\text{-}KO}$ mice had significantly decreased proportions of Igλ^{+} cells, whereas Igλ usage was elevated in the most mature IgD^{hi}IgM^{lo} B cells in peripheral immune compartments. It is possible that *Tnfaip3*$^{CD11c\text{-}KO}$ mice have a reduced Igλ locus accessibility which would subsequently affect Igλ recombination and receptor editing events. However, it appears much more likely that in *Tnfaip3*$^{CD11c\text{-}KO}$ mice the BCR repertoire selection is abnormal, leading to reduced receptor editing in the bone marrow and decreased selection against Igλ^{+} B cells in the periphery[37]. This could e.g. be related to reduced survival of B cells in these mice.

Further experiments, e.g. involving crosses with transgenic mice expressing autoreactive and non-autoreactive BCRs are likely to show whether or not deletion of the *Tnfaip3* gene in DCs affects selection of the BCR repertoire in mice.

B-1 cell progenitors develop independently of IL-7[39] and the bone marrow[38]. Although in *Tnfaip3*$^{CD11c\text{-}KO}$ mice B-1 cells were reduced in numbers and had an altered BCR repertoire, as evidenced by reduced PtC-binding, we found that serum IgM and IgG3 levels were normal and that B-1 cells were able to mount a normal response to the type II T cell-independent antigen DNP-Ficoll. In contrast to this relatively unaffected B-1 cell compartment, we detected severe defects in B-2 cells. Serum levels of IgG1, IgG2b and IgG2c were increased, but B cells were unable to mount a specific T cell-dependent antibody response towards OVA *in vivo,* suggesting that B cells in *Tnfaip3*$^{CD11c\text{-}KO}$ mice received aberrant stimulatory signals from T-cells. This might well be related to the disturbed micro-architecture of the spleen observed in *Tnfaip3*$^{CD11c\text{-}KO}$ mice[10]. Although we did not check for autoreactive IgG in 6-week-old mice, it was already demonstrated that 12-week-old mice had enhanced anti-dsDNA IgG and one 10-week-old mice had positivity for self-antigen RNP-A[10].

Naïve splenic B cells from *Tnfaip3*$^{CD11c\text{-}KO}$ mice showed an enhanced response to activating stimuli. A minor proportion of B cells might have been targeted by CD11c-cre-mediated deletion[47], because CD11c can be expressed by a small fraction of B cells, associated with aging and autoimmunity[48]. However, such CD11c^{+} B cells were hardly present in the B cell fractions of our *in vitro* experiments, because we negatively selected for CD11c during our magnetic B cell purification procedure. More likely, the enhanced responsiveness of B cells was a result of activating signals *in vivo*, which appear to be present in a very early phase of the developing autoimmune pathology. Similar co-stimulatory molecule enhancements was also seen in autoimmune disease, as CD80 MFI values were higher in unstimulated naïve peripheral B cells of multiple sclerosis patients[49] and CD80/CD86 MFI values were elevated in CD40-stimulated naïve B cells from SLE patients[50], compared to healthy controls. Although increased MZ B cells[51] and memory B cells[52] could explain rapid and enhanced activation or class switched immu-

noglobulin production, this is not likely to underlie the increased responsiveness of B cells in *Tnfaip3*$^{CD11c\text{-}KO}$ mice: these mice have reduced MZ B cell numbers and no presence of memory B cells, as suggested by equal memory B cell marker CD80[53] levels at baseline as WT controls.

To conclude, we demonstrated that loss of A20/*Tnfaip3* in DCs mainly affects B cell development, BCR repertoire selection and function. Improper signals from the bone marrow microenvironment are likely responsible for the age-dependent arrest of B cell development. B cells that reach the periphery act differently to stimuli, indicating that either (i) B cell selection in bone marrow might alter the activation threshold of B cells, or (ii) that the activation status of DCs and T cells in lymphoid organs have a large impact on B cell activation and function. These findings in mice indicate that humoral B cell-driven diseases including SLE, may develop from primary defects in immune cells from a different compartment, such as DCs.

Acknowledgements

This project was supported by The Dutch Arthritis Association (12-2-410). We would like to thank Mirjam Kool, Odilia Corneth, as well as the Erasmus MC Animal Facility (EDC) staff for their assistance during the project.

Conflict of interest

The authors declare no conflict of interest.

REFERENCES

1. Crispin JC, Liossis SN, Kis-Toth K, Lieberman LA, Kyttaris VC, Juang YT *et al.* Pathogenesis of human systemic lupus erythematosus: recent advances. *Trends in molecular medicine* 2010; 16(2): 47-57.
2. Hampe CS. B Cell in Autoimmune Diseases. *Scientifica* 2012; 2012.
3. Steinman RM, Hawiger D, Nussenzweig MC. Tolerogenic dendritic cells. *Annual review of immunology* 2003; 21: 685-711.
4. Pao LI, Lam KP, Henderson JM, Kutok JL, Alimzhanov M, Nitschke L *et al.* B cell-specific deletion of protein-tyrosine phosphatase Shp1 promotes B-1a cell development and causes systemic autoimmunity. *Immunity* 2007; 27(1): 35-48.
5. Lamagna C, Hu Y, DeFranco AL, Lowell CA. B cell-specific loss of Lyn kinase leads to autoimmunity. *Journal of immunology (Baltimore, Md : 1950)* 2014; 192(3): 919-928.
6. Kaneko T, Saito Y, Kotani T, Okazawa H, Iwamura H, Sato-Hashimoto M *et al.* Dendritic cell-specific ablation of the protein tyrosine phosphatase Shp1 promotes Th1 cell differentiation and induces autoimmunity. *Journal of immunology (Baltimore, Md : 1950)* 2012; 188(11): 5397-5407.
7. Lamagna C, Scapini P, van Ziffle JA, DeFranco AL, Lowell CA. Hyperactivated MyD88 signaling in dendritic cells, through specific deletion of Lyn kinase, causes severe autoimmunity and inflammation. *Proceedings of the National Academy of Sciences of the United States of America* 2013; 110(35): E3311-3320.
8. Sun SC, Chang JH, Jin J. Regulation of nuclear factor-kappaB in autoimmunity. *Trends in immunology* 2013; 34(6): 282-289.
9. Wertz IE, O'Rourke KM, Zhou H, Eby M, Aravind L, Seshagiri S *et al.* De-ubiquitination and ubiquitin ligase domains of A20 downregulate NF-kappaB signalling. *Nature* 2004; 430(7000): 694-699.
10. Kool M, van Loo G, Waelput W, De Prijck S, Muskens F, Sze M *et al.* The ubiquitin-editing protein A20 prevents dendritic cell activation, recognition of apoptotic cells, and systemic autoimmunity. *Immunity* 2011; 35(1): 82-96.
11. Tavares RM, Turer EE, Liu CL, Advincula R, Scapini P, Rhee L *et al.* The ubiquitin modifying enzyme A20 restricts B cell survival and prevents autoimmunity. *Immunity* 2010; 33(2): 181-191.
12. Gay D, Saunders T, Camper S, Weigert M. Receptor editing: an approach by autoreactive B cells to escape tolerance. *The Journal of experimental medicine* 1993; 177(4): 999-1008.
13. Tiegs SL, Russell DM, Nemazee D. Receptor editing in self-reactive bone marrow B cells. *The Journal of experimental medicine* 1993; 177(4): 1009-1020.
14. Nemazee D, Buerki K. Clonal deletion of autoreactive B lymphocytes in bone marrow chimeras. *Proceedings of the National Academy of Sciences of the United States of America* 1989; 86(20): 8039-8043.
15. Goodnow CC, Crosbie J, Adelstein S, Lavoie TB, Smith-Gill SJ, Brink RA *et al.* Altered immunoglobulin expression and functional silencing of self-reactive B lymphocytes in transgenic mice. *Nature* 1988; 334(6184): 676-682.
16. Meffre E. The establishment of early B cell tolerance in humans: lessons from primary immunodeficiency diseases. *Annals of the New York Academy of Sciences* 2011; 1246: 1-10.
17. Samuels J, Ng YS, Coupillaud C, Paget D, Meffre E. Impaired early B cell tolerance in patients with rheumatoid arthritis. *The Journal of experimental medicine* 2005; 201(10): 1659-1667.
18. Bensimon C, Chastagner P, Zouali M. Human lupus anti-DNA autoantibodies undergo essentially primary V kappa gene

rearrangements. *The EMBO journal* 1994; 13(13): 2951-2962.

19. Dorner T, Farner NL, Lipsky PE. Ig lambda and heavy chain gene usage in early untreated systemic lupus erythematosus suggests intensive B cell stimulation. *Journal of immunology (Baltimore, Md : 1950)* 1999; 163(2): 1027-1036.
20. Dorner T, Foster SJ, Farner NL, Lipsky PE. Immunoglobulin kappa chain receptor editing in systemic lupus erythematosus. *The Journal of clinical investigation* 1998; 102(4): 688-694.
21. Henry-Bonami RA, Williams JM, Rachakonda AB, Karamali M, Kendall PL, Thomas JW. B lymphocyte "original sin" in the bone marrow enhances islet autoreactivity in type 1 diabetes-prone nonobese diabetic mice. *Journal of immunology (Baltimore, Md : 1950)* 2013; 190(12): 5992-6003.
22. Lamoureux JL, Watson LC, Cherrier M, Skog P, Nemazee D, Feeney AJ. Reduced receptor editing in lupus-prone MRL/lpr mice. *The Journal of experimental medicine* 2007; 204(12): 2853-2864.
23. Vereecke L, Sze M, Mc Guire C, Rogiers B, Chu Y, Schmidt-Supprian M *et al.* Enterocyte-specific A20 deficiency sensitizes to tumor necrosis factor-induced toxicity and experimental colitis. *The Journal of experimental medicine* 2010; 207(7): 1513-1523.
24. Caton ML, Smith-Raska MR, Reizis B. Notch-RBP-J signaling controls the homeostasis of CD8- dendritic cells in the spleen. *The Journal of experimental medicine* 2007; 204(7): 1653-1664.
25. Vroman H, Bergen IM, Li BW, van Hulst JA, Lukkes M, van Uden D *et al.* Development of eosinophilic inflammation is independent of B-T cell interaction in a chronic house dust mite-driven asthma model. *Clinical and experimental allergy : journal of the British Society for Allergy and Clinical Immunology* 2017; 47(4): 551-564.
26. Hardy RR, Carmack CE, Shinton SA, Kemp JD, Hayakawa K. Resolution and characterization of pro-B and pre-pro-B cell stages in normal mouse bone marrow. *The Journal of experimental medicine* 1991; 173(5): 1213-1225.
27. Dorshkind K. IL-1 inhibits B cell differentiation in long term bone marrow cultures. *Journal of immunology (Baltimore, Md : 1950)* 1988; 141(2): 531-538.
28. Morrissey P, Charrier K, Bressler L, Alpert A. The influence of IL-1 treatment on the reconstitution of the hemopoietic and immune systems after sublethal radiation. *Journal of immunology (Baltimore, Md : 1950)* 1988; 140(12): 4204-4210.
29. Lin Q, Dong C, Cooper MD. Impairment of T and B cell development by treatment with a type I interferon. *The Journal of experimental medicine* 1998; 187(1): 79-87.
30. Wang J, Lin Q, Langston H, Cooper MD. Resident bone marrow macrophages produce type 1 interferons that can selectively inhibit interleukin-7-driven growth of B lineage cells. *Immunity* 1995; 3(4): 475-484.
31. Grawunder U, Melchers F, Rolink A. Interferon-gamma arrests proliferation and causes apoptosis in stromal cell/interleukin-7-dependent normal murine pre-B cell lines and clones in vitro, but does not induce differentiation to surface immunoglobulin-positive B cells. *European journal of immunology* 1993; 23(2): 544-551.
32. Ueda Y, Yang K, Foster SJ, Kondo M, Kelsoe G. Inflammation controls B lymphopoiesis by regulating chemokine CXCL12 expression. *The Journal of experimental medicine* 2004; 199(1): 47-58.
33. ten Boekel E, Melchers F, Rolink A. The status of Ig loci rearrangements in single cells from different stages of B cell development. *International immunology* 1995; 7(6): 1013-1019.
34. McGuire KL, Vitetta ES. kappa/lambda Shifts do not occur during maturation of murine B cells. *Journal of immunology (Baltimore, Md : 1950)* 1981; 127(4): 1670-1673.

35. Hieter PA, Korsmeyer SJ, Waldmann TA, Leder P. Human immunoglobulin kappa light-chain genes are deleted or rearranged in lambda-producing B cells. *Nature* 1981; 290(5805): 368-372.
36. Dingjan GM, Middendorp S, Dahlenborg K, Maas A, Grosveld F, Hendriks RW. Bruton's tyrosine kinase regulates the activation of gene rearrangements at the lambda light chain locus in precursor B cells in the mouse. *The Journal of experimental medicine* 2001; 193(10): 1169-1178.
37. Nemazee D. Mechanisms of central tolerance for B cells. *Nature reviews Immunology* 2017; 17(5): 281-294.
38. Hayakawa K, Hardy RR, Herzenberg LA, Herzenberg LA. Progenitors for Ly-1 B cells are distinct from progenitors for other B cells. *The Journal of experimental medicine* 1985; 161(6): 1554-1568.
39. Carvalho TL, Mota-Santos T, Cumano A, Demengeot J, Vieira P. Arrested B lymphopoiesis and persistence of activated B cells in adult interleukin 7(-/-)- mice. *The Journal of experimental medicine* 2001; 194(8): 1141-1150.
40. Cox KO, Hardy SJ. Autoantibodies against mouse bromelain-modified RBC are specifically inhibited by a common membrane phospholipid, phosphatidylcholine. *Immunology* 1985; 55(2): 263-269.
41. Mercolino TJ, Arnold LW, Hawkins LA, Haughton G. Normal mouse peritoneum contains a large population of Ly-1+ (CD5) B cells that recognize phosphatidyl choline. Relationship to cells that secrete hemolytic antibody specific for autologous erythrocytes. *The Journal of experimental medicine* 1988; 168(2): 687-698.
42. Shlomchik MJ. Activating systemic autoimmunity: B's, T's, and tolls. *Current opinion in immunology* 2009; 21(6): 626-633.
43. Rennick D, Yang G, Muller-Sieburg C, Smith C, Arai N, Takabe Y *et al.* Interleukin 4 (B-cell stimulatory factor 1) can enhance or antagonize the factor-dependent growth of hemopoietic progenitor cells. *Proceedings of the National Academy of Sciences of the United States of America* 1987; 84(19): 6889-6893.
44. Hayashi S, Gimble JM, Henley A, Ellingsworth LR, Kincade PW. Differential effects of TGF-beta 1 on lymphohemopoiesis in long-term bone marrow cultures. *Blood* 1989; 74(5): 1711-1717.
45. Lee G, Namen AE, Gillis S, Ellingsworth LR, Kincade PW. Normal B cell precursors responsive to recombinant murine IL-7 and inhibition of IL-7 activity by transforming growth factor-beta. *Journal of immunology (Baltimore, Md : 1950)* 1989; 142(11): 3875-3883.
46. Popov AV, Zou X, Xian J, Nicholson IC, Bruggemann M. A human immunoglobulin lambda locus is similarly well expressed in mice and humans. *The Journal of experimental medicine* 1999; 189(10): 1611-1620.
47. Lindquist RL, Shakhar G, Dudziak D, Wardemann H, Eisenreich T, Dustin ML *et al.* Visualizing dendritic cell networks in vivo. *Nat Immunol* 2004; 5(12): 1243-1250.
48. Rubtsov AV, Rubtsova K, Kappler JW, Jacobelli J, Friedman RS, Marrack P. CD11c-Expressing B Cells Are Located at the T Cell/B Cell Border in Spleen and Are Potent APCs. *Journal of immunology (Baltimore, Md : 1950)* 2015; 195(1): 71-79.
49. Fraussen J, Claes N, Van Wijmeersch B, van Horssen J, Stinissen P, Hupperts R *et al.* B cells of multiple sclerosis patients induce autoreactive proinflammatory T cell responses. *Clin Immunol* 2016; 173: 124-132.
50. Sim JH, Kim HR, Chang SH, Kim IJ, Lipsky PE, Lee J. Autoregulatory function of interleukin-10-producing pre-naive B cells is defective in systemic lupus erythematosus. *Arthritis Res Ther* 2015; 17: 190.
51. Oliver AM, Martin F, Kearney JF. IgMhighCD21high lymphocytes enriched in the splenic marginal zone generate effector cells more rapidly than the bulk of follicular B cells. *Journal of immunology*

(Baltimore, Md : 1950) 1999; 162(12): 7198-7207.

52. Kurosaki T, Kometani K, Ise W. Memory B cells. *Nature reviews Immunology* 2015; 15(3): 149-159.
53. Zuccarino-Catania GV, Sadanand S, Weisel FJ, Tomayko MM, Meng H, Kleinstein SH *et al.* CD80 and PD-L2 define functionally distinct memory B cell subsets that are independent of antibody isotype. *Nat Immunol* 2014; 15(7): 631-637.

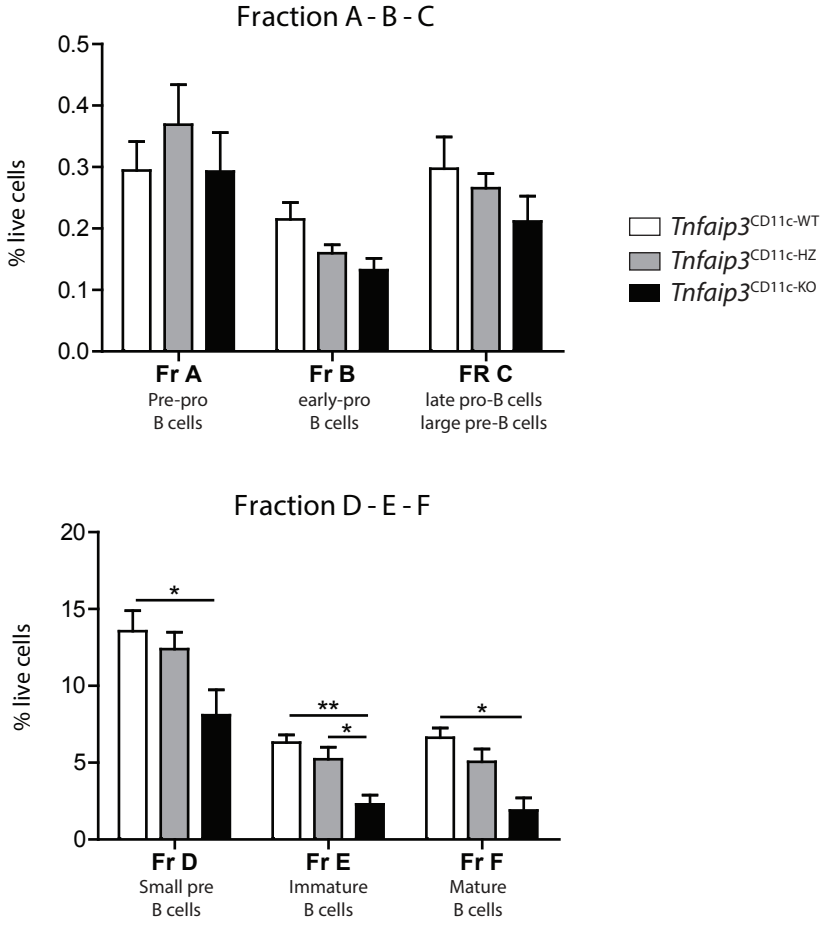

Supplementary Figure 1: Pro B cell stages are unaffected in *Tnfaip3*$^{CD11c\text{-}KO}$ mice.

The indicated developmental B-lineage fractions, according to the Hardy nomenclature[26] in the bone marrow of the three mouse groups, calculated as a percentage of living cells. Results are representative of 3 independent experiments and are presented as mean values ± SEM of $n = 6$ per group. *P<0.05, **P < 0.01 using the Mann-whitney U statistical test.

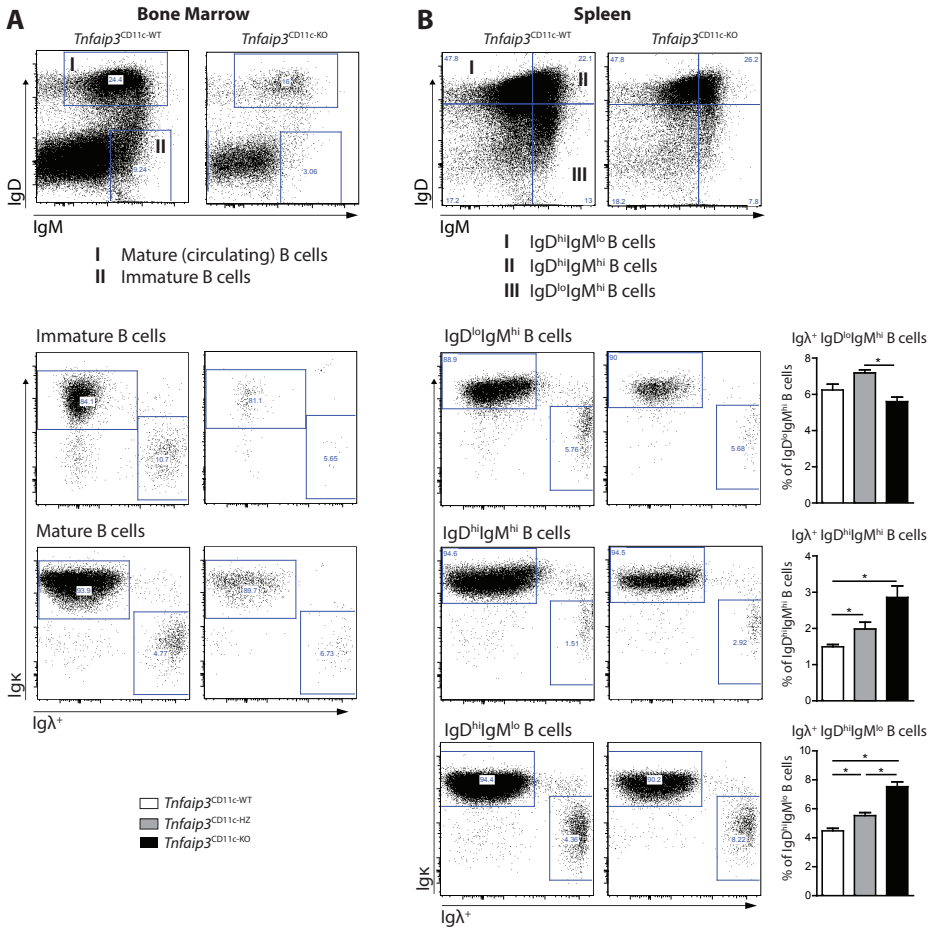

Supplementary Figure 2: Igκ$^+$ and Igλ$^+$ light chains in bone marrow and spleens in *Tnfaip3*$^{CD11c\text{-}KO}$ mice. (**A**) Flow cytometric analysis Igκ$^+$ and Igλ$^+$ light chains in bone marrow immature B cells (B220$^+$CD19$^+$IgD^{lo}IgM^{hi}) and mature B cells (B220$^+$CD19$^+$IgD^{hi}IgM^{hi}), in the indicated mice. Gating strategy according to Dingjan et al[36]. (**B**) Flow cytometric analysis Igκ$^+$ and Igλ$^+$ light chains in splenic immature B cells (B220$^+$CD19$^+$IgD^{lo}IgM^{hi}), IgD^{hi}IgM^{hi} B cells (B220$^+$CD19$^+$IgD^{hi}IgM^{hi}) and mature B cells (B220$^+$CD19$^+$IgD^{hi}IgM^{lo}), with enumeration of the proportion Igλ$^+$ light chain across all indicated genotypes.

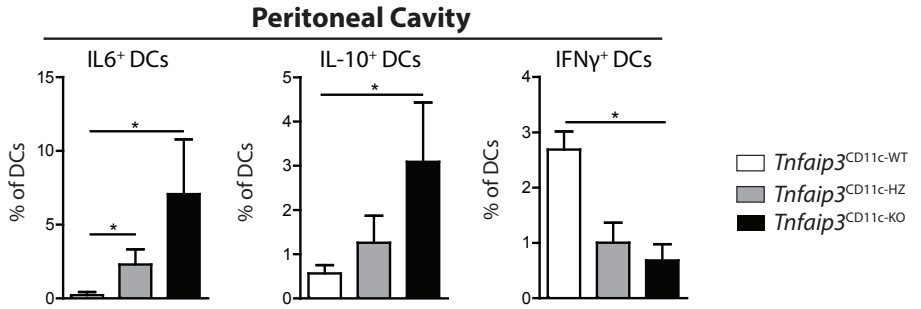

Supplementary Figure 3: Peritoneal cavity DCs from *Tnfaip3*$^{CD11c\text{-}KO}$ mice express increased IL-6, IL-10 and reduced IFN-γ.

6-week-old *Tnfaip3*^{CD11c} mice were analyzed for peritoneal cavity DCs. Quantification of DC (CD11c^{+}MHC-II^{+}) that expressed IL-6, IL-10 and IFN-γ, using flow cytometry. Results are from a single experiment and are presented as mean values ± SEM of $n = 6$ per group. *$P<0.05$ using the Mann-whitney U statistical test.

Supplementary Table 1: Antibodies used for flow cytometry

Antibody	Conjugate	Clone	Company
B220	PE-Cy7	RA3-6B2	eBioscience
B220	Alexa Fluor 700	RA3-6B2	eBioscience
B220	Biotin	RA3-6B2	BD
BP-1 (Ly-51)	Biotin	6C3/BP	BD
CD11c	PE-Texas Red	N418	Invitrogen
CD138	Brilliant Violet 605	281-2	BD
CD19	PerCP-Cy5.5	eBio1D3	eBioscience
CD2	PE	RM2-5	eBioscience
CD24	Briljant Violet 650	M1/69	BD
CD25	Brilliant Violet 605	PC61	BioLegend
CD4	Brilliant Violet 711	RM4-5	BD
CD34	Alexa Fluor 700	RAM34	eBioscience
CD43	Briljant Violet 605	S7	BD
CD5	PE	53-7.3	eBioscience
CD5	Biotin	53-7.3	BD
cKit	APC-eFluor780	2B8	eBioscience
IFNγ	PE-Cy7	XMG1.2	eBioscience
IgD	APC	11-26c	eBioscience
Ig λ	FITC	R26-46	BD
Ig λ	Biotin	R26-46	BD
IgM	APC	II/41	eBioscience
IgM	PE-Cy7	II/41	eBioscience
IL-10	Alexa Fluor 488	JES5-16E3	eBioscience
IL-6	PE	MP5-20F3	BD
Ig κ	FITC	187.1	BD
PtC	FITC		
Streptavidin	Brilliant Violet 711		BD

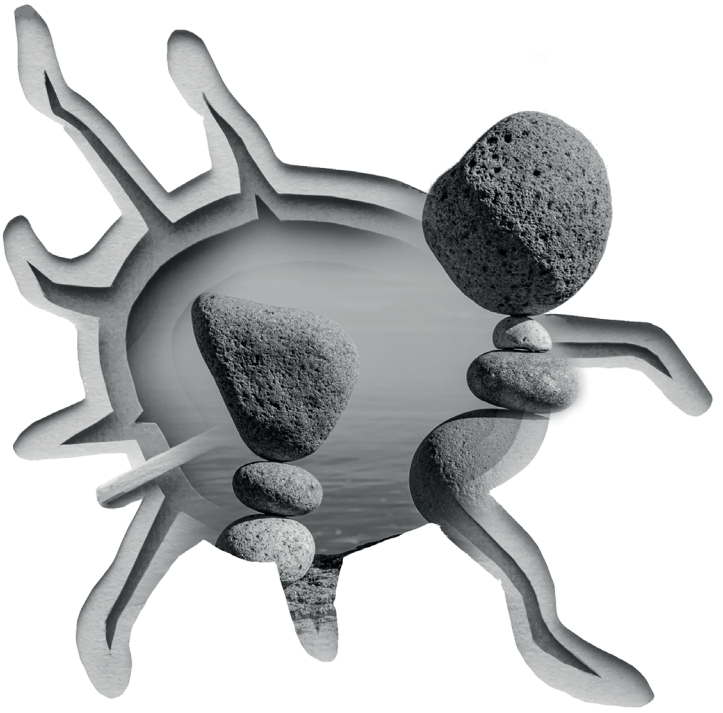

Chapter 6

Tnfaip3/A20 deficient dendritic cells induce autoimmune pathology in mice, independent of T-B cell communication.

Tridib Das, Ingrid M. Bergen, Anne Huber, Menno van Nimwegen, Jennifer van Hulst, Geert van Loo, Bart N. Lambrecht, Mirjam Kool, Rudi W. Hendriks

Manuscript in preparation

ABSTRACT

Dendritic cells (DCs) are sentinel cells regulating both immune homeostasis and immunogenic responses. Ablation of *Tnfaip3*/A20, a negative regulator of the NF-κB pathway, in DCs (*Tnfaip3*$^{CD11c\text{-}KO}$ mice) induces DC activation. As a result, activation of T cells and B cells occurs leading to spontaneous germinal center (GC) formation and an autoimmune phenotype. *In vitro Tnfaip3*-deficient DCs are potent activators of naïve B cells that develop into IgG1- and IgA-producing plasma cells. We hypothesize that T cells might be dispensable for B cell-driven autoimmunity in *Tnfaip3*$^{CD11c\text{-}KO}$ mice.

Tnfaip3^{CD11c} mice were crossed to *Cd40lg*^{KO} mice to hamper communication between T cells and B cells and immune activation and tissue inflammation were examined. In 10-week-old *Tnfaip3*$^{CD11c\text{-}KO}$ mice, splenic DCs harbor an activated phenotype as evidenced by higher CD40 surface expression, both on a WT and on a *Cd40lg*^{KO} background. As expected, both follicular T helper (Tfh)-cells and GC B cells were reduced in CD40L-deficient mice. Marginal zone B cells, but not follicular B cells, expressed GC-associated cytokine receptors in *Tnfaip3*$^{CD11c\text{-}KO}$*Cd40lg*^{KO} mice. In 24-week-old *Tnfaip3*$^{CD11c\text{-}KO}$ mice, splenic IgG1^{+} plasma cells and memory B cells were highly abundant, together with elevated anti-dsDNA IgG1 in serum and IgG deposition in the kidneys. Importantly, *Tnfaip3*$^{CD11c\text{-}KO}$*Cd40lg*^{KO} mice presented with kidney pathology, in which IgA was deposited and serum anti-dsDNA IgM and IgA levels were enhanced.

These findings indicate that kidney pathology can occur in the absence of CD40L-dependent communication between T cells and B cells in mice harboring *Tnfaip3*-deficient DCs. We conclude that therapies interfering with CD40-CD40L interaction may not fully prevent organ inflammation in autoimmune disorders.

INTRODUCTION

Immune homeostasis is critically controlled by dendritic cells (DCs)[1]. In order to respond to pathogens, DCs are activated and induce an appropriate immune response to clear the infection. In autoimmunity, unfortunately, DCs are activated with deleterious consequences[2]. For instance, artificial activation of DCs, by *in vivo* ablation of *Tnfaip3*/A20, a negative regulator of NF-κB signaling, resulted in T cell and B cell activation, antibody class switching, systemic inflammation and glomerulonephritis. When mice were 24 weeks old, they developed an autoimmune phenotype resembling either inflammatory bowel disease[3] or systemic lupus erythematosus (SLE)[4].

SLE is a multifactorial disease in which multiple immune cells, such as DCs, T cells and B cells play a role[5]. The presence of antinuclear antibodies (ANA) in serum is generally considered a decisive diagnostic sign of SLE. These antibodies are produced by plasma cells, which develop from B cells that are either activated in germinal centers (GC) or by extrafollicular responses in a T cell-independent (TI) manner[6]. B-cell activation is initiated by engagement of specific antigens to the B-cell receptor (BCR), resulting in a T cell dependent or TI humoral response[7]. GC B cells are dependent on T cell help, whereby CD40L expression on activated T cells and their IL-21 production is crucial for communication with B cells[8]. Within the GC, T cell help promotes immunoglobulin (Ig) class switch, especially to IgG1[9] and IgG2[10]. However, B cells can also be activated, differentiate, and isotype-switch independent of antigen-specific T cell help, CD40L signaling, and IL-21 signaling to B cells. When B cells are activated in extrafollicular responses in a TI manner, antigen presenting cells such as DCs or macrophages can replace the function of T cells to instruct plasma cell formation[11]. Nevertheless, T cells do dramatically enhance the response, and this occurs via CD40L and IL-21 signals.

Intriguingly, *Tnfaip3*-deficient bone marrow-derived DCs (BM-DCs), when cultured with naïve B cells, could induce plasma cell formation and IgG1 and IgA class switch in a TI manner[4]. This was partially dependent on the presence of IL-6, and not due to IL-21 or other familiar TI-cytokines, such as B lymphocyte stimulator protein (BLyS, also known as BAFF) or a proliferation-inducing ligand (APRIL)[4].

It is currently unknown whether B cell activation *in vivo* in autoimmune *Tnfaip3*$^{CD11c\text{-}KO}$ mice is dependent on T cell help or directly induced by activated DCs. To determine whether T cell dependent contact was necessary, we hampered T cell communication with B cells by deletion of CD40L and crossed *Tnfaip3*$^{CD11c\text{-}KO}$ mice to CD40L-deficient mice[12].

MATERIALS AND METHODS

Mice

C57BL/6 *Tnfaip3*$^{fl/fl}$*Cd11c*$^{cre/+}$ mice[4] were crossed with *Cd40lg*^{KO} mice[12] (The Jackson Laboratory, Bar Harbor, ME, USA). Male and female mice were analyzed at 10 weeks or 24 weeks of age. The cre-deficient littermates served as wild-type (WT) controls. Mice were bred and housed under specific pathogen-free conditions in the Erasmus MC experimental animal facility. All experiments were approved by the animal ethical committee of the Erasmus MC (EMC3329).

Generation of bone marrow-derived dendritic cells (BM-DCs)

To obtain BM-DCs, BM cells were cultured for 9 days in DC culture medium (RPMI 1640 containing GlutaMAX (Invitrogen, Waltham, MA, USA, with 5% FCS (Hyclone, South Logan, UT, USA), 50 µM 2-mercaptoethanol (Sigma-Aldrich Co., St. Louis, MO, USA) and 50 µg/ml gentamycin (Invitrogen), with 20 ng/ml of granulocyte-macrophage colony-stimulating factor (GM-CSF)[13].

RNA Sequencing

Total RNA was extracted from BM-DCs as described[14]. Single-end reads were aligned to the mouse genome (UCSC Genome Browser mm9) using TopHat (Tophat version 2.0.8). Gene expression levels as fragments per kilobase of a transcript per million mapped reads (FPKMs) were calculated using Cufflinks[15]. RNA-Seq Data Analysis Differential gene expression assessment was done in the R environment (version 3.1.1) with CuffDiff[16]. Gene set enrichment analysis (GSEA)[17] was performed using a pre-ranked list of all genes. The MySigDB collection "H: Hallmark Genes" was used to align for enrichment. From the top 3 most enriched gene sets results, we further specified cytokines and chemokines as published on www.genenames.org.

Tissue preparation

Spleens were taken from sacrificed mice. One half was stored in Tissue-Tek® O.C.T.™ compound (Sakura Finetek Europe B.V., Alphen aan den Rijn, The Netherlands) and slowly frozen at -20 °C. Cryo sections were cut using a CryoStar™ NX70 Cryostat (Thermo Fisher Scientific Inc., Waltham, MA, USA).

The other half was used to obtain single cell suspensions. Spleens were homogenized through a 100-µm cell strainer (Corning Inc., Corning, NY, USA) and collected in Gibco™ RPMI Medium 1640 (1 x) + GlutaMAX™-1 (Thermo Fisher Scientific Inc., Waltham, MA, USA). Spleen red blood cells were lysed using osmotic lysis buffer (0.15 M NH_4CL, 10 mM $KHCO_3$, 0.1 mM EDTA, pH 7.1-7.4; sterile-filtered with 0.22 µm filter).

Freshly isolated kidneys, liver, and pancreas were incubated 24 hrs on Roti-Histofix 4% (Carl-Roth, Karlsruhe, Germany) and then embedded in paraffin wax. Paraffin embedded tissue sections were stained with hematoxylin and eosin, using standard procedures.

Flow cytometry and cell sorting

Flow cytometric surface and intracellular staining procedures have been described previously[18]. Monoclonal antibodies used for flow cytometric analyses were (Target, Clone, Manufacturer): CD11b (M1/70, BD Biosciences), CD11c (N418, Invitrogen), CD19 (1D3, BD Biosciences), CD21 (4E3, eBioscience), CD23 (B3B4, eBioscience), CD3e (17A2, eBioscience), CD4 (GK1.5, eBioscience), CD80 (16-10A1, eBioscience), CD86 (GL1, BD Biosciences), CD95 (Jo2, BD Biosciences), CXCR5 (2G8, BD Biosciences), GL7 (RUO, BD Biosciences), IgD (11-26c.2a, BD Biosciences), IgG1 (R19-15, BD Biosciences), IgM (II/41, eBioscience), MHC-II (M5/114.15.3, eBioscience), PD-1 (J43, BD Biosciences), The following monoclonal antibodies were used for cell sorting (Target, Clone, Manufacturer): CD19 (eBio1D3, eBioscience), CD21 (4E3, eBioscience), CD23 (B3B4, eBioscience), CD3e (145-2C11, BD Biosciences). Sorting was conducted using a BD FACSAria™ II (BD Biosciences, San Jose, CA, USA). Data analysis was performed in FlowJo version 9 Workspace (FlowJO LLC, Ashland, OR, USA).

RNA isolation and cDNA synthesis

Total RNA was isolated from sorted follicular (FO) B cells and marginal zone (MZ) B cells, using the RNeasy® Micro Kit (QIAGEN, Venlo, Netherlands) according to the manufacturer's instructions. cDNA was synthesized using the RevertAid H Minus First Strand cDNA Synthesis Kit (Thermo Fisher Scientific Inc., Waltham, MA, USA). 11 µl of the isolated total RNA was used and 1 µl of random hexamer primer was added, then mixed, centrifuged and incubated for 5 min at 65 °C. The mixture was chilled on ice, centrifuged and 4 µl of 5x Reaction Buffer, 1 µl of RiboLock RNase Inhibitor (20U/µl), 2 µl 10 mM dNTP Mix and 1 µl RevertAid H Minus Reverse Transcriptase (200U/µl) were added. After incubation for 5 min at 25 °C, the mixture was incubated for 60 min at 42 °C. To terminate the reaction, the sample was heated to 70 °C for 5 min. The cDNA was stored at -20 °C until it was used in quantitative RT-PCR.

Quantitative RT-PCR

Quantitative RT-PCR (real-time reverse-transcription PCR) analysis was performed using the SYBR® Select Master Mix Kit (Thermo Fisher Scientific Inc., Waltham, MA, USA) and primers (Target, Forward, Reverse) for Fasl (F: GCAGAAGGAACTGGCAGAAC, R: TTAAATGGGCCACACTCCTC), Il-4r (F: GAGTGGAGTCCTAGCATCACG, R: CAGTGGAAGGCGCTGTATC), Il-21 (F: CCATCAAACCCTGGAAACAA, R: TCACAGGAAGGGCATTTAGC) and Il-21r (F: AGTGCCCCAGCCTAAAGAAT, R: ACTGAGTATGCTGGGGTTGG) on an Applied Biosystems™

7300 Real Time PCR System (Thermo Fisher Scientific Inc., Waltham, MA, USA). Ubiquitin C (UBC) mRNA expression was used as housekeeping gene to normalize gene transcription. Data were extracted from the linear range of amplification.

Immunoglobulin levels and autoreactivity assessment

Serum total immunoglobulin levels were assessed by ELISA, as previously described[19]. Briefly, goat-anti-mouse immunoglobulins were plated overnight. Wells were blocked and serum was incubated for 3 hrs at room temperature. Depending on the isotype of interest, anti-mouse biotin labeled against the isotype of interest was incubated and developed. The optical density (OD) was measured at 450 nm on a Microplate Reader (Bio-Rad, Hercules, CA, USA). Immunoglobulin autoreactivity assessment was assessed as previously described[19].

Periodic Acid Schiff Diastase staining (PAS-D or PAS+ staining)

Three-µm-thick paraffin embedded kidney sections were stained with Periodic Acid Schiff (PAS; Sigma-Aldrich). Briefly, paraffin embedded sections were dewaxed and hydrated to water using Xylene (Sigma-Aldrich) and ethanol dilutions in MilliQ. One part human saliva (containing the enzyme diastase) was diluted 1:10 with MilliQ and incubated on slides for 30 min on room temperature. Slides were placed for 5 min in freshly prepared periodic acid solution (Sigma-Aldrich) and then in Schiff's reagent for 5 min and counterstained with Gill's hematoxylin (Merck Millipore) for 2 sec. Lastly, slides were dehydrated using Xylene and mounted in Entallan (Merck Millipore).

Immunohistochemistry of Cryosections

For immunohistochemistry, 6 µm acetone or 4 % formalin fixed spleen sections were blocked in peroxidase blocking buffer (PBS, 0.67 % H_2O_2, 2 % NaN_3) for 30 min at room temperature. Aspecific secondary antibody binding was prevented by blocking the sections in Blocking Buffer (1% Blocking Reagent (Roche Diagnostics GmbH, Mannheim, Germany) in PBS) containing 10% normal goat or donkey serum. Sections were stained with primary antibodies for 1 hr at room temperature, washed three times with PBS and incubated with alkaline phosphatase (AP) or peroxidase (PO) conjugated secondary antibodies for 30 min at room temperature. Used antibodies are listed (Target, clone, dilution, manufacturer, secondary antibody, dilution, manufacturer): CD21 (Biotin, 1:100, Streptavidin PO, 1:50), MOMA1 (1:100, Bioceros, Goat anti-Rat AP, 1:50, Jackson Immunoresearch), GL7 (RUO, 1:50, eBioscience, Goat anti-Rat AP, 1:50, Jackson Immunoresearch) and IgD (11-26, 1:50, eBioscience, Goat anti-PE PO, 1:50, Rockland Immunochemichals). First the alkaline phosphatase was detected in 30 minutes using a mixture containing N-(4-Amino-2,5-diethoxyphenyl)benzamide (Fast Blue BB, Sigma-Aldrich), 2 M HCl, 4 % $NaNO_2$, Naphthol AS-MX phosphate (VWR International, Radnor,

PA, USA), N,N-dimethylformamide (DMF) (Sigma-Aldrich), Tris-HCl buffer (pH 8.5) and (-)-tetramisole hydrochloride (Sigma-Aldrich). The substrate was filtered using filtration paper. Subsequently, peroxidase was detected within 30 min with a mixture containing 3-amino-9-ethylcarbazole (AEC) in DMF, 0.1 M NaAC (pH 4.6), 30% H_2O_2 (Merck Millipore, Darmstadt and double-filtered. Stained tissue sections were embedded in Kaiser's Glycerol/Gelatin (Boom B.V., Meppel, The Netherlands). Micrographs were made using a Leica DM2000 microscope (Leica Microsystems GmbH, Wetzlar, Germany), a Leica DFC450 camera (Leica Microsystems GmbH, Wetzlar, Germany) and Leica Application (LAS) Software Version 4.5.0 (Leica Microsystems GmbH, Wetzlar, Germany).

Immunohistochemistry of Paraffin embedded sections

For immunohistochemical stainings on paraffin embedded sections, antigen retrieval was established using citrate buffer (Sigma Aldrich) pH 6.0 for 10 min in the microwave. 3 µm-thick paraffin kidney sections were stained with biotinylated primary antibody against total Immunoglobulin Isotypes (Primary antibody target, dilution, manufacturer): IgA (Biotin, 1:200, Southern Biotech), IgM (Biotin, 1:200, Southern Biotech) and IgG (Biotin, 1:200, Southern Biotech). After washing with PBS, slides were incubated for 1 hr with Avidin/Biotinylated Enzyme Complex (ABC) from the anti-Rat ABC Peroxidase Kit (Vector Laboratories). 10mg 3,3'-Diaminobenzene (DAB) (Sigma-Aldrich) was dissolved in Tris-HCl buffer (pH 7,6) with 12µl H_2O_2 to retrieve specific staining and slides were coated with Kaiser's glycerol.

Confocal Microscopy

For confocal imaging, 12 µm-thick spleen cryostat sections were stained as explained above. Primary and secondary antibodies were (Target, clone, dilution, manufacturer, with respective secondary antibody target, dilution, manufacturer): B220 (RA3-6B2, 1:50, BD Biosciences, Donkey anti-Rat Cy5, 1:200, Jackson Immunoresearch), CD11c (N418, 1:10, eBioscience, Goat anti-Hamster Cy3, 1:1000, Jackson Immunoresearch), CD3e (KT3, 1:50, Bioceros, Donkey anti-Rat Cy3, 1:1000, Jackson Immunoresearch). Slides were counterstained with *4',6-diamidino-2-phenylindole (*DAPI), mounted with VECTASHIELD® HardSet™ Antifade Mounting Medium (Vector Laboratries, Burlingame, CA, USA) and analyzed on a Zeiss LSM 510 META confocal microscope (Carl Zeiss AG, Oberkochen, Germany). Images were analyzed using ImageJ software (Rasband, W.S., ImageJ, U. S. National Institutes of Health, Bethesda, Maryland, USA).

Statistics

Statistical significance of data was calculated using the non-parametric Mann-Whitney U test. P-values <0.05 were considered significant. All analyses were performed using Prism (GraphPad Software version 9, La Jolla, CA, USA). All data are presented as the mean with the standard error of the mean (SEM).

RESULTS

Loss of *Tnfaip3*/A20 in BM-DCs increases the expression of cytokines involved in B cell activation.

As *in vitro Tnfaip3*/A20-deficient BM-DCs can directly activate B cells[4], an unbiased transcriptome analysis using mRNA-sequencing was performed[14] to examine differences between *Tnfaip3*^{WT}, *Tnfaip3*^{HZ}, and *Tnfaip3*^{KO} BM-DCs that could explain the TI B cell activating capacity. A large number of differentially expressed genes (DEG) were identified between *Tnfaip3*^{WT}, *Tnfaip3*^{HZ}, and *Tnfaip3*^{KO} BM-DCs (**Figure 1A**). Gene set enrichment analysis (GSEA) revealed that several cytokine-signaling pathways are highly active in *Tnfaip3*^{KO} BM-DCs, with the 'TNF-α signaling via NF-κB' pathway as the most enriched gene set in *Tnfaip3*^{KO} BM-DCs compared to *Tnfaip3*^{WT} BM-DCs (**Figure 1B/C**). This pathway was also significantly enriched in *Tnfaip3*^{KO} BM-DCs when compared to *Tnfaip3*^{HZ} BM-DCs as well as in *Tnfaip3*^{HZ} BM-DCs compared to *Tnfaip3*^{WT} BM-DCs (**Supplementary Figure 1A/B**). mRNA expression of several cytokines and chemokines was increased in *Tnfaip3*^{KO} BM-DCs compared to *Tnfaip3*^{WT} BM-DCs (**Figure 1D**), including cytokines involved in activation of B cells and T cells, such as *Il6*, *Il1b*, and *Il1a* (**Figure 1E**). However, mRNA expression of some cytokines, including *Tnf* and *Lta* was reduced in *Tnfaip3*^{KO} BM-DCs compared to *Tnfaip3*^{WT} BM-DCs (**Figure 1F**). Expression of TI cytokines regulating B cell activation and survival, such as APRIL, BAFF and TGFβ were not significantly altered in *Tnfaip3*^{KO} BM-DCs (data not shown).

Taken together, cytokine signaling pathways were highly dependent on the expression of *Tnfaip3* in BM-DCs and these pathways were inversely correlated with *Tnfaip3* gene expression. *Tnfaip3*-deficient DCs harbored elevated mRNA expression of cytokines, such as IL-6, IL-1β and IL-1α that may directly influence B cell activation, particularly in the context of autoimmunity[20, 21].

Splenic DCs from *Tnfaip3*$^{CD11c\text{-}KO}$*Cd40lg*^{KO} mice show enhanced expression of activation markers.

To test whether T cell help is needed for B cell activation in *Tnfaip3*$^{CD11c\text{-}KO}$ mice, CD40L-CD40 interaction between T cells and B cells was abrogated by crossing *Tnfaip3*$^{CD11c\text{-}KO}$ mice with *Cd40lg*^{KO} mice. Spleens of 10-week-old *Tnfaip3*$^{CD11c\text{-}KO}$ mice and *Tnfaip3*$^{CD11c\text{-}KO}$*Cd40lg*^{KO} mice showed splenomegaly in comparison to their respective WT controls and *Tnfaip3*$^{CD11c\text{-}Hz}$ mice (**Supplementary Figure 1C**). However, no differences in splenic cellularity (**Supplementary Figure 1D**) was seen, consistent with the previously demonstrated extramedullary hematopoiesis in *Tnfaip3*$^{CD11c\text{-}KO}$ mice[4]. Also, the number of splenic DCs (**Supplementary Figure 1E/F**) did not differ across the six genotypes. Splenic DCs of *Tnfaip3*$^{CD11c\text{-}HZ}$ and *Tnfaip3*$^{CD11c\text{-}KO}$ mice showed a slight increase of CD40 expression, which reached significance for *Tnfaip3*$^{CD11c\text{-}HZ}$ mice, compared to WT mice

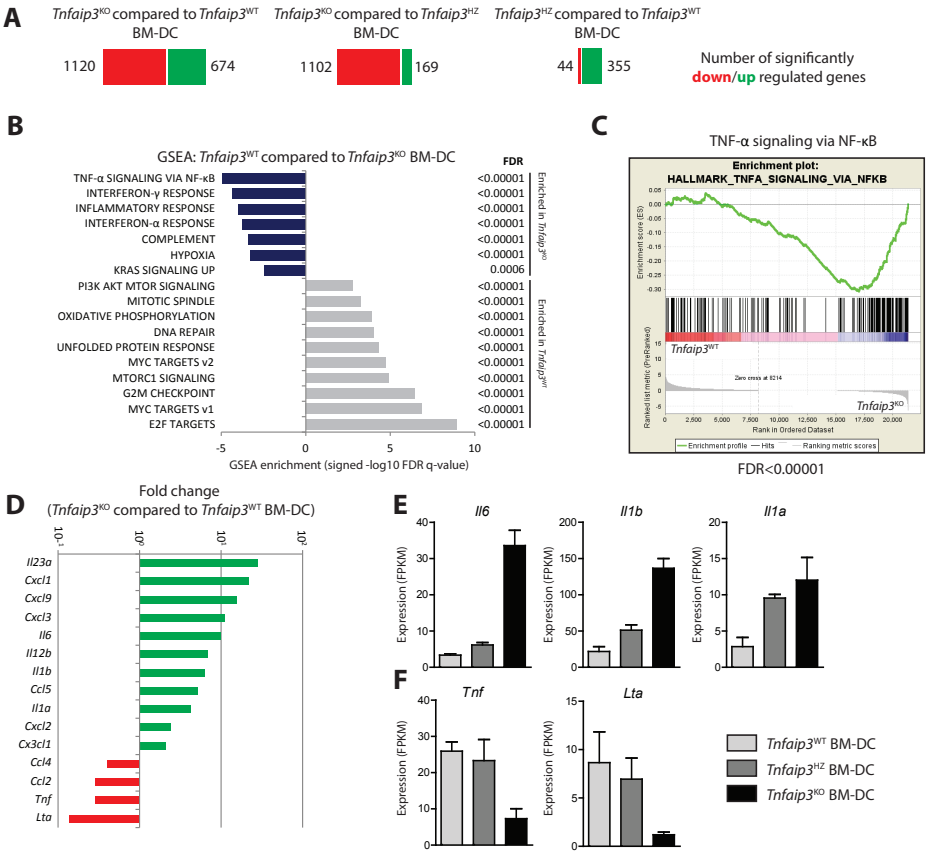

Figure 1: Loss of *Tnfaip3*/A20 in BM-DCs increases the expression of cytokines involved in B cell activation.

Bone marrow-derived DCs (BM-DCs) were analyzed by RNA Next generation sequencing (NGS). (**A**) The significant up and down-regulated gene numbers are listed according to Cuff diff-tools between *Tnfaip3*^{WT} mice, *Tnfaip3*^{HZ} mice and *Tnfaip3*^{KO} BM-DCs. (**B**) Gene set enrichment analysis (GSEA) performed for the ranked list of significantly altered genes between BM-DCs from *Tnfaip3*$^{CD11c\text{-}KO}$ mice and *Tnfaip3*$^{CD11c\text{-}WT}$ mice. The top 10 results with a False Discovery Rate (FDR)<0.25 are shown. (**C**) The top result of the GSEA with 'signal to noise'. (**D**) Using the three most enriched results (being "TNF-α SIGNALING VIA NF-κB", "INTERFERON-γ RESPONSE" and "INFLAMMATORY RESPONSE"), we characterized all cytokines and chemokines and expressed the fold changes between *Tnfaip3*^{KO} BM-DCs and *Tnfaip3*^{WT} BM-DCs. (**E-F**) Quantification of the Fragments Per Kilobase of transcript per Million mapped reads (FPKM) values of IL-6 (*Il6*), IL-1β (*Il1b*) and IL-1α (*Il1a*) (**E**) and TNF-α (*Tnfa*) and TNF-β (*Lta*) (**F**) between all BM-DC genotypes, as assessed directly from raw sequence data. NGS results are presented as mean values ± SEM of $n = 4$ mice per group.

(**Figure 2A/B**). The expression of PD-L1, but not CD86, was moderately enhanced on DCs from *Tnfaip3*$^{CD11c\text{-}KO}$ mice compared to WT controls (**Figure 2A/B**). Remarkably, in the absence of CD40L, expression of CD40, CD86, and PD-L1 were significantly increased on DCs from *Tnfaip3*$^{CD11c\text{-}KO}$*Cd40lg*^{KO} mice, compared to *Cd40lg*^{KO} mice (**Figure 2A/B**).

In short, in splenic DCs of *Tnfaip3*$^{CD11c\text{-}KO}$ mice, CD40L signals appear to restrain the expression of co-stimulatory molecules such as CD40, CD86, and PD-L1.

Reduction of MZ B cells in *Tnfaip3*$^{CD11c\text{-}KO}$ mice is restored by *Cd40lg* deletion.

In *Tnfaip3*$^{CD11c\text{-}KO}$ mice the numbers of CD4$^+$ T cells and CD8$^+$ T cells were not significantly affected (**Figure 3A**). However, the absence of CD40L signals is known to influence T cell and B cell homeostasis[22]. Both splenic CD8$^+$ and CD4$^+$ T cell numbers were reduced in 10-week-old *Cd40lg*^{KO} mice compared to WT mice (**Figure 3A**, see for gating strategy: **Supplementary Figure 2A**). Within the GC, follicular T-helper cells (Tfh-cells) are crucial for B cell activation and plasma cell formation, partly through CD40L-CD40 interaction[23]. The proportions of Tfh cells from total CD4$^+$ T cells were reduced in spleens of *Cd40lg*^{KO} mice compared to WT mice (**Figure 3B**, see for gating strategy: **Supplementary Figure 2A**). The numbers of B cells were significantly decreased in *Tnfaip3*$^{CD11c\text{-}KO}$ mice as well as in *Cd40lg*^{KO} mice compared to WT mice (**Figure 3C**, see for gating strategy: **Supplementary Figure 2B**). The proportions of GC B cells were increased in *Tnfaip3*$^{CD11c\text{-}KO}$ mice compared to WT controls and *Tnfaip3*$^{CD11c\text{-}HZ}$ mice, but these were virtually absent in mice lacking *Cd40lg* (**Figure 3C**). Despite the lack of GC B cells in all three *Tnfaip3* genotypes on the *CD40lg*^{KO} background, substantial number of plasma cells were present (**Figure 3C**, see for gating strategy: **Supplementary Figure 2B**).

Whereas the absence of the *Tnfaip3* gene in DCs did not significantly affect the proportions of follicular (FO) B cells in the spleen, marginal zone (MZ) B cell frequencies were dramatically reduced in *Tnfaip3*$^{CD11c\text{-}KO}$ mice compared to WT or *Tnfaip3*$^{CD11c\text{-}HZ}$ mice (**Figure 3D/E**). The percentages of FO B cells were slightly reduced in *Cd40lg*^{KO} mice compared to WT controls and likewise in *Tnfaip3*$^{CD11c\text{-}KO}$*Cd40lg*^{KO} mice compared to *Tnfaip3*$^{CD11c\text{-}KO}$ mice (**Figure 3E**). Intriguingly, the proportions of MZ B cells were increased in *Tnfaip3*$^{CD11c\text{-}KO}$*Cd40lg*^{KO} mice compared to *Tnfaip3*$^{CD11c\text{-}KO}$ mice, to similar frequencies as observed in WT mice (**Figure 3E**).

Next, we used immunohistochemistry to examine the splenic architecture. In WT mice rings of MOMA1$^+$ MZ macrophages were bordered by CD21$^+$ FO B cells and MZ B cells on the inside and outside, respectively (**Figure 3F**). Similar staining patterns were observed in spleens of *Cd40lg*^{KO} mice. However, the architecture was completed distorted in *Tnfaip3*$^{CD11c\text{-}KO}$ mice, as previously described[4] (**Figure 3F**), with only very few B cells and MZ macrophages. Strikingly, white pulp regions containing MZ macrophages, FO and MZ B cells were slightly reestablished in *Tnfaip3*$^{CD11c\text{-}KO}$*Cd40lg*^{KO} mice, compared to *Tnfaip3*$^{CD11c\text{-}KO}$ mice, although these regions were still smaller than those in *Cd40lg*^{KO} or WT mice (**Figure 3F**). In 24-week-old mice, the marked reduction in FO and MZ B cell was still apparent in *Tnfaip3*$^{CD11c\text{-}KO}$ mice, but less so in *Tnfaip3*$^{CD11c\text{-}KO}$*Cd40lg*^{KO} mice (**Supplementary Figure 2C**).

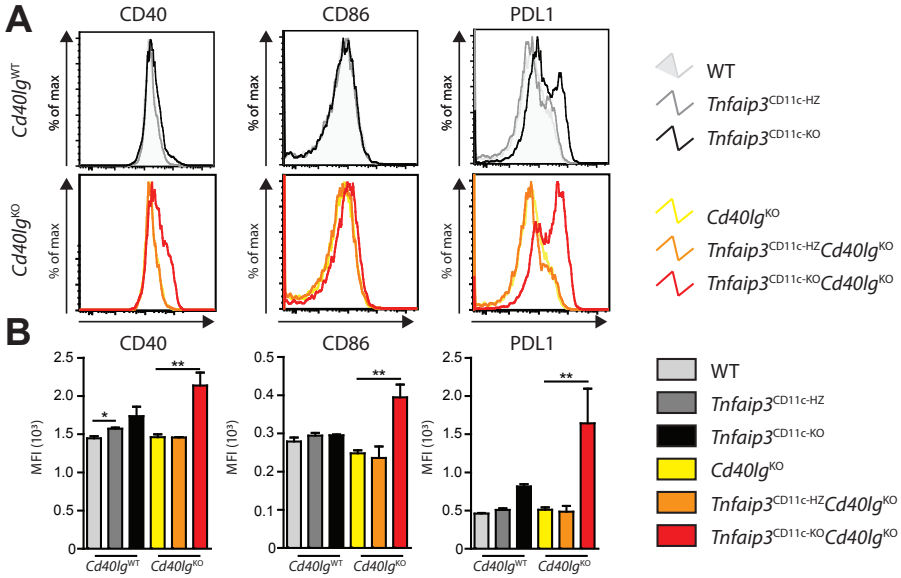

Figure 2: Splenic DCs from *Tnfaip3*$^{CD11c\text{-}KO}$*Cd40lg*^{KO} mice show enhanced expression of activation markers.

Spleens of naïve 10-week-old *Tnfaip3*^{CD11c}*Cd40lg* mice were analyzed for DCs (CD11c^{+}MHC-II^{+}) (**A-B**) Quantification of DC activation for CD40, CD86 and PD-L1 histograms (**A**) and bar-plot (**B**) using flow cytometry. Results are presented as mean values ± SEM of *n* = 2-5 mice per group. **P<0.01.

Taken together, in the absence of CD40L expression, mice harboring *Tnfaip3*-deficient DCs have strongly reduced Tfh-cell and GC B cell numbers. While young *Tnfaip3*$^{CD11c\text{-}KO}$ mice have very low MZ B cell proportions, these are considerably restored in the absence of CD40L, particularly in aging mice.

B cells from *Tnfaip3*$^{CD11c\text{-}KO}$*Cd40lg*^{KO} mice have an activated phenotype and T cells show robust expression of B cell-activating cytokines.

We next examined the phenotype of FO and MZ B cells. Whereas deletion of *Tnfaip3* did not affect their phenotype, we found that both FO and MZ B cells from 10-week-old *Tnfaip3*$^{CD11c\text{-}KO}$*Cd40lg*^{KO} mice displayed enhanced surface expression of CD80, CD86 and PD-L2 compared to *Cd40lg*^{KO} mice (**Figure 4A**). While both FO B cells and MZ B cell expressed enhanced CD95 in *Tnfaip3*$^{CD11c\text{-}KO}$*Cd40lg*^{KO} mice compared to *Cd40lg*^{KO} mice, only MZ B cells displayed enhanced MHC-II expression, which however did not reach significance (**Supplementary Figure 3A**).

Since interleukin IL-21 and IL-4 direct GC B cell responses[24], the expression of the IL-21 receptor (IL-21R) and IL-4R was examined in purified splenic FO and MZ B cell fractions by RT-PCR (See for sorting strategy: **Supplementary Figure 3B**). Whereas no differences were detected for IL-21R and IL-4R mRNA expression in FO B cells, minor increases were

observed in splenic MZ B cells from *Tnfaip3*$^{CD11c\text{-}KO}$*Cd40lg*^{KO} mice compared to *Cd40lg*^{KO} mice (**Supplementary Figure 3C**).

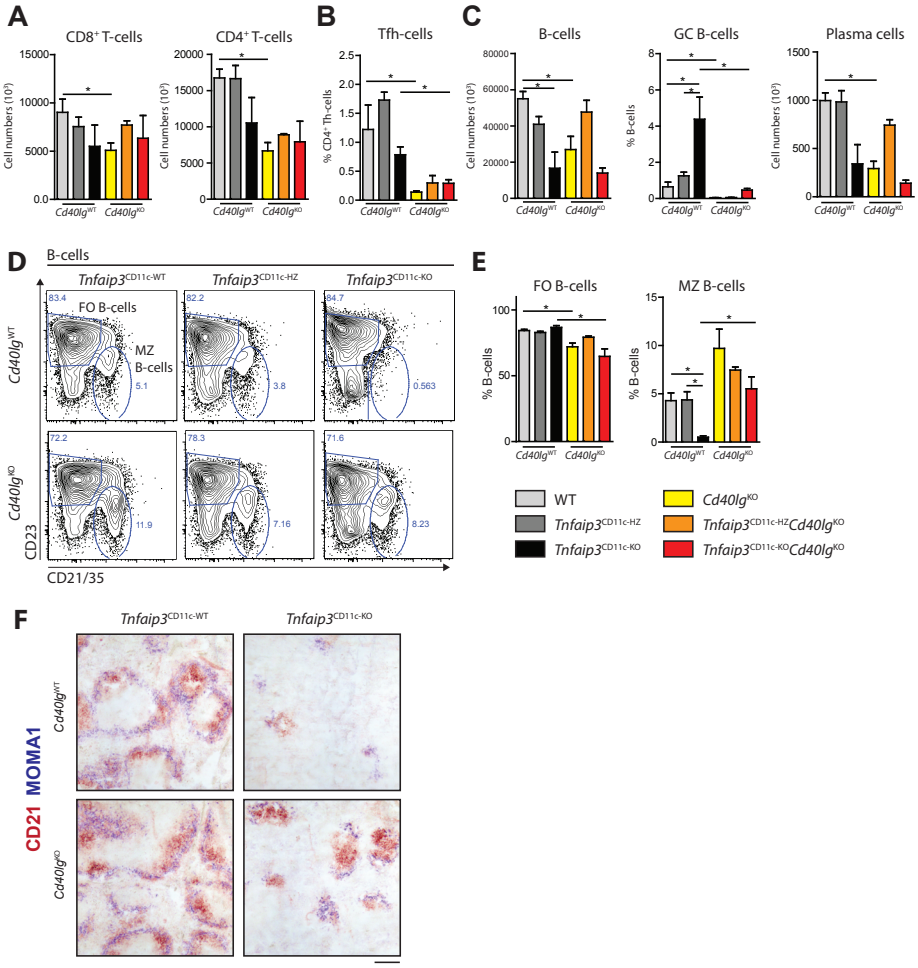

Figure 3: Reduction of MZ B cells in *Tnfaip3*$^{CD11c\text{-}KO}$ mice is restored by *Cd40lg* deletion.
Naïve 10-week-old *Tnfaip3*^{CD11c}*Cd40lg* mice spleens were analyzed for T cells and B cells. (**A-E**) Quantification of splenic CD8$^+$ T cells (CD3$^+$CD8$^+$CD4$^-$), CD4$^+$ T cells (CD3$^+$CD4$^+$CD8$^-$) (**A**), Follicular T-helper cells (Tfh-cells; CD3$^+$CD4$^+$CXCR5$^+$PD1^{hi}) (**B**), B cells (B220$^+$), Germinal center B cells (B220$^+$CD138$^-$CD95$^+$IgD$^-$), Plasma cells (B220$^-$CD138$^+$) (**C**) using flow cytometry. (**D**) Flow cytometric analysis of Follicular B cells (FO B cells; B220$^+$CD23$^+$, CD21/35^{int}) and Marginal zone B cells (MZ B cells; B220$^+$CD23$^-$, CD21/35$^+$) (**E**) Quantification of splenic FO B cell and MZ B cell proportions using flow cytometry. (**F**) Immunohistochemistry of spleens for MOMA1$^+$ (Blue) macrophages and CD21$^+$ (red) MZ B cells. Scale bars represent 200µm. Representative data is shown from one out of two independent experiments. Results are presented as mean values ± SEM of *n* = 2-5 mice per group. *P<0.05, **P<0.01.

We next investigated cytokine expression in splenic T cells. IL-21 mRNA expression in $CD3^+CD4^+CD44^+$ effector $CD4^+$ T-cells was apparently not affected by *Tnfaip3* deletion (**Figure 4B**), but was decreased in $Cd40lg^{KO}$ mice and $Tnfaip3^{CD11c\text{-}HZ}Cd40lg^{KO}$ mice compared to their $Cd40lg^{WT}$ counterparts (**Figure 4B**). Interestingly, IL-21 mRNA expression in effector $CD4^+$ T-cells appeared to be rescued in $Tnfaip3^{CD11c\text{-}KO}Cd40lg^{KO}$ mice compared to $Cd40lg^{KO}$ mice (**Figure 4B**). The splenic total $CD4^+$ T cell population from $Tnfaip3^{CD11c\text{-}KO}$ mice contained elevated proportions of IL-4^+ cells compared to $Tnfaip3^{CD11c\text{-}HZ}$ mice and WT mice, as determined by intracellular flow cytometry (**Figure 4C**). Likewise, the proportions of IL-4^+ $CD4^+$ T cells from $Tnfaip3^{CD11c\text{-}KO}Cd40lg^{KO}$ mice were increased compared to $Cd40lg^{KO}$ mice (**Figure 4C**).

Other T cell-derived cytokines such as IFNγ, IL-6 and IL-17 can also promote B cell responses[25, 26]. The proportion of IFN-γ^+ splenic $CD4^+$ T cell did not differ within the three *Tnfaip3* genotypes on the $Cd40lg^{WT}$ background, but were decreased in $Cd40lg^{KO}$ mice (**Figure 4C**). A minor significant increment of IFN-γ-expressing $CD4^+$ T cells was seen in the spleen of $Tnfaip3^{CD11c\text{-}KO}Cd40lg^{KO}$ mice compared to $Cd40lg^{KO}$ mice (**Figure 4C**). The frequency of IL-6^+ $CD4^+$ T cells within $Tnfaip3^{CD11c\text{-}KO}$ mice was enhanced compared to $Tnfaip3^{CD11c\text{-}HZ}$ mice and WT mice (**Figure 4C**).

Interestingly, the most pronounced increase in IL-6^+ $CD4^+$ T cells was observed in $Tnfaip3^{CD11c\text{-}KO}Cd40lg^{KO}$ mice (**Figure 4C**). The proportions of IL-17^+ $CD4^+$ T cells were enhanced in $Tnfaip3^{CD11c\text{-}KO}$ mice and $Tnfaip3^{CD11c\text{-}KO}Cd40lg^{KO}$ mice (**Figure 4C**). The proportions of IFN-γ^+ $CD8^+$ T cells did not significantly differ between the six genotypes (**Figure 4D**). A prominent increase in IL-6^+ $CD8^+$ T cells was seen in $Tnfaip3^{CD11c\text{-}KO}Cd40lg^{KO}$ mice compared to the other five groups of mice (**Figure 4D**).

In summary, in the absence of CD40L, FO B cells and MZ B cells from $Tnfaip3^{CD11c\text{-}KO}$ mice show increased expression of cell surface activation markers. Although the interaction of T cells with B cells is hampered by the absence of CD40L, $CD4^+$ and $CD8^+$ T cells from $Tnfaip3^{CD11c\text{-}KO}Cd40lg^{KO}$ mice still produce B cell-activating cytokines, such as IL-21, IL-4, IFN-γ, IL-17 and IL-6.

Aged $Tnfaip3^{CD11c\text{-}KO}$ mice do not develop GC B cell clusters in the absence of CD40L.

As previously reported[4], aged ~24-week-old $Tnfaip3^{CD11c\text{-}HZ}$ mice and $Tnfaip3^{CD11c\text{-}KO}$ mice harbor enlarged spleens in comparison to WT mice, largely due to extramedullary hematopoiesis (**Figure 5A**). Likewise, spleens of $Tnfaip3^{CD11c\text{-}HZ}Cd40lg^{KO}$ mice and $Tnfaip3^{CD11c\text{-}KO}Cd40lg^{KO}$ mice were enlarged compared to $Cd40lg^{KO}$ mice (**Figure 5A**). Similar to young mice, spleens of aged $Tnfaip3^{CD11c\text{-}KO}$ mice and $Tnfaip3^{CD11c\text{-}KO}Cd40lg^{KO}$ mice lacked normal lymphoid structures compared to $Tnfaip3^{CD11c\text{-}HZ}$ and $Tnfaip3^{CD11c\text{-}WT}$ mice on a WT or $Cd40lg^{KO}$ background (**Figure 5B**). The total numbers of $CD4^+$ T cells were similar in spleens in all six genotypes of aged mice (**Figure 5C**). Within the splenic $CD4^+$ T

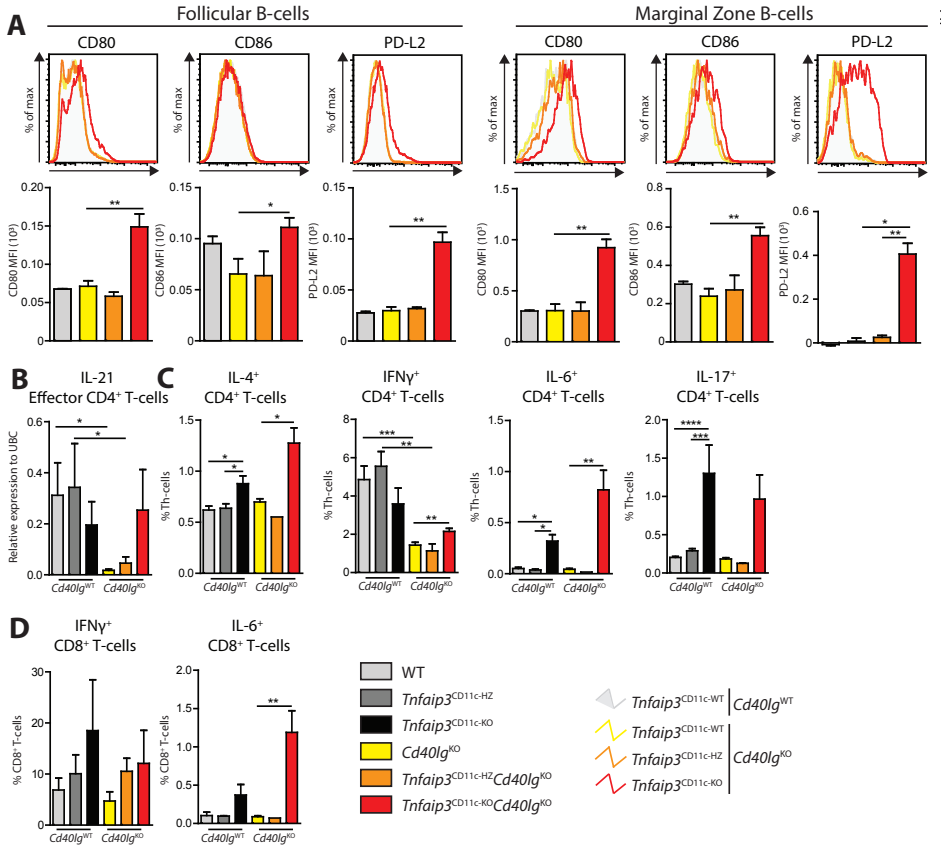

Figure 4: B cells from *Tnfaip3*$^{CD11c\text{-}KO}$*Cd40lg*^{KO} mice have an activated phenotype and T cells show robust expression of B cell-activating cytokines.

Naïve 10-week-old *Tnfaip3*^{CD11c}*Cd40lg* mice spleens were analyzed for FO B cells (CD19$^+$CD23$^+$CD21/35^{int}) and MZ B cells (CD19$^+$CD23$^-$CD21/35$^+$). Since MZ B cells were virtually absent in *Tnfaip3*$^{CD11c\text{-}KO}$ mice, only FO B cells and MZ B cells from *Tnfaip3*$^{CD11c\text{-}WT}$ mice were compared with all three *Cd40lg*^{KO} genotypes. (**A**) Histograms and bar-chart quantification of B cell activation markers CD80, CD86 and PD-L2. (**B**) Quantification of cytokines IL-21 expression in sorted effector T cells (CD3$^+$CD4$^+$CD44$^+$) using RT-PCR. (**C**) Enumeration of the proportions of intracellular IL-4$^+$, IFN-γ$^+$, IL-6$^+$ and IL-17$^+$ splenic CD4$^+$ T cells using flow cytometry. (**D**) Quantification of the proportions intracellular IFN-γ$^+$ and IL-6$^+$ CD8$^+$ T cells using flow cytometry. Data is shown from one experiment in (**A**-**B**) and pooled data from two experiments (**C**-**D**). Results are presented as mean values ± SEM of *n* = 2-7 mice per group. *P<0.05, **P<0.01, ***P<0.001, ****P<0.0001.

cells, the proportions of Tfh-cells were increased in *Tnfaip3*$^{CD11c\text{-}HZ}$ mice compared to WT mice and *Tnfaip3*$^{CD11c\text{-}KO}$ mice, but were severely reduced in the three *Tnfaip3* genotypes on the *Cd40lg*^{KO} background (**Figure 5D**). Splenic B cell numbers were reduced in aged *Tnfaip3*$^{CD11c\text{-}KO}$ mice compared to WT or *Tnfaip3*$^{CD11c\text{-}HZ}$ mice, but did not differ between the three *Tnfaip3* genotypes on the *Cd40lg*^{KO} background (**Figure 5E**). Whereas the frequencies of GC B cells were increased in spleens of *Tnfaip3*$^{CD11c\text{-}HZ}$ and *Tnfaip3*$^{CD11c\text{-}KO}$ mice, GC B

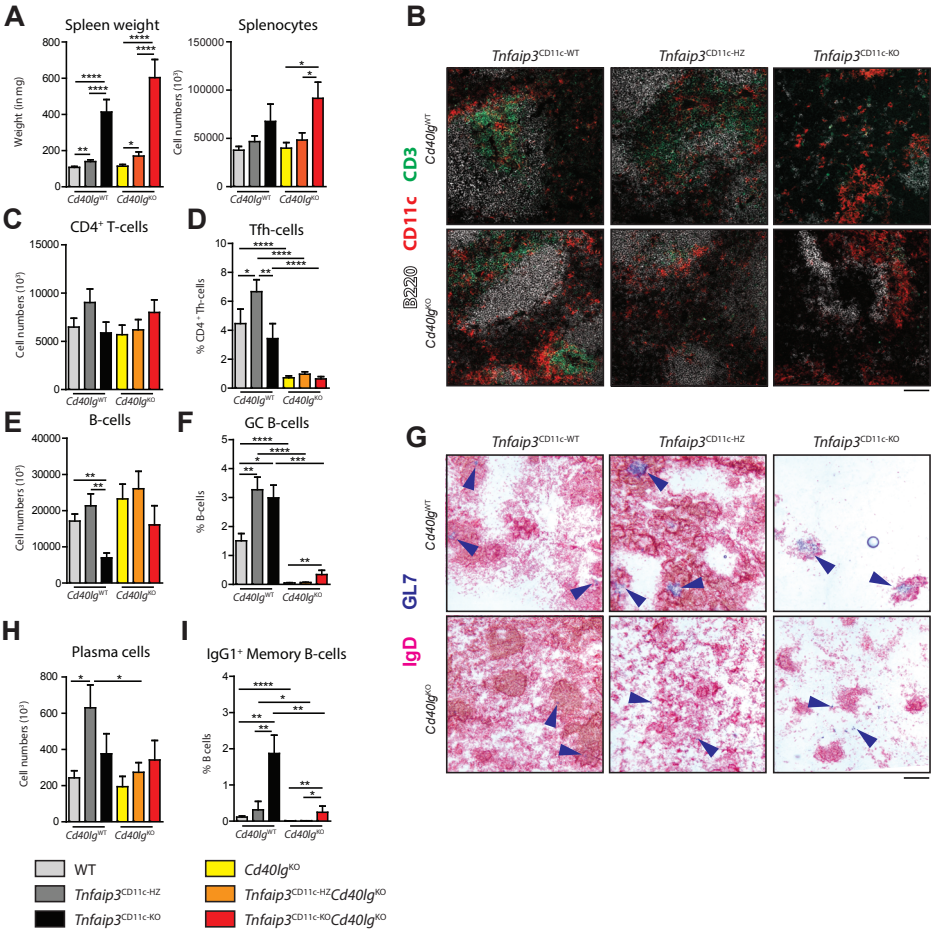

Figure 5: Aged *Tnfaip3*$^{CD11c\text{-}KO}$ mice do not develop GC B cell clusters in the absence of CD40L.
Naïve 24-week-old *Tnfaip3*^{CD11c}*Cd40lg* mice spleens were analyzed. (**A**) Enumeration of splenic weight and cellularity. (**B**) Confocal histology of spleens for CD3$^+$ (green); CD11c$^+$ (red) and B220$^+$ (white) cells. (**C-F**) Quantification of splenic CD4$^+$ T cell numbers (CD3$^+$CD4$^+$) (**C**), proportions of splenic Follicular Th-cells (Tfh-cells; CD3$^+$CD4$^+$CXCR5$^+$PD1^{hi}) (**D**), B cell (B220$^+$) numbers (**E**), and the proportions of splenic GC B cells (B220$^+$CD138$^-$CD95$^+$IgD$^-$) (**F**) using flow cytometry. (**G**) Immunohistochemistry of spleens for IgD$^+$ (Pink) and GL7$^+$ (Blue). (**H-I**) Quantification of splenic plasma cells (B220$^-$CD138$^+$) (**H**) and splenic memory IgG1$^+$ memory B cells (B220$^+$CD138$^-$IgG1$^{+(surface)}$) using flow cytometry. Results are pooled from 5-7 independent experiments and are presented as mean values ± SEM of *n* = 11-16 mice per group. Scale bars represent 200µm. *P<0.05, **P<0.01, ***P<0.001, ****P<0.0001.

cells were virtually absent in aged *Cd40lg*^{KO} and *Tnfaip3*$^{CD11c\text{-}HZ}$*Cd40lg*^{KO} mice (**Figure 5F**). Although B cells with a GC surface phenotype were detected in *Tnfaip3*$^{CD11c\text{-}KO}$*Cd40lg*^{KO} mice (**Figure 5F**), GL7$^+$ B cells were only present as isolated B cells and no GC B cell clusters could be observed (**Figure 5G**). The numbers of splenic plasma cells were elevated in old *Tnfaip3*$^{CD11c\text{-}HZ}$ mice compared to WT controls (**Figure 5H**). Comparable to

young mice, splenic plasma cell counts did not differ significantly between three *Tnfaip3* genotypes on the *Cd40lg*^{KO} background (**Figure 5H**). IgG1^{+} memory B cells were significantly increased in *Tnfaip3*$^{CD11c\text{-}KO}$ compared to *Tnfaip3*$^{CD11c\text{-}HZ}$ mice and *Tnfaip3*$^{CD11c\text{-}WT}$ mice (**Figure 5I**). However, only a minor increase was observed in *Tnfaip3*$^{CD11c\text{-}KO}$*Cd40lg*^{KO} mice (**Figure 5I**).

Taken together, similar to young mice, aged *Tnfaip3*$^{CD11c\text{-}KO}$ mice develop splenomegaly irrespective of the presence of CD40L, with a disturbed splenic architecture. In aged *Tnfaip3*$^{CD11c\text{-}KO}$*Cd40lg*^{KO} mice, GC B cell clusters were absent.

Aged *Tnfaip3*$^{CD11c\text{-}KO}$*Cd40lg*^{KO} mice have IgM and IgA but not IgG1 autoantibodies.

Next, we used flow cytometry to asses IgM^{+}, IgG1^{+} and IgA^{+} plasma cells in the spleens of the six groups of mice. On the *Cd40lg*^{WT} background the proportions of plasma cells that were IgM^{+} were reduced in *Tnfaip3*$^{CD11c\text{-}KO}$ mice, which showed an increase in isotype switched plasma cells, in particular IgG1^{+} (**Figure 6A**). In contrast, the splenic plasma cells in all three *Tnfaip3* genotypes on the *Cd40lg*^{KO} background were mainly IgM^{+}. The remaining (~10%) immunoglobulin positive plasma cells, likely IgG2b, IgG2c or IgG3-positive plasma cells that can occur independently of T-cell interaction[9], did not differ between the genotypes.

Autoreactive anti-dsDNA IgG1 and IgA, but not IgM, were increased in the serum of *Tnfaip3*$^{CD11c\text{-}KO}$ mice compared to WT and *Tnfaip3*$^{CD11c\text{-}HZ}$ controls (**Figure 6B**), as previously shown[4]. Anti-dsDNA IgM was increased in *Tnfaip3*$^{CD11c\text{-}KO}$*Cd40lg*^{KO} mice, compared with *Cd40lg*^{KO} and *Tnfaip3*$^{CD11c\text{-}HZ}$*Cd40lg*^{KO} mice (**Figure 6B**). The absence of CD40L abrogated anti-dsDNA IgG1 and reduced the levels of anti-dsDNA IgA in the serum of the three *Tnfaip3* genotypes. Interestingly however, anti-dsDNA IgA in *Tnfaip3*$^{CD11c\text{-}KO}$*Cd40lg*^{KO} mice was enhanced compared to *Cd40lg*^{KO} mice (**Figure 6B**). Total IgM levels in serum were increased in *Tnfaip3*$^{CD11c\text{-}HZ}$ mice (**Figure 6C**). On *Cd40lg*^{KO} background serum IgM was elevated in both *Tnfaip3*$^{CD11c\text{-}HZ}$*Cd40lg*^{KO} and *Tnfaip3*$^{CD11c\text{-}KO}$*Cd40lg*^{KO} mice (**Figure 6C**). Serum total IgG1 and IgA was elevated in *Tnfaip3*$^{CD11c\text{-}KO}$ mice compared to WT mice and *Tnfaip3*$^{CD11c\text{-}HZ}$ mice, but was significantly lower in *Tnfaip3*$^{CD11c\text{-}KO}$*Cd40lg*^{KO} mice (**Figure 6C**).

Bone marrow (BM) of 24-week-old mice displayed non-significant increases in IgG1^{+} and IgA^{+} memory B-cells in *Tnfaip3*$^{CD11c\text{-}KO}$ mice, which were reduced in *Tnfaip3*$^{CD11c\text{-}KO}$*Cd40lg*^{KO} mice (**Supplementary Figure 4A**). In contrast to spleen, BM plasma cells were reduced in *Tnfaip3*$^{CD11c\text{-}KO}$*Cd40lg*^{KO} mice compared to *Tnfaip3*$^{CD11c\text{-}KO}$ mice (**Supplementary Figure 4B**). The proportions of IgM^{+} plasma cells in BM was lowest in *Tnfaip3*$^{CD11c\text{-}KO}$ mice and *Tnfaip3*$^{CD11c\text{-}KO}$*Cd40lg*^{KO} mice compared to the other four genotypes (**Supplementary Figure 4C**). The high proportions of bone marrow IgG1^{+} and IgA^{+} plasma cells were similar to the results seen in *Tnfaip3*$^{CD11c\text{-}KO}$ mice spleens, with

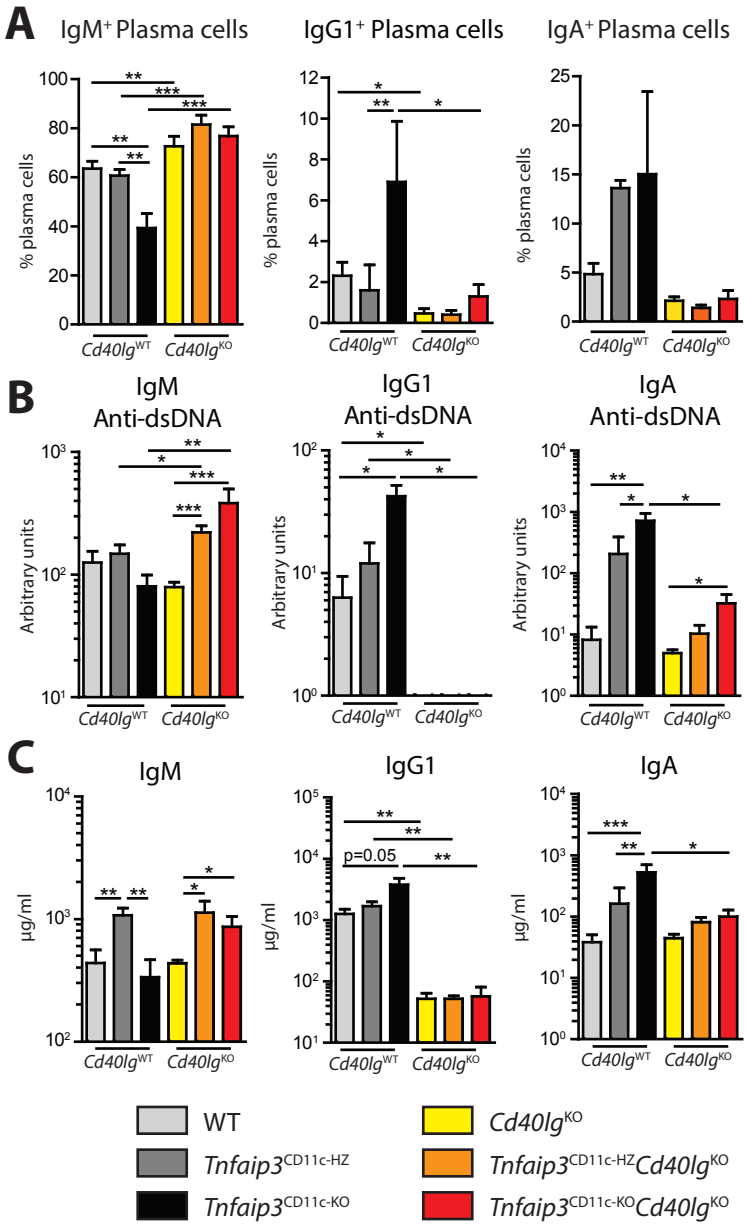

Figure 6: Aged *Tnfaip3*$^{CD11c\text{-}KO}$*Cd40lg*^{KO} mice have IgM and IgA but not IgG1 auto-antibodies.
Naïve 24-week-old *Tnfaip3*^{CD11c}*Cd40lg* mice serum were analyzed. (**A**) Quantification of IgM$^+$ plasma cells (B220$^-$CD138$^+$IgM$^+$), IgG1$^+$ plasma cells (B220$^-$CD138$^+$IgG1$^+$) and IgA$^+$ plasma cells (B220$^-$CD138$^+$IgA$^+$) using flow cytometry. (**B**) Quantification of serum autoreactive IgM, IgG1 and IgA immunoglobulins against ds-DNA using ELISA. **(C)** Quantification of total serum IgM, IgG1 and total IgA using ELISA. Results are pooled from 2-5 independent experiments and are presented as mean values ± SEM of *n* = 11-16 mice per group. *P<0.05, **P<0.01, ***P<0.001, ****P<0.0001. Scale bars represent 200µm.

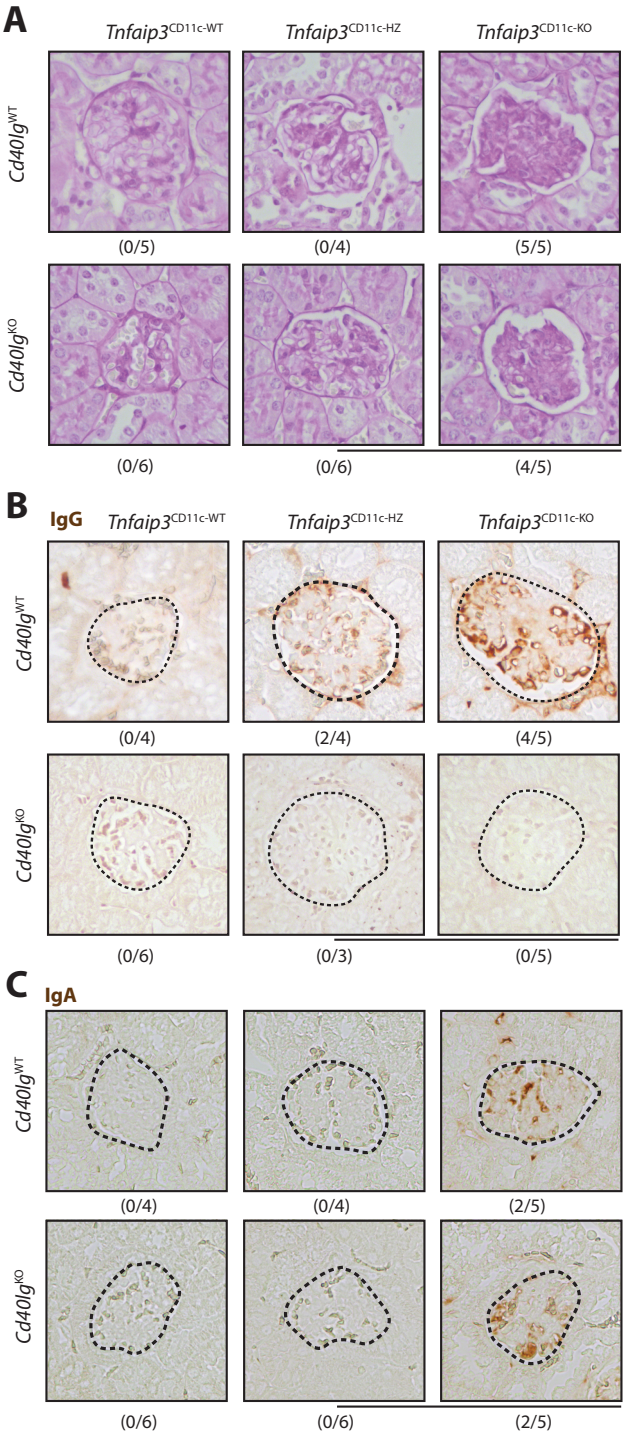

Figure 7: Basement membrane thickening and IgA deposition in kidneys of *Tnfaip3*$^{CD11c\text{-}KO}$*Cd40lg*^{KO} mice. Naïve 24-week-old *Tnfaip3*^{CD11c}*Cd40lg* mice kidneys were analyzed. (**A**) Kidney paraffin slides were stained using Periodic Acid Schiff (PAS)$^{+}$ staining (or PAS-diastase staining). (**B**) Kidney paraffin slides were stained for IgG-positivity using immunohistochemistry. (**C**) Kidney paraffin slides were stained for IgA-positivity using immunohistochemistry. Results are from 4 independent experiments. Scale bars represent 200µm.

drastic reductions of these plasma cells on an *CD40lg*^{KO} background (**Supplementary Figure 4D/E**). A relatively large population of non-IgM/IgG1/IgA plasma cells was seen in *Tnfaip3*$^{CD11c\text{-}KO}$*Cd40lg*^{KO} mice (**Figure 4F**), likely expressing IgG2b, IgG2c or IgG3, given their CD40L-independence[9].

In short, the absence of CD40L hampered the formation of IgG1^{+} plasma cells, leading to a lack of total IgG1 and autoreactive IgG1 in the serum of *Tnfaip3*$^{CD11c\text{-}KO}$*Cd40lg*^{KO} mice. Interestingly, in these mice anti-dsDNA IgM was higher than in the *Tnfaip3*$^{CD11c\text{-}KO}$*Cd40lg*^{WT} counterparts and anti-dsDNA IgA remained detectable.

Basement membrane thickening and IgA deposition in kidneys of *Tnfaip3*$^{CD11c\text{-}KO}$*Cd40lg*^{KO} mice.

Aged *Tnfaip3*$^{CD11c\text{-}KO}$ mice developed inflammatory infiltrates in livers and pancreas islets of Langerhans, which were still present in *Tnfaip3*$^{CD11c\text{-}KO}$*Cd40lg*^{KO} mice but absent in control mice (**Supplementary Figure 5A/B**). As previously demonstrated[4], aged *Tnfaip3*$^{CD11c\text{-}KO}$ mice developed membranoproliferative glomerulonephritis with increased glomerular cellularity and thickening of the basement membranes, compared with *Tnfaip3*$^{CD11c\text{-}HZ}$ mice and WT mice (**Figure 7A**). Interestingly, basement membrane thickening was also observed in kidneys of *Tnfaip3*$^{CD11c\text{-}KO}$*Cd40lg*^{KO} mice, but not in *Cd40lg*^{KO} controls (**Figure 7A**).

Basement membrane thickening in kidneys in lupus glomerulonephritis patients develops due to immunoglobulin complex deposition[27]. Indeed, confirming previous results[4], kidneys of *Tnfaip3*$^{CD11c\text{-}KO}$ mice showed IgG deposition in the glomeruli (**Figure 7B**). However, IgG staining was completely absent in kidneys from all three *Tnfaip3*^{CD11c} genotypes on a *Cd40lg*^{KO} background (**Figure 7B**). Interestingly however, positive glomerular IgA staining could be observed in 2 out of 5 *Tnfaip3*$^{CD11c\text{-}KO}$ mice and *Tnfaip3*$^{CD11c\text{-}KO}$*Cd40lg*^{KO} mice, but was completely absent in the other genotypes (**Figure 7C**).

In summary, basement membrane thickening in *Tnfaip3*$^{CD11c\text{-}KO}$ mice occurs in the absence of CD40L-derived signals and is independent of glomerular IgG deposition. Since IgA deposits were observed in the kidney glomeruli of *Tnfaip3*$^{CD11c\text{-}KO}$*Cd40lg*^{KO} mice, these may well be involved in the induction of basement membrane thickening in the kidneys.

DISCUSSION

DCs critically control immune homeostasis[1]. Mice harboring activated DCs, through ablation of *Tnfaip3*/A20 develop autoimmunity, with increased T cell and B cell activation[3, 4]. *In vitro* B cells could be activated by *Tnfaip3*-deficient BM-DCs without T cell help[4]. In this study, we abrogated T-B cell communication through ablation of CD40L

to examine whether B cell activation could be provoked by *Tnfaip3*-deficient DCs *in vivo* without T cell help[8]. While IgG1 was drastically reduced in *Tnfaip3*$^{CD11c\text{-}KO}$ mice lacking CD40L-signaling, they still developed kidney pathology and (autoreactive) IgA and IgM. T-B cell communication appears therefore not necessary for autoimmune organ inflammation in *Tnfaip3*$^{CD11c\text{-}KO}$ mice.

Using an unbiased approach, we first confirmed by GSEA[17] that full or heterozygote loss of *Tnfaip3* in BM-DCs caused activation, shown by the enrichment for several cytokine-signaling pathways, most prominently "TNF-α signaling via NF-κB". The *in vitro* B cell response driven by *Tnfaip3*-deficient BM-DCs was facilitated by high IL-6 production[4]. *Tnfaip3*-deficient BM-DCs harbored an increased expression of prominent T cell differentiating cytokines, such as IL-12 and IL-23[28] as well as several TI cytokines, such as IL-6[29] and IL-1β[30]. It is puzzling that in our analyses the TI hallmark genes BAFF and APRIL[11] were not significantly upregulated in *Tnfaip3*$^{CD11c\text{-}KO}$ BM-DCs, in contrast to previous publication[4]. In any case, these proteins were not involved in the *in vitro* B cell immunoglobulin production induced by *Tnfaip3*-deficient BM-DCs[4].

As expected, *Tnfaip3*-deficient DCs in spleens of mice harbored an activated phenotype, shown by elevated CD40, CD86 and PD-L1 expression, which appeared to be further elevated when CD40L was absent. Most likely this is not a direct consequence of CD40L-CD40 interaction on DCs, as CD40 signaling in DCs is known to promote the expression of CD80/CD86[31]. It is conceivable that other signals, such as proinflammatory cytokines, promote the increased activation status of DCs.

GC formation critically depends on CD40L-CD40 interaction[32], which we confirmed in both young and aged *Cd40lg*^{KO} mice, as the number of both GC B cells and Tfh-cells were strongly decreased. Despite the absence of clusters of GC B cells and Tfh-cells in *Tnfaip3*$^{CD11c\text{-}KO}$*Cd40lg*^{KO} mice, some B cells could still acquire a GL7^{+} GC B-cell phenotype. During TI immunizations, also in T cell-deficient mice, short-lived GC B cell responses can be induced[33, 34]. As we could not detect clusters of GC B cells in the spleens of *Tnfaip3*$^{CD11c\text{-}KO}$*Cd40lg*^{KO} mice, the GL7^{+} B cell phenotype might be induced by sporadic interaction of B cells and *Tnfaip3*-deficient DCs, promoting their TI activation. In particular MZ B cells are specialized in TI responses[35]. Strikingly, MZ B cells were almost absent in *Tnfaip3*$^{CD11c\text{-}KO}$ mice, but their proportions increased in *Tnfaip3*$^{CD11c\text{-}KO}$*Cd40lg*^{KO} mice. These MZ B cells displayed an activated phenotype, and in contrast to FO B cells, receptors for IL-21 and IL-4 were detected[36, 37]. Elevated expression of IL-4 and IL-21 was seen in CD4^{+} T cells of *Tnfaip3*$^{CD11c\text{-}KO}$*Cd40lg*^{KO} mice. Therefore, these cytokine signals can still be provided by T cells, thereby supporting activation of B cells, in particular of MZ B cells that express receptors for these cytokines.

Unexpectedly, in the absence of appropriate T-B cell communication, *Tnfaip3*$^{CD11c\text{-}KO}$ mice developed glomerulonephritis with glomerular basement membrane thickening. Anti-dsDNA IgG is well-known to cause kidney pathology by depositing in glomeruli

and forming immune complexes[38]. Indeed, IgG was present in kidneys of *Tnfaip3*$^{CD11c\text{-}KO}$ mice, but completely absent in the three *Tnfaip3* genotypes lacking CD40L. Instead, IgA was detected in the glomeruli of a fraction of *Tnfaip3*$^{CD11c\text{-}KO}$*Cd40lg*^{KO} mice, possibly contributing to glomerular membrane thickening, as indeed two out of five mice with IgA deposition had simultaneous glomerular membrane thickening present. Further research is required to identify the mechanisms involved in the kidney pathology in *Tnfaip3*$^{CD11c\text{-}KO}$*Cd40lg*^{KO} mice, particularly in mice that lack IgA complex deposition in the glomeruli. In this context, some SLE patients with glomerulonephritis have high anti-dsDNA IgA titers present[39], which may support the involvement of IgA in kidney pathology. IgA class switch can be induced by IL-6[40] and TGF-β[41]. As IL-6 expression was increased, but TGF-β mRNA expression was low in *Tnfaip3*-deficient BM-DCs (**Figure 1** and previously demonstrated[4, 14] it is conceivable that DC-derived IL-6 may play a prominent role in the induction of heavy chain class switch to IgA in our model. In support of this, in B cell cultures that were stimulated by *Tnfaip3*-deficient BM-DCs neutralization of IL-6 reduced IgA production by ~50%, indicating an important role for IL-6 in mediating increased Ig production when A20 is lacking in DCs. Nevertheless, IL-6 can be produced by a variety of cells, including splenic CD4$^+$ T cells, CD8$^+$ T cells and B cells in *Tnfaip3*$^{CD11c\text{-}KO}$ and *Tnfaip3*$^{CD11c\text{-}KO}$*Cd40lg*^{KO} mice. Therefore, the role of IL-6 in the pathology observed in *Tnfaip3*$^{CD11c\text{-}KO}$*Cd40lg*^{KO} mice is an interesting topic of research in the future. IL-6 is already well recognized as a promising therapeutic target to treat autoimmune diseases[42, 43]. In addition, the increased production of IFN-γ and IL-17 by CD4$^+$ T cells present in *Tnfaip3*$^{CD11c\text{-}KO}$*Cd40lg*^{KO} mice, compared with *Cd40lg*^{KO} mice, may contribute to the autoimmune pathology. Apart from IgA, anti-dsDNA IgM was enhanced in *Tnfaip3*$^{CD11c\text{-}KO}$*Cd40lg*^{KO} mice. We also found total IgM depositions in the glomeruli of these mice, and not in *Tnfaip3*$^{CD11c\text{-}KO}$ mice (data not shown). It is unlikely that these are pathologic immunoglobulin depositions, since autoreactive IgM anti-dsDNA is shown to delay glomerulonephritis in lupus mice[44].

In conclusion, T-B cell communication via CD40-CD40L interaction is not critical for B cell activation, Ig heavy chain class-switch, and autoimmune pathology including glomerulonephritis - possibly mediated by autoreactive IgA - in *Tnfaip3*$^{CD11c\text{-}KO}$ mice. In the context of therapies targeting CD40 or CD40L in human autoimmune diseases[45], it is of relevance that glomerular nephritis can develop independently of IgG deposition and CD40L in mice. However, whether this mechanism also occurs in humans and whether this would involve IgA auto-antibodies remains unknown.

Acknowledgements

We would like to thank Odilia Corneth and the Erasmus MC Animal Facility (EDC) staff for their assistance during the project. This project was supported by The Dutch Arthritis

Association (12-2-410) and the European Framework program 7 (FP7-MC-CIG grant 304221).

Conflict of interest

The authors declare no conflict of interest.

REFERENCES

1. Steinman RM. Decisions about dendritic cells: past, present, and future. *Annu Rev Immunol* 2012; 30: 1-22.
2. Sozzani S, Del Prete A, Bosisio D. Dendritic cell recruitment and activation in autoimmunity. *J Autoimmun* 2017; 85: 126-140.
3. Hammer GE, Turer EE, Taylor KE, Fang CJ, Advincula R, Oshima S *et al.* Expression of A20 by dendritic cells preserves immune homeostasis and prevents colitis and spondyloarthritis. *Nat Immunol* 2011; 12(12): 1184-1193.
4. Kool M, van Loo G, Waelput W, De Prijck S, Muskens F, Sze M *et al.* The ubiquitin-editing protein A20 prevents dendritic cell activation, recognition of apoptotic cells, and systemic autoimmunity. *Immunity* 2011; 35(1): 82-96.
5. Pan L, Lu MP, Wang JH, Xu M, Yang SR. Immunological pathogenesis and treatment of systemic lupus erythematosus. *World J Pediatr* 2019.
6. Malkiel S, Barlev AN, Atisha-Fregoso Y, Suurmond J, Diamond B. Plasma Cell Differentiation Pathways in Systemic Lupus Erythematosus. *Front Immunol* 2018; 9: 427.
7. Fagarasan S, Honjo T. T-Independent immune response: new aspects of B cell biology. *Science* 2000; 290(5489): 89-92.
8. Han S, Hathcock K, Zheng B, Kepler TB, Hodes R, Kelsoe G. Cellular interaction in germinal centers. Roles of CD40 ligand and B7-2 in established germinal centers. *J Immunol* 1995; 155(2): 556-567.
9. Whitmire JK, Slifka MK, Grewal IS, Flavell RA, Ahmed R. CD40 ligand-deficient mice generate a normal primary cytotoxic T-lymphocyte response but a defective humoral response to a viral infection. *J Virol* 1996; 70(12): 8375-8381.
10. Xu J, Foy TM, Laman JD, Elliott EA, Dunn JJ, Waldschmidt TJ *et al.* Mice deficient for the CD40 ligand. *Immunity* 1994; 1(5): 423-431.
11. Xu W, Banchereau J. The antigen presenting cells instruct plasma cell differentiation. *Front Immunol* 2014; 4: 504.
12. Renshaw BR, Fanslow WC, 3rd, Armitage RJ, Campbell KA, Liggitt D, Wright B *et al.* Humoral immune responses in CD40 ligand-deficient mice. *J Exp Med* 1994; 180(5): 1889-1900.
13. van Rijt LS, Prins JB, Leenen PJ, Thielemans K, de Vries VC, Hoogsteden HC *et al.* Allergen-induced accumulation of airway dendritic cells is supported by an increase in CD31(hi)Ly-6C(neg) bone marrow precursors in a mouse model of asthma. *Blood* 2002; 100(10): 3663-3671.
14. Vroman H, Bergen IM, van Hulst JAC, van Nimwegen M, van Uden D, Schuijs MJ *et al.* TNF-alpha-induced protein 3 levels in lung dendritic cells instruct TH2 or TH17 cell differentiation in eosinophilic or neutrophilic asthma. *J Allergy Clin Immunol* 2018; 141(5): 1620-1633 e1612.
15. Trapnell C, Williams BA, Pertea G, Mortazavi A, Kwan G, van Baren MJ *et al.* Transcript assembly and quantification by RNA-Seq reveals unannotated transcripts and isoform switching during cell differentiation. *Nat Biotechnol* 2010; 28(5): 511-515.
16. Trapnell C, Hendrickson DG, Sauvageau M, Goff L, Rinn JL, Pachter L. Differential analysis of gene regulation at transcript resolution with RNA-seq. *Nat Biotechnol* 2013; 31(1): 46-53.
17. Subramanian A, Tamayo P, Mootha VK, Mukherjee S, Ebert BL, Gillette MA *et al.* Gene set enrichment analysis: a knowledge-based approach for interpreting genome-wide expression profiles. *Proc Natl Acad Sci U S A* 2005; 102(43): 15545-15550.
18. Vroman H, Bergen IM, Li BW, van Hulst JA, Lukkes M, van Uden D *et al.* Development of eosinophilic inflammation is independent of B-T cell interaction in a chronic

house dust mite-driven asthma model. *Clin Exp Allergy* 2017; 47(4): 551-564.
19. Das T, Bergen IM, Koudstaal T, van Hulst JAC, van Loo G, Boonstra A *et al.* DNGR1-mediated deletion of A20/Tnfaip3 in dendritic cells alters T and B-cell homeostasis and promotes autoimmune liver pathology. *J Autoimmun* 2019; 102: 167-178.
20. Hunter CA, Jones SA. IL-6 as a keystone cytokine in health and disease. *Nat Immunol* 2015; 16(5): 448-457.
21. Ritvo PG, Klatzmann D. Interleukin-1 in the Response of Follicular Helper and Follicular Regulatory T Cells. *Front Immunol* 2019; 10: 250.
22. Corneth OB, de Bruijn MJ, Rip J, Asmawidjaja PS, Kil LP, Hendriks RW. Enhanced Expression of Bruton's Tyrosine Kinase in B Cells Drives Systemic Autoimmunity by Disrupting T Cell Homeostasis. *J Immunol* 2016; 197(1): 58-67.
23. Vinuesa CG, Linterman MA, Yu D, MacLennan IC. Follicular Helper T Cells. *Annu Rev Immunol* 2016; 34: 335-368.
24. Gonzalez DG, Cote CM, Patel JR, Smith CB, Zhang Y, Nickerson KM *et al.* Nonredundant Roles of IL-21 and IL-4 in the Phased Initiation of Germinal Center B Cells and Subsequent Self-Renewal Transitions. *J Immunol* 2018; 201(12): 3569-3579.
25. Subbarayal B, Chauhan SK, Di Zazzo A, Dana R. IL-17 Augments B Cell Activation in Ocular Surface Autoimmunity. *J Immunol* 2016; 197(9): 3464-3470.
26. Kopf M, Herren S, Wiles MV, Pepys MB, Kosco-Vilbois MH. Interleukin 6 influences germinal center development and antibody production via a contribution of C3 complement component. *J Exp Med* 1998; 188(10): 1895-1906.
27. Yung S, Yap DY, Chan TM. Recent advances in the understanding of renal inflammation and fibrosis in lupus nephritis. *F1000Res* 2017; 6: 874.
28. Zhu J, Yamane H, Paul WE. Differentiation of effector CD4 T cell populations (*). *Annu Rev Immunol* 2010; 28: 445-489.
29. Hirano T, Taga T, Nakano N, Yasukawa K, Kashiwamura S, Shimizu K *et al.* Purification to homogeneity and characterization of human B-cell differentiation factor (BCDF or BSFp-2). *Proc Natl Acad Sci U S A* 1985; 82(16): 5490-5494.
30. Nakae S, Asano M, Horai R, Iwakura Y. Interleukin-1 beta, but not interleukin-1 alpha, is required for T-cell-dependent antibody production. *Immunology* 2001; 104(4): 402-409.
31. Caux C, Massacrier C, Vanbervliet B, Dubois B, Van Kooten C, Durand I *et al.* Activation of human dendritic cells through CD40 cross-linking. *J Exp Med* 1994; 180(4): 1263-1272.
32. Kawabe T, Naka T, Yoshida K, Tanaka T, Fujiwara H, Suematsu S *et al.* The immune responses in CD40-deficient mice: impaired immunoglobulin class switching and germinal center formation. *Immunity* 1994; 1(3): 167-178.
33. Dianda L, Gulbranson-Judge A, Pao W, Hayday AC, MacLennan IC, Owen MJ. Germinal center formation in mice lacking alpha beta T cells. *European journal of immunology* 1996; 26(7): 1603-1607.
34. Lentz VM, Manser T. Cutting edge: germinal centers can be induced in the absence of T cells. *J Immunol* 2001; 167(1): 15-20.
35. Cerutti A, Cols M, Puga I. Marginal zone B cells: virtues of innate-like antibody-producing lymphocytes. *Nat Rev Immunol* 2013; 13(2): 118-132.
36. Turqueti-Neves A, Otte M, Prazeres da Costa O, Hopken UE, Lipp M, Buch T *et al.* B-cell-intrinsic STAT6 signaling controls germinal center formation. *European journal of immunology* 2014; 44(7): 2130-2138.
37. Zotos D, Coquet JM, Zhang Y, Light A, D'Costa K, Kallies A *et al.* IL-21 regulates germinal center B cell differentiation and proliferation through a B cell-intrinsic

mechanism. *J Exp Med* 2010; 207(2): 365-378.

38. Madaio MP, Carlson J, Cataldo J, Ucci A, Migliorini P, Pankewycz O. Murine monoclonal anti-DNA antibodies bind directly to glomerular antigens and form immune deposits. *J Immunol* 1987; 138(9): 2883-2889.
39. Villalta D, Bizzaro N, Bassi N, Zen M, Gatto M, Ghirardello A *et al.* Anti-dsDNA antibody isotypes in systemic lupus erythematosus: IgA in addition to IgG anti-dsDNA help to identify glomerulonephritis and active disease. *PLoS One* 2013; 8(8): e71458.
40. Beagley KW, Eldridge JH, Lee F, Kiyono H, Everson MP, Koopman WJ *et al.* Interleukins and IgA synthesis. Human and murine interleukin 6 induce high rate IgA secretion in IgA-committed B cells. *J Exp Med* 1989; 169(6): 2133-2148.
41. Sonoda E, Matsumoto R, Hitoshi Y, Ishii T, Sugimoto M, Araki S *et al.* Transforming growth factor beta induces IgA production and acts additively with interleukin 5 for IgA production. *J Exp Med* 1989; 170(4): 1415-1420.
42. Ho LJ, Luo SF, Lai JH. Biological effects of interleukin-6: Clinical applications in autoimmune diseases and cancers. *Biochem Pharmacol* 2015; 97(1): 16-26.
43. Wallace DJ, Strand V, Merrill JT, Popa S, Spindler AJ, Eimon A *et al.* Efficacy and safety of an interleukin 6 monoclonal antibody for the treatment of systemic lupus erythematosus: a phase II dose-ranging randomised controlled trial. *Ann Rheum Dis* 2017; 76(3): 534-542.
44. Werwitzke S, Trick D, Kamino K, Matthias T, Kniesch K, Schlegelberger B *et al.* Inhibition of lupus disease by anti-double-stranded DNA antibodies of the IgM isotype in the (NZB x NZW)F1 mouse. *Arthritis Rheum* 2005; 52(11): 3629-3638.
45. Nakamura M, Tanaka Y, Satoh T, Kawai M, Hirakata M, Kaburaki J *et al.* Autoantibody to CD40 ligand in systemic lupus erythematosus: association with thrombocytopenia but not thromboembolism. *Rheumatology (Oxford)* 2006; 45(2): 150-156.

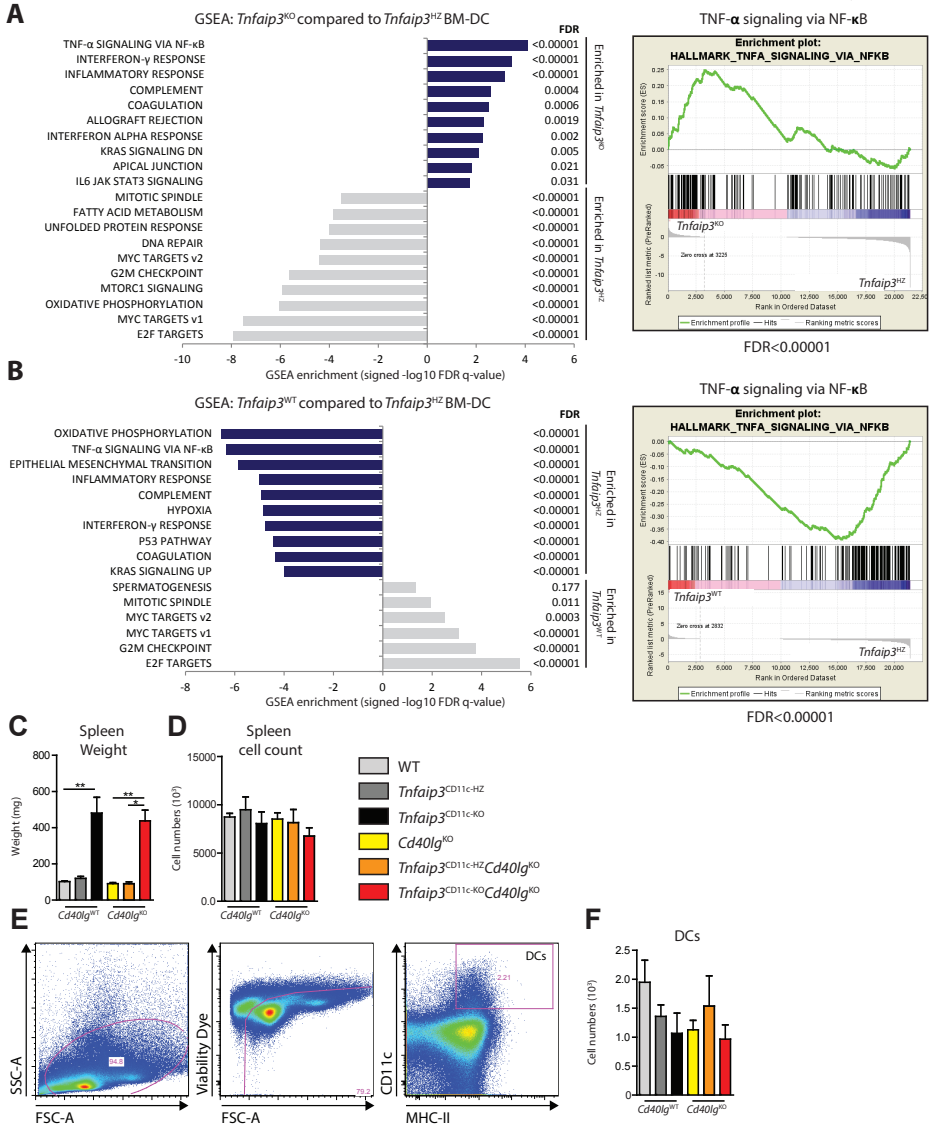

Supplementary Figure 1: BM-DCs and Dendritic cells are activated with loss of Tnfaip3/A20.
BM-derived dendritic cells (BM-DCs) were analyzed by RNA Next generation sequencing (NGS). (**A-B**) Gene set enrichment analysis (GSEA) performed for the ranked list of significantly altered genes between BM-DCs from *Tnfaip3*$^{CD11c\text{-}KO}$ mice and *Tnfaip3*$^{CD11c\text{-}HZ}$ mice (**A**) and *Tnfaip3*$^{CD11c\text{-}WT}$ mice and *Tnfaip3*$^{CD11c\text{-}HZ}$ mice (**B**). Only the top results with a False Discovery Rate (FDR)<0.25 are shown. Enrichments plots for the Hallmark gene set TNFα signaling via NF-κB is also displayed. (**C-F**) Naïve 10-week-old *Tnfaip3*^{CD11c}*Cd40lg* mice spleens were analyzed for (**C-D**) Enumeration of splenic weight (**C**) and cellularity (**D**) using flow cytometry. (**E-F**) Gating strategy for splenic DCs (CD11c^{+}MHC-II^{+}) (**E**) and DC numbers (**F**) using flow cytometry. NGS data is from n=4 BM-DC cultures per genotype. Data in (**C-F**) shown from 2 independent experiments and results are presented as mean values ± SEM of n = 2-7 mice per group. *P<0.05, **P<0.01.

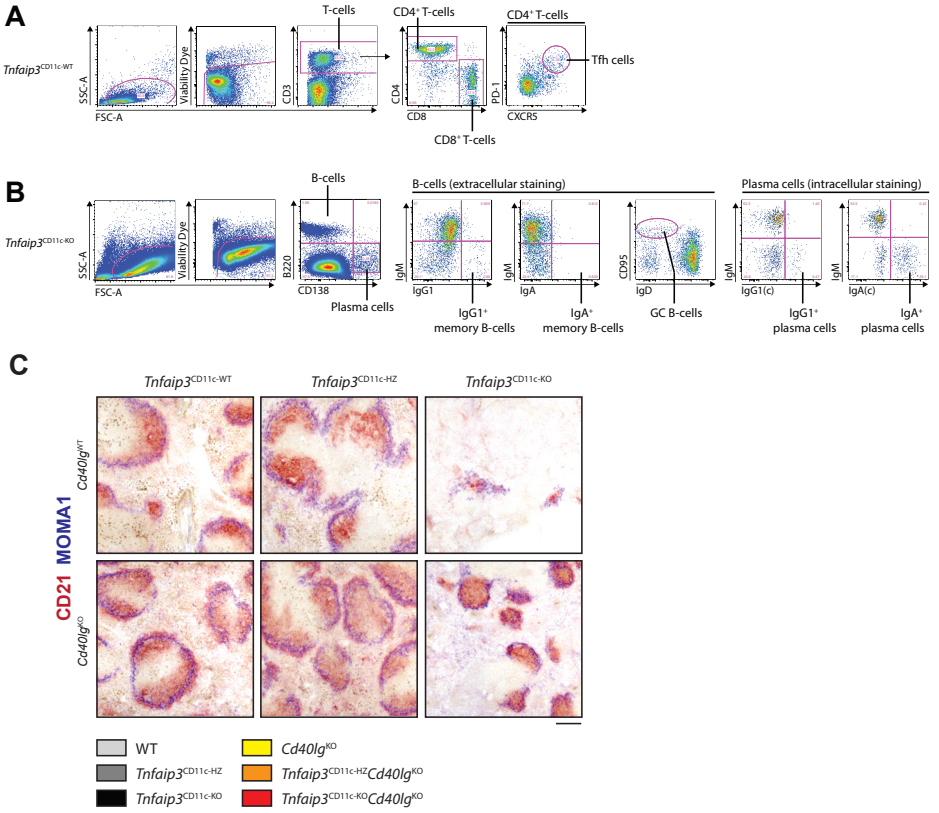

Supplementary Figure 2: Old *Tnfaip3*$^{CD11c\text{-}KO}$ mice have restored MZ B-cells proportions and histology. Gating strategy in naïve *Tnfaip3*^{CD11c}*Cd40lg* spleens to determine T-cells (**A**) and B-cells (**B**) mentioned in Figure 3 and Figure 5. (**C**) Naïve 24-week-old *Tnfaip3*^{CD11c}*Cd40lg* spleens were analyzed by immunohistochemistry. (**C**) Immunohistochemistry of spleens for MOMA1^{+} (Blue) macrophages and CD21^{+} (red) MZ B-cells. Scale bars represent 200µm.

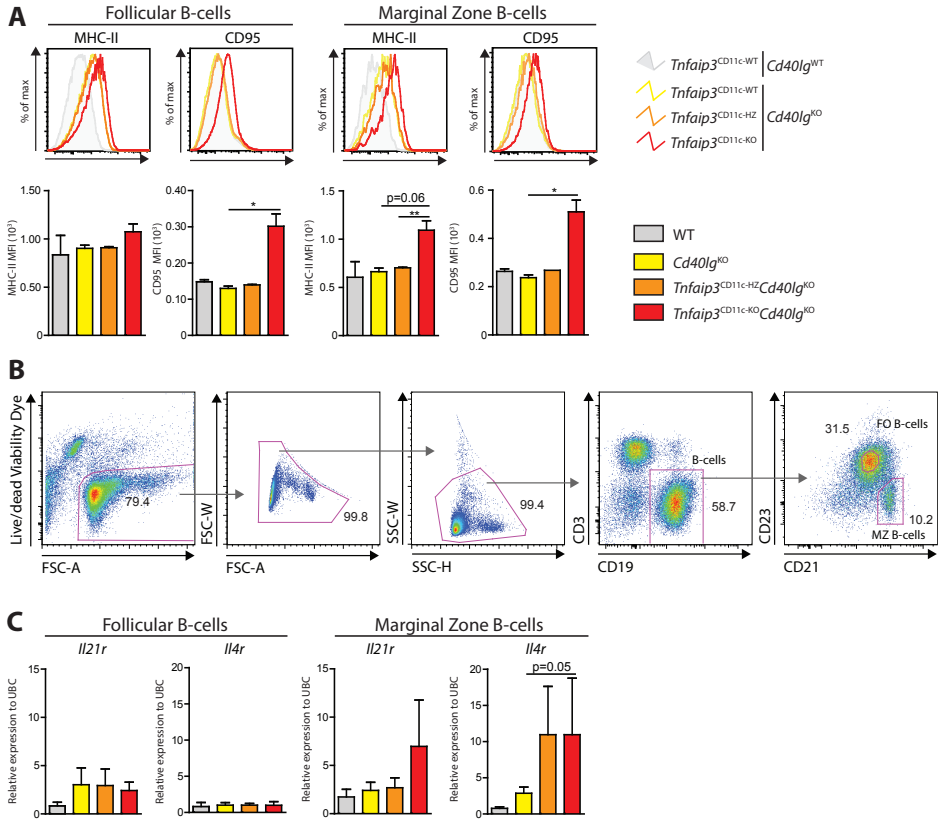

Supplementary Figure 3: Follicular B-cells in Tnfaip3CD11c-KOCd40lgKO mice are also activated, but do not express GC receptors.

Naïve 10-week-old *Tnfaip3*^{CD11c}*Cd40lg* mice spleens were analyzed for FO B-cells (CD19^{+}CD23^{+}, CD21/35^{int}) and MZ B-cells (CD19^{+}CD23^{-}CD21/35^{+}). (**A**) Histograms and barchart quantification of FO B-cell and MZ B-cell MHC-II and CD95 using flow cytometry. (**B**) Flow cytometry sorting gating strategy for both splenic FO B-cells and splenic MZ B-cells. (**C**) Sorted FO B-cells and MZ B-cells from spleens were analyzed using RT-PCR to quantify mRNA levels of Il21r and Il4r. Data is shown from one experiment. Results are presented as mean values ± SEM of n = 2-6 mice per group. *P<0.05, **P<0.01.

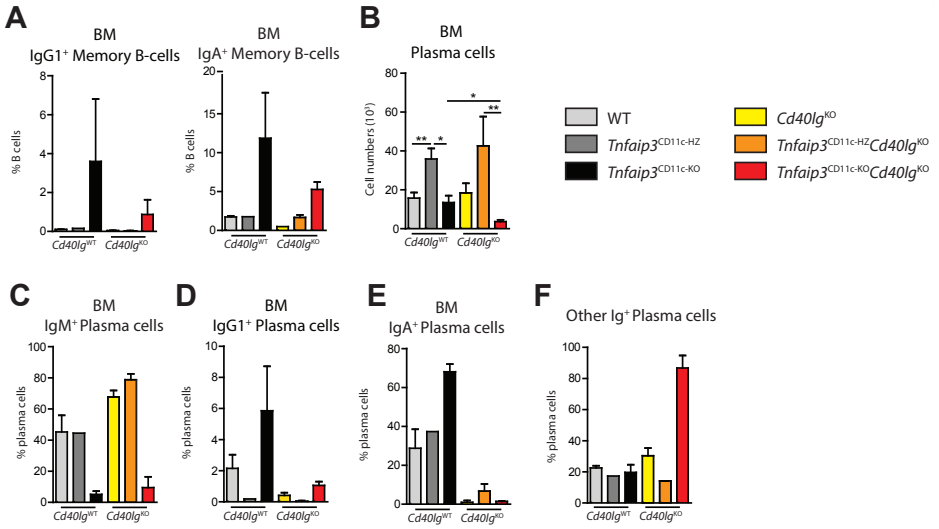

Supplementary Figure 4: Bone marrows of *Tnfaip3*$^{CD11c\text{-}KO}$ mice have enhanced IgG1 B-cells, but not without CD40L signaling.

Analysis of Naïve 24-week-old *Tnfaip3*^{CD11c}*Cd40lg* mice serum and bone marrows. (**A-F**) Enumeration of proportions of IgG1$^+$ Memory B-cells (B220$^+$CD138$^-$IgG1$^+$) and IgA$^+$ memory B-cells (B220$^+$CD138$^-$IgA$^+$) (**A**), plasma cell (numbers B220$^+$CD138$^+$) (**B**) IgM$^+$ plasma cells (B220$^-$CD138$^+$IgM$^+$) (**C**), IgG1$^+$ plasma cells (B220$^-$CD138$^+$IgG1$^+$) (**D**), IgA$^+$ plasma cells (B220$^-$CD138$^+$IgA$^+$) (**E**) and other immunoglobulin-positive plasma cells (B220$^-$CD138$^+$IgM$^-$IgG1$^-$IgA$^-$) (**F**) using flow cytometry. Data is shown of n = 3 independent experiments (in B) and 1 experiments (in A,C-F) and results are presented as mean values ± SEM of n = 2-9 mice per group. *P<0.05, **<P0.01.

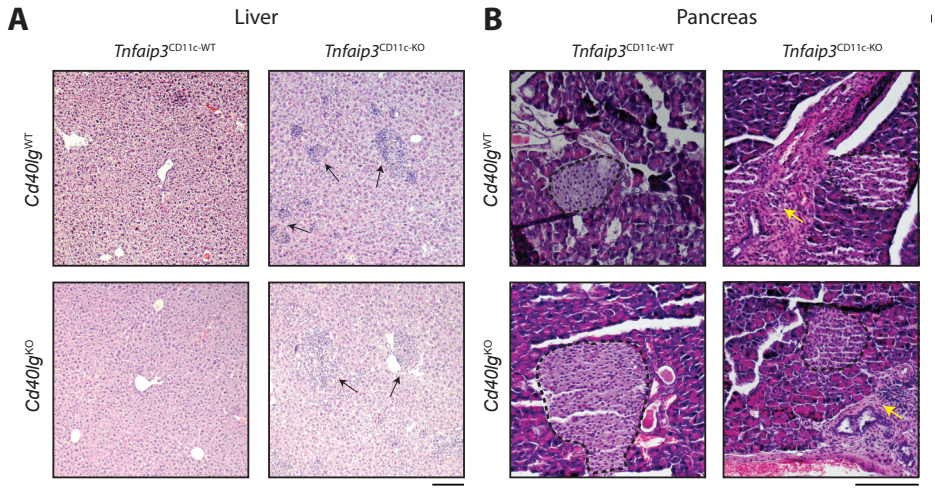

Supplementary Figure 5: Multiorgan inflammation in *Tnfaip3*$^{CD11c\text{-}KO}$ mice occurs independently of T-cell help.

Naïve 24-week-old *Tnfaip3*^{CD11c}*Cd40lg* mice tissues were stained using Hematoxylin and Eosin. Representative Liver (**A**) and Pancreas (**B**) tissues are shown. Liver inflammatory infiltrates (black arrows), islets of Langerhans (Dashed-circle) and Perivascular invlammation (yellow arrows) are depicted. Scale bars represent 200µm.

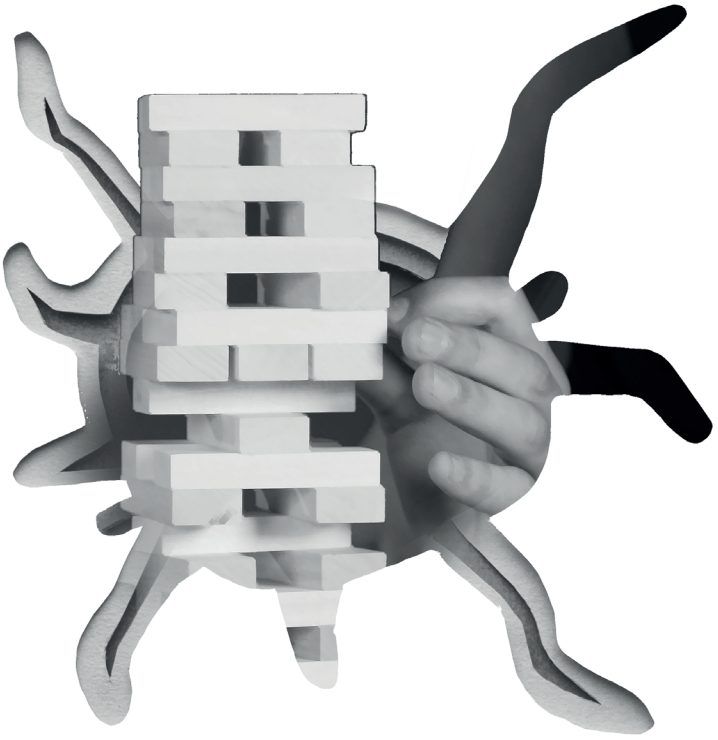

Chapter 7

Evidence that the autoimmune phenotype in mice with dendritic cell-specific deletion of Tnfaip3/A20 is independent of the IL-23/ IL-17 axis.

Tridib Das, Ingrid Bergen, Menno van Nimwegen, Jennifer van Hulst, Geert van Loo, Bart N. Lambrecht, Mirjam Kool, Rudi W. Hendriks

Manuscript in preparation

ABSTRACT

Background: Dendritic cells (DCs) are sentinel cells within the immune system that direct tolerogenic and immune conditions. Mice that lack *Tnfaip3*/A20, a negative regulator of NF-κB signaling, specifically in DCs (*Tnfaip3*$^{CD11c\text{-}KO}$ mice) have a lupus-like autoimmune phenotype characterized by autoantibodies and glomerulonephritis. *Tnfaip3*/A20-deficient DCs display spontaneous activation and thereby induce T and B cell activation. *In vitro* co-cultures of stimulated bone marrow-derived *Tnfaip3*$^{CD11c\text{-}KO}$ DCs with T cells display increased IL-17 production.

Objective: We investigated the role of IL-23, a key cytokine for T helper 17 (Th17) cell maintenance and expansion, in the pathology of the lupus-like autoimmune phenotype of *Tnfaip3* $^{CD11c\text{-}KO}$ mice.

Methods: *Tnfaip3*$^{CD11c\text{-}KO}$ mice were crossed to *Il23*^{KO} mice and *in vivo* Th subsets, B cell activation, levels of (auto-)antibodies and kidney inflammation were assessed in 24-week-old mice.

Results: Spleens of *Tnfaip3*$^{CD11c\text{-}KO}$ mice were enlarged, but additional loss of IL-23 resulted in a substantial reduction of spleen size, granulocytes and monocytes/macrophage counts. Although DCs from *Il23*^{KO}*Tnfaip3*$^{CD11c\text{-}KO}$ had a more activated phenotype than DCs from *Il23*^{WT}*Tnfaip3*$^{CD11c\text{-}KO}$ mice, their numbers in the spleen remained very low. *In vivo* Th17 cell differentiation was not enhanced in *Tnfaip3*$^{CD11c\text{-}KO}$ mice, compared to wild-type controls littermates. Loss of IL-23 did not significantly affect the numbers of Th17 cells in the spleen. Although splenic plasma cells were essentially not altered in *Tnfaip3*$^{CD11c\text{-}KO}$ mice, they were reduced by additional IL-23-deficiency. Total IgG1 or autoreactive IgG1 was increased in the serum of both *Il23*^{KO} and *Il23*^{WT} *Tnfaip3*$^{CD11c\text{-}KO}$ mice. Only IgA was greatly reduced in *Il23*^{KO}*Tnfaip3*$^{CD11c\text{-}KO}$ mice compared to *Il23*^{WT}*Tnfaip3*$^{CD11c\text{-}KO}$ mice. Finally, IL-23-deficiency did not affect glomerulonephritis in *Tnfaip3*$^{CD11\text{-}KO}$ mice.

Conclusion: These findings indicate that the lupus-like autoimmune pathology in *Tnfaip3*$^{CD11c\text{-}KO}$ mice is independent of the IL-23/IL-17 axis.

INTRODUCTION

Systemic lupus erythematosus (SLE) is the prototypical systemic autoimmune disorder in which multiple innate and adaptive immune cells, such as dendritic cells (DCs), T cells and B cells play an important role[1]. B lymphocytes are the primary effector cells in SLE pathogenesis[2]. As they become plasma cells, they produce autoreactive antibodies and thereby facilitate immune complexes that trigger kidney inflammation[3]. In addition, an imbalanced T-helper (Th) cell differentiation has been implicated in lupus pathology, because an increase of Th17 cells or their primary cytokine IL-17 was observed in patients compared to healthy controls and correlated with more disease activity[4, 5]. Further downstream, Th17 cells are known to facilitate differentiation of B cells into plasma cells and antibody production by secretion of cytokines[6, 7]. It has been demonstrated in mice that IL-17 is indispensable for the production of several autoantibodies and for the development of lupus nephritis[8].

Differentiation and stabilization of Th17 cells is dependent on IL-23[9], which is primarily produced by activated antigen presenting cells including DCs or monocytes/macrophages[10]. IL-23R signaling is responsible for increasing RORγt expression and IL-17 via STAT3[11]. Next to its function in survival and expansion of Th17 cells[12], IL-23 is also involved in unlocking the full pathogenic potential of Th17 cells[13]. The observation that the addition of ustekinumab, a monoclonal antibody that inhibits IL-23 and IL-12, to standard-of-care treatment resulted in a better efficacy in clinical and laboratory parameters than placebo, supports further development of ustekinumab as a novel therapeutic strategy in SLE[14, 15].

Ablation of the *Tnfaip3* gene encoding A20, a negative regulator of the NF-κB signaling pathway, specifically in DCs *in vivo* (in *Tnfaip3*$^{CD11c\text{-}KO}$ mice), resulted in T cell and B cell activation, antibody class switching, systemic inflammation, and glomerulonephritis, generating a phenotype resembling SLE[16]. Stimulated DCs lacking A20/Tnfaip3 produced high levels of IL-23 and promoted IL-17 production in *in vitro* co-cultures with T cells[16]. Moreover, we recently demonstrated that A20/Tnfaip3-deficient DCs induced Th17 cell differentiation via production of the pro-inflammatory cytokines IL-1β, IL-6 and IL-23 *in vivo* in a model of allergic airway inflammation[17].

In this report, we investigated whether ablation of IL-23 would alter Th17 cell induction in *Tnfaip3*$^{CD11c\text{-}KO}$ mice *in vivo*. Th17 cells promote B cell proliferation and trigger antibody production and immunoglobulin (Ig) heavy chain class switch recombination *in vivo*[7]. Therefore, we wondered whether IL-23 abrogation would affect plasma cell differentiation and Ig production and consequently renal pathology. We found that absence of IL-23 in *Tnfaip3*$^{CD11c\text{-}KO}$ mice reduced the splenic myeloid cell populations, while increasing DC activation markers. Surprisingly, Th17 cells were not increased in 24-week-old *Tnfaip3*$^{CD11c\text{-}KO}$ mice, compared to *Tnfaip3*$^{CD11c\text{-}WT}$ mice. Moreover, the absence of IL-23 in

Tnfaip3$^{CD11c\text{-}KO}$ mice did not alter the numbers of Th17 cells or plasma cells in the spleen. Serum levels of total IgG1 and autoreactive IgG1 and kidney inflammation were also not dependent on IL-23.

MATERIALS AND METHODS

Mice

Cd11c-cre^{+} transgenic *Tnfaip3*$^{fl/fl}$ mice[16] were crossed with *Il23p19*$^{-/-}$ on a C57BL/6 background[18] to obtain *Il23*^{WT} *and Il23*^{KO} *Tnfaip3*$^{CD11c\text{-}KO}$ mice. Male and female mice were analyzed at 24-weeks of age and cre-deficient littermates were used as wild-type (WT) controls. Mice were bred and housed under specific pathogen-free conditions in the Erasmus MC experimental animal facility. All experiments were approved by the animal ethical committee of the Erasmus MC (EMC3329).

Tissue preparation

Spleens and bone marrow (BM) were taken from sacrificed mice to obtain single cell suspensions. One femur per mouse was crushed using a pestle and mortar and spleens were homogenized through a 100 µm cell strainer (Corning Inc., Corning, NY, USA) and collected in Gibco™ RPMI Medium 1640 (1 x) + GlutaMAX™-1 (Thermo Fisher Scientific Inc., Waltham, MA, USA). Red blood cells were lysed using osmotic lysis buffer (0.15 M NH_4CL, 10 mM $KHCO_3$, 0.1 mM EDTA, pH 7.1 - 7.4; sterile-filtered with 0.22 µm filter). Viable cells were counted using Tryptan blue and a Buerker-Tuerk counting chamber (Paul Marienfeld GmbH & Co. KG, Lauda Königshofen, Germany). Freshly isolated kidneys were incubated on Roti-Histofix 4% (Carl-Roth, Karlsruhe, Germany) for 24 hrs and then embedded in paraffin wax.

Periodic Acid Schiff Diastase (PAS-D) staining

Three µm-thick paraffin-embedded kidney sections were stained according to the PAS-D Staining protocol. Briefly, paraffin-embedded sections were dewaxed and hydrated to water using Xylene (Sigma-Aldrich) and ethanol dilutions in MilliQ. One part human saliva (containing the enzyme diastase) was diluted 1:10 with MilliQ and incubated on slides at room temperature for 30 min. Slides were placed in freshly prepared periodic acid solution for 5 min (Sigma-Aldrich) and subsequently in Schiff's reagent for 5 min and counterstained with Gill's hematoxylin (Merck Millipore) for 2 seconds. Finally, slides were dehydrated using Xylene and mounted in Entallan (Merck Millipore).

Immunohistochemistry of Cryosections

For immunohistochemistry, 6 µm acetone or 4 % formalin-fixed spleen sections were blocked in peroxidase blocking buffer (PBS, 0.67 % H_2O_2, 2 % NaN_3) at room temperature for 30 min. Blocking Buffer (1% Blocking Reagent (Roche Diagnostics GmbH, Mannheim, Germany) in PBS) containing 10% normal goat or donkey serum was used to prevent aspecific secondary antibody binding. Sections were stained with primary antibodies at room temperature for 1 hr, washed with PBS and incubated with alkaline phosphatase (AP) or peroxidase (PO) conjugated secondary antibodies at room temperature for 30 min. Used antibodies were: anti-GL7 (clone RUO, 1:50, eBioscience) and anti-IgD-PE (clone 11-26, 1:50, eBioscience) with alkaline phosphatase (AP)-conjugated goat anti-rat (1:50, Jackson Immunoresearch) and peroxidase-labeled goat anti-PE, 1:50, Rockland Immunochemichals) as secondary antibody, respectively. AP was detected first during 30 min using a mixture containing N-(4-Amino-2,5-diethoxyphenyl)benzamide (Fast Blue BB, Sigma-Aldrich), 2 M HCl, 4 % $NaNO_2$, Naphthol AS-MX phosphate (VWR International, Radnor, PA, USA), N,N-dimethylformamide (DMF) (Sigma-Aldrich), Tris-HCl buffer (pH 8.5) and (-)-tetramisole hydrochloride (Sigma-Aldrich). The substrate was filtered using filtration paper. Secondly, peroxidase was detected within 30 min with a mixture containing 3-amino-9-ethylcarbazole (AEC) in DMF, 0.1 M NaAC (pH 4.6), 30% H_2O_2 (Merck Millipore, Darmstadt and double-filtered. Kaiser's Glycerol/Gelatin (Boom B.V., Meppel, The Netherlands) was used to embed tissue sections and micrographs were made using a Leica DM2000 microscope (Leica Microsystems GmbH, Wetzlar, Germany), a Leica DFC450 camera (Leica Microsystems GmbH, Wetzlar, Germany) and Leica Application (LAS) Software Version 4.5.0 (Leica Microsystems GmbH, Wetzlar, Germany).

Confocal Microscopy

For confocal imaging, 12 µm-thick spleen cryostat sections were stained as explained above. Primary and secondary antibodies were (Target, clone, dilution, manufacturer, with respective secondary antibody target, dilution, manufacturer): B220 (RA3-6B2, 1:50, BD Biosciences, Donkey anti-Rat Cy5, 1:200, Jackson Immunoresearch), CD11c (N418, 1:10, eBioscience, Goat anti-Hamster Cy3, 1:1000, Jackson Immunoresearch), CD3e (KT3, 1:50, Bioceros, Donkey anti-Rat Cy3, 1:1000, Jackson Immunoresearch). Slides were counterstained with 4′,6-diamidino-2-phenylindole (DAPI), mounted with VECTASHIELD® HardSet™ Antifade Mounting Medium (Vector Laboratries, Burlingame, CA, USA) and analyzed on a Zeiss LSM 510 META confocal microscope (Carl Zeiss AG, Oberkochen, Germany). Images were analyzed using ImageJ software (Rasband, W.S., ImageJ, U. S. National Institutes of Health, Bethesda, Maryland, USA).

Flow cytometry

Flow cytometry surface and intracellular staining procedures have been described previously[19]. Monoclonal antibodies used for flow cytometric analyses are listed in **Supplementary Table S1A.**

Immunoglobulin levels

For quantification of total immunoglobulin levels, Nunc Microwell plates (Life technologies, Carlsbad, CA, USA) were coated with 1 µg/ml goat-anti-mouse IgM, IgA, IgG1, IgG2b, IgG2c, or IgG3 (Southern Biotech, Birmingham, AL, USA) overnight at 4C°. Wells were blocked with 10% FCS (Capricorn Scientific, Ebsdorfergrund, Germany) in PBS (Thermo Scientific, Waltham, MA, USA) for 1 hr. Standards and serum were diluted in PBS and incubated at room temperature for 3 hrs. Depending on the isotype of interest, biotin labeled anti-mouse IgM, IgA, IgG1, IgG2b, IgG2c, or IgG3 (Southern Biotech) was incubated for 1 hr. Streptavidin-horseradish peroxidase (eBioscience) and 3,3',5,5'-tetramethylbenzidine substrate (eBioscience) was used to develop the ELISA and then optical density was measured at 450 nm on a Microplate Reader (Bio-Rad, Hercules, CA, USA). Ig autoreactivity assessment was assessed as previously described[20].

Statistics

If the Kruskal-Wallis 1-way ANOVA test was significant, we further used the non-parametric Mann Whitney U test to determine significant differences between two groups. P-values <0.05 were considered significant. All analyses were performed using Prism (GraphPad Software version 9, La Jolla, CA, USA). All data are presented as mean values with the standard error of the mean (SEM).

RESULTS

Lack of IL-23 strongly reduces the numbers of neutrophils, monocytes/ macrophage and DCs in *Tnfaip3*$^{CD11c\text{-}KO}$ mice.

To assess the effect of IL-23 abrogation on the phenotype of *Tnfaip3*$^{CD11c\text{-}KO}$ mice, we analyzed spleens of *Tnfaip3*$^{CD11c\text{-}WT}$, *Tnfaip3*$^{CD11c\text{-}HZ}$ and *Tnfaip3*$^{CD11c\text{-}KO}$ mice that were either WT or KO for the *IL-23* gene, at the age of 24 weeks. Spleens of the aged *Tnfaip3*$^{CD11c\text{-}KO}$ mice were enlarged, compared to *Tnfaip3*$^{CD11c\text{-}WT}$ and *Tnfaip3*$^{CD11c\text{-}HZ}$ mice (**Figure 1A**), as previously described[16]. Also, spleens of *Il23*^{KO}*Tnfaip3*$^{CD11c\text{-}KO}$ mice were enlarged in comparison to *Il23*^{KO} control mice, but they were significantly smaller than spleens of *Il23*^{WT}*Tnfaip3*$^{CD11c\text{-}KO}$ mice (**Figure 1A**). Despite the large size of the spleens in *Il23*^{KO}*Tnfaip3*$^{CD11c\text{-}KO}$mice, their cellularity was drastically reduced compared to *Il23*^{KO}*Tnfaip3*$^{CD11c\text{-}WT}$mice and to *Il23*^{WT}*Tnfaip3*$^{CD11c\text{-}KO}$mice (**Figure 1A**).

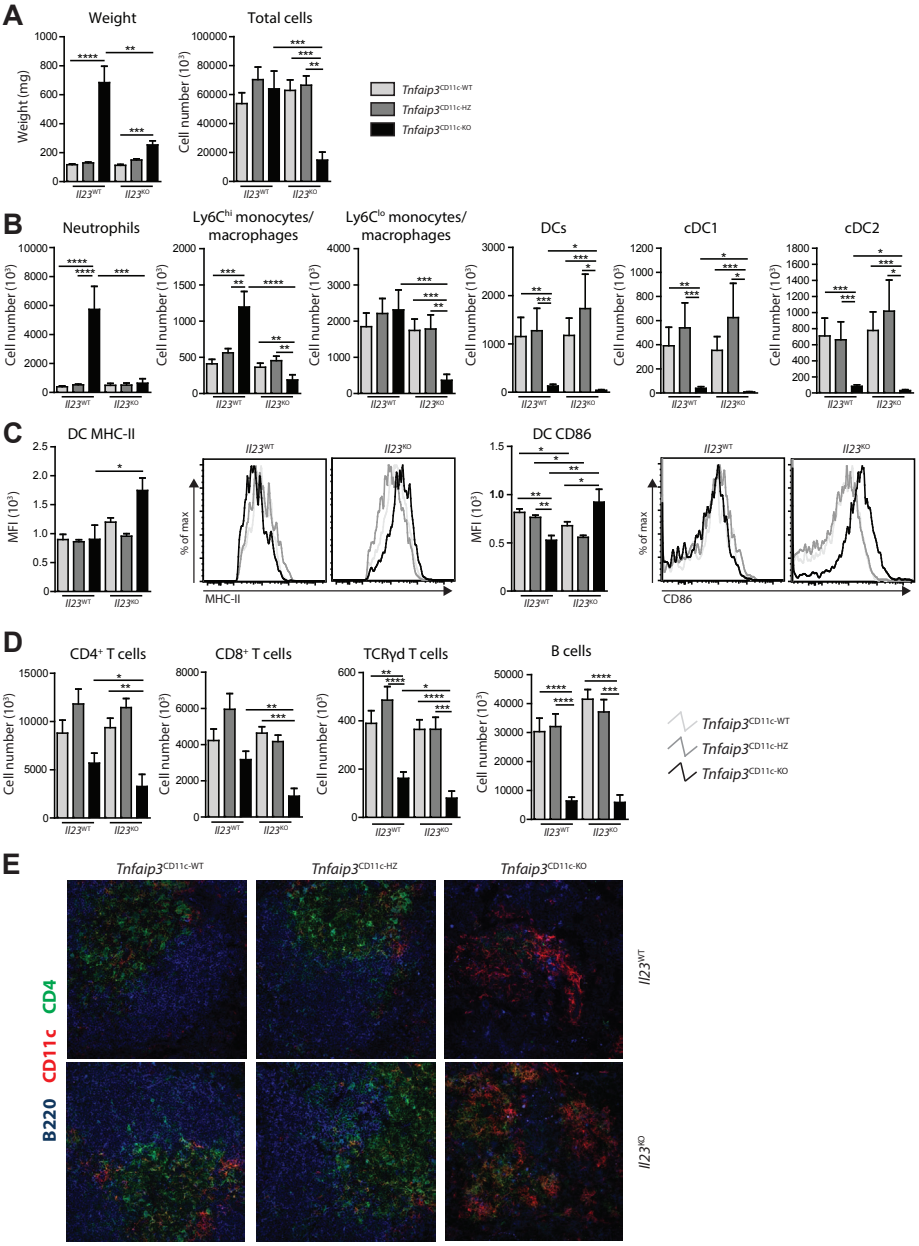

Figure 1: IL-23-deficiency strongly reduces myeloid cell populations in *Tnfaip3*$^{CD11c\text{-}KO}$ mice, but has moderate effects on lymphoid cells.

Spleens from 24-week-old naïve mice of the indicated genotypes were analyzed for myeloid and lymphoid cells. (**A**) Quantification of splenic weight and cellularity. (**B**) Enumeration of splenic neutrophils ($CD45^+CD11b^+GR1^+$), $Ly6C^{hi}$ monocytes/macrophages ($CD45^+CD11b^+GR1^-Ly6C^{hi}$), $Ly6C^{lo}$ monocytes/macrophages ($CD45^+CD11b^+GR1^-Ly6C^{lo}$), total DCs ($CD45^+CD11c^+$MHC-$II^+$), cDC1s ($CD45^+CD11c^+$MHC-$II^+CD11b^-$) and cDC2s ($CD45^+CD11c^+$MHC-$II^+CD11b^+$), using flow cytometry. (**C**) Quantification surface

expression of MHC-II and CD86 on splenic DCs, using flow cytometry (*left*) and representative histogram overlays (*right*). (**D**) Quantification of splenic $CD4^+$ T cells ($CD3^+CD4^+CD8^-$), $CD8^+$ Th cells ($CD3^+CD8^+CD4^-$), TCRγδ T cells ($CD3^+TCR\gamma\delta^+$) and B cells ($B220^+CD138^-$) using flow cytometry. (**E**) Confocal imaging of spleens for CD4 (Green), B220 (Blue) and CD11c (Red). Pooled data is shown from four independent experiments (in A/B/D) and a single experiment (in C/E). Results are presented as mean values ± SEM of n = 2-19 mice per group. Kruskal-Wallis test for multiple comparisons was performed and followed by a Mann-Whitney U test. *P<0.05, **P<0.01, ***P<0.001, ****P<0.0001.

The numbers of neutrophils were significantly increased in *Il23*^{WT}*Tnfaip3*$^{CD11c\text{-}KO}$ mice, compared to WT mice, *Tnfaip3*$^{CD11c\text{-}HZ}$ mice and *Il23*^{KO}*Tnfaip3*$^{CD11c\text{-}KO}$ mice (**Figure 1B**; see for gating strategy[21]: **Supplementary Figure S1**). Whereas absolute cell counts of Ly6C^{hi} monocytes/macrophage were increased in *Il23*^{WT}*Tnfaip3*$^{CD11c\text{-}KO}$ mice, compared to *Il23*^{WT} *Tnfaip3*$^{CD11c\text{-}WT}$ and *Tnfaip3*$^{CD11c\text{-}HZ}$ mice, they did not differ for the Ly6C^{lo} monocyte/macrophage population (**Figure 1B**, see for gating strategy: **Supplementary Figure S1**). Both Ly6C^{hi} and Ly6c^{lo} monocytes were reduced in *Il23*^{KO}*Tnfaip3*$^{CD11c\text{-}KO}$ mice compared to the other mouse groups (**Figure 1B**).

The absolute numbers of total DCs, as well as the cDC1 and cDC2 subsets (see for gating strategy: **Supplementary Figure S1**), were strongly reduced in the spleens of *Il23*^{WT}*Tnfaip3*$^{CD11c\text{-}KO}$ mice and even significantly further reduced in *Il23*^{KO}*Tnfaip3*$^{CD11c\text{-}KO}$ mice, compared to their *Tnfaip3*$^{CD11c\text{-}WT}$ and *Tnfaip3*$^{CD11c\text{-}HZ}$ counterparts (**Figure 1B**). Next, we evaluated splenic DCs for the expression of the MHC class II and CD86 surface markers, which are associated with DC activation. Surface MHC-II was significantly increased in *Il23*^{KO}*Tnfaip3*$^{CD11c\text{-}KO}$ mice, compared to *Il23*^{WT}*Tnfaip3*$^{CD11c\text{-}KO}$ mice (**Figure 1C**). While CD86 expression was significantly reduced in *Il23*^{WT}*Tnfaip3*$^{CD11c\text{-}KO}$ mice, compared to *Tnfaip3*$^{CD11c\text{-}WT}$ and*Tnfaip3*$^{CD11c\text{-}HZ}$ mice, it was significantly higher in *Il23*^{KO}*Tnfaip3*$^{CD11c\text{-}KO}$ mice compared to *Il23*^{KO} mice and *Il23*^{WT}*Tnfaip3*$^{CD11c\text{-}KO}$ mice (**Figure 1C**).

In conclusion, the concomitant absence of IL-23 in *Tnfaip3*$^{CD11c\text{-}KO}$ mice resulted in significantly reduced splenic cell counts, with lower numbers of neutrophils, monocytes/macrophage and in particular DCs. The DCs in these *Il23*^{KO}*Tnfaip3*$^{CD11c\text{-}KO}$ mice had a more activated phenotype.

Lack of IL-23 has moderate effects on lymphocyte cells in the spleen.

At 24 weeks of age, the numbers of splenic $CD4^+$ T cells and $CD8^+$ T cells did not differ between *Tnfaip3*$^{CD11c\text{-}KO}$ and *Tnfaip3*$^{CD11c\text{-}WT}$ mice on the *Il23*^{WT} background (**Figure 1D**). However, they were moderately reduced in *Il23*^{KO} *Tnfaip3*$^{CD11c\text{-}KO}$ mice, compared to *Il23*^{WT}*Tnfaip3*$^{CD11c\text{-}KO}$ mice (**Figure 1D**). Both $TCR\gamma\delta^+$ T cells and B cells were reduced in *Tnfaip3*$^{CD11c\text{-}KO}$ mice, irrespective of the *Il23* genotype, when compared to the other four groups of mice (**Figure 1D**).

The very low absolute cell counts of the spleens of *Tnfaip3*$^{CD11c\text{-}KO}$*Il23*^{KO} mice, prompted us to investigated their architecture. We previously observed a disturbed splenic

architecture in *Tnfaip3*$^{CD11c\text{-}KO}$ mice in comparison to *Tnfaip3*$^{CD11c\text{-}WT}$ and *Tnfaip3*$^{CD11c\text{-}HZ}$ mice[16]. Likewise, also on the *Il23*^{KO} background the *Tnfaip3*$^{CD11c\text{-}KO}$ mice had spleens with a disturbed architecture: very few B220$^+$ cells, and a few clusters of CD11c$^+$ cells, without clearly separated B and T cell areas (**Figure 1E**). In a smaller magnification, immunohistochemical analyses revealed a drastic reduction of IgD$^+$ B cells in the spleens of both *Il23*^{WT} and *Il23*^{KO} *Tnfaip3*$^{CD11c\text{-}KO}$ mice, compared to the *Tnfaip3*$^{CD11c\text{-}WT}$ counterparts (**Supplementary Figure S2**). Large regions were devoid of IgD$^+$ B cells, most likely representing red pulp areas with myeloid cells. Nevertheless, the absence of IL-23 appeared to result in a slight rescue of IgD$^+$ B cells clusters in *Tnfaip3*$^{CD11c\text{-}KO}$ spleens. This would be consistent with the flow cytometry findings of reduced total numbers of cells, but similar numbers of B cells in the spleens of *Il23*^{KO}*Tnfaip3*$^{CD11c\text{-}KO}$ mice, compared with *Il23*^{WT} *Tnfaip3*$^{CD11c\text{-}KO}$ mice.

In conclusion, despite the substantial reduction of spleen weight and total cell count in *Il23*^{KO} *Tnfaip3*$^{CD11c\text{-}KO}$ mice compared to *Il23*^{WT} *Tnfaip3*$^{CD11c\text{-}KO}$ mice, T cell numbers were only moderately reduced and B cell numbers were comparable between the two mouse groups.

IL-23-deficiency reduces the numbers of both Th17 and non-Th17 cycling T cells in *Tnfaip3*$^{CD11c\text{-}KO}$ mice.

Because IL-23 plays a primary role in Th17-cell homeostasis and is important for the expansion of Th17 cells[10, 22], we further investigated splenic CD4$^+$ T-cell subsets.

Antigen-experienced CD44$^+$ effector and memory CD4$^+$ T cells in the spleen were highest in both *Il23*^{WT} and *Il23*^{KO} *Tnfaip3*$^{CD11c\text{-}HZ}$ mice (**Figure 2A**). This population was decreased in *Il23*^{KO}*Tnfaip3*$^{CD11c\text{-}KO}$ mice compared to *Il23*^{WT}*Tnfaip3*$^{CD11c\text{-}KO}$ mice. This was probably linked to the overall reduction of splenic CD4$^+$ T cells in *Il23*^{KO}*Tnfaip3*$^{CD11c\text{-}KO}$ mice: when we calculated the proportions of antigen-experienced CD44$^+$ effector and memory CD4$^+$ T cells as a percentage of total CD4$^+$ T cells, there was no detectable effect of the loss of IL-23 (**Supplementary Figure S3A**).

Loss of IL-23 also did not appear to affect the total numbers of RORγt$^+$ Th17 cells in the spleen of *Tnfaip3*$^{CD11c\text{-}KO}$ mice (**Figure 2B, 2C**), although their proportions within the total CD4$^+$ T cell population in the spleen were increased (**Supplementary Figure S3B**).

The numbers of cycling Ki67$^+$ CD4$^+$ T cells, non-Th17 cells and CD8$^+$ T cells in the spleen of the six groups of mice essentially reflected the total numbers of cells in these populations (**Figure 2D;** see for proportions of Ki67$^+$ cells within these populations: **Supplementary Figure S3C**). In contrast, a pattern emerged that both the absolute numbers and the proportions of Ki67$^+$ RORγt$^+$ Th17 cells were reduced in the three *Il23*^{KO} genotypes, compared with the *Il23*^{WT} counterparts (**Figure 2D**; **Supplementary Figure S3C**).

The numbers of intracellular IL-17$^+$, IFN-γ$^+$ and IL-10$^+$ splenic CD4$^+$ T cells were significantly reduced in both *Il23*^{WT} and *Il23*^{KO} *Tnfaip3*$^{CD11c\text{-}KO}$ mice, compared to their *Tnfaip3*$^{CD11c\text{-}WT}$ or *Tnfaip3*$^{CD11c\text{-}HZ}$ counterparts (**Figure 2E,2F,2G**). However, as a proportion of CD4$^+$ T cells, IL17$^+$, IFNγ$^+$ and IL-10$^+$ cells were significantly higher in *Il23*^{KO}*Tnfaip3*$^{CD11c\text{-}KO}$ mice compared to *Il23*^{KO}*Tnfaip3*$^{CD11c\text{-}WT}$ or *Il23*^{KO}*Tnfaip3*$^{CD11c\text{-}HZ}$ controls (**Supplementary Figure S3D, S3E, S3F**).

Absence of IL-23 had limited effects on the numbers of antigen-experienced CD44$^+$ effector and memory CD8$^+$ T cells in the spleen of the three mouse genotypes. Although *Il23*^{KO}*Tnfaip3*$^{CD11c\text{-}KO}$ mice had lower absolute numbers of CD44$^+$CD8$^+$ T cells than *Il23*^{WT}*Tnfaip3*$^{CD11c\text{-}KO}$ mice (**Figure 2H**), their frequencies (as proportions of CD8$^+$ T cells) were increased (**Supplementary Figure S3G**). In parallel, the absolute numbers of IFNγ$^+$ CD8$^+$ T cells tended to be lower in *Il23*^{KO}*Tnfaip3*$^{CD11c\text{-}KO}$ than in *Il23*^{WT}*Tnfaip3*$^{CD11c\text{-}KO}$ mice (**Figure 2I**), but their frequencies (as proportions of CD8$^+$ T cells) were increased (**Supplementary Figure S3H**).

In conclusion, in *Tnfaip3*$^{CD11c\text{-}KO}$ mice the lack of IL-23 did not reduce the absolute numbers or proportions of RORγ$^+$ or IL-17$^+$ Th17 cells in the spleen. Nevertheless, in these mice the absolute numbers of cycling Ki67$^+$Th17 cells, as well as the proportions of Ki67$^+$ cells within the Th17 population was reduced in the spleen in the absence of IL-23. These findings suggest that an ongoing induction of Th17 cells can compensate for the absence of IL-23-driven expansion of Th17 cells in *Il23*^{KO}*Tnfaip3*$^{CD11c\text{-}KO}$mice.

IL-23-deficiency reduces splenic plasma cells numbers and IgA serum levels in *Tnfaip3*$^{CD11c\text{-}KO}$ mice.

Since Th17 cells are known to mediate B cell differentiation and Ig heavy chain class switch recombination[7], we assessed the effects of *Il23* gene deletion on germinal center (GC) B cells and plasma cells in the spleen at the age of 24 weeks. GC B-cell numbers were reduced in *Tnfaip3*$^{CD11c\text{-}KO}$ mice, irrespective of the presence of IL-23 (**Figure 3A**). However, as a proportion of B cells, splenic GC B cells were enhanced in *Tnfaip3*$^{CD11c\text{-}KO}$ mice and also in *Il23*^{KO}*Tnfaip3*$^{CD11c\text{-}HZ}$ mice, compared to *Tnfaip3*$^{CD11c\text{-}WT}$ mice and *Il23*^{KO} mice respectively (**Supplementary Figure 4A**). Splenic plasma cell numbers were elevated in *Il23*^{WT}*Tnfaip3*$^{CD11c\text{-}HZ}$ mice in comparison to *Il23*^{WT}*Tnfaip3*$^{CD11c\text{-}WT}$ and *Il23*^{WT}*Tnfaip3*$^{CD11c\text{-}KO}$ mice (**Figure 3A**). Importantly, whereas the effect of the absence of IL-23 on *Tnfaip3*$^{CD11c\text{-}WT}$ and *Tnfaip3*$^{CD11c\text{-}HZ}$ mice was limited, plasma cells were very low in *Il23*^{KO}*Tnfaip3*$^{CD11c\text{-}KO}$ mice (**Figure 3A).** This pattern was similar for IgM$^+$, IgG1$^+$ and IgA$^+$ plasma cell counts (**Figure 3A**). When we analyzed the Ig heavy chain class distribution in the plasma cells, we noticed that proportions of IgG1$^+$ plasma cells were increased in *Tnfaip3*$^{CD11c\text{-}KO}$ mice, in particular in *Il23*^{KO}*Tnfaip3*$^{CD11c\text{-}KO}$ mice, compared to *Tnfaip3*$^{CD11c\text{-}WT}$ mice on an *Il23*^{WT} or *Il23*^{KO} background (**Supplementary Figure 4B,** see also pie-chart).

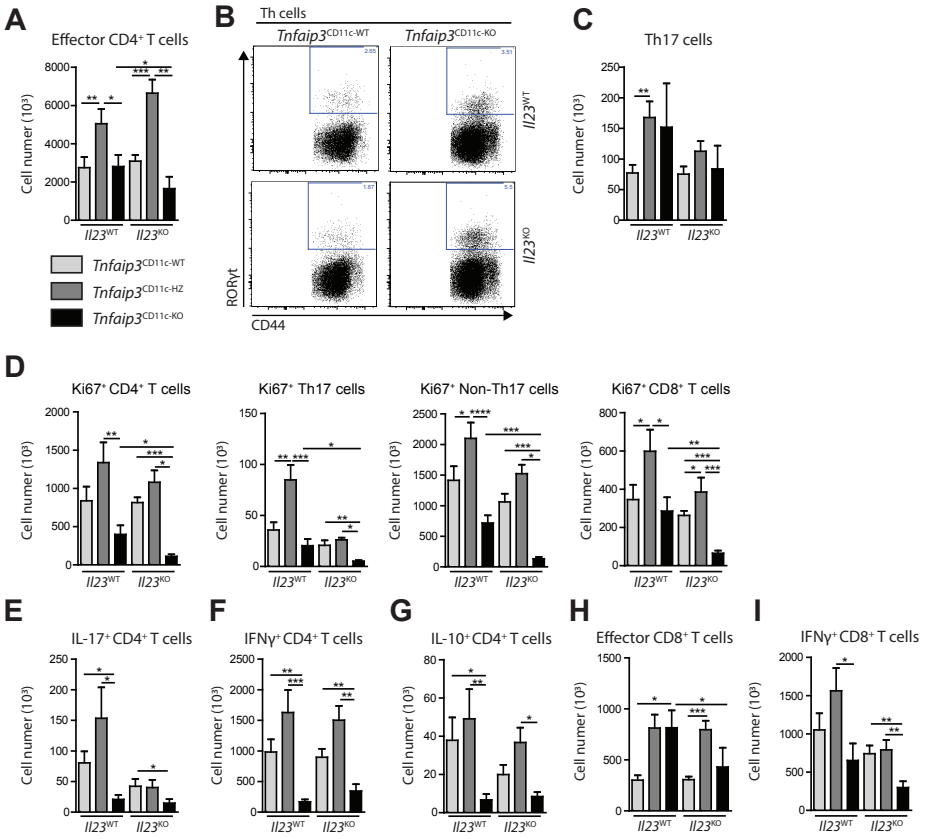

Figure 2: IL-23-deficiency reduces the numbers of both Th17 and non-Th17 cycling T cells in *Tnfaip3*$^{CD11c\text{-}KO}$ mice.

Spleens from 24-week-old naïve mice of the indicated genotypes were analyzed for T cell populations. (**A**) Quantification of splenic antigen-experienced effector CD4$^+$ T cells (CD3$^+$CD4$^+$CD44$^+$) using flow cytometry. (**B-C**) Flow cytometry profiles of gated CD4$^+$ T cells for surface CD44 and intracellular RORγt$^+$ (**B**) and enumeration of splenic Th17 cells (CD3$^+$CD4$^+$RORγt$^+$)(**C**) using flow cytometry. (**D**) Quantification of Ki67$^+$ proliferating CD4$^+$ T cells (CD3$^+$CD4$^+$Ki67$^+$), Th17 cells (CD3$^+$CD4$^+$Roryt$^+$Ki67$^+$), Non-Th17 cells (CD3$^+$CD4$^+$Roryt$^-$Ki67$^+$) and CD8$^+$ T cells (CD3$^+$CD8$^+$Ki67$^+$) (**E-I**) Quantification of IL-17$^+$ CD4$^+$ T cells (CD3$^+$CD4$^+$IL-17$^+$) (**E**), IFNγ$^+$ CD4$^+$ T cells (CD3$^+$CD4$^+$IFNγ$^+$) (**F**), IL-10$^+$ CD4$^+$ T cells (CD3$^+$CD4$^+$IL-10$^+$) (**G**) antigen experienced effector CD8$^+$ T cells (CD3$^+$CD8$^+$CD44$^+$) (**H**) and IFNγ$^+$ CD8$^+$ T cells (CD3$^+$CD8$^+$IFNγ$^+$) (**I**), using flow cytometry. Pooled data are shown from four independent experiments, except for panels D, E and G, which were from two independent experiments. Results are presented as mean values ± SEM of *n* = 3-19 mice per group. Kruskal-Wallis test for multiple comparisons was performed and followed by a Mann-Whitney U test. *P<0.05, **P<0.01, ***P<0.001, ****P<0.0001.

The remaining fraction of splenic plasma cells, expressing IgG2b, IgG2c and IgG3 appeared to be increased in the absence of IL-23.

The total numbers of B220$^+$ B-lineage cells in the bone marrow (BM) of *Il23*^{WT}*Tnfaip3*$^{CD11c\text{-}KO}$ mice were significantly decreased (**Figure 3B**), pointing to a developmental

B cell defect (described in greater detail in chapter 5 of this thesis) and thus providing an explanation for the reduced numbers of B cells present in the spleen of these mice. Also, the absolute numbers of total plasma cells were highest in *Il23*^{WT} *Tnfaip3*$^{CD11c\text{-}HZ}$ mice, but reduced in *Il23*^{WT} and *Il23*^{KO} *Tnfaip3*$^{CD11c\text{-}KO}$ mice compared to the other mouse groups (**Figure 3B**). All three *Tnfaip3* genotypes had lower numbers of IgM$^+$ plasma cells on the *Il23*^{KO} than on the *Il23*^{WT} background. IgM$^+$ plasma cells were virtually absent in *Il23*^{KO} *Tnfaip3*$^{CD11c\text{-}KO}$ mice (**Figure 3B**). In contrast, the complete absence of Tnfaip3/A20 or IL-23 did not significantly affect the numbers of BM IgG1$^+$ or IgA$^+$ plasma cells. An IL-23-dependent rise was seen for BM IgG1$^+$ and IgA$^+$ BM plasma cells in *Tnfaip3*$^{CD11c\text{-}HZ}$ mice compared to the control mice (**Figure 3B**).

Altogether, regarding the Ig heavy chain class distribution in BM plasma cells, we observed a reduction of the proportions of IgM$^+$ plasma cells in *Il23*^{WT}*Tnfaip3*$^{CD11c\text{-}KO}$ mice and a virtual absence of IgM$^+$ plasma cells in *Il23*^{KO}*Tnfaip3*$^{CD11c\text{-}KO}$ mice (**Supplementary Figure 4C**, see also pie-chart). Concomitantly, the proportions of BM IgG1$^+$ and IgA$^+$ plasma cells were increased in *Tnfaip3*$^{CD11c\text{-}KO}$ mice compared to *Tnfaip3*$^{CD11c\text{-}WT}$ mice and *Tnfaip3*$^{CD11c\text{-}HZ}$ mice, irrespective of the presence of IL-23 (**Supplementary Figure 4C**, see also pie-chart).

Next, we assessed serum Ig levels and observed a differential effect of the absence of Tnfaip3/A20 on individual subclasses: IgM and Ig2b were unaffected, IgG1 and IgA were increased and IgG2c and IgG3 were decreased (**Figure 3C**). In *Il23*^{WT}*Tnfaip3*$^{CD11c\text{-}HZ}$ mice, we found that only IgA levels were increased. For most subclasses this pattern was largely unaffected by the absence of IL-23, except that levels of IgA were lower in all three *Il23*^{KO} *Tnfaip3* genotypes compared to their *Il23*^{WT} equivalents (**Figure 3C**). Thus, in *Il23*^{KO}*Tnfaip3*$^{CD11c\text{-}KO}$ mice the levels of IgA in serum were in the normal range, similar to *Il23*^{WT}*Tnfaip3*$^{CD11c\text{-}WT}$ mice.

In summary, the absence of IL-23 resulted in strong reduction of IgM$^+$, IgG1$^+$ and IgA$^+$ splenic plasma cells specifically in the group of *Tnfaip3*$^{CD11c\text{-}KO}$ mice. By contrast, in the BM the absence of IL-23 reduced the numbers of IgM$^+$ plasma cells in all three *Tnfaip3* genotypes, but did not significantly affect IgG1$^+$ and IgA$^+$ plasma cell counts in *Tnfaip3*$^{CD11c\text{-}KO}$ mice. Serum IgG1 and IgA were the primary isotypes increased in *Tnfaip3*$^{CD11c\text{-}KO}$ mice, but additional loss of IL-23 in these mice only reduced serum IgA levels, leaving IgG1 levels unaffected.

IL-23-deficiency does not affect autoreactive IgG1 levels or kidney glomerulonephritis in *Tnfaip3*$^{CD11c\text{-}KO}$ mice.

Since aged *Tnfaip3*$^{CD11c\text{-}KO}$ mice expressed autoantibodies *in vivo*[16], we analyzed the presence of autoreactive anti-dsDNA and anti-cardiolipin IgG1 in serum of 24-week-old mice. Anti-dsDNA and anti-cardiolipin IgG1 was higher in *Tnfaip3*$^{CD11c\text{-}KO}$ mice than *Tnfaip3*$^{CD11c\text{-}HZ}$ or *Tnfaip3*$^{CD11c\text{-}KO}$ mice, regardless of IL-23-deficiency, although this

did not reach significance (**Figure 4A, 4B**). Since autoreactive immunoglobulins may cause tissue damage in glomeruli, we assessed histology of the kidney glomeruli in the six groups of mice. We previously reported that aged *Tnfaip3*$^{CD11c\text{-}KO}$ mice developed membranoproliferative glomerulonephritis with increased glomerular cellularity and thickening of the basement membranes[16]. Using PAS-D staining we confirmed that ~80% of the *Il23*^{WT}*Tnfaip3*$^{CD11c\text{-}KO}$ mice had thicker glomerular basement membranes, compared to 0% and ~25% in *Il23*^{WT}*Tnfaip3*$^{CD11c\text{-}WT}$ and *Il23*^{WT}*Tnfaip3*$^{CD11c\text{-}HZ}$ mice respectively (**Figure 4C**). Lack of IL-23 lead to similar basement membrane thickening in 100% of *Il23*^{KO} *Tnfaip3*$^{CD11c\text{-}KO}$ mice compared to 0% and ~40% in *Il23*^{KO}*Tnfaip3*$^{CD11c\text{-}WT}$ and *Il23*^{KO}*Tnfaip3*$^{CD11c\text{-}HZ}$ mice respectively (**Figure 4C**).

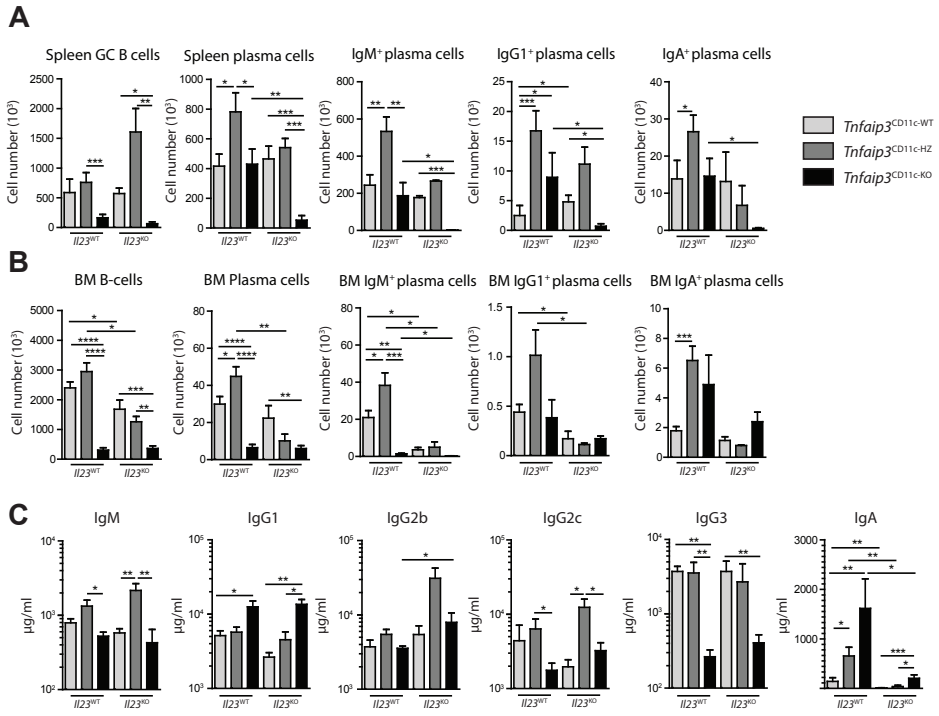

Figure 3: IL-23-deficiency reduces splenic plasma cells numbers and IgA serum levels in *Tnfaip3*$^{CD11c\text{-}KO}$ mice.

Spleens and bone marrow (BM) from 24-week-old naïve mice of the indicated genotypes were analyzed for B-cell populations. (**A-B**) Quantification of GC B-cells (B220$^+$CD138$^-$IgD$^-$CD95$^+$), plasma cells (B220$^-$CD138$^+$), IgM$^+$ plasma cells (B220$^-$CD138$^+$IgM$^+$), IgG1$^+$ plasma cells (B220$^-$CD138$^+$IgG1$^+$) and IgA$^+$ plasma cells B-cells (B220$^-$CD138$^+$IgA$^+$) in spleens (**A**) and BM (**B**) (Total B-lineage cells in BM gated as B220$^+$CD138$^-$) using flow cytometry. (**C**) Serum concentrations of IgM, IgG1, IgG2b, IgG2c, IgG3 and IgA, determined by ELISA. Pooled data are shown from three independent experiments (panels A and B). Serum Ig levels are from two (IgM, IgG2b, IgG2c, IgG3) or four (IgG1, IgA) independent experiments. Results are presented as mean values ± SEM of *n* = 5-15 mice per group. Kruskal-Wallis test for multiple comparisons was performed and followed by a Mann-Whitney U test. *P<0.05, **P<0.01, ***P<0.001, ****P<0.0001.

Thus, lack of IL-23 did not abrogate the formation of IgG1 autoantibodies nor thickening of the glomerular basement membrane in *Tnfaip3*$^{CD11c\text{-}KO}$ mice.

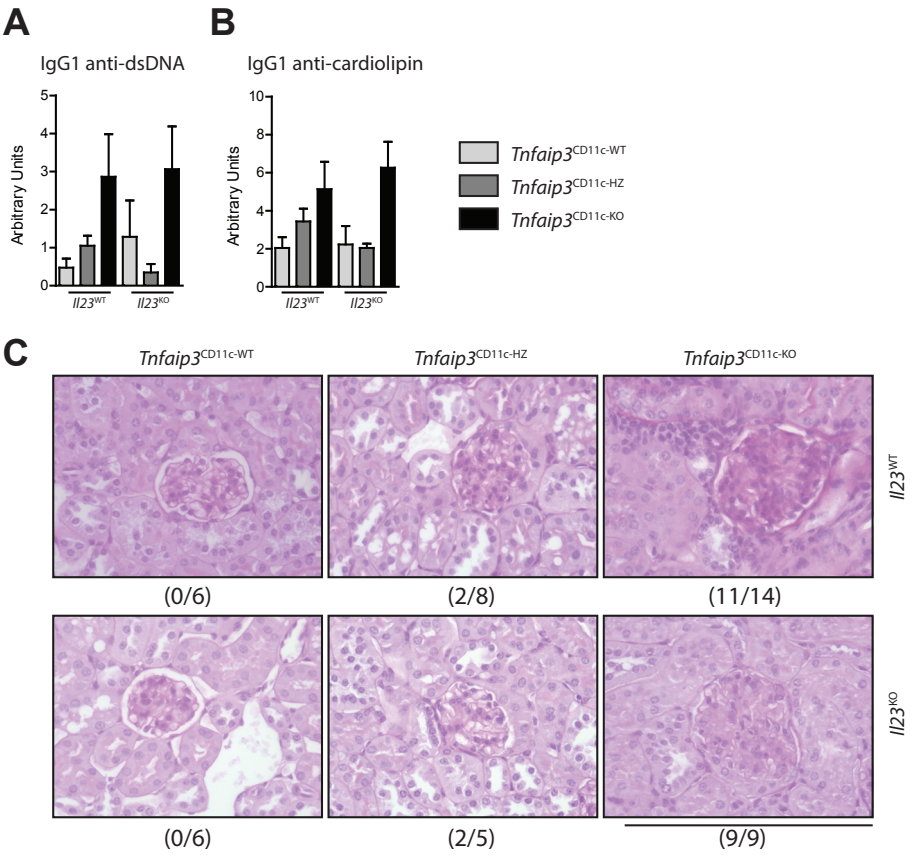

Figure 4: IL-23-deficiency does not affect autoreactive IgG1 levels or kidney glomerulonephritis in *Tnfaip3*$^{CD11c\text{-}KO}$ mice.

Serum of naïve 24-week-old mice of the indicated genotypes was analyzed for autoreactive IgG1 towards dsDNA (**A**) and cardiolipin (**B**) using ELISA. (**C**) PAS-D staining on paraffin-embedded kidneys. Scale bars represent 200µm. Representative histology images are shown from three independent experiments. Results are presented as mean values ± SEM of *n* = 2-10 mice per group.

DISCUSSION

Since the start of the millennium, the discovery of IL-23 and the primary acting cytokine IL-17 has redefined the understanding of autoimmune disorders[22]. In several autoimmune disorders such as psoriasis, inflammatory bowel disease (IBD) or SLE, common subunit p40 blockade of IL-12 and IL-23 or selective blockade of IL-23 has shown

promising clinical results[15, 23]. Also, in lupus mouse models the role of IL-23/IL-17 is of importance[24]. We studied our *Tnfaip3*$^{CD11c\text{-}KO}$ lupus mouse model, in which Tnfaip3/A20, a negative regulator for NF-κB, is specifically deleted in DCs, leading to hyperactivated DCs[16]. As a result, activity of T and B cells is dysregulated and mice express autoantibodies and develop lupus nephritis. BM-derived DCs from *Tnfaip3*$^{CD11c\text{-}KO}$ mice produced high IL-23 and induced Th17 cell differentiation *in vitro*[16]. In this report, we addressed the question whether loss of IL-23 *in vivo* would restore Th17 cell homeostasis and thereby alleviate the lupus phenotype. We found, however, that *in vivo* Th17 cell differentiation was not enhanced in 24-week-old *Tnfaip3*$^{CD11c\text{-}KO}$ mice, compared to *Tnfaip3*$^{CD11c\text{-}WT}$ mice. Moreover, loss of IL-23 expression did not significantly affect the numbers of Th17 cells in the spleen, serum levels of IgG1 or anti-dsDNA IgG1 or kidney glomerulonephritis. Taken together, these findings indicate that the autoimmune pathology in *Tnfaip3*$^{CD11c\text{-}KO}$ mice is independent of the IL-23/IL-17 axis.

While *Tnfaip3*$^{CD11c\text{-}KO}$ mice had enlarged spleens with various proliferating myeloid cells[16], these were significantly reduced in the absence of IL-23. This was possibly due to survival signals to myeloid cells provided by IL-23, as shown during *C. albicans* infection[25]. Neutrophils were the myeloid cells that expanded most in *Il23*^{WT}*Tnfaip3*$^{CD11c\text{-}KO}$ mice. Although IL-23 deficiency may be associated with defects in granulopoiesis[26, 27], no differences were seen between *Il23*^{WT}and *Il23*^{KO} mice of the *Tnfaip3*$^{CD11c\text{-}WT}$ or *Tnfaip3*$^{CD11c\text{-}HZ}$ genotype.

All conventional DC subsets, including the cDC2 subset known to primarily produce IL-23[28] were reduced in number, both in *Il23*^{WT} and *Il23*^{KO} *Tnfaip3*$^{CD11c\text{-}KO}$ mice. Surprisingly, splenic DC activation status, as measured by surface MHC-II and CD86 expression was higher in *Il23*^{KO} than *Il23*^{WT} *Tnfaip3*$^{CD11c\text{-}KO}$ mice. *In vitro,* Tnfaip3/A20-deficient BM-derived DCs showed no differences for CD40, CD86 or MHC-II expression between IL-23^{WT} and IL-23^{KO} mice, indicating that IL-23 had no effect on their activation status *in vitro*. An autocrine effect of IL-23 on DCs has been suggested, influencing IL-12 production and improving antigen presentation in a skin reactivity test[29, 30]. Furthermore, human *in vitro* studies show that IL-23 promotes T cell proliferation, without affecting DC maturation[31]. In a naïve state only ~4% of CD11c^{+} DCs express IL-23R[32]. This did not differ across the six mouse groups in our study (T.D., unpublished. data), suggesting that the absence of this autocrine IL-23 effect is not a likely explanation for enhanced activation of DCs in *Il23*^{KO}*Tnfaip3*$^{CD11c\text{-}KO}$ mice. In contrast to previous findings[16], we saw a reduction of splenic DCs at the age of 24 weeks in *Il23*^{WT} *Tnfaip3*$^{CD11c\text{-}KO}$ mice, and even more so in *Il23*^{KO}*Tnfaip3*$^{CD11c\text{-}KO}$ mice. It may be argued that a higher activation status of this minor population of DCs is not likely to contribute to the systemic phenotype in *Il23*^{KO}*Tnfaip3*$^{CD11c\text{-}KO}$ mice. However, despite having such low DC counts, both *Il23*^{WT} and *Il23*^{KO}*Tnfaip3*$^{CD11c\text{-}KO}$ mice still developed the lupus-like phenotype. This suggests that secondary activated cells that were in proximity to the DCs, such as T-cells or monocytes/macrophages contribute to the

phenotype, e.g. by elevated cytokine production such as the previously demonstrated IL-6 and TNF-α[16].

In contrast to previously reported *in vitro* studies[16], *Tnfaip3*$^{CD11c\text{-}KO}$ mice did not have increased RORγt^{+} Th17 cells or IL-17^{+} CD4^{+} T cells *in vivo,* compared to *Tnfaip3*$^{CD11c\text{-}WT}$ mice. It remains however unclear whether this originates from differences between *in vivo* and *in vitro* findings, or from differences between mouse facilities or microbiome. The latter would be supported by our analyses of the B cell compartment in the spleens of 24-week-old *Tnfaip3*$^{CD11c\text{-}KO}$ mice, showing reduced numbers of GC B cells and similar numbers of plasma cells compared to WT control mice, whereas Kool *et al.* reported that both cell populations were increased (although not significantly) in 25-week-old *Tnfaip3*$^{CD11c\text{-}KO}$ mice[16]. In this context, it is of note that another strain of C57Bl/6 mice with a DC-specific deficiency of Tnfaip3/A20, also based on CD11c-Cre-mediated gene targeting developed a phenotype characterized by IBD-associated arthritis[33]. This phenotype is quite different from the SLE-like phenotype in our *Tnfaip3*$^{CD11c\text{-}KO}$ mice[16], which would support an important role of microbiome or other environmental factors on the *in vivo* immunological and pathological effects of Tnfaip3/A20 deletion.

We were surprised to see that whereas antigen-experienced effector/memory CD4^{+} T-cells were reduced in the spleens of *Il23*^{KO}*Tnfaip3*$^{CD11c\text{-}KO}$ mice, this was not observed for RORγt^{+} Th17 cells or IL-17^{+} CD4^{+} T cells. Rather, the proportions of RORγt^{+} Th17 cells and IL-17^{+} CD4^{+} T cells appeared to rise in *Il23*^{KO}*Tnfaip3*$^{CD11c\text{-}KO}$ mice compared to *Il23*^{WT}*Tnfaip3*$^{CD11c\text{-}KO}$ mice. Two roles of IL-23 have been proposed, namely induction of T cell expansion and induction of T cell pathogenicity. Whereas initially IL-23 was regarded as an inducing factor for Th17 cells[34], later studies show that primarily TGF-β and IL-6 are responsible for the induction and IL-23 is more important for survival and expansion of Th17 cells[12]. T cell proliferation was overall reduced in *Il23*^{KO} mice, however, as a proportion of CD4^{+} T cells, only the Th17 cell population - and not non-Th17 cells - showed a reduction in proliferation due to absence of IL-23. The limited effects of IL-23 on the size of the splenic Th17 population, together with a reduction of Ki67^{+} proliferating Th17 cells, suggest an ongoing *de novo* induction of Th17 cells, or an increased migration of resting Th17 cells into the spleen. Both of these mechanisms may compensate for the absence of IL-23-driven expansion of Th17 cells in *Il23*^{KO}*Tnfaip3*$^{CD11c\text{-}KO}$mice.

Another concept would be that IL-23 unlocks the full pathogenic potential of autoreactive T-cells, while only the TGF-β/IL-6 combination induces more suppressive IL-10^{+} T-cells[13]. Indeed, in our data a significant increase of the proportions – but not absolute numbers - of splenic IL-10^{+} T-cells was seen in *Il23*^{KO}*Tnfaip3*$^{CD11c\text{-}KO}$ mice, compared to *Il23*^{WT}*Tnfaip3*$^{CD11c\text{-}KO}$ mice, suggesting that relatively more immunosuppressive CD4^{+} T cells were present in the absence of IL-23. In our hands cytokine and transcription factor expression could unfortunately not reliably be combined to analyze on the single-cell level whether RORγt^{+} Th17 cells had altered IL-10 production. Regardless of these

suppressive IL-10^{+} Th-cells, however, autoantibody production or tissue inflammation assessed by basement membrane thickening in kidney glomeruli was unaltered in *Tnfaip3*$^{CD11c\text{-}KO}$ mice in absence of IL-23. Further experiments are necessary to determine whether other Th17-associated cytokines, such as IL-22 and GM-CSF, which is normally induced by IL-23[35], are changed in *Il23*^{WT} and *Il23*^{KO}*Tnfaip3*$^{CD11c\text{-}KO}$ mice.

The numbers of splenic IL-17^{+} or IFNγ^{+} Th cells was not different between *Il23*^{WT} and *Il23*^{KO}*Tnfaip3*$^{CD11c\text{-}KO}$ mice. As a proportion, however, substantial increases in IFNγ^{+} Th cells were seen. This is not likely caused by IL-23-deficiency alone, because IL-23 has only a marginal effect on IFNγ expression[36]. Although IL-23 does not induce Th17 commitment, it helps to maintain a Th17 phenotype[37], which might explain why in its absence higher levels of Th1 cytokines are produced when DCs have an activated phenotype. Nevertheless, although it has been shown that plasticity of Th17 cells towards IFNγ^{+} Th1 cells is dependent on IL-23[38], we did not find evidence for such a role of IL-23 in our *Tnfaip3*$^{CD11c\text{-}KO}$ mice: IL-17^{+}IFNγ^{+} Th cells were not decreased in *Il23*^{KO} *Tnfaip3*$^{CD11c\text{-}KO}$ mice (T.D., unpublished data). Taken together, our findings suggests that the proportions of IFNγ^{+} CD4^{+} Th-cells in *Il23*^{KO} *Tnfaip3*$^{CD11c\text{-}KO}$mice may rise due to (i) *de novo* induction of Th1 cells over Th17 cells, possibly supported by IL-12 from *Tnfaip3*$^{CD11c\text{-}KO}$ DCs[17] or to (ii) migration of IFNγ^{+} CD4^{+} Th-cells into the spleen or migration of IFNγ^{-} CD4^{+} cells out of the spleen.

Th17 cells influence B-cell activation and Ig production by plasma cells into isotypes IgG1, IgG2a/c and IgG2b[7]. Since Th17 cells were not reduced in *Il23*^{KO} *Tnfaip3*$^{CD11c\text{-}KO}$ mice compared to *Il23*^{WT}*Tnfaip3*$^{CD11c\text{-}KO}$ mice, it was expected that also serum Ig levels were essentially unaffected. This was indeed the case, except that IgA was substantially reduced. Given the low numbers of IgA^{+} plasma cells in the spleens of *Tnfaip3*$^{CD11c\text{-}KO}$ *Il23*^{KO} mice, while the bone marrow plasma cells were unaffected, it might be possible that a major fraction of serum IgA in *Tnfaip3*$^{CD11c\text{-}KO}$ mice was produced in the spleen. However, IgA could also be derived from the intestine[39], but we did not observe intestinal autoimmune inflammation in *Il23*^{WT} or *Il23*^{KO}*Tnfaip3*$^{CD11c\text{-}KO}$ mice (T.D., unpublished data), despite a previous report of gut inflammation in another published *Tnfaip3*$^{CD11c\text{-}KO}$ mouse model[33]. Yet, lack of IL-23 did not appear to affect the autoimmune phenotype in that a similar basement membrane thickening was found in the kidney glomeruli of *Il23*^{WT} and *Il23*^{KO}*Tnfaip3*$^{CD11c\text{-}KO}$ mice. Given the differential effects of the absence of Tnfaip3/A20 or IL-23-deficiency on the individual subclasses, additional experiments are required to evaluate the autoreactivity of the individual Ig subclasses in the serum of *Il23*^{WT} and *Il23*^{KO}*Tnfaip3*$^{CD11c\text{-}KO}$ mice. Likewise, it will be informative to investigate the presence and nature of immune complex depositions in the glomeruli in *Il23*^{WT} and *Il23*^{KO}*Tnfaip3*$^{CD11c\text{-}KO}$ mice.

In conclusion, the absence of IL-23 resulted in a substantial reduction of granulocytes and monocytes/macrophage in the spleens of *Tnfaip3*$^{CD11c\text{-}KO}$ mice. Although

splenic DCs from *Il23*^{KO}*Tnfaip3*$^{CD11c\text{-}KO}$ had a more activated phenotype than DCs from *Il23*^{WT}*Tnfaip3*$^{CD11c\text{-}KO}$ mice, their numbers remained very low. Deletion of the *Tnfaip3* gene in DCs did not enhance Th17 cell differentiation *in vivo* and further loss of IL-23 did not affect the numbers of splenic Th17 cells. Despite a severe reduction of plasma cells in the spleen, the serum of *Il23*^{KO}*Tnfaip3*$^{CD11c\text{-}KO}$ mice contained autoreactive IgG1. Glomerular membrane thickening seen in *Tnfaip3*$^{CD11c\text{-}KO}$ mice was also unaffected by IL-23-deficiency. From these findings we conclude that the autoimmune pathology in *Tnfaip3*$^{CD11c\text{-}KO}$ mice is independent of the IL-23/IL-17 axis.

Acknowledgements

We would like to thank Odilia Corneth and the Erasmus MC Animal Facility (EDC) staff for their assistance during the project. This project was supported by The Dutch Arthritis Association (12-2-410) and the European Framework program 7 (FP7-MC-CIG grant 304221).

Conflict of interest

The authors declare no conflict of interest.

REFERENCES

1. Crispin JC, Liossis SN, Kis-Toth K, Lieberman LA, Kyttaris VC, Juang YT *et al.* Pathogenesis of human systemic lupus erythematosus: recent advances. *Trends in molecular medicine* 2010; 16(2): 47-57.
2. Nashi E, Wang Y, Diamond B. The role of B cells in lupus pathogenesis. *The international journal of biochemistry & cell biology* 2010; 42(4): 543-550.
3. Flores-Mendoza G, Sanson SP, Rodriguez-Castro S, Crispin JC, Rosetti F. Mechanisms of Tissue Injury in Lupus Nephritis. *Trends in molecular medicine* 2018; 24(4): 364-378.
4. Wong CK, Lit LC, Tam LS, Li EK, Wong PT, Lam CW. Hyperproduction of IL-23 and IL-17 in patients with systemic lupus erythematosus: implications for Th17-mediated inflammation in auto-immunity. *Clinical immunology (Orlando, Fla)* 2008; 127(3): 385-393.
5. Xing Q, Wang B, Su H, Cui J, Li J. Elevated Th17 cells are accompanied by FoxP3+ Treg cells decrease in patients with lupus nephritis. *Rheumatology international* 2012; 32(4): 949-958.
6. Hsu HC, Yang P, Wang J, Wu Q, Myers R, Chen J *et al.* Interleukin 17-producing T helper cells and interleukin 17 orchestrate autoreactive germinal center development in autoimmune BXD2 mice. *Nature immunology* 2008; 9(2): 166-175.
7. Mitsdoerffer M, Lee Y, Jager A, Kim HJ, Korn T, Kolls JK *et al.* Proinflammatory T helper type 17 cells are effective B-cell helpers. *Proceedings of the National Academy of Sciences of the United States of America* 2010; 107(32): 14292-14297.
8. Amarilyo G, Lourenco EV, Shi FD, La Cava A. IL-17 promotes murine lupus. *Journal of immunology (Baltimore, Md : 1950)* 2014; 193(2): 540-543.
9. McGeachy MJ, Chen Y, Tato CM, Laurence A, Joyce-Shaikh B, Blumenschein WM *et al.* The interleukin 23 receptor is essential for the terminal differentiation of interleukin 17-producing effector T helper cells in vivo. *Nature immunology* 2009; 10(3): 314-324.
10. Oppmann B, Lesley R, Blom B, Timans JC, Xu Y, Hunte B *et al.* Novel p19 protein engages IL-12p40 to form a cytokine, IL-23, with biological activities similar as well as distinct from IL-12. *Immunity* 2000; 13(5): 715-725.
11. Ghoreschi K, Laurence A, Yang XP, Tato CM, McGeachy MJ, Konkel JE *et al.* Generation of pathogenic T(H)17 cells in the absence of TGF-beta signalling. *Nature* 2010; 467(7318): 967-971.
12. Veldhoen M, Hocking RJ, Atkins CJ, Locksley RM, Stockinger B. TGFbeta in the context of an inflammatory cytokine milieu supports de novo differentiation of IL-17-producing T cells. *Immunity* 2006; 24(2): 179-189.
13. McGeachy MJ, Bak-Jensen KS, Chen Y, Tato CM, Blumenschein W, McClanahan T *et al.* TGF-beta and IL-6 drive the production of IL-17 and IL-10 by T cells and restrain T(H)-17 cell-mediated pathology. *Nature immunology* 2007; 8(12): 1390-1397.
14. Larosa M, Zen M, Gatto M, Jesus D, Zanatta E, Iaccarino L *et al.* IL-12 and IL-23/Th17 axis in systemic lupus erythematosus. *Experimental biology and medicine (Maywood, NJ)* 2019; 244(1): 42-51.
15. van Vollenhoven RF, Hahn BH, Tsokos GC, Wagner CL, Lipsky P, Touma Z *et al.* Efficacy and safety of ustekinumab, an IL-12 and IL-23 inhibitor, in patients with active systemic lupus erythematosus: results of a multicentre, double-blind, phase 2, randomised, controlled study. *Lancet (London, England)* 2018; 392(10155): 1330-1339.
16. Kool M, van Loo G, Waelput W, De Prijck S, Muskens F, Sze M *et al.* The ubiquitin-editing protein A20 prevents dendritic cell activation, recognition of apoptotic cells,

and systemic autoimmunity. *Immunity* 2011; 35(1): 82-96.

17. Vroman H, Bergen IM, van Hulst JAC, van Nimwegen M, van Uden D, Schuijs MJ *et al.* TNF-alpha-induced protein 3 levels in lung dendritic cells instruct TH2 or TH17 cell differentiation in eosinophilic or neutrophilic asthma. *The Journal of allergy and clinical immunology* 2018; 141(5): 1620-1633. e1612.
18. Ghilardi N, Kljavin N, Chen Q, Lucas S, Gurney AL, De Sauvage FJ. Compromised humoral and delayed-type hypersensitivity responses in IL-23-deficient mice. *Journal of immunology (Baltimore, Md : 1950)* 2004; 172(5): 2827-2833.
19. Vroman H, Bergen IM, Li BW, van Hulst JA, Lukkes M, van Uden D *et al.* Development of eosinophilic inflammation is independent of B-T cell interaction in a chronic house dust mite-driven asthma model. *Clinical and experimental allergy : journal of the British Society for Allergy and Clinical Immunology* 2017; 47(4): 551-564.
20. Das T, Bergen IM, Koudstaal T, van Hulst JAC, van Loo G, Boonstra A *et al.* DNGR1-mediated deletion of A20/Tnfaip3 in dendritic cells alters T and B-cell homeostasis and promotes autoimmune liver pathology. *Journal of autoimmunity* 2019; 102: 167-178.
21. Cossarizza A, Chang HD, Radbruch A, Acs A, Adam D, Adam-Klages S *et al.* Guidelines for the use of flow cytometry and cell sorting in immunological studies (second edition). *European journal of immunology* 2019; 49(10): 1457-1973.
22. Gaffen SL, Jain R, Garg AV, Cua DJ. The IL-23-IL-17 immune axis: from mechanisms to therapeutic testing. *Nature reviews Immunology* 2014; 14(9): 585-600.
23. Kashani A, Schwartz DA. The Expanding Role of Anti-IL-12 and/or Anti-IL-23 Antibodies in the Treatment of Inflammatory Bowel Disease. *Gastroenterology & hepatology* 2019; 15(5): 255-265.
24. Kyttaris VC, Zhang Z, Kuchroo VK, Oukka M, Tsokos GC. Cutting edge: IL-23 receptor deficiency prevents the development of lupus nephritis in C57BL/6-lpr/lpr mice. *Journal of immunology (Baltimore, Md : 1950)* 2010; 184(9): 4605-4609.
25. Nur S, Sparber F, Lemberg C, Guiducci E, Schweizer TA, Zwicky P *et al.* IL-23 supports host defense against systemic Candida albicans infection by ensuring myeloid cell survival. *PLoS pathogens* 2019; 15(12): e1008115.
26. Smith E, Zarbock A, Stark MA, Burcin TL, Bruce AC, Foley P *et al.* IL-23 is required for neutrophil homeostasis in normal and neutrophilic mice. *Journal of immunology (Baltimore, Md : 1950)* 2007; 179(12): 8274-8279.
27. Stark MA, Huo Y, Burcin TL, Morris MA, Olson TS, Ley K. Phagocytosis of apoptotic neutrophils regulates granulopoiesis via IL-23 and IL-17. *Immunity* 2005; 22(3): 285-294.
28. Satpathy AT, Briseno CG, Lee JS, Ng D, Manieri NA, Kc W *et al.* Notch2-dependent classical dendritic cells orchestrate intestinal immunity to attaching-and-effacing bacterial pathogens. *Nature immunology* 2013; 14(9): 937-948.
29. Belladonna ML, Renauld JC, Bianchi R, Vacca C, Fallarino F, Orabona C *et al.* IL-23 and IL-12 have overlapping, but distinct, effects on murine dendritic cells. *Journal of immunology (Baltimore, Md : 1950)* 2002; 168(11): 5448-5454.
30. Li Y, Yu X, Ma Y, Hua S. IL-23 and dendritic cells: What are the roles of their mutual attachment in immune response and immunotherapy? *Cytokine* 2019; 120: 78-84.
31. Vaknin-Dembinsky A, Balashov K, Weiner HL. IL-23 is increased in dendritic cells in multiple sclerosis and down-regulation of IL-23 by antisense oligos increases dendritic cell IL-10 production. *Journal of immunology (Baltimore, Md : 1950)* 2006; 176(12): 7768-7774.

32. Awasthi A, Riol-Blanco L, Jager A, Korn T, Pot C, Galileos G *et al.* Cutting edge: IL-23 receptor gfp reporter mice reveal distinct populations of IL-17-producing cells. *Journal of immunology (Baltimore, Md : 1950)* 2009; 182(10): 5904-5908.
33. Hammer GE, Turer EE, Taylor KE, Fang CJ, Advincula R, Oshima S *et al.* Expression of A20 by dendritic cells preserves immune homeostasis and prevents colitis and spondyloarthritis. *Nature immunology* 2011; 12(12): 1184-1193.
34. Harrington LE, Hatton RD, Mangan PR, Turner H, Murphy TL, Murphy KM *et al.* Interleukin 17-producing CD4+ effector T cells develop via a lineage distinct from the T helper type 1 and 2 lineages. *Nature immunology* 2005; 6(11): 1123-1132.
35. El-Behi M, Ciric B, Dai H, Yan Y, Cullimore M, Safavi F *et al.* The encephalitogenicity of T(H)17 cells is dependent on IL-1- and IL-23-induced production of the cytokine GM-CSF. *Nature immunology* 2011; 12(6): 568-575.
36. Chackerian AA, Chen SJ, Brodie SJ, Mattson JD, McClanahan TK, Kastelein RA *et al.* Neutralization or absence of the interleukin-23 pathway does not compromise immunity to mycobacterial infection. *Infection and immunity* 2006; 74(11): 6092-6099.
37. Stritesky GL, Yeh N, Kaplan MH. IL-23 promotes maintenance but not commitment to the Th17 lineage. *Journal of immunology (Baltimore, Md : 1950)* 2008; 181(9): 5948-5955.
38. Hirota K, Duarte JH, Veldhoen M, Hornsby E, Li Y, Cua DJ *et al.* Fate mapping of IL-17-producing T cells in inflammatory responses. *Nature immunology* 2011; 12(3): 255-263.
39. Gutzeit C, Magri G, Cerutti A. Intestinal IgA production and its role in host-microbe interaction. *Immunological reviews* 2014; 260(1): 76-85.

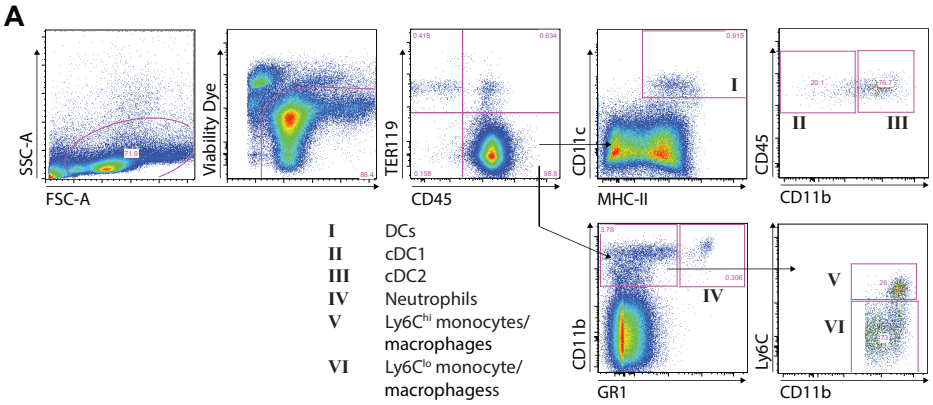

Supplementary Figure 1: Gating strategy for the indicated myeloid cell fractions in the spleen of naïve 24-week-old mice, using flow cytometry.

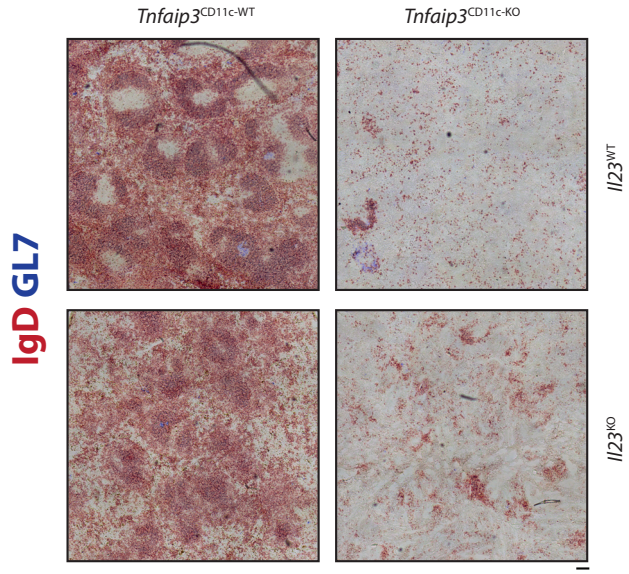

Supplementary Figure 2: IL-23-deficiency has no major effects on the splenic architecture in *Tnfaip3*$^{CD11c\text{-}KO}$ mice.

Spleens from naïve 24-week-old mice from the indicated genotypes were analyzed by immunohistochemistry for IgD (Red) and GL7 (Blue). Scale bars represent 200μm.

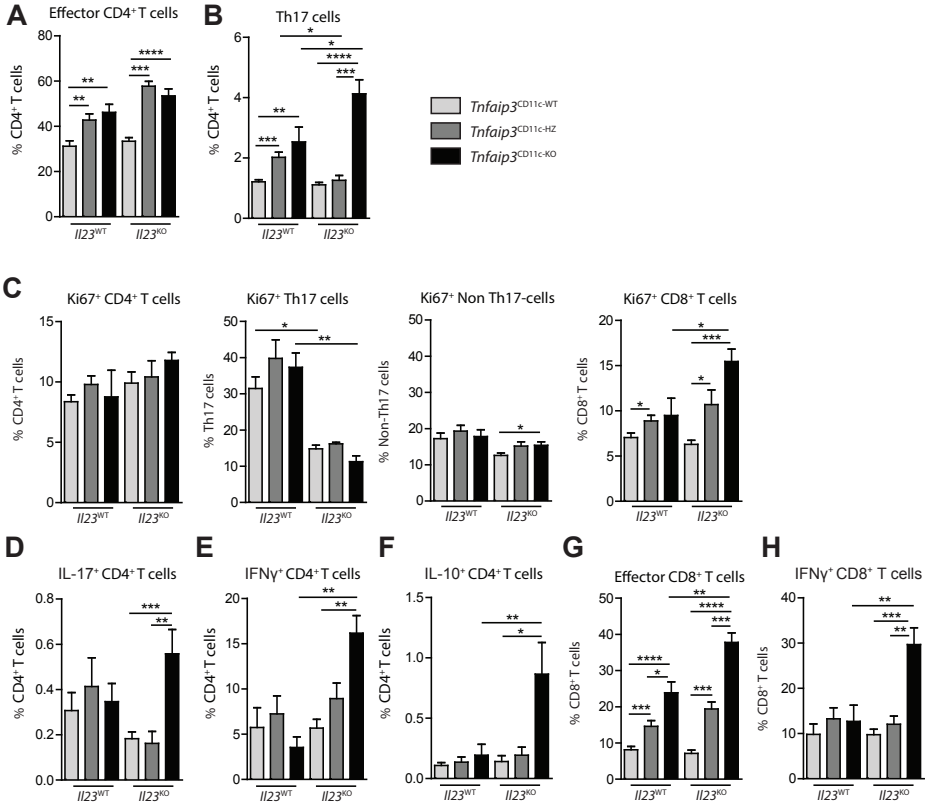

Supplementary Figure 3: Effects of IL-23-deficiency on the proportions of T cell subsets, T cell proliferation and cytokine production.

Spleens from naïve 24-week-old mice from the indicated genotypes were analyzed for T cell populations. (**A-B**) Quantification of proportions splenic effector CD4+ T-cells ($CD3^+CD4^+CD44^+$)(A) and $ROR\gamma t^+$ Th17 cells ($CD3^+CD4^+ROR\gamma t^+$) (**B**) using flow cytometry. (**C**) Quantification of proportions $Ki67^+$ proliferating $CD4^+$ T cells ($CD3^+CD4^+Ki67^+$), Th17 cells ($CD3^+CD4^+Ror\gamma t^+Ki67^+$), Non-Th17 cells ($CD3^+CD4^+Ror\gamma t^-$ $Ki67^+$) and $CD8^+$ T cells ($CD3^+CD8^+$ $Ki67^+$) (**D-H**) Proportion $IL\text{-}17^+$ $CD4^+$ T cells ($CD3^+CD4^+IL\text{-}17^+$) (**D**) $IFN\gamma^+$ $CD4^+$ T cells ($CD3^+CD4^+IFN\gamma^+$) (**E**) and $IL\text{-}10^+$ $CD4^+$ T cells ($CD3^+CD4^+IL\text{-}10^+$)(**F**) and effector $CD8^+$ T-cells ($CD3^+CD8^+CD44^+$) (**G**) and $IFN\gamma^+$ $CD8^+$ T-cells ($CD3^+CD8^+IFN\gamma^+$) (**H**) using flow cytometry. Pooled data are shown from four independent experiments, except for panels C,D and F, which are from two independent experiments. Results are presented as mean values ± SEM of n = 3-19 mice per group. Kruskal-Wallis test for multiple comparisons was performed, followed by a Mann-Whitney U test. *P<0.05, **P<0.01, ***P<0.001, ****P<0.0001.

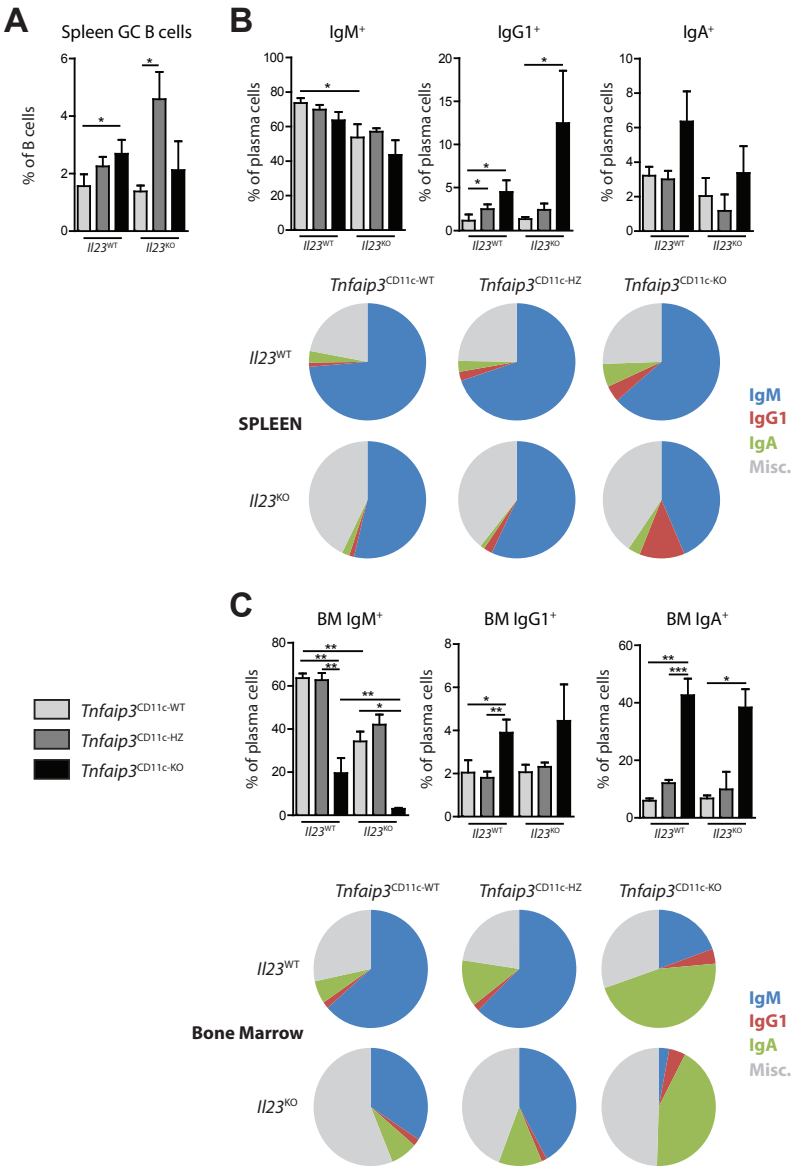

Supplementary Figure 4: Splenic and BM proportions of IgA$^+$ and IgG1$^+$ plasma cells are elevated regardless of IL-23 in *Tnfaip3*$^{CD11c\text{-}KO}$ mice.

Naïve 24-week-old *Tnfaip3*^{CD11c}*Il23* mice spleens and BM were analyzed for B cell and plasma cell proportions. (**A**) Quantification of proportion splenic GC B cells (B220$^+$IgD$^-$CD95$^+$) using flow cytometry. (**B-C**) Enumeration of the proportion IgM$^+$ plasma cells (B220$^-$CD138$^+$IgM$^+$), IgG1$^+$ plasma cells (B220$^-$CD138$^+$IgG1$^+$) and IgA$^+$ plasma cells (B220$^-$CD138$^+$IgA$^+$) in spleen (**B**) and BM (**C**) using flow cytometry. Pie charts have been included of these proportions. Pooled data is shown from three independent experiments, except panels (**B/C**) which are from one experiment. Results are presented as mean values ± SEM of n = 2-15 mice per group. Kruskal-Wallis test for multiple comparisons was used, followed by Mann-Whitney U test. *P<0.05, **P<0.01, ***P<0.001.

Supplementary Table 1: Antibodies used for flow cytometry

Antibody	Conjugate	Clone	Company
B220	AF700	RA3-6B2	eBioscience
CD11b	PercP-Cy5.5	M1/70	BD
CD11c	BV786	HL3	BD
CD138	BV605	281-2	BD
CD19	APC-Cy7	1D3	BD
CD3e	PE-CF594	145-2C11	BD
CD4	BV711	RM4-5	BD
CD44	Percp-Cy5.5	IM7	eBioscience
CD44	APC-cy7	IM7	BD
CD45	PE TxR	I3/2.3	Abcam
CD62L	APC-Cy7	MEL-14	BD
CD8a	PE-Cy7	53-6.7	eBioscience
CD86	PE-Cy7	GL1	BD
Gr-1	PE-Cy7	D7	eBioscience
IFN-y	ef450	XMG1.2	eBioscience
IgD	APC	11-26c	eBioscience
IgG1	Biotin	A85-1	BD
IgG2a/b	Biotin	R2-40	BD
IgG3	Biotin	R40-82	BD
IgM	PE-Cy7	II/41	eBioscience
IL-10	Percp-EF710	JES5-16E3	eBioscience
IL17A	AF700	TC11-18A10.1	BD
Ki67	eFluor 660	SolA15	eBioscience
MHC II	AF700	I-Ad/I-Ed	eBioscience
RORyt	PE	Q31-378	BD

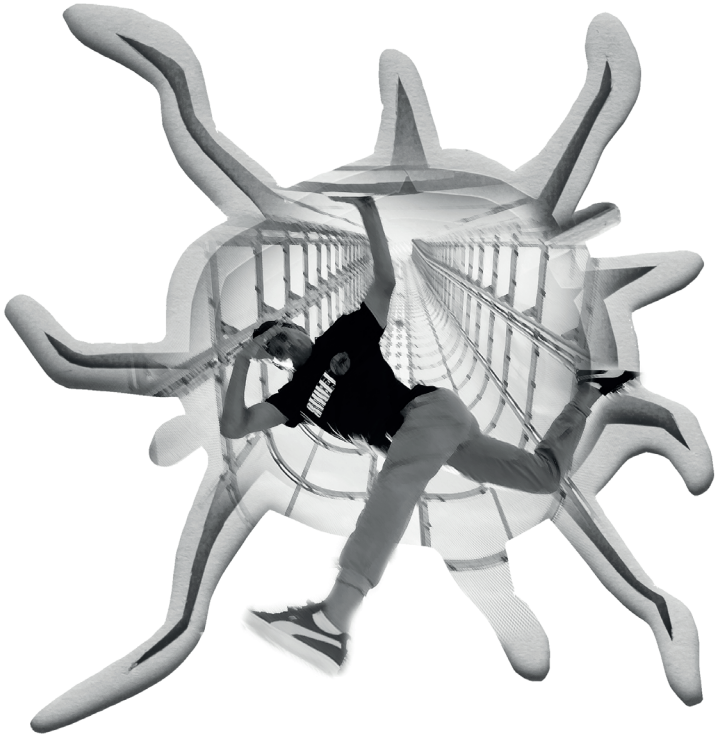

Chapter 8

Discussion and future directions

Tridib Das

In this thesis we addressed the role of A20/Tnfaip3, a negative regulator of NF-κB signaling in dendritic cells (DCs) in immune regulation that is essential to prevent autoimmune disease. We examined a novel DNGR1-cre mediated targeted deletion of the *Tnfaip3* gene in mice, which primarily affects cDC1s and studied their activation in the context of a spontaneous chronic autoimmune liver disease (**Chapter 3**). In a house dust mite (HDM)-induced neutrophilic airway inflammation, based on LysM-cre-mediated deletion of A20/*Tnfaip3* from myeloid cells, we examined the role of IL-17RA-signaling (**Chapter 4**). We surprisingly found that IL-17RA-signaling played no detectable role in HDM-induced neutrophilic airway inflammation. In aged *Tnfaip3*$^{CD11c\text{-}KO}$ mice, which lack A20/Tnfaip3 expression essentially in all DCs, we noticed that splenic B cell numbers were significantly reduced. We therefore examined the developmental stages of B cells in these mice in detail in **Chapter 5** and found that B cell development in the bone marrow was hampered at the immature B cell stage in 6-week-old *Tnfaip3*$^{CD11c\text{-}KO}$ mice and at the pre-B cell stage in 24-week-old Tnfaip3$^{CD11c\text{-}KO}$ mice. It had been previously demonstrated that A20/Tnfaip3-deficient bone marrow-derived (BM)-DCs could directly activate B cells *in vitro* independent of T cell help. Using this model crossed onto a *Cd40lg*^{KO} background, we examined whether this also occurred *in vivo* (**Chapter 6**). Despite the crucial role of CD40L in T-B cell communication in acquiring germinal center (GC) B cells and IgG1 class-switched plasma cells, we still observed glomerular membrane thickening in *Tnfaip3*$^{CD11c\text{-}KO}$*Cd40lg*^{KO} mice. We concluded that in these mice the kidney pathology was most likely mediated by autoreactive, T cell independent IgA, because IgA was deposited and serum anti-dsDNA IgM and IgA levels were enhanced. Finally, we aimed to investigate how IL-23 signaling affected Th17 and B cell populations in *Tnfaip3*$^{CD11c\text{-}KO}$ mice (**Chapter 7**). We observed that the autoimmune phenotype in mice with dendritic cell-specific deletion of Tnfaip3/A20 was independent of the IL-23/IL-17 axis.

In this chapter, we discuss the role of A20/Tnfaip3, primarily in DCs, but also other immune cells, to keep the immune system in balance and prevent autoimmunity. We translate our findings to patients and discuss the outlook of A20 research in autoimmunity.

A STEP INTO THE PAST, EQUALS A STEP INTO THE FUTURE: UNDERSTANDING DC ONTOGENY

Nobel laureate Ralph Steinman's discovery of DCs in the 1970's boosted our knowledge of immune homeostasis[1]. DCs are orchestrators of the immune system from tolerance to immunity[2]. This delicate balance is maintained by the expression of tolerogenic or immunogenic co-stimulators and cytokines[3, 4]. Over the years various types of DCs were

discovered and this led to a confusing nomenclature of DC subsets in different organs and different species, and challenged the comparison of individual experimental studies. At one point in time, questions were asked whether DCs are truly any different from monocytes at all[5]. In 2014, when experiments described in this thesis were ongoing, a consensus was proposed on the basis of DC ontogeny, which corresponded well across different species[6]. Deciphering various transcription factors or cell-specific expression markers to isolate DC subsets became a 'hot topic', either by targeted deletion of those transcription factors[7] or by genetic tracing using fluorescent reporters in mice[8, 9]. Promising results were found for cDC1s and pDCs, but to date, cDC2s have no single transcription factor with exclusive control over their development. This is due to (i) key transcription factors such as IRF4, which are also used by other myeloid or adaptive immune cells[10] and (ii) the finding that cDC2s can also be derived from lymphoid progenitors during certain conditions[11]. An overview of the main pDC and cDC transcription factors is depicted in **Figure 1**. Very recent work identified a subdivision of cDC2s into cDC2A and cDC2B based on T-bet or RORγt expression, respectively, and divides them into anti-inflammatory and pro-inflammatory cDC2s[12]. Our work did not take these ongoing divisions of cDC subsets into account.

Our interest settled on loxP-Cre-mediated gene deletion, whereby the DNGR1-cre (Clec9a-cre) was shown to mostly affect cDC1s, and a smaller proportion cDC2s and moDCs in steady state[8]. By crossing our *Tnfaip3*^{DNGR1} mice with ROSA-EYFP mice we demonstrated, in parallel to the work of Schraml *et al.* in the kidney[8], that primarily cDC1s (~95%) were affected in the liver (**Chapter 3**). A proportion cDC2s and moDCs (~30-40%) also showed deletion, as evidenced by YFP expression, in steady state. Interestingly, during inflammation these proportions were reduced for cDC1s from ~95% YFP-positivity to ~60% YFP-positivity. While Schraml *et al* did not report the exact percentages of YFP$^+$ cells in DC subsets during *L. monocytogenes* inflammation, their CD11c$^+$GR1$^-$ population had ~55% YFP-positivity and likely encompassed most DC subsets. Thus, during inflammation, there appears to be a positive selection for the YFP-negative (reflecting the Tnfaip3-sufficient) population of cDC1s in our study. What the origin of these cells are is yet unknown, but they could be derived from monocytes as they can express cDC markers in tumors[13]. In the time that the experiments described were ongoing, several novel cDC1 specific conditional cre transgenic mouse models became available such as XCR1-cre or Karma-cre[14] that are superior to the DNGR1-cre mouse. Even during viral infection, these models remain specific for cDC1[14]. The utilization of these models would have given cleaner results in comparison to the DNGR1-cre mice when analyzing the systemic effects of activated cDC1s, as described in **chapter 3**. Nevertheless, in *Tnfaip3*$^{DNGR1\text{-}KO}$ mice cDC and moDC activation was associated with T cell activation, elevated IFN-γ production and plasma cell differentiation (**Figure 2**). Specifically, plasma cells were present that produced autoreactive IgA recognizing periportal

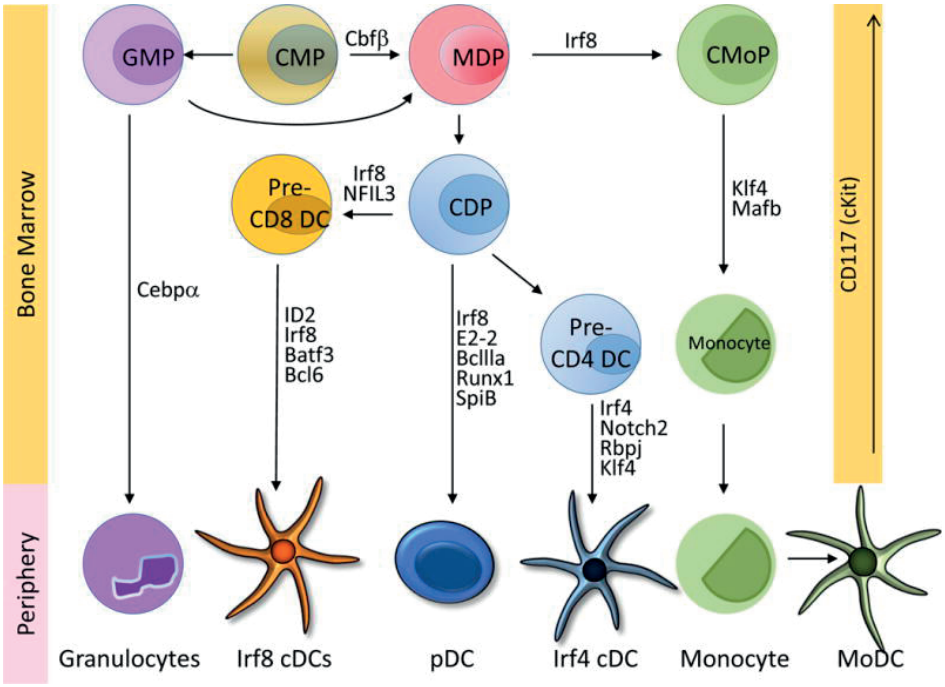

Figure 1: Differential expression of transcription factors regulating DC differentiation
From the common myeloid progenitor (CMP), stems off a granulocyte-monocyte progenitor (GMP) and macrophage-dendritic cell progenitor (MDP). The latter splits off into a common monocyte progenitor (CMoP) that may develop into monocytes or into the common DC progenitor (CDP). The CDP may give rise to pDCs or a precursor DC (pre-DC) for $CD4^+$ or $CD8^+$ DCs. ID2, inhibitor of DNA binding 2; BATF3, basic leucine zipper transcription factor ATF-like 3; IRF, interferon-regulatory factor; Bcl6 or Bcl11a, B cell lymphoma 6 or 11a; Runx1, Runt related transcription factor; Rbpj, Recombination signal binding protein for immunoglobulin Kappa J Region; Klf4, Krueppel-like Factor; Mafb, MAF BZIP transcription factor B. From Murphy et al, Annu Rev Immunol, 2016[7].

cytoplasmic liver antigens, possibly leading to inflammatory infiltrates in those areas. By administering anti-IL-6 antibodies *in vivo*, we blocked IL-6 for multiple weeks and found a simultaneous absence of Th17 cells (Thomas Koudstaal et al., unpublished data). Thus, lack of IL-6 and Th17 did not reduce the liver inflammation. We were unable to demonstrate whether IFN-γ was responsible for the inflammation, which likely contributes to the pathology as IFN-γ transgenic mice on a liver specific promoter (serum amyloid P component) resembled our liver phenotype[15]. Evidence was obtained for an indispensable role for cDC1s in a *Batf3*$^{-/-}$ mice in a primary biliary cirrhosis model (Reuveni/Zigmund, pers. commun.), which would support our findings of liver pathology in the *Tnfaip3*^{DNGR1} model of activated cDC1s. Liver inflammation was previously demonstrated in the context of multiorgan inflammation by Kool *et al* in the SLE-like phenotype[16] and by Xuan et al with CD11c-cre mediated deletion of *Tnfaip3*[17]. Another group indepen-

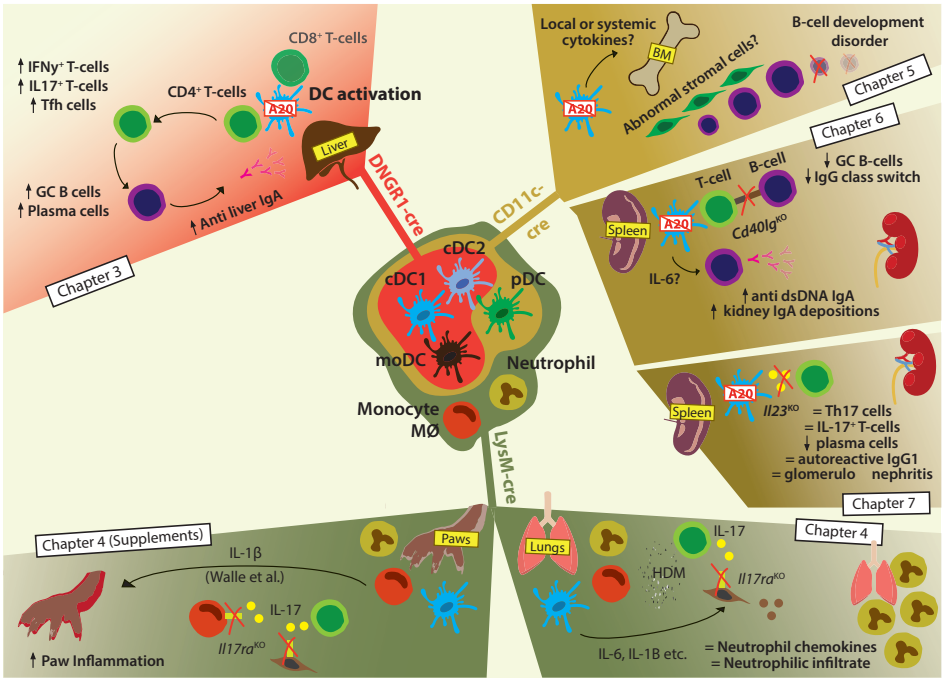

Figure 2: A summary of the Tnfaip3$^{fl/fl}$ and Cre-LoxP models (DNGR1-cre (red), CD11c-cre (brown) and LysM-cre (Green) applied in this thesis, as well as the studied organs. Additional crosses onto other backgrounds (*Cd40lg*^{KO}, *Il23*^{KO} and *Il17ra*^{KO}), which are described in the specific chapter blocks are indicated. "↑" means a significant increase, "↓" means a significant decrease and "=" means no significant differences.

dently generated a similar *Tnfaip3*$^{CD11c\text{-}KO}$ mouse model that had an IBD phenotype[18]. We confirmed that the *Tnfaip3*$^{DNGR1\text{-}KO}$ mice differed from these phenotypes, since we found no intestinal or kidney inflammation. It is of note that cDC activation in the lungs of *Tnfaip3*$^{DNGR1\text{-}KO}$ mice, could result in a pulmonary hypertension phenotype (Koudstaal et al., manuscript submitted). Differences in phenotype between laboratories, using a similar *Tnfaip3*$^{CD11c\text{-}KO}$ model are likely caused by microbiome differences, although effects of genetic background or minor differences in the targeting construct cannot be excluded. How the microbiome affects genetic models deserves future attention, because they can cloud the conclusions of genetic murine studies.

A20/TNFAIP3, MYELOID CELLS AND TH17-IL-23 AXIS IN CHRONIC DISEASES

Since the original discovery of the Th17 cell lineage in 2005[19], the Th17-IL-23 axis has been a prime topic in autoimmune research. Arthritis, IBD and psoriasis are classic ex-

amples with deregulations in this axis[20]. Other chronic diseases such as COPD or asthma should deserve this attention too. Patients with severe asthma may have a neutrophilic infiltrate[21] and elevated serum IL-17 levels[22] in comparison to moderate asthma patients. In an HDM-driven mouse model of airway inflammation, our group demonstrated that myeloid deficiency of A20 lead to a neutrophilic rather than an eosinophilic airway infiltrate[23]. Since IL-17 levels coordinate neutrophil chemoattractants such as CXCL1 from airway epithelial cells[24], we hypothesized that HDM-induced neutrophil airway inflammation would be reduced in *Tnfaip3*$^{LysM\text{-}KO}$ mice when crossed onto an *Il17ra*^{KO} background (**Figure 2**). Surprisingly, this did not seem to be the case (**Chapter 4**). An equal extent of neutrophilic airway infiltration was seen in the broncho-alveolar lavage (BAL) fluid in HDM-exposed *Il17ra*^{WT} and *Il17ra*^{KO} *Tnfaip3*$^{LysM\text{-}KO}$ mice. Although IL-17Rα-signaling was absent, chemokines such as CXCL1, CXCL2 and CXCL12 were still formed, possibly due to high unaltered levels of IL-1β and IL-6. The clinical relevance of A20 in asthma patients was recently highlighted by reports of reduced TNFAIP3 mRNA and protein levels, isolated from PBMCs from asthmatic children compared to healthy controls[25]. DCs also showed a non-significant reduction of TNFAIP3 mRNA levels in asthmatic children[25].

Increased numbers of Th17 cells were present in spleens and inguinal lymph nodes of *Tnfaip3*$^{LysM\text{-}KO}$ mice[26] and these mice were originally demonstrated to have paw inflammation resembling arthritis. Although the arthritis was independent of T or B cells[26], myeloid cells such as monocytes[27] or neutrophils[28] can also produce IL-17. We thus wanted to examine the role of IL-17Rα signaling on arthritis. Surprisingly, despite having no IL-17Rα-signaling, there was equal paw inflammation in *Tnfaip3*$^{LysM\text{-}KO}$*Il17ra*^{KO} mice (**Supplementary Figure Chapter 4, Figure 2**), which was explained in a subsequent paper by evidence that IL-1β is the responsible cytokine[29]. A novel function for A20 was deciphered: it regulates the inflammasome NLRP3 and secondary IL-1β release from myeloid cells[29]. The effect of A20 on the inflammasome was confirmed in a few families around the world that had a loss-of-function mutation in A20. These patients have a rare disease called "A20 Haploinsufficiency"[30] and their PBMCs have elevated inflammasome activation, NLRP3 and IL-1β protein and mRNA production[30, 31]. Phenotypes ranged from autoinflammatory diseases such as Behçets disease[30] to autoimmune disorders[32].

In the same *Tnfaip3*$^{LysM\text{-}KO}$ mouse, another role of A20 was discovered: A20-deficiency in IFN-γ-stimulated bone marrow derived macrophages (BM-DM), resulted in higher STAT1 mRNA transcription in comparison to STAT3 mRNA transcription, indicating that A20 may regulate STAT gene transcription ratios[33]. Understanding the potent molecular functions of A20 is still of high interest, illustrated by two recent papers that studied the functional domains of A20. The Zinc Finger (ZF) 7 domain was most important to prevent a spontaneous autoimmune psoriatic-arthritis/like phenotype[34, 35], whereas abrogating the ZF4 or OTU domain of A20 surprisingly did not reveal any phenotype[36, 37]. The

psoriatic-arthritis like symptoms were dependent on T cells, IL-17 and TNFα[35]. Although DC co-stimulatory molecules were not assessed (except for MHC-II), this does suggest their involvement to activate the adaptive immune system.

In vitro, it was shown that A20-deficient BM-DCs[16], produce high levels of IL-23 and IL-6 (Vroman et al[23] and this thesis, **Chapter 6**), and could elicit IL-17 production from naïve T cells. We wondered whether *in vivo* Th17 cells could be reduced, and consecutive B cell activation as well, since Th17 cells can stimulate immunoglobulin production[38]. We thus crossed *Tnfaip3*$^{CD11c\text{-}KO}$ mice to *Il23*^{KO} mice and analyzed the resulting phenotype (**Chapter 7, Figure 2**). We surprisingly did not see a reduction of Th17 cells or IL-17^{+} CD4^{+} T-cells in the spleen when we abrogated IL-23 in *Tnfaip3*$^{CD11c\text{-}KO}$ mice. This corresponds with the literature that IL-23 is mostly important for maintenance of Th17 cells and inducing its pathogenicity, but that IL-6 and TGF-β cause Th17 cell induction[39]. Since Th17 cells influence plasma cell class switch by cytokines[38], we also assessed serum immunoglobulins. We found no differences in *Tnfaip3*$^{CD11c\text{-}KO}$ mice concerning serum IgM, IgG2b, IgG2c or IgG3 in absence of IL-23. IgA which was elevated in *Tnfaip3*$^{CD11c\text{-}KO}$ mice was lowered in *Tnfaip3*$^{CD11c\text{-}KO}$*Il23*^{KO} mice. The increase of total IgG1 levels in the serum of *Tnfaip3*$^{CD11c\text{-}KO}$ mice was independent of IL-23, nor was the amount of autoreactive IgG1 and kidney glomerulonephritis. We therefore concluded that the SLE-phenotype in *Tnfaip3*$^{CD11c\text{-}KO}$ mice acts independently from the IL-23/Th17 axis. These findings are in contrast to studies that show a crucial role of IL-23 in other SLE models, such as the lupus prone MRL.*Fas*^{lpr} mice[40, 41]. Therefore, distinct immunological mechanisms may lead to a similar SLE phenotype: in the *lpr* mice there is a greater dependency on the Th17/IL-23 axis. In our model, future studies to identify the primary responsible cytokine may include blocking IL-6, TNF-α or IFN-γ since these were elevated in *Tnfaip3*$^{CD11c\text{-}KO}$ mice *in vivo*[16-18].

A20/TNFAIP3 AND DIRECT ACTIVATION OF B CELLS BY DCS, INDEPENDENTLY FROM T CELLS

The most classic route of adaptive immune cell activation is by antigen presenting cells (APCs), via T cells, which in turn activate B cells. However, a direct interaction between APCs and B cells is also described[42], whereby DCs are shown to interact directly with B cells and present antigen to them[43]. Our group was able to demonstrate *in vitro* that BM-DCs from *Tnfaip3*$^{CD11c\text{-}KO}$ mice in combination with only naïve B cells, stimulated plasmablast and plasma cell formation leading to IgA and IgG1 release[16]. Interestingly, characteristic T cell independent activators of plasma cells such as BAFF and APRIL[44], were not necessary in this *in vitro* activation of plasma cells[16]. Only IL-6 was found to stimulate IgA release[16]. Using mRNA sequencing, we compared *Tnfaip3*^{KO}, *Tnfaip3*^{HZ} and *Tnfaip3*^{WT}

BM-DCs[23] for a comprehensive genome-wide identification of differentially transcribed genes including candidate factors that may orchestrated B cell activation by DCs (**chapter 6**). However, even by gene-set enrichment analysis (GSEA), we did not find new targets except IL-6, IL-1α and IL-1β. Factors such as BAFF and APRIL were not significantly differentially expressed in our analysis. We proceeded to analyze whether activated DCs in *Tnfaip3*$^{CD11c\text{-}KO}$ mice could also activate B cells *in vivo* and could direct class-switched plasma cells without T cell help by crossing these mice onto a *Cd40lg*^{KO} background (**Chapter 6, Figure 2**). GC B cells are dependent on CD40 ligand interaction[45]. However, while *Tnfaip3*$^{CD11c\text{-}KO}$*Cd40lg*^{KO} displayed a detectable elevation of GC-like B cells on flow cytometry in comparison to *Cd40lg*^{KO} mice, GC structures containing these cells could not be visualized using immunohistochemistry (**Chapter 6**). These findings indicating that these GC-like B cells were most likely activated B cells, rather than true GC B cells. While some studies provided evidence that GC B cells can be formed without T cell help[46, 47], these were short-lived GC B cells that did not allow the immunoglobulin variable regions to undergo somatic hypermutation. Interestingly, despite having no regular GC B cells, we did see equal number of plasma cells in double KO mice, compared to *Tnfaip3*$^{CD11c\text{-}KO}$ mice, suggesting that extrafollicular B cell activation was likely responsible for plasma cell formation. Within lupus models, the short-lived plasmablasts are the main source of autoantibodies[48, 49], which derive from extrafollicular loci instead of long-lived plasma cells that originate from germinal centers. In these extrafollicular loci, DCs are in close proximity to autoantibody-positive B cells and are thought to provide survival signals to them[49]. In accordance, it has been reported that constitutive DC depletion in MRL.*Fas*^{lpr} mice reduced plasma blast numbers, autoantibodies and glomerulonephritis[50]. Interestingly, despite the absence of T-B cell communication, IgG formation or glomerular IgG deposition, we still found glomerulonephritis in *Cd40lg*^{KO}*Tnfaip3*$^{CD11c\text{-}KO}$ mice. Possibly, autoreactive IgA contributed to the basement membrane thickening, as IgA depositions were detected in ~40% of the double KO mice. This knowledge is valuable, since therapies that inhibit T-B cell communication in patients with SLE, may not be sufficient to prevent end-stage renal disease.

A20/TNFAIP3, DCS AND B-CELL DEVELOPMENT IN THE BONE MARROW

The function of DCs in the lymph nodes, the splenic compartment and mucosa are pronounced and well-studied, but what could the roles of DCs be in the bone marrow (BM)? BM-resident DCs have been identified and are known to resemble cDC2s, but simultaneously differ from splenic cDC2s in their chemokines and chemokine receptors[51]. They are thought to provide survival signals to mature B cells in the BM[52]**.** Could DCs that are resident in the BM influence the BM environment and thereby also affect developing

B cells or play a role in their development? And what will be the effects of DCs in the BM on the functionality of developing B cells later in their life once they have left the BM? We specifically asked these questions, because we found reduced numbers of mature B cells in the spleen, but also in BM of 24-week-old Tnfaip3$^{CD11c\text{-}KO}$ mice.

In young 6-week-old mice we therefore analyzed the different stages of B cell development in BM and found a disorder around the small pre-B cell stage in **Chapter 5** (**Figure 2**). Using an *in vitro* co-culture with IL-7, we identified that the CD19^{negative} BM fraction from *Tnfaip3*$^{CD11c\text{-}KO}$ mice could negatively influence development of B cells that were derived from both WT or from *Tnfaip3*$^{CD11c\text{-}KO}$ mice. This implies that there is a non-cell intrinsic defect in B cell differentiation in these mice. Using several washing steps, we also hypothesize that cytokines are not likely responsible for defects in B cell differentiation. We however cannot exclude that during the *in vitro* study, new cytokines were produced that hampered B cell development. Future experiments may be conducted to explore the presence of any elevated inhibitory cytokines in such IL-7-driven co-cultures, including IFN α/β/γ, IL-1 α/β, IL-4 or TGF-β, or stromal cell chemokines such as CXCL12[53] that are known to influence B cell development. It is attractive to speculate that local DCs in the BM of *Tnfaip3*$^{CD11c\text{-}KO}$ mice have critical effects on B cell differentiation in the BM. It would be informative to assess activation markers and cytokines on BM-resident DCs in *Tnfaip3*$^{CD11c\text{-}KO}$ mice.

Since BM is a compartment that is difficult to access in humans, relatively little is known about possible defects in B cell development in autoimmune patients. A small cohort of SLE patients, however, revealed reduced BM CD20^{+} B cells[54], which may parallel our findings of reduced mature B cells in the BM of *Tnfaip3*$^{CD11c\text{-}KO}$ mice. Unstimulated peripheral B cells from MS patients and stimulated B cells from SLE patients had elevated CD80/CD86 expression in comparison to healthy donor B cells[55, 56]. This also corresponds to our *in vitro* findings in **Chapter 5** where peripheral mature B cells from *Tnfaip3*$^{CD11c\text{-}KO}$ mice expressed higher levels of CD80/CD86 on different stimuli. In an SLE cohort, it was found that more apoptotic cells were present in the BM, together with elevated numbers of T cells, macrophages and pDCs, thus reflecting a more pro-inflammatory environment[54]. Signs of a type 1 IFN-rich environment in the BM of SLE patients have been found[57] and it was recently shown that transitional B cells in SLE patients indeed have a type 1, and also a type 2 IFN-stimulated signature derived from the BM environment[58]. All in all, understanding of abnormal BM and B cell development in SLE patients may contribute to knowledge that is important for the future development of new therapies for this autoimmune disease.

CONCLUSIONS AND FUTURE DIRECTIONS

Immune cell activation may tip the balance from tolerance to autoimmunity. In all our murine studies we deleted A20/TNFAIP3, a negative regulator of NF-κB signaling, to lean different immune cells towards activation (**Figure 2**). How relevant is A20 deficiency in humans? Besides a very rare disorder, haploinsufficiency of A20 (HA20)[30], it is more reasonable that subtle defects in A20 expression levels or its induction is affected than general A20 deficiency. One *TNFAIP3* missense mutation near the OTU domain with the most subtle effect on function (T108A/I207L), was seen in Australian families from Maori ancestry[59]. The allele variation was also identified in Denovisan archaic human species, but not present in Neanderthals, which lived in the same Siberian cave, suggesting that this allele arose after Denovisan and Neanderthal lineage divergence more than 170,000 years ago[59]. What could be the advantage of this allele? A heightened immune response with e.g. release of TNF-α or CXCL2 could be seen in stimulated PBMCs from these families versus controls. Using a humanized mouse model with CRISPR-Cas9 genome editing, the authors elegantly demonstrate that the T108A/I207L mutation increases survival by 1.8x in male mice compared to WT mice when exposed to coxsackie virus infection[59]. Mice with more severe missense mutations, one of which was based on the HA20 phenotype in humans[30], never died of this coxsackie virus infection. But this came at a price: a range of subclinical spontaneous tissue inflammation was detectable in one variation, whereas fatal intestinal inflammation was seen in another. Thus, protection from foreign invaders may be more efficient, at the price of suffering from responses e.g. to microbes that should be tolerated.

One of A20's functions is thus to create a balanced immune system, which is primarily important in DCs. We were most interested to study the role of A20/Tnfaip3 in DCs. Given the division of labor it is important to study DC subsets specifically, and not as a whole population. We have made a first step using the DNGR1-cre model to decipher the role of A20/Tnfaip3-depletion primarily in the cDC1 subset. However, more specific cre models such as the XCR1-cre or Karma-cre can be used in future experiments to ablate A20 in only cDC1s, since the DNGR1-cre model also targets a proportion cDC2s and moDCs. When translating findings from murine studies to patients, it is crucial to consider this subdivision of DCs. Although human DCs have been properly classified[60], to date only a few studies on cDC changes in autoimmune patients have been reported. The *Tnfaip3*$^{CD11c\text{-}KO}$ model demonstrated the consequence of active DCs, but it raised several more questions. When we crossed *Tnfaip3*$^{CD11c\text{-}KO}$ mice to *Cd40lg*^{KO} mice, we saw no class switched IgG, but we did find autoreactive IgA and also IgA depositions in the kidneys. Two clinical diseases are known with similar findings: X-linked Hyper-IgM syndrome patients lack CD40LG and therefore have drastically reduced class-switched immunoglobulins, including reduced levels of IgA[61]. IgA nephropathy is characterized by a

dominance of IgA that leads to deposition in the kidney glomeruli, in contrast to IgG[62]. Although the pathogenesis of these two disorders is different, it appears that they may merge in our *Cd40lg*^{KO}*Tnfaip3*$^{CD11c\text{-}KO}$ mice, because we did find IgA depositions in the kidney glomeruli without IgG immunoglobulins present. There are case reports available of IgA nephropathy and SLE occurring in the same patients[62, 63]. Several clinical trials are currently performed with anti-CD40L or anti-CD40 biologicals in SLE[64], whereby clinical activity scores are improved over placebo controls that also include kidney function parameters. Our findings, however, suggest that in a diseased state with activated DCs, such inhibitors may still result in unexpected outcomes of kidney glomerulonephritis.

The Th17-IL23-axis was contra intuitively not of importance in our model of Tnfaip3-deficiency in DCs and other myeloid cells, concerning endpoints of kidney glomerulonephritis (**Chapter 7**, **Figure 2**), paw inflammation and neutrophilic airway inflammation (**Chapter 4, Figure 2**). Ustekinumab, the biological anti-p40 subunit against both IL-23 and IL-12 has been approved for diseases such as Crohn's disease, psoriasis and psoriatic arthritis. It is still under investigation for SLE, although promising results have been reported[65]. Ustekinumab does not seem to be effective in RA[66]. There are no ongoing clinical trials in asthma, which reflects our findings of similar neutrophilic airway inflammation with or without IL-17RA-signaling in a HDM-induced airway inflammation model in *Tnfaip3*$^{LysM\text{-}KO}$ mice. It has been demonstrated in one case study, however, that Ustekinumab also relieved an asthmatic patient of her chronic airway medication, while she was treated for psoriasis[67], suggesting that Th17 responses could be underlying asthma pathogenesis in some patients. Further investigations are needed to characterize the group of asthma patients that may benefit from IL-17 blockade, before ustekinumab may be tested in clinical trials for a subgroup of therapeutically refractive patients.

In conclusion, our studies have shown that activated DCs lie at the initiation phase of the autoimmune response, with extensive secondary consequences. Blocking an intermediate cytokine sometimes may not inhibit a primary endpoint such as kidney glomerulonephritis, because activated DCs can activate multiple cells prior to the release of the cytokine in question. Future autoimmunity treatments could be focused on inhibiting NF-κB activation. However, these treatment strategies need to be designed carefully as they might reduce acute inflammation, while causing long-lasting side effects. For example, interference with NF-κB in enterocytes prevented systemic inflammation in an intestinal-ischemia reperfusion model, but led to apoptotic mucosal damage as well[68], since NF-κB acts as an anti-apoptotic factor. For that reason, NF-κB blockade has already been an attractive candidate in cancer therapy NF-κB[69]. While IKK inhibitors pose toxicity issues, a lot of research is conducted to pharmacologically modulate ubiquitination and degradation of NF-κB components[69], thus nearing the functions of A20. Another therapeutic option in accordance to our findings, would be to treat autoimmunity with tolerogenic DCs. To date, two studies with the induction of tolerogenic DCs with an

AMPK activator and an AhR antagonist showed promising results in SLE[70]. Perhaps the induction of tolerogenic-DCs holds a future in the treatment or prevention of autoimmune diseases, and should thus be investigated.

REFERENCES

1. Steinman RM, Witmer MD. Lymphoid dendritic cells are potent stimulators of the primary mixed leukocyte reaction in mice. *Proceedings of the National Academy of Sciences of the United States of America* 1978; 75(10): 5132-5136.
2. Steinman RM. Decisions about dendritic cells: past, present, and future. *Annu Rev Immunol* 2012; 30: 1-22.
3. Tan JK, O'Neill HC. Maturation requirements for dendritic cells in T cell stimulation leading to tolerance versus immunity. *J Leukoc Biol* 2005; 78(2): 319-324.
4. Steinman RM, Nussenzweig MC. Avoiding horror autotoxicus: the importance of dendritic cells in peripheral T cell tolerance. *Proc Natl Acad Sci U S A* 2002; 99(1): 351-358.
5. Hume DA. Differentiation and heterogeneity in the mononuclear phagocyte system. *Mucosal immunology* 2008; 1(6): 432-441.
6. Guilliams M, Ginhoux F, Jakubzick C, Naik SH, Onai N, Schraml BU *et al.* Dendritic cells, monocytes and macrophages: a unified nomenclature based on ontogeny. *Nature reviews Immunology* 2014; 14(8): 571-578.
7. Murphy TL, Grajales-Reyes GE, Wu X, Tussiwand R, Briseño CG, Iwata A *et al.* Transcriptional Control of Dendritic Cell Development. *Annual review of immunology* 2016; 34: 93-119.
8. Schraml BU, van Blijswijk J, Zelenay S, Whitney PG, Filby A, Acton SE *et al.* Genetic tracing via DNGR-1 expression history defines dendritic cells as a hematopoietic lineage. *Cell* 2013; 154(4): 843-858.
9. Abram CL, Roberge GL, Hu Y, Lowell CA. Comparative analysis of the efficiency and specificity of myeloid-Cre deleting strains using ROSA-EYFP reporter mice. *Journal of immunological methods* 2014; 408: 89-100.
10. Mittrücker HW, Matsuyama T, Grossman A, Kündig TM, Potter J, Shahinian A *et al.* Requirement for the transcription factor LSIRF/IRF4 for mature B and T lymphocyte function. *Science (New York, NY)* 1997; 275(5299): 540-543.
11. Salvermoser J, van Blijswijk J, Papaioannou NE, Rambichler S, Pasztoi M, Pakalniškytė D *et al.* Clec9a-Mediated Ablation of Conventional Dendritic Cells Suggests a Lymphoid Path to Generating Dendritic Cells In Vivo. *Frontiers in immunology* 2018; 9: 699.
12. Brown CC, Gudjonson H, Pritykin Y, Deep D, Lavallée VP, Mendoza A *et al.* Transcriptional Basis of Mouse and Human Dendritic Cell Heterogeneity. *Cell* 2019; 179(4): 846-863.e824.
13. Sharma MD, Rodriguez PC, Koehn BH, Baban B, Cui Y, Guo G *et al.* Activation of p53 in Immature Myeloid Precursor Cells Controls Differentiation into Ly6c(+) CD103(+) Monocytic Antigen-Presenting Cells in Tumors. *Immunity* 2018; 48(1): 91-106.e106.
14. Mattiuz R, Wohn C, Ghilas S, Ambrosini M, Alexandre YO, Sanchez C *et al.* Novel Cre-Expressing Mouse Strains Permitting to Selectively Track and Edit Type 1 Conventional Dendritic Cells Facilitate Disentangling Their Complexity in vivo. *Frontiers in immunology* 2018; 9: 2805.
15. Toyonaga T, Hino O, Sugai S, Wakasugi S, Abe K, Shichiri M *et al.* Chronic active hepatitis in transgenic mice expressing interferon-gamma in the liver. *Proc Natl Acad Sci U S A* 1994; 91(2): 614-618.
16. Kool M, van Loo G, Waelput W, De Prijck S, Muskens F, Sze M *et al.* The ubiquitin-editing protein A20 prevents dendritic cell activation, recognition of apoptotic cells, and systemic autoimmunity. *Immunity* 2011; 35(1): 82-96.
17. Xuan NT, Wang X, Nishanth G, Waisman A, Borucki K, Isermann B *et al.* A20 expression in dendritic cells protects mice from LPS-induced mortality. *European journal of immunology* 2015; 45(3): 818-828.

18. Hammer GE, Turer EE, Taylor KE, Fang CJ, Advincula R, Oshima S *et al.* Expression of A20 by dendritic cells preserves immune homeostasis and prevents colitis and spondyloarthritis. *Nature immunology* 2011; 12(12): 1184-1193.
19. Langrish CL, Chen Y, Blumenschein WM, Mattson J, Basham B, Sedgwick JD *et al.* IL-23 drives a pathogenic T cell population that induces autoimmune inflammation. *The Journal of experimental medicine* 2005; 201(2): 233-240.
20. Tang C, Chen S, Qian H, Huang W. Interleukin-23: as a drug target for autoimmune inflammatory diseases. *Immunology* 2012; 135(2): 112-124.
21. Green RH, Brightling CE, Woltmann G, Parker D, Wardlaw AJ, Pavord ID. Analysis of induced sputum in adults with asthma: identification of subgroup with isolated sputum neutrophilia and poor response to inhaled corticosteroids. *Thorax* 2002; 57(10): 875-879.
22. Agache I, Ciobanu C, Agache C, Anghel M. Increased serum IL-17 is an independent risk factor for severe asthma. *Respiratory medicine* 2010; 104(8): 1131-1137.
23. Vroman H, Bergen IM, van Hulst JAC, van Nimwegen M, van Uden D, Schuijs MJ *et al.* TNF-alpha-induced protein 3 levels in lung dendritic cells instruct TH2 or TH17 cell differentiation in eosinophilic or neutrophilic asthma. *J Allergy Clin Immunol* 2018; 141(5): 1620-1633 e1612.
24. Wonnenberg B, Jungnickel C, Honecker A, Wolf L, Voss M, Bischoff M *et al.* IL-17A attracts inflammatory cells in murine lung infection with P. aeruginosa. *Innate immunity* 2016; 22(8): 620-625.
25. Krusche J, Twardziok M, Rehbach K, Böck A, Tsang MS, Schröder PC *et al.* TNF-α-induced protein 3 is a key player in childhood asthma development and environment-mediated protection. *The Journal of allergy and clinical immunology* 2019; 144(6): 1684-1696.e1612.
26. Matmati M, Jacques P, Maelfait J, Verheugen E, Kool M, Sze M *et al.* A20 (TNFAIP3) deficiency in myeloid cells triggers erosive polyarthritis resembling rheumatoid arthritis. *Nat Genet* 2011; 43(9): 908-912.
27. Starnes T, Robertson MJ, Sledge G, Kelich S, Nakshatri H, Broxmeyer HE *et al.* Cutting edge: IL-17F, a novel cytokine selectively expressed in activated T cells and monocytes, regulates angiogenesis and endothelial cell cytokine production. *Journal of immunology (Baltimore, Md : 1950)* 2001; 167(8): 4137-4140.
28. Ferretti S, Bonneau O, Dubois GR, Jones CE, Trifilieff A. IL-17, produced by lymphocytes and neutrophils, is necessary for lipopolysaccharide-induced airway neutrophilia: IL-15 as a possible trigger. *Journal of immunology (Baltimore, Md : 1950)* 2003; 170(4): 2106-2112.
29. Vande Walle L, Van Opdenbosch N, Jacques P, Fossoul A, Verheugen E, Vogel P *et al.* Negative regulation of the NLRP3 inflammasome by A20 protects against arthritis. *Nature* 2014; 512(7512): 69-73.
30. Zhou Q, Wang H, Schwartz DM, Stoffels M, Park YH, Zhang Y *et al.* Loss-of-function mutations in TNFAIP3 leading to A20 haploinsufficiency cause an early-onset autoinflammatory disease. *Nature genetics* 2016; 48(1): 67-73.
31. Rajamäki K, Keskitalo S, Seppänen M, Kuismin O, Vähäsalo P, Trotta L *et al.* Haploinsufficiency of A20 impairs protein-protein interactome and leads into caspase-8-dependent enhancement of NLRP3 inflammasome activation. *RMD open* 2018; 4(2): e000740.
32. Kadowaki T, Ohnishi H, Kawamoto N, Hori T, Nishimura K, Kobayashi C *et al.* Haploinsufficiency of A20 causes autoinflammatory and autoimmune disorders. *The Journal of allergy and clinical immunology* 2018; 141(4): 1485-1488.e1411.
33. De Wilde K, Martens A, Lambrecht S, Jacques P, Drennan MB, Debusschere K *et*

al. A20 inhibition of STAT1 expression in myeloid cells: a novel endogenous regulatory mechanism preventing development of enthesitis. *Annals of the rheumatic diseases* 2017; 76(3): 585-592.
34. Polykratis A, Martens A, Eren RO, Shirasaki Y, Yamagishi M, Yamaguchi Y *et al.* A20 prevents inflammasome-dependent arthritis by inhibiting macrophage necroptosis through its ZnF7 ubiquitin-binding domain. *Nature cell biology* 2019; 21(6): 731-742.
35. Razani B, Whang MI, Kim FS, Nakamura MC, Sun X, Advincula R *et al.* Non-catalytic ubiquitin binding by A20 prevents psoriatic arthritis-like disease and inflammation. *Nature immunology* 2020; 21(4): 422-433.
36. De A, Dainichi T, Rathinam CV, Ghosh S. The deubiquitinase activity of A20 is dispensable for NF-κB signaling. *EMBO reports* 2014; 15(7): 775-783.
37. Lu TT, Onizawa M, Hammer GE, Turer EE, Yin Q, Damko E *et al.* Dimerization and ubiquitin mediated recruitment of A20, a complex deubiquitinating enzyme. *Immunity* 2013; 38(5): 896-905.
38. Mitsdoerffer M, Lee Y, Jäger A, Kim HJ, Korn T, Kolls JK *et al.* Proinflammatory T helper type 17 cells are effective B-cell helpers. *Proceedings of the National Academy of Sciences of the United States of America* 2010; 107(32): 14292-14297.
39. Veldhoen M, Hocking RJ, Atkins CJ, Locksley RM, Stockinger B. TGFbeta in the context of an inflammatory cytokine milieu supports de novo differentiation of IL-17-producing T cells. *Immunity* 2006; 24(2): 179-189.
40. Kyttaris VC, Kampagianni O, Tsokos GC. Treatment with anti-interleukin 23 antibody ameliorates disease in lupus-prone mice. *BioMed research international* 2013; 2013: 861028.
41. Kyttaris VC, Zhang Z, Kuchroo VK, Oukka M, Tsokos GC. Cutting edge: IL-23 receptor deficiency prevents the development of lupus nephritis in C57BL/6-lpr/lpr mice. *Journal of immunology (Baltimore, Md : 1950)* 2010; 184(9): 4605-4609.
42. Xu W, Banchereau J. The antigen presenting cells instruct plasma cell differentiation. *Frontiers in immunology* 2014; 4: 504.
43. Qi H, Egen JG, Huang AY, Germain RN. Extrafollicular activation of lymph node B cells by antigen-bearing dendritic cells. *Science (New York, NY)* 2006; 312(5780): 1672-1676.
44. Mackay F, Schneider P, Rennert P, Browning J. BAFF AND APRIL: a tutorial on B cell survival. *Annual review of immunology* 2003; 21: 231-264.
45. Han S, Hathcock K, Zheng B, Kepler TB, Hodes R, Kelsoe G. Cellular interaction in germinal centers. Roles of CD40 ligand and B7-2 in established germinal centers. *Journal of immunology (Baltimore, Md : 1950)* 1995; 155(2): 556-567.
46. Dianda L, Gulbranson-Judge A, Pao W, Hayday AC, MacLennan IC, Owen MJ. Germinal center formation in mice lacking alpha beta T cells. *European journal of immunology* 1996; 26(7): 1603-1607.
47. Lentz VM, Manser T. Cutting edge: germinal centers can be induced in the absence of T cells. *Journal of immunology (Baltimore, Md : 1950)* 2001; 167(1): 15-20.
48. Hoyer BF, Moser K, Hauser AE, Peddinghaus A, Voigt C, Eilat D *et al.* Short-lived plasmablasts and long-lived plasma cells contribute to chronic humoral autoimmunity in NZB/W mice. *The Journal of experimental medicine* 2004; 199(11): 1577-1584.
49. William J, Euler C, Christensen S, Shlomchik MJ. Evolution of autoantibody responses via somatic hypermutation outside of germinal centers. *Science (New York, NY)* 2002; 297(5589): 2066-2070.
50. Teichmann LL, Ols ML, Kashgarian M, Reizis B, Kaplan DH, Shlomchik MJ. Dendritic cells in lupus are not required for activation of T and B cells but promote their expansion,

resulting in tissue damage. *Immunity* 2010; 33(6): 967-978.

51. Zhang J, Supakorndej T, Krambs JR, Rao M, Abou-Ezzi G, Ye RY *et al.* Bone marrow dendritic cells regulate hematopoietic stem/progenitor cell trafficking. *The Journal of clinical investigation* 2019; 129(7): 2920-2931.
52. Sapoznikov A, Pewzner-Jung Y, Kalchenko V, Krauthgamer R, Shachar I, Jung S. Perivascular clusters of dendritic cells provide critical survival signals to B cells in bone marrow niches. *Nature immunology* 2008; 9(4): 388-395.
53. Ueda Y, Yang K, Foster SJ, Kondo M, Kelsoe G. Inflammation controls B lymphopoiesis by regulating chemokine CXCL12 expression. *The Journal of experimental medicine* 2004; 199(1): 47-58.
54. Park JW, Moon SY, Lee JH, Park JK, Lee DS, Jung KC *et al.* Bone marrow analysis of immune cells and apoptosis in patients with systemic lupus erythematosus. *Lupus* 2014; 23(10): 975-985.
55. Fraussen J, Claes N, Van Wijmeersch B, van Horssen J, Stinissen P, Hupperts R *et al.* B cells of multiple sclerosis patients induce autoreactive proinflammatory T cell responses. *Clinical immunology (Orlando, Fla)* 2016; 173: 124-132.
56. Sim JH, Kim HR, Chang SH, Kim IJ, Lipsky PE, Lee J. Autoregulatory function of interleukin-10-producing pre-naïve B cells is defective in systemic lupus erythematosus. *Arthritis research & therapy* 2015; 17(1): 190.
57. Palanichamy A, Bauer JW, Yalavarthi S, Meednu N, Barnard J, Owen T *et al.* Neutrophil-mediated IFN activation in the bone marrow alters B cell development in human and murine systemic lupus erythematosus. *Journal of immunology (Baltimore, Md : 1950)* 2014; 192(3): 906-918.
58. Dieudonné Y, Gies V, Guffroy A, Keime C, Bird AK, Liesveld J *et al.* Transitional B cells in quiescent SLE: An early checkpoint imprinted by IFN. *Journal of autoimmunity* 2019; 102: 150-158.
59. Zammit NW, Siggs OM, Gray PE, Horikawa K, Langley DB, Walters SN *et al.* Denisovan, modern human and mouse TNFAIP3 alleles tune A20 phosphorylation and immunity. *Nature immunology* 2019; 20(10): 1299-1310.
60. Collin M, Bigley V. Human dendritic cell subsets: an update. *Immunology* 2018; 154(1): 3-20.
61. Conley ME, Larché M, Bonagura VR, Lawton AR, 3rd, Buckley RH, Fu SM *et al.* Hyper IgM syndrome associated with defective CD40-mediated B cell activation. *The Journal of clinical investigation* 1994; 94(4): 1404-1409.
62. Saha MK, Julian BA, Novak J, Rizk DV. Secondary IgA nephropathy. *Kidney international* 2018; 94(4): 674-681.
63. Perazzio SF, Granados Á, Salomão R, Silva NP, Carneiro-Sampaio M, Andrade LE. High frequency of immunodeficiency-like states in systemic lupus erythematosus: a cross-sectional study in 300 consecutive patients. *Rheumatology (Oxford, England)* 2016; 55(9): 1647-1655.
64. Karnell JL, Rieder SA, Ettinger R, Kolbeck R. Targeting the CD40-CD40L pathway in autoimmune diseases: Humoral immunity and beyond. *Advanced drug delivery reviews* 2019; 141: 92-103.
65. Larosa M, Zen M, Gatto M, Jesus D, Zanatta E, Iaccarino L *et al.* IL-12 and IL-23/Th17 axis in systemic lupus erythematosus. *Experimental biology and medicine (Maywood, NJ)* 2019; 244(1): 42-51.
66. Smolen JS, Agarwal SK, Ilivanova E, Xu XL, Miao Y, Zhuang Y *et al.* A randomised phase II study evaluating the efficacy and safety of subcutaneously administered ustekinumab and guselkumab in patients with active rheumatoid arthritis despite treatment with methotrexate. *Annals of the rheumatic diseases* 2017; 76(5): 831-839.

67. Amarnani A, Rosenthal KS, Mercado JM, Brodell RT. Concurrent treatment of chronic psoriasis and asthma with ustekinumab. *The Journal of dermatological treatment* 2014; 25(1): 63-66.
68. Chen LW, Egan L, Li ZW, Greten FR, Kagnoff MF, Karin M. The two faces of IKK and NF-kappaB inhibition: prevention of systemic inflammation but increased local injury following intestinal ischemia-reperfusion. *Nature medicine* 2003; 9(5): 575-581.
69. Herrington FD, Carmody RJ, Goodyear CS. Modulation of NF-κB Signaling as a Therapeutic Target in Autoimmunity. *Journal of biomolecular screening* 2016; 21(3): 223-242.
70. Ritprajak P, Kaewraemruaen C, Hirankarn N. Current Paradigms of Tolerogenic Dendritic Cells and Clinical Implications for Systemic Lupus Erythematosus. *Cells* 2019; 8(10).

English Summary
Dutch Summary
Portfolio
Curriculum Vitae
Acknowledgements

ENGLISH SUMMARY

Our immune system consists of a complex network of multiple players. These serve to keep foreign pathogens away, while tolerating our own proteins or harmless organisms. In other words, the immune system requires a balance between immunity on one hand, and tolerance on the other hand. Excessive activation can tip the balance into the domain of autoimmune disorders. Typical autoimmune disorders are rheumatoid arthritis, inflammatory bowel disease (IBD), psoriasis and systemic lupus erythematosus (SLE). It is estimated that within Europe and USA 6-7% of the population has a diagnosed autoimmune disorder. Studying the pathogenesis of autoimmune disorders has been an ongoing quest, as many immune cells take part in it.

Genome-wide association studies (GWAS) reveal a wide range of genes that could be implicated in autoimmune disorders. One of these genes, TNFAIP3 (A20), is associated to multiple autoimmune disorders and is a protein that inhibits the NF-κB pathway that is essential for the activation and survival of many immune cells. In simple terms, A20/TNFAIP3 is one of the most important brake-mechanism protein on immune cell activation.

A unique immune cell, discovered in the 1970s by Nobel laureate Ralph Steinman, termed dendritic cells, is the prime orchestrator of the balance of the immune system. By genetic engineering in mice, the *Tnfaip3* gene could specifically be removed from DCs, which resulted in their activation. This led to activation of several other primary immune cells such as T cells and B cells, and a phenotype that resembled human autoimmune diseases. Our group saw a phenotype resembling SLE, while another research group documented a phenotype of inflammatory bowel disease.

In **chapter 2** we highlight all mouse models known to date in which a targeted deletion of the *Tnfaip3* gene was performed in different immune cells that are known to be involved in autoimmune disorders. We summarize small DNA mutations (single nucleotide polymorphisms (SNPs)) in the human A20/TNFAIP3 locus that have functional and therapeutic consequences for autoimmune patients.

While the population of DCs became more defined over the course of the last 10 years, we utilized a specific Cre-LoxP model (Dngr1-cre) to delete the *A20/Tnfaip3* gene from the conventional type 1 DC (cDC1s) (**Chapter 3**). We found that cDC1s were also activated in these mice, and that by the age of ~31 weeks they developed autoimmune liver inflammation. T cells and B cells were activated, which resulted in antibody producing cells (plasma cells) that made auto-antibodies of the IgA isotype to components of liver cells.

Another highlight in autoimmune research was the unraveling of the Th17/IL-23 axis, which is important in autoimmune diseases such as arthritis, IBD and psoriasis, but also in other chronic diseases such as asthma. In a house dust mite (HDM)-driven model of airway inflammation, our group demonstrated previously that deficiency of Tnfaip3/A20

in myeloid cells lead to neutrophilic rather than eosinophilic airway infiltration, which condition might resemble therapy-resistant asthma patients. We determined whether neutrophilic infiltrates would be reduced in the absence of IL-17 receptor A (IL-17RA) signaling (**Chapter 4**), because IL-17 is known to control neutrophil attractants such as the CXCL1 chemokine production by airway epithelial cells. Surprisingly, this did not seem to be the case, as other cytokines including IL-1β, IL-23 and GM-CSF, which also have the capacity to induce neutrophilic-attracting chemokines, were still produced. We also determined whether the arthritis-like phenotype in mice that lack Tnfaip3 in myeloid cells was reduced in the absence of IL-17RA-signaling (**Chapter 4**). The paw inflammation seen in these aged mice was not dependent on IL-17, but was later demonstrated by another group to be mostly driven by IL-1β.

When studying *Tnfaip3*$^{CD11c\text{-}KO}$ mice, that developed an SLE-like phenotype, we noticed a reduction of B cells in the spleens of aged mice. This could be explained by a development disorder of B cells in the bone marrow. We thus examined all developmental stages of B cells in young and aged mice in **Chapter 5.** We found that B cell development in the bone marrow was hampered at the immature B cell stage in 6-week-old *Tnfaip3*$^{CD11c\text{-}KO}$ mice and at the pre-B cell stage in 24-week-old *Tnfaip3*$^{CD11c\text{-}KO}$ mice. The developmental disorder might well explain the reduced numbers of mature B cells in the periphery of aged *Tnfaip3*$^{CD11c\text{-}KO}$ mice. Using *in vitro* studies, we determined that systemic effects of DC activation leading to changes in the cytokine milieu in bone marrow was most likely not responsible for the observed defect in B cell development. Rather, the observed age-dependent developmental arrest of B-lineage cells most likely reflected changes in non-B cells, most likely A20/Tnfaip3-deficient DCs in the bone marrow. This indicated that activated DCs in a different compartment than spleen, such as bone marrow, could also hamper B cell development and perhaps their function. Interestingly, B cells that reached the periphery were more easily activated compared to B cells from healthy mice.

Antibody producing plasma cells are derived from B cells. The normal route of B cell activation is as follows: DCs activate T cells, and they in turn activate B cells. However, in certain circumstances DCs can also directly activate B cells without the help of T cells. It had been previously demonstrated that A20/Tnfaip3-deficient bone marrow DCs could activate B cells in *in vitro*, independently of T cell help. In **Chapter 6**, we determined whether T cell-independent activation of B cells also occurs in a mice *in vivo,* if we would disable T-B cell communication by abrogating CD40L expression in mice lacking A20 in dendritic cells. CD40L is an essential protein expressed on activated T cells that is essential for their capacity to support B cell activation. Although T-B cell communication was required to achieve germinal centers and IgG1 antibody production, we found that antibodies of the IgA subclass could still be formed. Kidney glomerular basement membrane thickening was also seen, despite the absence of IgG induction, possibly facilitated by IgA depositions that we could demonstrate in the kidneys of a consider-

able fraction of CD40L-deficient mice with CD11c-Cre-driven deletion of the *A20/Tnfaip3* gene.

Since Th17 cells are so important in autoimmunity, and their development is facilitated by IL-23, we wondered how Th17 cell homeostasis would be affected if we induce IL-23-deficiency in mice with abrogated Tnfaip3 expression from DCs (**Chapter 7**). Surprisingly, Th17 cell homeostasis was not altered in absence of IL-23. Levels of immunoglobulins, autoreactive immunoglobulins and kidney glomerular changes were also unaltered in these mice. We thus concluded that the SLE phenotype seen in mice with Tnfaip3-deficient DCs was independent of the Th17/IL-23 axis.

Taken together, DCs maintain the balance between tolerance to autoimmunity. The A20/Tnfaip3 protein in DCs helps in keeping the balance: loss of this protein tips the immune system into a state of autoimmunity. By utilizing several genetic mouse models of targeted A20/Tnfaip3 deletion from specific DC subsets, we have seen that the absence of A20/Tnfaip3 can result in different autoimmune phenotypes, e.g. an autoimmune liver phenotype or SLE. In more detail, the SLE phenotype is quite robust, because despite inhibiting the Th17/IL-23 axis or T-B cell communication, the mice still developed a disease phenotype with characteristics of SLE. This highlights that future of therapies may need to be targeted to the start of an autoimmune reaction, for example at the level of DCs, because at a later point in disease development many other immune players and cytokines are involved, perhaps irreversibly. Those future therapies will be crucial to help DCs to maintain their *Act of balance*.

NEDERLANDSE SAMENVATTING

Ons immuunsysteem bestaat uit een complex netwerk van verschillende immunologische spelers. Zij werken samen om vreemde lichamen zoals virussen en bacteriën te weren, terwijl ze andere eiwitten of organismen welke ongevaarlijk zijn moeten tolereren. Met andere woorden: ons immuunsysteem heeft een balans nodig tussen immuniteit aan de ene kant en tolerantie aan de andere kant. Te veel activatie van het immuunsysteem leidt tot gezondheidsproblemen op het gebied van auto-immuunziekten, waarin lichaamseigen eiwitten worden aangevallen. Karakteristieke auto-immuunziekten zijn reumatoïde artritis, inflammatoire darm aandoeningen (IBD), psoriasis en systemische lupus erythomatodes (SLE). Naar schatting heeft 6 à 7% van de Europese en Amerikaanse bevolking een auto-immuun aandoening. Onderzoek naar het ontstaan van auto-immuunziekten is een zoektocht die al tientallen jaren speelt vanwege de complexiteit van de vele immuuncellen die er aan deelnemen.

Door genetisch onderzoek via genoombrede associatie studies zijn vele genen gevonden die betrokken kunnen zijn bij auto-immuun aandoeningen. Één van die genen is TNFAIP3 (ook bekend als A20), welke geassocieerd is met verscheidene auto-immuun ziekten. Het is een eiwit dat de NF-κB signaleringsroute remt, die zeer belangrijk is voor cel activatie en overleving. Eenvoudig gezegd: TNFAIP3/A20 is één van de belangrijkste regulatoren die als rem functioneert in immuuncel activatie.

Eén unieke immuuncel, de dendritische cel (DC), ontdekt in de jaren '70 door Nobelprijswinnaar Ralph Steinman, is de dirigent van het immuunsysteem. Door middel van extra signalen op het celoppervlak (co-stimulatoire en co-inhibitoire moleculen) kan de DC bepalen of een volgende immuuncel, de T cel, geactiveerd wordt. Met behulp van genetische muismodellen is het mogelijk om Tnfaip3/A20 specifiek weg te halen in een enkel celtype, bijvoorbeeld de DC. Dit leidt dan tot spontane activatie van deze DCs. Als je deze muizen, die A20/Tnfaip3 missen uit DCs (deze zijn *Tnfaip3*$^{CD11c\text{-}KO}$ muizen genoemd), oud laat worden treedt activatie op van andere immuuncellen, zoals T en B cellen. Als gevolg daarvan ontwikkelen deze dieren een ziektebeeld dat grote overeenkomsten vertoont met autoimmuunziekten bij de mens. Onze groep heeft aangetoond dat *Tnfaip3*$^{CD11c\text{-}KO}$ muizen SLE-achtige verschijnselen ontwikkelen, terwijl een andere onderzoeksgroep heeft laten zien dat vergelijkbare muizen een IBD ziektebeeld kunnen ontwikkelen. In **Hoofdstuk 2** geven we een overzicht van de nu bekende muismodellen waarin A20/Tnfaip3 specifiek is verwijderd uit verschillende immunologische cellen die een rol spelen bij autoimmuun reacties. We noemen ook de kleine DNA variaties (de zgn. enkel-nucleotide polymorfismen of SNPs) die bij patiënten worden gevonden en een mogelijke verklaring kunnen zijn voor functionele veranderingen in hun immuunsysteem en mogelijk therapeutische consequenties hebben.

Doordat de populatie van DCs steeds beter gedefinieerd werd in de laatste 10 jaar, werd ook steeds duidelijker dat er verschillende DC typen waren. Onze interesse viel op een nieuw genetisch model om A20/Tnfaip3 specifiek te verwijderen uit een subtype van DCs, de zgn. conventioneel type 1 dendritische cel (cDC1) (**Hoofdstuk 3**). We zagen in deze *Tnfaip3*$^{Dngr1\text{-}KO}$ muizen dat de cDC1s inderdaad geactiveerd raakten en dat rond de leeftijd van 31 weken deze muizen een autoimmuun leverontsteking hadden ontwikkeld. T cellen en B cellen waren geactiveerd en er waren antistof producerende cellen (plasma cellen) aantoonbaar, die antistoffen van het IgA isotype tegen lichaamseigen levereiwitten produceerden.

Nog een belangrijke ontwikkeling in het onderzoek over auto-immuun ziekten was de ontdekking van de Th17 cel, die de belangrijke signaalstof, het IL-17 cytokine, produceert. De zgn. Th17/IL-23 as van inflammatoire cytokinen en de Th17 cel bleek betrokken te zijn bij auto-immuun ziekten zoals reuma, IBD en psoriasis, maar ook bij andere chronische aandoeningen zoals astma. In een huisstofmijt-geïnduceerd model van luchtwegontsteking in muizen met myeloïde cel-specifieke deficiëntie van A20/Tnfaip3 (*Tnfaip3*$^{LysM\text{-}KO}$) heeft onze groep eerder aangetoond dat muizen een neutrofiel infiltraat in de longen ontwikkelden in tegenstelling tot een eosinofiel infiltraat. Een dergelijk ziekteprofiel met een neutrofiel infiltraat in de longen vertoont overeenkomsten met het immunologisch profiel van patiënten met moeilijk te behandelen astma. We vroegen ons af of de aantrekking en opeenhoping van neutrofielen zou afnemen als we de signaalstof IL-17 zouden wegnemen, aangezien IL-17 betrokken is bij de productie van stoffen die neutrofielen aantrekken zoals het CXCL1 chemokine dat door de cellen van de luchtwegwand wordt geproduceerd onder invloed van IL-17 (**Hoofdstuk 4**). In tegenstelling tot onze verwachting bleek dit niet het geval te zijn, aangezien andere cytokinen zoals IL-1β, IL-23 en GM-CSF nog steeds geproduceerd werden en deze ook in luchtwandcellen de productie van chemokinen die neutrofielen aantrekken kunnen stimuleren. We hebben in deze myeloid-specifieke Tnfaip3-deficiënte *Tnfaip3*$^{LysM\text{-}KO}$ muizen ook gekeken naar een reuma-achtig ziektebeeld dat door een andere onderzoeksgroep was beschreven, en onderzocht of dergelijke ziekteverschijnselen zouden afnemen in afwezigheid van IL-17 receptor signalering. Dit bleek ook niet het geval te zijn. Later werd aangetoond in een ander onderzoek dat cytokine IL-1β hoofdverantwoordelijk is voor het reuma-achtig beeld in myeloid-specifieke Tnfaip3-deficiënte muizen.

Tijdens het bestuderen van de muis welke dendritische cel-specifiek Tnfaip3-deficient is (*Tnfaip3*$^{CD11c\text{-}KO}$ muizen) en een SLE-achtig beeld ontwikkeld, viel het ons op dat de B cellen aanzienlijk verminderd waren in de milt. Omdat deze bevinding wijst op een defect in de aanmaak van B cellen in het beenmerg hebben we in **hoofdstuk 5** de ontwikkeling van B cellen onderzocht in zowel jonge als oudere *Tnfaip3*$^{CD11c\text{-}KO}$ muizen. Er bleek een leeftijdsafhankelijke B cel ontwikkelingsstoornis te zijn, gekenmerkt door een sterke blokkade op het immature B cel en het eerdere pre-B cel stadium in, respec-

tievelijk, 6 en 24 weken oude *Tnfaip3*$^{CD11c\text{-}KO}$ muizen. Deze stoornis is een aannemelijke verklaring voor de afname van B cellen in perifere lymphoïde organen zoals de milt op oudere leeftijd. Door laboratoriumproeven in een beenmerg celkweek systeem hebben we kunnen aantonen dat circulerende signaalstoffen waarschijnlijk niet de afwijking in B cel ontwikkeling probleem induceren, maar dat Tnfaip3-deficiëntie DCs in het beenmerg zelf waarschijnlijk deze afwijkingen in de B cel ontwikkeling veroorzaken. Een andere interessante bevinding was dat volgroeide B cellen die het beenmerg verlaten, wel gemakkelijker geactiveerd raken op eenzelfde stimulus dan B cellen uit een normale gezonde muis. Onze proeven laten zien dat de geactiveerde DCs in ons muis model ook in een ander orgaan dan de milt, zoals dus in het beenmerg, B cel ontwikkeling kan verstoren en mogelijk hun uiteindelijke functie kan beïnvloeden.

Normaalgesproken verloopt de activatie van B cellen via antigeen presenterende cellen zoals DCs, die T cellen activeren, die vervolgens hulp bieden aan B cellen in nauwe B-T cel interactie. Er is echter aangetoond dat Tnfaip3-deficiënte DCs, zonder de hulp van T cellen, in een celkweeksysteem (*in vitro*) B cellen konden activeren. In **hoofdstuk 6**, vroegen we ons af of deze directe activatie van B cellen door Tnfaip3-deficiënte DCs ook in de muis (*in vivo*) plaatsvindt. Om dit te onderzoeken hebben we T en B cel communicatie geblokkeerd door genetisch tevens CD40L weg te halen (een eiwit dat door de T cel na activatie op het celoppervlak wordt gezet en dat belangrijk is voor functionele T-B cel interactie). Deze T-B cel communicatie bleek essentieel te zijn voor het ontwikkelen van kiemcentrum B cellen, een subgroep van B cellen die zich bevinden in kiemcentra waar B cellen na activatie een interactie aangaan met T cellen om vervolgens verder te kunnen uitrijpen o.a. tot antistof-producerende plasma cellen. In de afwezigheid van CD40L werd er geen IgG1 gevormd, maar vonden we dat een andere antistof, IgA, wel gevormd kon worden. Het circulerende IgA in het serum bevatte ook reactiviteit tegen lichaamseigen stoffen. Structurele veranderingen in de glomeruli – dit zijn de kluwens van haarvaatjes die belangrijk zijn voor de bloedfiltratie in de nier – die passen bij een SLE beeld, werden nog steeds aangetroffen ondanks de afwezigheid van IgG.

Omdat Th17 cellen zo belangrijk zijn in auto-immuunziekten en hun ontwikkeling ondersteund wordt door IL-23, vroegen we ons af of de auto-immuun afwijkingen in *Tnfaip3*$^{CD11c\text{-}KO}$ muizen zouden verminderen in de afwezigheid van IL-23 (**Hoofdstuk 7**). In tegenstelling tot de verwachting, was de ontwikkeling van Th17 cellen niet verstoord in afwezigheid van IL-23. Ook het niveau van antistoffen, ook die tegen lichaamseigen eiwitten zoals dubbelstrengs DNA in het serum en afwijkingen in de nieren was bij de IL-23-deficiënte *Tnfaip3*$^{CD11c\text{-}KO}$ niet veranderd ten opzichte van *Tnfaip3*$^{CD11c\text{-}KO}$ die wel IL-23 konden maken. We concludeerden dus dat het SLE fenotype in deze *Tnfaip3*$^{CD11c\text{-}KO}$ muizen onafhankelijk was van de Th17/IL-23 as.

Samenvattend is de DC belangrijk om een goede balans tussen tolerantie en immuniteit te bewaren. Het Tnfaip3/A20 eiwit in DCs speelt hierin een cruciale rol, want als DCs

dit eiwit missen slaat het immuun systeem teveel door richting auto-immuniteit. Door gebruik te maken van verschillende genetische muismodellen waarbij we heel specifiek bepaalde DC subgroepen deficiënt konden maken voor Tnfaip3/A20, zagen we dat deze muizen verschillende auto-immuun ziektebeelden ontwikkelden. Deze varieerden van auto-immuun leverontsteking tot een algehele immuunontsteking die duidelijke overeenkomsten had met SLE. Dit SLE beeld bleek robuust: ook als we T-B cel interactie of de Th17/IL-23 as blokkeerden waren er nog steeds diverse kenmerken van SLE meetbaar. Deze bevindingen benadrukken dat de toekomstige therapie ontwikkeling voor auto-immuunziekten gericht zou moeten zijn op ingrijpen in een vroeg stadium van het ziekteproces, zoals op het niveau van DCs. In een later stadium van de ziekte zijn er veel andere immuuncellen en signaalstoffen betrokken, waardoor het moeilijker wordt een afdoende effect van de behandeling te verkrijgen. Het is dus belangrijk om de DCs te helpen hun activatie strikt te moduleren en hun *act of balance* te ondersteunen.

PORTFOLIO

Tridib Das

Erasmus MC Department:	Pulmonary medicine
PhD Period:	2013 – 2017
Thesis Directors:	Prof. dr. R.W. Hendriks
	Prof. dr. B.N.M. Lambrecht
Research School:	Molecular Medicine

PhD Courses

2013 Animal Handling Course (MolMed)
2013 Functional imaging and super resolution
2013 Basic Course on R (MolMed)
2014 Advanced Immunology Course (MolMed)
2014 Research Management for PhD Students (MolMed)
2015 Research Integrity Course (MolMed)
2016 Writing a scientific article Course (MolMed)

(Inter)national conferences

2013 International Symposium on Regulators of Adaptive Immunity (Erlangen, Germany)
2014 ILD Winterschool (Davos, Switserland)
2014 IRC mini-symposium on Cell Signaling in inflammation and immunity (Ghent, Belgium)
2014 NVVI Lunteren (Lunteren, The Netherlands)

Presentations and posters

2014 MolMed Day (Rotterdam, the Netherlands) – Poster
2014 NVVI 50th Anniversary meeting (Kaatsheuvel, the Netherlands) – Oral
2014 Dendritic Cell conference (Tours, France) – Poster
2015 Keystone Macrophages and Dendritic Cells Re-united (Montreal, Canada) – Poster
2015 MolMed Day (Rotterdam, the Netherlands) – Poster
2016 MolMed Day (Rotterdam, the Netherlands) – Poster
2016 Dendritic Cell conference (Shanghai, China) – Oral

Coaching, Teaching and management activities

Supervision of Fatemeh Ahmedi (Master student)
Supervision of Anne Hubers (Master student)

Supervision of Zhongli Chen (Master student, guiding in writing a review article)
Mentor for 1st year medical graduate students
Board member of PROMERAS (PhD association Erasmus MC)

Publications

2018 **Das, T.**, Chen, Z., Kool, M. A20/Tumor Necrosis Factor α-Induced Protein 3 in Immune Cells Controls Development of Autoinflammation and Autoimmunity: Lessons from Mouse Models.
Front Immunol. 2018 Feb 21;9:104
Impact factor: 4.534

2018 Vroman, H., **Das, T.**, Bergen, I.M., van Hulst, J.A.C., Ahmadi, F., van Loo, G. Lubberts, E., Hendriks, R.W., Kool, M. House dust mite-driven neutrophilic airway inflammation in mice with TNFAIP3-deficient myeloid cells is IL-17-independent.
Clin Exp Allergy. 2018 Dec;48(12):1705-1714.
Impact factor: 4.641

2019 **Das, T.**, Bergen, I.M., Koudstaal, T., van Hulst, J.A.C., van Loo, G., Boonstra, A., Vanwolleghem, T., Leung, P.S.C., Gershwin, M.E., Hendriks, R.W., Kool, M.
J Autoimmun. 2019 Aug;102:167-178
Impact factor: 7.321

ABOUT THE AUTHOR

Tridib Das was born in New Delhi, India on 14th October 1988. He attended bilingual VWO at the Alfrink College in Zoetermeer, after which he studied medicine from Leiden University. In 2007 he went as an exchange student to the Karolinska University in Stockholm, at which time an interest in biomedical sciences started to grow. This steered him to enroll in a pre-master biomedical sciences at Leiden University. After achieving cum laude on his medicine degree in 2012, he completed his masters in biomedical sciences from Leiden University in 2013, which included a research internship at Tufts and Yale University in Boston and New Haven (USA).

Choosing a clinical career path could change for him every month during his clinical rotations, varying from pediatrician, to ENT-specialist to gynaecologist. His final choice was set for ophthalmology. One passion, however, was continuous throughout his studies and became evident from all his student research internships: the immune system. It intrigued him how it entangled every organ of our human body and was layered in so many different ways. Logically a PhD vacancy on autoimmune disorders at Erasmus MC became his choice for dedicating the next phase of life before starting a clinical residency. With positive responses from Boston through Skype interviews his future supervisors in Rotterdam from the pulmonary medicine department, Tridib jumped aboard the research line in 2013 on the role of A20/Tnfaip3 in dendritic cells to balance autoimmunity. The results of this thesis are now in front of you and were defended in Rotterdam on 24th February 2021.

As per June 2018 Tridib is in his residency to become an ophthalmologist from the Rotterdam Eye hospital. In his spare time he enjoys photography, traveling the world, tasting different cuisines and analyze movies of the silver screen. He lives with his wife Smriti in Rotterdam.

ACKNOWLEDGEMENTS

"*Always finish what you start*." After many years, I am happy to announce my thesis is finally complete and would hereby like to thank everyone who contributed to the completion of this thesis. Without them, this thesis would not have been possible.

Firstly, my sincere thanks is addressed to my thesis director **Prof. dr. Rudi Hendriks**. Dear Rudi, I still remember our first Skype meeting well. I was in Boston and you were in Rotterdam. You were immediately able to convey your enthousiasm for immunology and the various ongoing projects in your laboratory. Although it was quite a leap of faith into an unknown lab, I simply had a very good feeling about it when I heard you speak. Years later I still admire your knowledge of immunology, your adaptability in the field, and the way in which you communicate intricate problems with such simplicity. You have really brought forward my best abilities, by pointing out when that was necessary, but also by motivating me at less fortunate moments. Especially in the last phase of my PhD I am amazed at your almost poetic descriptions of my own data, when you gave clear feedback on my remaining chapters. I am very grateful for the opportunity that you have given me to perform my thesis at your laboratory, to be able to call you my mentor these years, and for your intense Olympic game-like coaching to guide me over the finish line.

My thesis would not have been possible without my second thesis director, **Prof. dr. Bart Lambrecht**. Dear Prof Lambrecht, I thank you for the inspiration of your research on the field of A20, that has been the base for the contents in this thesis. Whenever I heard you speaking on a conference or meeting and I was surprised by your ready-to-use knowledge about every relevant article in the field, I was myself pushed to get back to the literature or make long hours in the lab. Also thank you for assisting in the last phase of my thesis and that you are part of my PhD committee.

My heartiest thanks also to **ing. Dr. Mirjam Kool**. Dear Mirjam, from day one I was under your supervision. You have helped me over the years to tune my medical doctor brain into a researcher. You gave me freedom to research my own ideas, such as the time when I was intending to find ophthalmologic symptoms in our study mice. If a project ever ended in a dead-end, you could always give a positive twist to the material that we did find. I often received constructive feedback on weekends and evenings to make my data or presentations better. Thank you very much for all your input!

To **Prof. Dr. Henk Hoogsteden** and **Prof. dr. Joachim Aerts**, I express my gratefulness for giving me the opportunity to perform my research in the pulmonology laboratory.

In addition, my thanks go out to **Prof. dr. Frans Kroese**, **Dr. Erik Lubberts** and **Dr. Andre Boonstra** for participating in my PhD committee.

Acknowledgements

In our lab I am lucky to have had technicians to work together on my experiments. Dear **Ingrid**, all the hands-on-skills I have learned from you. On long experiment days I could really build on your knowledge and assistance. You have always kept an eye out for the various mouse lines of my project, for which I express my gratitude. Even though the field of autoimmunity was new to you, I felt that you tried your best to adapt and that you moved out of your comfort zone to help me out. Thank you for also sharing the load of supervising some students on the team when I was under a lot of work pressure finishing my thesis.

Dear **Menno**, "Fire-Ball", thank you for all the help at the mouse experiments in my first year. If I had you on my team, I knew we woudl have time to lunch that day, because you were simply so blazing fast. Amidst all the hard work, there would always be laughter with you around. **Jennifer, Marjolein** and **Melanie**, thank you for jumping in and assisting me on my large experiment days as well. Without your help I would still be pipetting on the lab.

Thankfully, even on the days that nothing in my PhD seemed to go in the right direction, I found solace within the Pulmonology Lab at the Erasmus MC, and made me look forward to go to the lab every morning. The atmosphere at the lab was simply phenomenal. Despite having a large lab, we regularly managed to go for lunch all together. My thanks go out to my fellow PhDs at the time: I had just moved to Rotterdam and felt we had become not only colleagues, but also friends.

Bobbi, I am glad we could relief our PhD stress during kickboxing and squash sessions. I will never forget your dedication to run and hit the ball, making Jackie Chan-style jumps through the hall. I was inspired by you to get my motorbike license and I hope that I can still make motor trips with you once I have finally bought one.

Irma, I remember that we both started on the same day at the lab and had some awesome conferences in the early days. Our cocktail choosing story is one for the books: I chose my cocktail super-fast and it was disgusting, and you took forever to choose one, but found by far the best cocktail on the list. Your theory does not always apply though: after all, you finished your PhD way faster than me, despite starting on the same day in the lab, and it was still with flying colours! Thanks also for the weekly movie nights we went to with the other PhDs and introducing me to delicious vegan cuisine.

Paulien, it was awesome that we independently joined the same Lindy hop dance classes and could checkmark some old-fashioned parties around Rotterdam. Thanks for your ongoing enthusiasm which really brought life to the lab, your co-founded Pulmonology LongDrinks will hopefully be carried on by the youngsters for many years to come.

Simar, if it was very late in the evening or sometime in the weekend, I was always sure that besides me there would be one more Indian roaming the lab. Your motivation transferred on to me to keep working hard and making the hours, which now at last pays

off. I am glad you could secure your career in Netherlands and wish you all the best in Nijmegen.

Next comes "The Roomies!", my co PhDs which probably had the most awesome room of the lab. **Denise**, it was never a dull moment with you around being an excellent talking partner. I will remember our 'Free' cinnamon punch in the coffee breaks. I wish you all the best in completing your PhD in the coming year. **Caroline** (the 'Mother' of our room), thanks for your kind and motivating words when things really became gloomy around my lowest PhD moments. **Heleen**, for helping me out with your pre-acquired knowledge around A20 and helpful tips to get most of my experiments. I am proud that we could publish an article together, putting both our experiments on the table and making a coherent story. **Peter**, also you were often around in the weekends and early mornings. I think we could often relate to similar problems having the doctor's brain in us. Last but definitely not least, **Thomas**, my fellow DNGR1-buddy, with you I will remember the record-setting long nights at the lab. Finishing at 3 or 4 'o clock in the morning almost became a normality with you and it was not a problem to work so late with your curated music beats in the background. I am very glad that you will support me as my paranymph on the defense date. Together with you and Peter, I will remember our 22-floor staircase race or plotting to rescue my brothers' new mobile phone from a Marktplaats criminal.

The "lab guys" really became a phenomenon in the early days of my PhD and I am thankful for the many adventurous activities like Escape rooms, Go-karts racing, Frisbee-football, you name it. **Koen**, you really knew how to constantly come up with new ideas, which even brought us on national TV during our 'prison escape-activity'. Also, thanks for making my childhood dreams come true of wearing an astronaut suit and a self-made Ghost buster costume to the pulmonology Christmas dinners.

To the younger PhDs of our lab: **Floris**, goodluck with finishing your remarkable PhD and thanks for your advice on helping me pass my American medical (USMLE) exams. **Jasper**, 'B-cell guy', thanks for your assistance in making me understand the complex world of B-cells which you really have mastered. I wish you luck on finishing your PhD. All the best on finishing your PhDs soon, **Stefan**, **Jelle**, **Esmee**, **Sai-Ping**, **Mandy**, **Joanne** and **Bob**. Another big thanks goes out to students that were courageous to join me in my projects: **Fatemeh**, for your vast motivation and even teaching me things about new laboratory techniques to study arthritis in the paws of the mice. All the best in Lund on completing your PhD. **Anne**, for mastering germinal center histology and helping me on my project which will hopefully be published after this PhD. I'm glad you collaborated further with the pulmonology lab and wish you all the best in your PhD.

I would lastly also like to express my thanks to the Post-Docs in our lab, **Odilia**, **Alex**, **Ralph** and **Saravanan** for their advice and creative thinking to help my auto-immune research off the ground, varying from histology tips to genome research. For any one

that I have missed to mention from our lab: thanks for the 'Gezelligheid' and I hope we will see each other soon.

Being kind of a 'black sheep' amidst all the pulmonology research, often made me seek advice from other departments. I would like to thank dr. **Janneke Samsom**, **Celia** and **Dicky** for advice on intestinal autoimmunity, **dr. Thomas Van Wolleghem** en **dr. Andre Boonstra** for helping me on my liver autoimmune project. I am proud we have published such a beautiful paper together in an impactful journal.

Performing mouse experiments is not possible without the excellent support of the members of the EDC under supervision of **Mr. Mahabier**. Thank you very much for all those years of pleasurable cooperation.

Making it to the PhD finish line would have never been possible, were it not for the ground work that has been set in me by my student supervisors. It is thanks to each of you, who believed in me while I was still a medical student. **Dr. Andreea Ioan** (Then: Leiden University), **Prof. dr. Sicco Scherjon** (Then: Leiden University), **Prof. dr. Diana Bianchi** (Tufts University, Boston) and **Prof. dr. Vicki Abrahams** (Yale University, New Haven). I have looked up to you almost as inspirational heroes. There have been times in my PhD when your visual images or quotes from you helped me picture how I wanted to become as a PhD. I hope that when you receive this thesis, you can visualize your contribution to this as well.

Beyond the lab, there are my friends I would like to thank for providing relaxations that were necessary to compensate the hard and broke PhD-life. **Jasper**, from high-school, thanks for making me exercise my PhD-kilo's away during our squash sessions at Erasmus University. **Kirty**, **Hadya** & **Viresh** for burning some calories during intense 30-second games. **Gert-Jan**, we immediately clicked with our similar reference TV humor and you have made my PhD time so much more memorable with our Rotterdam exploring adventures. It's a pity you live "far away" in London these days, but I look forward to taking you (and girlfriend **Laura**) to a Nando's restaurant soon! **David**, ever since our animal-handling course, we always miraculously came across each other in the Erasmus MC elevator. Thanks for the social (and also very intellectual) beer-drinking and tea/coffee drinking meetings we have shared. Wish you all the best in finishing your PhD soon too and hope to receive many more traveling tips for the world after the whole corona-virus episode hopefully flies over. To my "gentlemen" friends, **Clothaire**, **Dirk**, **Michel** and **Jesse**, thanks for keeping the friendship alive even though all live in different cities since our Medical days. In line of our tradition: it's time to visit a new city, taste a new burger and play a new board game in a random café. **Annemarij**, I hope you are proud to see me have my degree today, ever since we went to study in Sweden

together and I was head-strong that one day I wanted to become a professor. **Vaasu**, my childhood friend, our yearly Eurotrips were something that really shows the boundaries of your imagination. I really looked forward to our historic "Euro-Trips" during my PhD all across Europe where we tasted as much good food, soaked as much sun and heard all the music we could. **Daisy**, I am sure to have a to-do list of movie watching after I have spoken to you which helped me relax during the PhD. Last, but definitely not the least, **Jelle**, since our breakdancing days you have been around as my friend, turned up to be my best-man during my wedding and now even became my paranimf. We could always balance the intense working week with a good old party. I hope we continue to cherish this friendship and explore many more quality burgers, beers and wines in the future.

I also express my thanks to my current supervisors in my Ophthalmology training, **Prof. dr. Jan van Meurs** and **Prof. dr. Dion Paridaens**, who have given me the space and motivation to finish my PhD during a residency at the Eye Hospital Rotterdam. To all my fellow residents there, thanks for these last two years, and the rest of our residencies to come. It's going to be an awesome time!

My thanks go out to my in-laws who have accepted me as their son. Your support from 9000 kilometers away has reached me even so.

Dear **Mom** and **Dad**, thank you for your unconditional love which has motivated and soothed me on so many countless occasions. Mom ("Maa"), I remember that you actually went online to help me find articles on A20 that you thought were helpful (even though they might not have been, actually). This gesture and your support meant so much to me! Dad ("Baba"), even though I had to explain my projects so many times to you, I have loved that you cared to ask with the same curiosity each time when I visited. I hope I have made both of you proud by becoming not only the first medical doctor, but now also the first doctorate dr Das of our family. To my little brother **Tuhin**, while you were small, I was probably an example to you. But now you continue to amaze me with all your talents. I am grateful that despite our almost 12-year difference, we have so many similar interests and can still laugh over similar jokes. I wish you all the best in completing your university degree from TU delft in the coming years!

Smriti, my dear. No words can really describe your support. We got to know each other as I was at the beginning phase of my PhD, first as a friend, then my girlfriend, and eventually my wife. With your past experience of a PhD yourself you guided me with tips and tricks, which really helped over the years. But mostly it was you who was always there when I returned home while the PhD life reached its lowest moments and experiments had failed on me. I will especially remember how you would wait for me, even if it became 10 or 11PM, until I returned home and we would eat our dinner together. I am

grateful for your immense pool of patience to support your partner in his everlasting PhD. If you ask me now "Shall we do this?" you will no longer hear my excuse "I have a PhD to finish". I will say "Yes!" to all upcoming adventures that we will share, and look forward to each one of them. *Ami tomai khub bhalo bashi, amar shona!*